NOVEL INHIBITORS OF DIHYDRODIPICOLINATE SYNTHASE

A Thesis Submitted to the
College of Graduate Studies and Research
In Partial Fulfillment of the Requirements for the Degree of
Doctor of Philosophy in the Department of Chemistry
University of Saskatchewan, Saskatoon
By

Yulia Skovpen

PERMISSION TO USE

In presenting this thesis in partial fulfillment of the requirements for a Postgraduate degree from the University of Saskatchewan, I agree that the Libraries of this University may make it freely available for inspection. I further agree that permission for copying of this thesis in any manner, in whole or in part, for scholarly purposes may be granted by the professor or professors who supervised my thesis work or, in their absence, by the Head of Department or the Dean of the College in which my thesis work was done. It is understood that any copying or publication or use of this thesis or parts thereof for financial gain shall not be allowed without my written permission. It is also understood that due recognition shall be given to me and to the University of Saskatchewan in any scholarly use which may be made of any material in my thesis. Requests for permission to copy or to make other use of material in this thesis in whole or part should be addressed to:

Head of the Department of Chemistry
University of Saskatchewan
Saskatoon, Saskatchewan (S7N 5C9)

ABSTRACT

Dihydrodipicolinate synthase (DHDPS) catalyzes the first committed step of L-lysine and *meso*-diaminopimelate biosynthesis, which is the condensation of (*S*)-aspartate-β-semialdehyde (ASA) and pyruvate into dihydrodipicolinate via an unstable heterocyclic intermediate, (4*S*)-hydroxy-2,3,4,5-tetrahydro-(2*S*)-dipicolinic acid. DHDPS has been an attractive antibiotic target because L-lysine and *meso*-diaminopimelate are cross-linking components between peptidoglycan heteropolysaccharide chains in bacterial cell walls. Studies revealed that mutant auxotrophs for diaminopimelate undergo lysis in the absence of diaminopimelate in the medium; therefore the assumption is that strong inhibition of DHDPS would result in disruption of *meso*-diaminopimelate and L-lysine biosynthesis in bacteria and would stop or decrease bacterial growth (eventually leading to bacterial death). In this work, the DHDPS inhibitor design is focused on the allosteric site of the enzyme. It was proposed that a compound mimicking binding of two L-lysine molecules at the allosteric site at the enzyme's dimer-dimer interface would be a more potent inhibitor than the natural allosteric inhibitor of this enzyme, L-lysine. This inhibitor (*R,R*-bislysine) was synthesized as a racemic mixture, which was then separated with the aid of chiral HPLC. The mechanism of feedback inhibition of DHDPS from *Campylobacter jejuni* with its natural allosteric modulator, L-lysine, and its synthetic mimic, *R,R*-bislysine, is studied in detail. It is found that L-lysine is a partial uncompetitive inhibitor with respect to pyruvate and a partial mixed inhibitor with respect to ASA. *R,R*-bislysine is a mixed partial inhibitor with respect to pyruvate and a noncompetitive partial inhibitor with respect to ASA, with an inhibition constant of 200 nM. Kinetic evaluation of each DHDPS mutants (Y110F, H56A, H56N, H59A and H59N) has revealed amino acids responsible for the inhibitory effect of L-lysine, *R,R*-bislysine, and we have found that *R,R*-bislysine is a strong submicromolar inhibitor of Y110F, H56A, H56N and H59N.

ACKNOWLEDGMENTS

I would like to acknowledge my supervisor Dr. David R. J. Palmer for the opportunity to work in his lab and on such an interesting research project, which combines organic synthetic chemistry and enzymology/molecular biology. I am thankful for his wisdom and guidance, his patience, support and the degree of independence he gave me during these years.

I greatly appreciate the help, support and expertise of our lab manager, Natasha Vetter. I am also grateful for our fruitful discussions of all aspects of my work.

I am thankful to professor Dr. David A. R. Sanders, Cuylar Conly and Shuo Li for their valuable contribution to this research project. I very much appreciate Dr. David A. R. Sanders' suggestions, consulting and expertise.

I would like to thank Dr. Janet Hill and Dr. Bonnie Chaban (Department of Veterinary Microbiology, Western College of Veterinary Medicine, University of Saskatchewan) for providing *C. jejuni* genomic DNA, as well as Ken Thoms, Dr. Keith Brown, and other staff of the Saskatchewan Structural Sciences Centre.

Thank you to the former and present members of the Palmer Lab (Julie Boisvert-Martel, Dr. Shazia Anjum, Dr. Rajendra Jagdhane, Hari Babu Aamudalapalli, Aarti Bhagwat, Bernardo Jung, Theerawat Prasertanan), and of the Sanders Lab (Dr. Karin E. van Straaten, Dr. Sean Dalrymple, Jijin Raj Ayanath Kuttiyatveetil, Carla Protsko, Drew Bertwistle, Dr. Mary Yang and Siddharth Tiwari) for their constant support and suggestions.

I would also like to thank the members of my Advisory Committee, Dr. Soledade Pedras, Dr. Ed Krol, and Dr. Tak Tanaka. I appreciate their time, knowledge and expertise to evaluate my work and student performance.

I am grateful to the Department of Chemistry, Dr. Palmer, NSERC and the Provincial Government for financial support to help complete this work.

DEDICATION

I dedicate this thesis to my father, Valeriy Skovpen, who supported me in making the decision to pursue a Doctorate Program in Canada, who always encouraged me to set higher goals, and who would be proud of his daughter's achievements.

TABLE OF CONTENTS

LIST OF TABLES

LIST OF FIGURES

LIST OF SCHEMES

LIST OF ABBREVIATIONS

ASA,	(*S*)-Aspartate-β-semialdehyde
DHDPS,	Dihydrodipicolinate Synthase
DHDPR,	Dihydrodipicolinate Reductase
DHDP,	2,3-Dihydrodipicolinate
DTT,	Dithiothreitol
DAD,	Diode array detector
DCM,	Dichloromethane
DIBOC,	Di-*tert*-butyl dicarbonate
DMF,	*N,N*-Dimethylformamide
EDTA,	Ethylenediaminetetraacetic acid
ELSD,	Evaporative light scattering detector
FCC,	Flash column chromatography
HMPA,	Hexamethylphosphoramide
HTPA,	(4*S*)-Hydroxy-2,3,4,5-tetrahydro-(2*S*)-dipicolinic acid
HPLC,	High performance liquid chromatography
HEPES,	4-(2-Hydroxyethyl)-1-piperazineethanesulfonic acid
ITC,	Isothermal titration calorimetry
IC_{50},	Half maximal inhibitory concentration
IPTG,	Isopropyl β-D-1-thiogalactopyranoside
LDA,	Lithium diisopropylamide
NADH,	Nicotinamide adenine dinucleotide, reduced form
NAD^+	Nicotinamide adenine dinucleotide, oxydized form
NADPH,	Nicotinamide adenine dinucleotide phosphate, reduced form
$NADP^+$,	Nicotinamide adenine dinucleotide phosphate, oxidized form
PDB,	Protein Data Bank
SDS-PAGE,	Sodium dodecyl sulfate polyacrylamide gel electrophoresis
TB,	Terrific broth
TEA,	Triethylamine
TFA,	Trifluoroacetic acid
THF,	Tetrahydrofuran
TIM,	Triosephosphate isomerase
TLC,	Thin layer chromatography
Tris,	2-Amino-2-hydroxymethyl-propane-1,3-diol

CHAPTER 1. INTRODUCTION

1.1 DHDPS as a herbicidal and antibiotic target

Dihydrodipicolinate synthase (DHDPS) is an enzyme that catalyzes the first committed reaction of the lysine biosynthesis pathway in plants, bacteria, and some fungi, which is the condensation of pyruvate with (*S*)-aspartate-β-semialdehyde (ASA) to form (4*S*)-hydroxy-2,3,4,5-tetrahydro-(2*S*)-dipicolinic acid, which then spontaneously dehydrates to (*S*)-2,3-dihydropyridine-2,6-dicarboxylate (dihydrodipicolinate) (*1-4*). There has been ongoing interest in DHDPS since the 1960s, and most of the attention was focused on plant and some bacterial DHDPS. The plant enzyme allosterically regulates the production of lysine within cells, whereby the allosteric modulator of this enzyme is the final product of the biosynthetic pathway, L-lysine. Low micromolar IC_{50} values of lysine are typical for plant DHDPS (*5-7*). Removal of the mechanisms suppressing lysine production in crops would allow for agricultural products with higher lysine content and increased nutritional quality. On the other hand, the highly conserved sequence of plant DHDPS provides the possibility of designing non-selective herbicides targeting DHDPS. While some progress was achieved to engineer crops insensitive to lysine regulation by modification of the allosteric site of the enzyme, there are no compounds to date that are able to inactivate DHDPS and work as herbicides.

Bacterial DHDPS have less sequence identity than plant DHDPS. The importance of lysine feedback inhibition in bacteria remains unclear; IC_{50} values of lysine range from micromolar and millimolar level for some DHDPS from Gram-negative bacteria (*8-10*) to fully insensitive to lysine inhibition for some enzymes from Gram-positive bacteria (*11, 12*). The lysine biosynthesis pathway is essential for bacteria; it produces L-lysine for protein biosynthesis and *meso*-diaminopimelate, an essential component of bacterial cell walls (*13*). Bacterial strains with a deleted *dapA* gene (encoding DHDPS) are not viable and undergo lysis in the absence of *meso*-diaminopimelate in the medium (*14-16*). DHDPS has an additional significance for sporulating bacteria. The product of the reaction catalyzed by DHDPS, dihydrodipicolinate, is a precursor for dipicolinate which can comprise up to 15% of dry weight of bacterial spores (*17, 18*). Mutants

lacking DHDPS are not able to sporulate without supplementation of the cultures with dipicolinate (*18*). The absence of this lysine biosynthetic pathway in humans and its necessity for bacteria make DHDPS an attractive target for drug development (*19*).

1.2 Structure of DHDPS

1.2.1 Active site and proposed catalytic mechanism

DHDPS from many species exists as a homotetramer in solution (*7, 20-22*), however dimeric forms also occur (*23, 24*). The monomer has a TIM barrel fold, a common versatile fold observed in many enzymes (*25*), consisting of eight α-helices and eight parallel β-strands (*26*). The N-terminal domain of DHDPS forms an 8-fold α/β barrel structure connected to the α-helical C-terminal domain (*26*). The active site of the enzyme is at the C-terminal ends of the β-strands, where one of the loops forms a short helix with a highly conserved Arg138 (in *E. coli* DHDPS) whose side-chain is situated over the β-barrel. The active site of DHDPS consists of the key residue, lysine, which forms a Schiff base with the first substrate, pyruvate, and a catalytic triad, threonine and two tyrosines, which is proposed to act as a proton relay, transferring protons to and from the active site (*27*). One of the tyrosines in the catalytic triad belongs to a chain of the adjacent monomer (Figure 1.1). DHDPS from *E. coli* is a homotetramer, which consists of a pair of "tight dimers" (*28*). A number of crystal structures of DHDPS from different species are available in the Protein Data Bank (PDB).

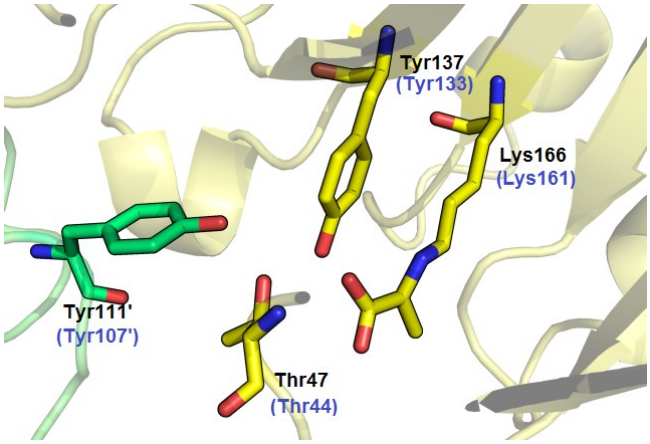

Figure 1.1 Active site of DHDPS. Crystal structure of *Campylobacter jejuni* DHDPS, PDB ID 3LER. *E. coli* numbering is shown in blue. K166 forms a Schiff base with pyruvate, while Y137, T47 and Y111' form the catalytic triad. Y111' belongs to the adjacent monomer (shown in green).

The proposed mechanism of DHDPS (Scheme 1.1) first involves binding of pyruvate in the active site and formation of a Schiff base with lysine, followed by deprotonation to the enamine. The second substrate, ASA, binds and reacts with the enamine, which then cyclizes into an unstable heterocyclic product, (4*S*)-4-hydroxy-2,3,4,5-tetrahydro-(2*S*)-dipicolinic acid (HTPA) (*27, 28*). HTPA can spontaneously dehydrate into dihydrodipicolinate or enter the next enzymatic step of the pathway, reduction (with dehydration), catalyzed by dihydrodipicolinate reductase (DHDPR) (*2*). Most of details of the proposed mechanism have not been determined experimentally. Involvement of specific residues in the mechanism has been inferred from protein crystallography (*1, 10*) and site-directed mutagenesis experiments (*27, 29*). Proton transfer from ASA to Gly186 is an alternative and arguably more likely mechanism.

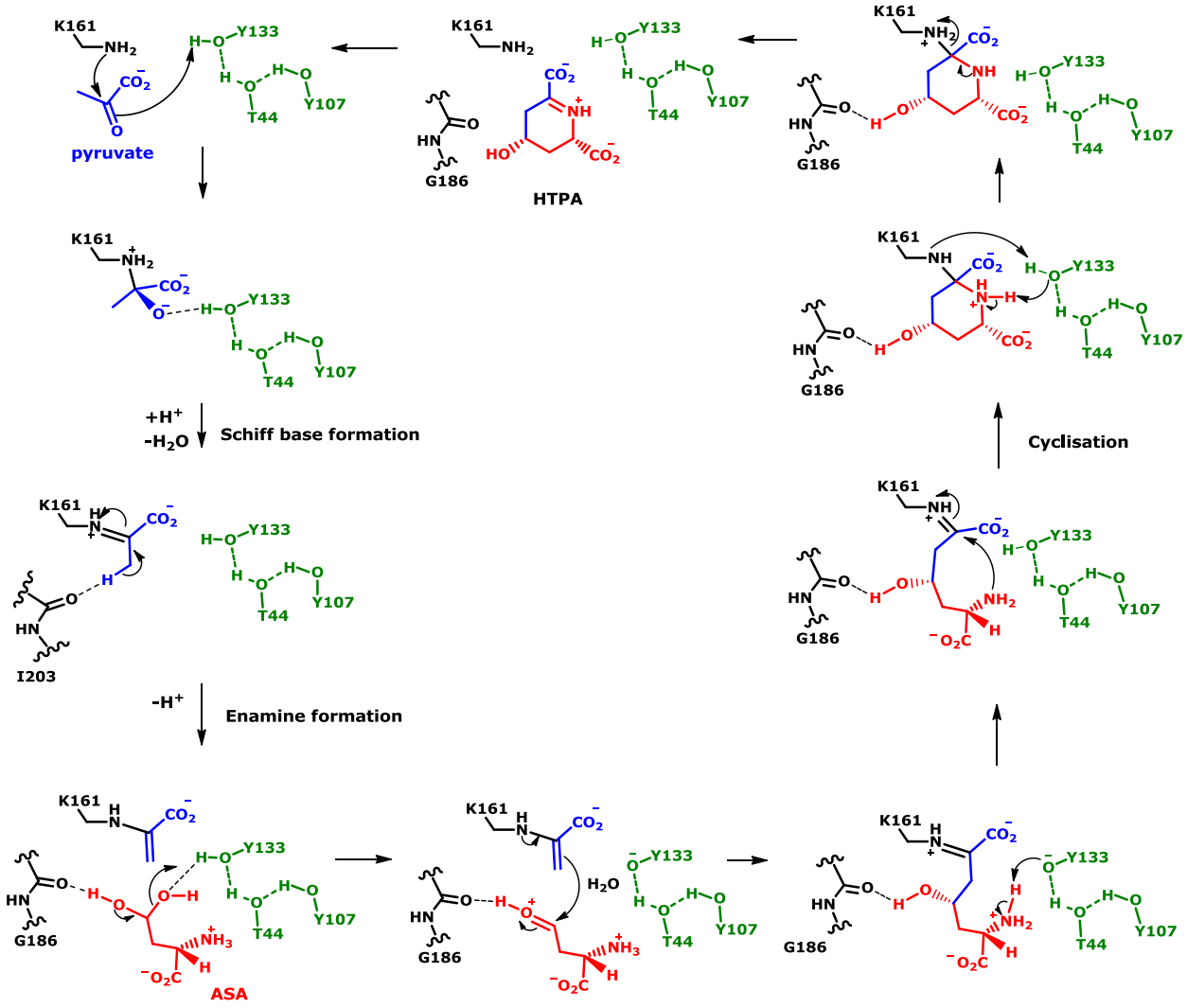

Scheme 1.1 Currently accepted mechanism of DHDPS from *E. coli* (*27, 28*).

1.2.2 Allosteric site and putative mechanisms of signal transduction

The allosteric site of DHDPS is located at the interface of the monomers forming each tight dimer in the tetramer. Lysine binding pockets are situated side by side on each monomer, forming a large regulatory site, where amino acid residues of both adjacent monomers are involved in binding of each molecule of lysine. The crystal structures of DHDPS with lysine bound at the allosteric site have been obtained for several species (*Arabidopsis thaliana, C. jejuni, E. coli*, *Pseudomonas aeruginosa*, *Vitis vinifera*,), and residues responsible for lysine

coordination are known for these DHDPS (*8, 22, 28, 30, 31*). The allosteric site of *C. jejuni* DHDPS is shown in Figure 1.2. Each molecule of lysine makes hydrogen bonds with Ser51, Ala52, Leu54, His59, Tyr110, Asn84', and Glu88', while His56 forms a cation π-interaction with the ε-amino group of lysine (the amino acid residues indicated with a prime belong to the adjacent monomer). The most conserved residues in the allosteric site of all DHDPS are Tyr110 and Asn84'. Despite the sequence divergence among bacterial DHDPS, including allosteric site residues, the architecture of allosteric sites of DHDPS from different species is very similar.

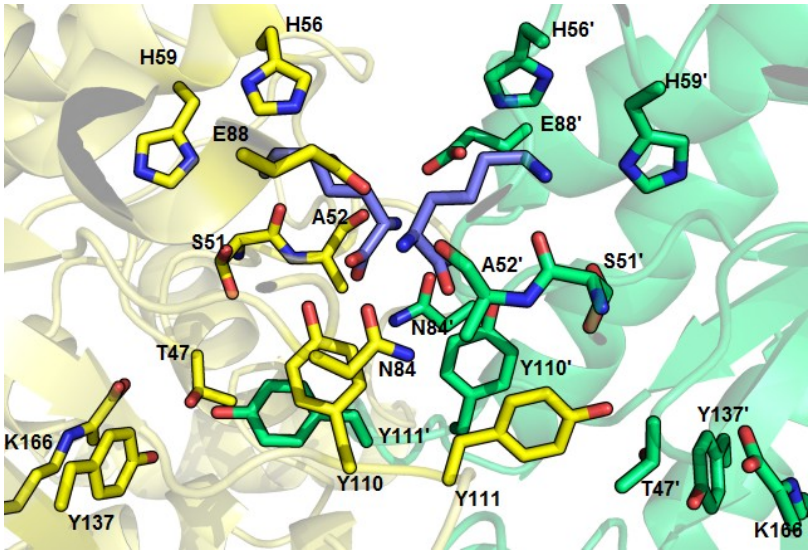

Figure 1.2 The allosteric site of DHDPS from *C. jejuni* (4M19). The residues of monomers A and B are shown in yellow and green, respectively. The active site residues Y111', T47, Y137 and K166 as a Schiff base are also shown for each monomer.

The exact mechanism of signal transduction from allosteric site to active site is not yet completely understood, although available crystal structures and molecular dynamics simulations allow us to propose a mechanism of allosteric regulation. The carboxylic group of the allosteric lysine creates a hydrogen bond with the phenolic OH of Tyr110, altering its position. This Tyr110 movement promotes a shift of Tyr111, which is a residue of the catalytic triad, and therefore its displacement causes a reduction in catalytic effectiveness within the active site. Furthermore, according to Atkinson *et al.* (who studied *V. vinifera* DHDPS), Tyr131 (equivalent of Tyr110 in *C. jejuni*) forms a hydrophobic stack with the catalytic triad residue Tyr132' (Tyr111' in *C. jejuni*) (*22*). This stack is disrupted upon lysine binding, displacing the hydroxyl

group of Tyr132' (Tyr111' in *C. jejuni*) and slowing down or discontinuing function of the catalytic triad.

1.3 Feedback inhibition of DHDPS by lysine in bacteria and plants

1.3.1 Kinetic models of lysine inhibition

Most DHDPS display partial lysine inhibition (*32*), meaning residual activity remains at saturating concentrations of lysine, although there are a few examples of plant DHDPS where full lysine inhibition was observed (*33*). The mechanism of lysine inhibition remains controversial, due to the contradictory nature of reported inhibition results. Various research groups have reported different mechanisms of lysine inhibition, for instance: it is a competitive inhibitor with respect to ASA and a noncompetitive inhibitor with respect to pyruvate (*5*); it is a competitive inhibitor versus pyruvate and mixed inhibitor with respect to ASA (*7*); it follows an uncompetitive partial mechanism with respect to pyruvate at pH 8 and mixed partial model of inhibition at low pH (*34*); it is a mixed partial inhibitor with respect to pyruvate and noncompetitive partial inhibitor with respect to ASA (*10, 22*), etc. Moreover, despite the known fact that lysine binds cooperatively to DHDPS (*5, 6, 22, 34-36*), cooperativity coefficients have not been taken into account while fitting kinetic models to experimental data, until the recent report of Atkinson *et al.* (*22*) and this present work (*8*).

1.3.2 DHDPS lacking lysine inhibition

All known plant DHDPS are sensitive to lysine inhibition, and this it is one of the reasons why unmodified crops do not accumulate lysine. To improve the nutritional value of crops, a number of research groups are working on the problem of increasing the lysine content in crops. A number of crops were genetically engineered to increase lysine levels by expressing bacterial DHDPS (lysine-insensitive or reduced lysine sensitivity). For some crops, the desired result has been achieved (*37, 38*), while other transgenic plants do not accumulate lysine in high concentrations, which is likely due to the existence of downregulation mechanisms of utilizing excess of lysine (*39*).

Certain mutations in the allosteric site can make DHDPS less sensitive or insensitive to lysine inhibition. For example, substitution of Trp53 (His53 in *E. coli*, His56 in *C. jejuni*) with Arg makes *A. thaliana* totally insensitive to lysine feedback inhibition (*33*). Mutations S157N,

E162K, A166T and A166V in *Zea mays* DHDPS (A79, E84 and L88, respectively, in *E. coli*) also make this enzyme insensitive to lysine (*40*). Maize cells transformed with a plasmid bearing the A166V mutated DHDPS maize gene resulted in increased lysine accumulation in this crop (*41*).

DHDPS from Gram-positive bacteria are weakly inhibited or insensitive to lysine. The reason for this is in variations in the allosteric site sequence, whereby the amino acid composition is unfavorable for lysine binding. For instance, Lys or Arg in position 56 creates a clash of positive charges with the side chain of the allosteric lysine, therefore preventing binding. DHDPS from Gram-positive *Corynebacterium glutamicum* has Lys in position 56, and is insensitive to lysine feedback inhibition, making this organism useful for industrial production of L-lysine (*42*). *Staphylococcus aureus*, known for its resistant strains to front-line antibiotics, contains dimeric DHDPS (*24*). This enzyme has Lys in positions 56 and 84, which makes the allosteric site shallow and changes the charge distribution in the binding pockets, and, as a result, this enzyme is insensitive to lysine inhibition (*24*). The design of inhibitors targeting the allosteric site of Gram-positive lysine-insensitive DHDPS seems to be an especially challenging task.

1.4 Inhibitors of DHDPS targeting the active site and the allosteric site

Most research groups working on inhibitors of DHDPS focus their attention on the active site. There are a few weak inhibitors that have been shown to be competitive with respect to ASA, such as succinate β-semialdehyde (*1*), and with respect to pyruvate, such as 2-ketobutyrate, 2-ketovalerate, 3-fluoropyruvate and glyoxalate (*34*). Several inhibitors of DHDPS are shown in Figure 1.3 and given in Table 1.1. Product mimics such as dipicolinic **1.1** and chelidamic **1.3** acids are weak millimolar inhibitors (*34, 43*). Interestingly, inhibition of growth of the late blight fungus *Phytophthora infestans* by millimolar concentrations of dipicolinic and chelidonic acids **1.1** and **1.2** was observed *in vivo* using infected potato leaf discs (*44*). Moderate inhibition of *E. coli* growth was observed for the piperidine diester **1.4** and chelidamic **1.3** acid at 20 mM (*45*). 2-Ketopimelic acid was found to be a weak irreversible inhibitor (*1*), and based on this observation, several compounds mimicking the acyclic enzyme-bound condensation product of ASA and pyruvate have been proposed (*46*). Two of them, bis(keto-acid) **1.5** and bis(oxime-ester) **1.6**, showed higher potency and the constrained acyclic-intermediate model was selected as a potential inhibitor lead (*46*). The continuation of that work was synthesis of phenolic

ketoacid derivatives **1.9** and **1.10**, which condense with the enzyme in a time-dependent manner (*47*). Analogs of 4-oxo-heptenedioic acid **1.7** and **1.8** proved to be irreversible millimolar inhibitors of DHDPS (*48*).

A number of millimolar inhibitors targeting the allosteric site of the enzyme have also been reported. Among them are homoserine lactone, 2-aminocyclopentanone, (*S*)-glutamic acid, (*S*)-aspartic acid (*49*), and *S*-(2-aminoethyl)-L-cysteine (thialysine), a sulfur-containing lysine mimic. Interestingly, despite a high structural similarity to L-lysine, thialysine binds ten times weaker to *E. coli* DHDPS than lysine (*34*).

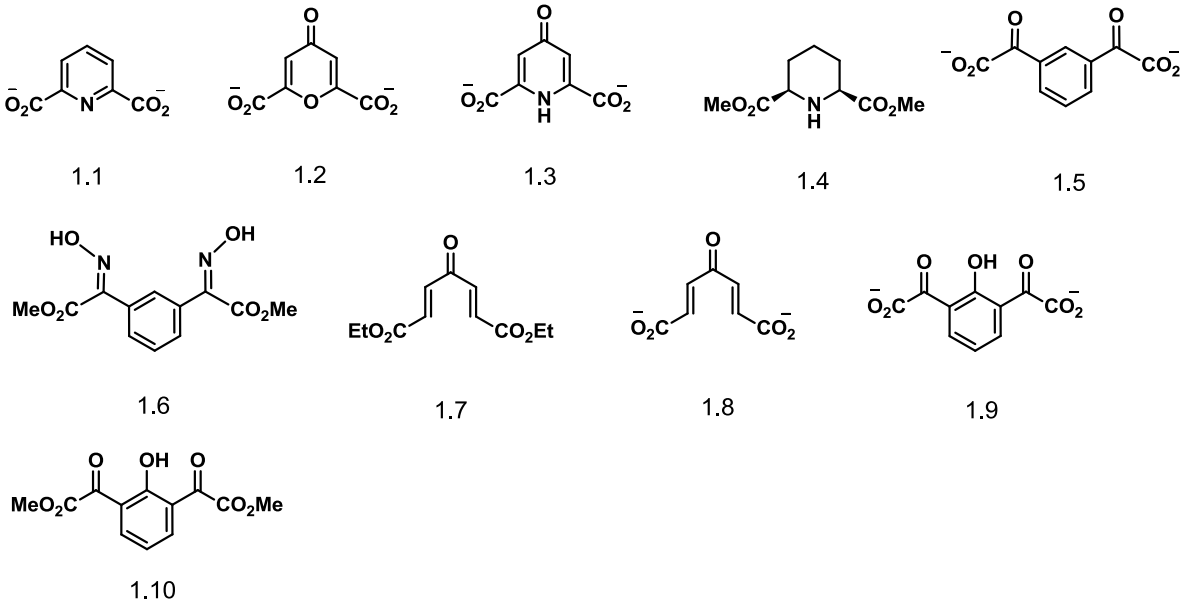

Figure 1.3 Inhibitors targeting the active site of DHDPS.

Table 1.1 Inhibitors targeting the active site of DHDPS.

Compound	Inhibition parameter	Organism	Reference
1.1	K_i 11 mM wrt pyr; 18 mM wrt ASA	*E. coli*	(*34, 43*)
	1 mM decrease activity by 75%	*P. infestans*	(*44*)
1.2	1 mM decrease activity by 54%	*P. infestans*	(*44*)
1.3	IC_{50} 22 mM	*E. coli*	(*43*)
1.4	IC_{50} 20 mM	*E. coli*	(*43*)
1.5	K_i^{app} 2.96 mM	*E. coli*	(*46*)
1.6	K_i^{app} 0.33 mM	*E. coli*	(*46*)
1.7	K_i^{app} 4.95 mM	*E. coli*	(*48*)
1.8	K_i^{app} 1.63 mM	*E. coli*	(*48*)
1.9	K_i^{app} 11.8 mM	*E. coli*	(*47*)
1.10	K_i^{app} 12.0 mM	*E. coli*	(*47*)

1.5 Proposal and research objectives

The main goal of this research is to find a potent inhibitor of DHDPS targeting the allosteric site. The attention of most research groups studying DHDPS is focused on inhibitors binding at the active site, and, aside from random inhibitor screening, no attempts have been made to develop an inhibitor to specifically target the allosteric site. The allosteric site was chosen as a target because noncompetitive inhibitors cannot compete with the substrates as competitive inhibitors do, so pyruvate and ASA inside the cell would not interfere with allosteric inhibitors. Until now there have been no known noncompetitive inhibitors stronger than the natural inhibitor L-lysine, and part of this project is to determine if it is possible to find a better inhibitor than L-lysine. Given the architecture of the allosteric site, it is possible for one molecule of inhibitor to fill two lysine binding pockets at the interface of adjacent monomers in the enzyme, so that only two inhibitor molecules would bind to the tetrameric enzyme. This strategy would decrease the entropy of binding of the inhibitor and increase the change of entropy of the system, which can lead to an overall decrease in free energy of the system (Equation 1.1).

$$\Delta G = \Delta H - T\Delta S \tag{1.1}$$

Phenix and Palmer (*36*) studied the binding of lysine to DHDPS from *Sinorhizobium meliloti* using ITC, and they concluded that lysine binds to the enzyme in a highly cooperative manner, where the first molecule of lysine binds loosely and the second one binds so tightly, that binding would be nearly simultaneous. The core of this proposal is that a molecule mimicking binding of two lysines will have higher affinity to the enzyme and will be a more potent inhibitor than lysine. The crystal structure of *E. coli* DHDPS (1YXD) with two lysines bound at the allosteric site provides a distance of 4.1 Å between the α-carbons of the two lysines. A two-carbon bridge would perfectly fit the space between the α-carbons, resulting in a structure of "*R,R*-bislysine" shown in Figure 1.4.

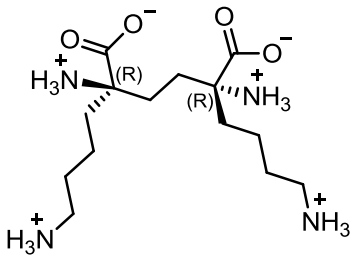

Figure 1.4 Structure of *R,R*-bislysine.

Here, we use DHDPS from *Campylobacter jejuni* as a model enzyme for assaying inhibitors. *C. jejuni* is a Gram-negative pathogen causing mostly gastroenteritis in humans, although more severe symptoms can also occur (*50, 51*). DHDPS from *C. jejuni* shares 37% sequence identity with *E. coli* DHDPS and two crystal structures are available in the Protein Data Bank (3LER and 3M5V).

The research objectives of this study are:

- Clone *dapA* and *dapB* genes from *C. jejuni* genomic DNA into the vector pQE-80L and transform *E. coli* XL1-Blue strain with this recombinant plasmid;
- Express and purify recombinant DHDPS and DHDPR;
- Kinetically evaluate DHDPS from *C. jejuni* using the coupled DHDPS-DHDPR assay;
- Determine the kinetic mechanism of lysine inhibition and calculate inhibition parameters;
- Synthesize *R,R*-bislysine and test its efficacy against *C. jejuni* DHDPS;
- Determine the kinetic mechanism of *R,R*-bislysine inhibition and calculate inhibition parameters;
- Perform site-directed mutagenesis on selected residues in the allosteric site to correlate structural changes of the protein with changes in binding affinity of the enzyme for the noncompetitive inhibitors;
- Examine the effectiveness of using the allosteric site of DHDPS as a target for development of new noncompetitive inhibitors.

1.6 Contributions of the author to the work presented in this thesis

Description of candidate's contribution to the manuscript (Chapter 2)

CHAPTER 2. Dihydrodipicolinate synthase from *Campylobacter jejuni*: Kinetic mechanism of cooperative Allosteric Inhibition and Inhibitor-Induced Substrate Cooperativity.

This chapter is an exact copy of a paper published in *Biochemistry*. Reprinted with permission from: Skovpen, Y. V., and Palmer, D. R. (2013) Dihydrodipicolinate synthase from *Campylobacter jejuni*: kinetic mechanism of cooperative allosteric inhibition and inhibitor-induced substrate cooperativity, *Biochemistry 52*, 5454-5462. Copyright (2013) American Chemical Society.

For this contribution, I performed all the experimental work: cloning of the genes, expression and purification of the proteins, synthesis of (*S*)-aspartate-*β*-semialdehyde and all kinetic experiments. I performed data analysis, results interpretation and wrote the initial draft of the work. Dr. David Palmer provided extensive guidance throughout the experimental work, supervised results interpretation, and was greatly involved in writing and editing the paper.

Description of candidate's contribution to the thesis (except Chapter 2)

In the rest of the thesis, all experimental work was performed by the candidate except:

- DHDPS mutant Y110F was generated by Shuo Li;
- preliminary kinetic experiments with H56A and H56N were performed by Shuo Li;
- crystal structures of *C. jejuni* DHDPS referred to throughout the text were generated by Cuylar Conly, supervised by Dr. David Sanders.

All experiments described in this thesis were part of the thesis work.

The co-author of the manuscript constituting Chapter 2, Dr. David Palmer, agrees that his contributions be included in this thesis, and with the description of his contributions. Other work referred to in the thesis performed by Shuo Li and Cuylar Conly is done so with their permission, and with that of their supervisors, Professor David Palmer and Professor David Sanders.

1.7 References

1. Blickling, S., Renner, C., Laber, B., Pohlenz, H. D., Holak, T. A., and Huber, R. (1997) Reaction mechanism of *Escherichia coli* dihydrodipicolinate synthase investigated by X-ray crystallography and NMR spectroscopy, *Biochemistry 36*, 24-33.
2. Devenish, S. R., Blunt, J. W., and Gerrard, J. A. (2010) NMR studies uncover alternate substrates for dihydrodipicolinate synthase and suggest that dihydrodipicolinate reductase is also a dehydratase, *J Med Chem 53*, 4808-4812.
3. Yugari, Y., and Gilvarg, C. (1965) The condensation step in diaminopimelate synthesis, *J Biol Chem 240*, 4710-4716.
4. Borthwick, E. B., Connell, S. J., Tudor, D. W., Robins, D. J., Shneier, A., Abell, C., and Coggins, J. R. (1995) *Escherichia coli* dihydrodipicolinate synthase: characterization of the imine intermediate and the product of bromopyruvate treatment by electrospray mass spectrometry, *Biochem J 305 (Pt 2)*, 521-524.
5. Kumpaisal, R., Hashimoto, T., and Yamada, Y. (1987) Purification and characterization of dihydrodipicolinate synthase from wheat suspension cultures, *Plant Physiol 85*, 145-151.
6. Dereppe, C., Bold, G., Ghisalba, O., Ebert, E., and Schar, H. P. (1992) Purification and characterization of dihydrodipicolinate synthase from pea, *Plant Physiol 98*, 813-821.
7. Frisch, D. A., Gengenbach, B. G., Tommey, A. M., Sellner, J. M., Somers, D. A., and Myers, D. E. (1991) Isolation and characterization of dihydrodipicolinate synthase from maize, *Plant Physiol 96*, 444-452.
8. Skovpen, Y. V., and Palmer, D. R. (2013) Dihydrodipicolinate synthase from *Campylobacter jejuni*: kinetic mechanism of cooperative allosteric inhibition and inhibitor-induced substrate cooperativity, *Biochemistry 52*, 5454-5462.
9. Devenish, S. R., Huisman, F. H., Parker, E. J., Hadfield, A. T., and Gerrard, J. A. (2009) Cloning and characterisation of dihydrodipicolinate synthase from the pathogen *Neisseria meningitidis*, *Biochim Biophys Acta 1794*, 1168-1174.
10. Dobson, R. C., Griffin, M. D., Roberts, S. J., and Gerrard, J. A. (2004) Dihydrodipicolinate synthase (DHDPS) from *Escherichia coli* displays partial mixed inhibition with respect to its first substrate, pyruvate, *Biochimie 86*, 311-315.
11. Domigan, L. J., Scally, S. W., Fogg, M. J., Hutton, C. A., Perugini, M. A., Dobson, R. C., Muscroft-Taylor, A. C., Gerrard, J. A., and Devenish, S. R. (2009) Characterisation of dihydrodipicolinate synthase (DHDPS) from *Bacillus anthracis*, *Biochim Biophys Acta 1794*, 1510-1516.
12. Rice, E. A., Bannon, G. A., Glenn, K. C., Jeong, S. S., Sturman, E. J., and Rydel, T. J. (2008) Characterization and crystal structure of lysine insensitive *Corynebacterium glutamicum* dihydrodipicolinate synthase (cDHDPS) protein, *Arch Biochem Biophys 480*, 111-121.
13. Bugg, T. D., and Walsh, C. T. (1992) Intracellular steps of bacterial cell wall peptidoglycan biosynthesis: enzymology, antibiotics, and antibiotic resistance, *Nat Prod Rep 9*, 199-215.
14. Yeh, P., Sicard, A. M., and Sinskey, A. J. (1988) General organization of the genes specifically involved in the diaminopimelate-lysine biosynthetic pathway of *Corynebacterium glutamicum*, *Mol Gen Genet 212*, 105-111.
15. Neidhardt, F. C., and Curtiss, R. (1996) *Escherichia coli and Salmonella: cellular and molecular biology*, 2nd ed., ASM Press, Washington, D.C.
16. Bukhari, A. I., and Taylor, A. L. (1971) Genetic analysis of diaminopimelic acid- and lysine-requiring mutants of *Escherichia coli*, *J Bacteriol 105*, 844-854.
17. Hoganson, D. A., and Stahly, D. P. (1975) Regulation of dihydrodipicolinate synthase during growth and sporulation of *Bacillus cereus*, *J Bacteriol 124*, 1344-1350.

18. Fukuda, A., and Gilvarg, C. (1968) The relationship of dipicolinate and lysine biosynthesis in *Bacillus megaterium*, *J Biol Chem 243*, 3871-3876.
19. Hutton, C. A., Southwood, T. J., and Turner, J. J. (2003) Inhibitors of lysine biosynthesis as antibacterial agents, *Mini Rev Med Chem 3*, 115-127.
20. Pearce, F. G., Perugini, M. A., McKerchar, H. J., and Gerrard, J. A. (2006) Dihydrodipicolinate synthase from *Thermotoga maritima*, *Biochem J 400*, 359-366.
21. Shedlarski, J. G., and Gilvarg, C. (1970) The pyruvate-aspartic semialdehyde condensing enzyme of *Escherichia coli*, *J Biol Chem 245*, 1362-1373.
22. Atkinson, S. C., Dogovski, C., Downton, M. T., Czabotar, P. E., Dobson, R. C., Gerrard, J. A., Wagner, J., and Perugini, M. A. (2013) Structural, kinetic and computational investigation of *Vitis vinifera* DHDPS reveals new insight into the mechanism of lysine-mediated allosteric inhibition, *Plant Mol Biol 81*, 431-446.
23. Burgess, B. R., Dobson, R. C., Bailey, M. F., Atkinson, S. C., Griffin, M. D., Jameson, G. B., Parker, M. W., Gerrard, J. A., and Perugini, M. A. (2008) Structure and evolution of a novel dimeric enzyme from a clinically important bacterial pathogen, *J Biol Chem 283*, 27598-27603.
24. Girish, T. S., Sharma, E., and Gopal, B. (2008) Structural and functional characterization of *Staphylococcus aureus* dihydrodipicolinate synthase, *FEBS Lett 582*, 2923-2930.
25. Wierenga, R. K. (2001) The TIM-barrel fold: a versatile framework for efficient enzymes, *FEBS Lett 492*, 193-198.
26. Mirwaldt, C., Korndorfer, I., and Huber, R. (1995) The crystal structure of dihydrodipicolinate synthase from *Escherichia coli* at 2.5 A resolution, *J Mol Biol 246*, 227-239.
27. Dobson, R. C., Valegard, K., and Gerrard, J. A. (2004) The crystal structure of three site-directed mutants of *Escherichia coli* dihydrodipicolinate synthase: further evidence for a catalytic triad, *J Mol Biol 338*, 329-339.
28. Dobson, R. C., Griffin, M. D., Jameson, G. B., and Gerrard, J. A. (2005) The crystal structures of native and (S)-lysine-bound dihydrodipicolinate synthase from *Escherichia coli* with improved resolution show new features of biological significance, *Acta Crystallogr D Biol Crystallogr 61*, 1116-1124.
29. Dobson, R. C., Devenish, S. R., Turner, L. A., Clifford, V. R., Pearce, F. G., Jameson, G. B., and Gerrard, J. A. (2005) Role of arginine 138 in the catalysis and regulation of *Escherichia coli* dihydrodipicolinate synthase, *Biochemistry 44*, 13007-13013.
30. Kaur, N., Gautam, A., Kumar, S., Singh, A., Singh, N., Sharma, S., Sharma, R., Tewari, R., and Singh, T. P. (2011) Biochemical studies and crystal structure determination of dihydrodipicolinate synthase from *Pseudomonas aeruginosa*, *Int J Biol Macromol 48*, 779-787.
31. Griffin, M. D., Billakanti, J. M., Wason, A., Keller, S., Mertens, H. D., Atkinson, S. C., Dobson, R. C., Perugini, M. A., Gerrard, J. A., and Pearce, F. G. (2012) Characterisation of the first enzymes committed to lysine biosynthesis in *Arabidopsis thaliana*, *PLoS One 7*, e40318.
32. Laber, B., Gomis-Ruth, F. X., Romao, M. J., and Huber, R. (1992) *Escherichia coli* dihydrodipicolinate synthase. Identification of the active site and crystallization, *Biochem J 288 (Pt 2)*, 691-695.
33. Vauterin, M., Frankard, V., and Jacobs, M. (2000) Functional rescue of a bacterial dapA auxotroph with a plant cDNA library selects for mutant clones encoding a feedback-insensitive dihydrodipicolinate synthase, *Plant J 21*, 239-248.
34. Karsten, W. E. (1997) Dihydrodipicolinate synthase from *Escherichia coli*: pH dependent changes in the kinetic mechanism and kinetic mechanism of allosteric inhibition by L-lysine, *Biochemistry 36*, 1730-1739.
35. Muscroft-Taylor, A. C., Soares da Costa, T. P., and Gerrard, J. A. (2010) New insights into the mechanism of dihydrodipicolinate synthase using isothermal titration calorimetry, *Biochimie 92*, 254-262.

36. Phenix, C. P., and Palmer, D. R. (2008) Isothermal titration microcalorimetry reveals the cooperative and noncompetitive nature of inhibition of *Sinorhizobium meliloti* L5-30 dihydrodipicolinate synthase by (S)-lysine, *Biochemistry 47*, 7779-7781.
37. Falco, S. C., Guida, T., Locke, M., Mauvais, J., Sanders, C., Ward, R. T., and Webber, P. (1995) Transgenic canola and soybean seeds with increased lysine, *Biotechnology (N Y) 13*, 577-582.
38. Ohnoutkova, L., Zitka, O., Mrizova, K., Vaskova, J., Galuszka, P., Cernei, N., Smedley, M. A., Harwood, W. A., Adam, V., and Kizek, R. (2012) Electrophoretic and chromatographic evaluation of transgenic barley expressing a bacterial dihydrodipicolinate synthase, *Electrophoresis 33*, 2365-2373.
39. Long, X., Liu, Q., Chan, M., Wang, Q., and Sun, S. S. (2013) Metabolic engineering and profiling of rice with increased lysine, *Plant Biotechnol J 11*, 490-501.
40. Shaver, J. M., Bittel, D. C., Sellner, J. M., Frisch, D. A., Somers, D. A., and Gengenbach, B. G. (1996) Single-amino acid substitutions eliminate lysine inhibition of maize dihydrodipicolinate synthase, *Proc Natl Acad Sci U S A 93*, 1962-1966.
41. Bittel, D. C., Shaver, J. M., Somers, D. A., and Gengenbach, B. G. (1996) Lysine accumulation in maize cell cultures transformed with a lysine-insensitive form of maize dihydrodipicolinate synthase, *Theoretical and Applied Genetics 92*, 70-77.
42. Sahm, H., Eggeling, L., Eikmanns, B., and Kramer, R. (1995) Metabolic design in amino-acid producing bacterium *Corinebacterium glutamicum*, *Fems Microbiology Reviews 16*, 243-252.
43. Turner, J. J., Gerrard, J. A., and Hutton, C. A. (2005) Heterocyclic inhibitors of dihydrodipicolinate synthase are not competitive, *Bioorg Med Chem 13*, 2133-2140.
44. Walters, D. R., McPherson, A., and Robins, D. J. (1997) Inhibition of lysine biosynthesis in *Phytophthora infestans*, *Mycological Research 101*, 329-333.
45. Mitsakos, V., Dobson, R. C., Pearce, F. G., Devenish, S. R., Evans, G. L., Burgess, B. R., Perugini, M. A., Gerrard, J. A., and Hutton, C. A. (2008) Inhibiting dihydrodipicolinate synthase across species: towards specificity for pathogens?, *Bioorg Med Chem Lett 18*, 842-844.
46. Boughton, B. A., Dobson, R. C., Gerrard, J. A., and Hutton, C. A. (2008) Conformationally constrained diketopimelic acid analogues as inhibitors of dihydrodipicolinate synthase, *Bioorganic & Medicinal Chemistry Letters 18*, 460-463.
47. Boughton, B. A., Hor, L., Gerrard, J. A., and Hutton, C. A. (2012) 1,3-Phenylene bis(ketoacid) derivatives as inhibitors of *Escherichia coli* dihydrodipicolinate synthase, *Bioorg Med Chem 20*, 2419-2426.
48. Boughton, B. A., Griffin, M. D., O'Donnell, P. A., Dobson, R. C., Perugini, M. A., Gerrard, J. A., and Hutton, C. A. (2008) Irreversible inhibition of dihydrodipicolinate synthase by 4-oxo-heptenedioic acid analogues, *Bioorg Med Chem 16*, 9975-9983.
49. Coulter, C. V., Gerrard, J. A., Kraunsoe, J. A. E., and Pratt, A. J. (1999) *Escherichia coli* dihydrodipicolinate synthase and dihydrodipicolinate reductase: kinetic and inhibition studies of two putative herbicide targets, *Pesticide Science 55*, 887-895.
50. Hughes, R. (2004) *Campylobacter jejuni* in Guillain-Barre syndrome, *Lancet Neurol 3*, 644.
51. Young, K. T., Davis, L. M., and Dirita, V. J. (2007) *Campylobacter jejuni*: molecular biology and pathogenesis, *Nat Rev Microbiol 5*, 665-679.

CHAPTER 2. DIHYDRODIPICOLINATE SYNTHASE FROM *CAMPYLOBACTER JEJUNI*: KINETIC MECHANISM OF COOPERATIVE ALLOSTERIC INHIBITION AND INHIBITOR-INDUCED SUBSTRATE COOPERATIVITY

2.1 Permission to use this manuscript

Skovpen, Y. V., and Palmer, D. R. (2013) Dihydrodipicolinate synthase from *Campylobacter jejuni*: kinetic mechanism of cooperative allosteric inhibition and inhibitor-induced substrate cooperativity, *Biochemistry 52*, 5454-5462.

This work fits naturally as a separate chapter prior to the remaining chapters of the thesis on novel inhibitor design, synthesis, and evaluation (Chapter 3); and on the generation, characterization, and inhibition of site-directed mutants (Chapter 4). A final chapter giving a discussion, conclusions, and future directions of the sum of the work will also be included.

2.2 Abstract

Dihydrodipicolinate synthase (DHDPS), an enzyme of the *meso*-diaminopimelate pathway of lysine biosynthesis, is essential for bacterial growth and is considered a target for novel antibiotics. We have studied DHDPS from *Campylobacter jejuni* for the first time, determining the kinetic mechanism of catalysis and inhibition with its natural allosteric feedback inhibitor, (*S*)-lysine. The tetrameric enzyme is known to have two allosteric sites, each of which binds two molecules of lysine. The results suggest that lysine binds highly cooperatively, and primarily to the F form of the enzyme during the ping-pong mechanism. By applying graphical methods and nonlinear regression, we have discriminated between the possible kinetic models and determined the kinetic and inhibition constants and Hill coefficients. We conclude that (*S*)-lysine is an uncompetitive partial inhibitor with respect to its first substrate, pyruvate, and a mixed partial inhibitor with respect to its second substrate, (*S*)-aspartate-*β*-semialdehyde (ASA), which differs from the kinetic models for inhibition reported for DHDPS from other sources. The Hill coefficients for the binding of lysine to different forms of the enzyme are all greater than 2, suggesting that the two allosteric sites are not independent. It has been found that ASA binds cooperatively in the presence of (*S*)-lysine and the cooperativity of binding increases at near-K_M concentrations of pyruvate. The incorporation of Hill coefficients into the kinetic equations was crucial for determining the kinetic model for this enzyme.

2.3 Introduction

Dihydrodipicolinate synthase (DHDPS, E.C. 4.2.1.52) is an allosterically regulated enzyme of the bacterial *meso*-diaminopimelate pathway, responsible for condensation of (*S*)-aspartate-*β*-semialdehyde (ASA) and pyruvate into an unstable heterocyclic product (4*S*)-hydroxy-2,3,4,5-tetrahydro-(2*S*)-dipicolinic acid (*1, 2*), which spontaneously dehydrates to (*S*)-2,3-dihydropyridine-2,6-dicarboxylate (dihydrodipicolinate) (*2-4*) (Figure 2.1). The reaction has been shown to follow a ping-pong, or "substituted-enzyme" mechanism, whereby pyruvate condenses with an active site lysine residue of the native or "E" form of the enzyme. This substituted or "F" form binds ASA and a new carbon-carbon bond is formed via an aldol reaction. The ligated intermediate then cyclizes by transimination and is released from the active site.

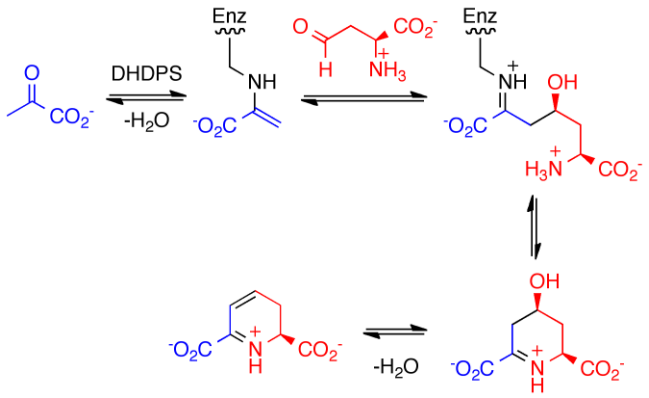

Figure 2.1 Reaction catalyzed by DHDPS. In the case of *C. jejuni* DHDPS, the active-site lysine residue is Lys166.

DHDPS is an attractive antibiotic target because (*S*)-lysine and *meso*-diaminopimelic acid are cross-linking components between peptidoglycan heteropolysaccharide chains in bacterial cell walls (*5, 6*). The activity of DHDPS can be affected by inhibitor molecules binding at the active or the allosteric site of the enzyme. A number of compounds targeting both active and allosteric sites have been proposed and described in the literature (*7-13*), but effective inhibitors of DHDPS have not yet been reported. In order to design an effective allosteric modulator of DHDPS, it is necessary to clarify the mechanism of allosteric interaction of DHDPS with its natural allosteric inhibitor (*S*)-lysine. There are several reports describing lysine inhibition of DHDPS isolated from different species, such as plants (*12, 14, 15*) and Gram-negative bacteria (*16, 17*), which are inhibited at very low concentrations of lysine, and Gram-positive bacteria

(*18-20*), which are weakly inhibited or insensitive to lysine. Despite this level of scrutiny, the kinetic mechanism of lysine inhibition is still not clear. Early papers using the wheat enzyme reported that lysine is a competitive inhibitor with respect to ASA and a noncompetitive inhibitor with respect to pyruvate (*12*). On the contrary, Frisch *et al.* reported that lysine is a competitive inhibitor versus pyruvate and mixed inhibitor with respect to ASA using the DHDPS from maize (*15*). Laber *et al*. described the mechanism of lysine inhibition of *E. coli* DHDPS as partial (*13*), which is in agreement with subsequent reports. Karsten (*21*), also working with the *E. coli* enzyme, determined that lysine binds to the F form of the enzyme at pH 8, suggesting an uncompetitive partial mechanism with respect to pyruvate. In the same article he showed that lysine can bind to the E form of the enzyme at low pH, which is an indication of a mixed model of inhibition. Over the last decade, research groups, particularly Gerrard and co-workers, have been describing the lysine inhibition mechanism as "partial mixed" with respect to pyruvate and "noncompetitive partial" with respect to ASA (*17*), except in the report of Soares da Costa *et al*. that defines the inhibition type as "partial uncompetitive" with respect to pyruvate (*22*). Atkinson *et al*. (*23*) also reports "mixed partial" and "noncompetitive partial" inhibition with respect to pyruvate and ASA respectively for the common grapevine DHDPS.

With the aid of isothermal titration calorimetry, it was shown that lysine binds cooperatively displaying a cooperative partial mixed model with respect to pyruvate for *E. coli* DHDPS (*24*), and lysine was also observed to bind to the E form of *S. meliloti* DHDPS (*25*). Importantly, the cooperative mode of lysine binding has been known as early as 1987 (*12*), but only a few authors reported cooperativity coefficient values (*12, 14, 21, 23*), and the cooperativity of binding is not accounted for in kinetic analyses. This may account for the variation in interpretation of kinetic data for DHDPS; although the determination of Hill coefficients and their incorporation into kinetic analyses makes the analysis more complex, it is likely an essential component for determining the best kinetic model of lysine inhibition. (As this manuscript was being prepared, Atkinson *et al*. (*23*) incorporated cooperativity coefficients for lysine binding derived from a nonlinear fit to kinetic models).

Here we report a kinetic analysis of the catalyzed reaction and its allosteric inhibition for the recombinant hexahistidine-tagged DHDPS from *Campylobacter jejuni*. *C. jejuni* is a Gram-negative pathogen that can cause gastroenteritis in humans, and can also lead to severe conditions such as Guillain-Barré syndrome, meningitis, and chronic colitis (*26, 27*). Sequence

alignment (*28, 29*) reveals that *C. jejuni* DHDPS shares 37% sequence identity with *E. coli* DHDPS. Kinetic parameters and lysine inhibition constants of *C. jejuni* DHDPS have not yet been reported, but X-ray crystal structures of *C. jejuni* DHDPS in the E form (RCSB Protein Data Bank ID 3M5V) and in the pyruvate-modified F form (PDB ID 3LER) have been deposited. These structures show conservation of the tertiary and quaternary structure: a $(\alpha/\beta)_8$ "TIM" barrel monomer forms a tetramer consisting of a loosely-associated dimer of more intimately connected dimers. Each "tight dimer" contains an allosteric regulatory site at the interface of the two monomers, and within these dimers each monomer contributes a tyrosine residue to the active site of the other. All active-site residues identified in DHDPS from other species are present in the *C. jejuni* DHDPS structure, as are the residues responsible for lysine binding at the allosteric site (*30*) which have been determined as a result of the crystal structure of *E. coli* DHDPS with bound lysine molecules (PDB ID 1YXD). As described herein, the surprisingly high affinity for lysine makes a thorough characterization of the cooperative allosteric inhibition of this enzyme an instructive model for discriminating between kinetic models for this and other complex enzymatic processes.

2.4 Materials and methods

2.4.1 ASA synthesis

ASA was synthesized according to the reported procedure (*31*). Due to the hygroscopic properties of ASA, the concentration of each newly prepared work solution of ASA was determined using the DHDPS-DHDPR coupled kinetic assay described below, in the presence of excess NADH.

2.4.2 Cloning of the *dapA* and *dapB* genes

C. jejuni genomic DNA was prepared by Dr. Bonnie Chaban, Western College of Veterinary Medicine, University of Saskatchewan. The *dapA* and *dapB* genes (encoding DHDPS and dihydrodipicolinate reductase (DHDPR) respectively) were PCR-amplified from genomic DNA using KAPA HiFi DNA polimerase (Kapa Biosystems) and forward and reverse primer pairs

5’-GAAAGGGGATCCATGGATAAAAATATTATCATTGGGGC -3’,

5’-ATTCTGCTGCAGTTAAAATCCTTTGATCTTATATTTTTTCATCACTTC-3’

respectively for *dapA*; 5’- TCAAGGGGATCCATGATTAAAATAGGAATTTATGGCG -3’,

5’-ACTGCACTGCAGTTAAATTCCTAAAAAATCATTGATTGAATAC-3’ respectively for *dapB*.

Each pair of genes was ligated into a pQE-80L vector (Qiagen) as *Bam*HI/*Pst*I restriction fragments using T4 DNA-ligase (New England BioLabs). Then *E. coli* XL1-Blue competent cells were transformed with the plasmids. Colonies containing correct recombinant plasmids were identified by analysis of restriction enzymes products, and positive candidates were sequenced by the DNA Technologies Unit of the National Research Council, Saskatoon, Canada.

2.4.3 Expression and purification of enzymes

TB media (*32*) (250 mL) containing ampicillin (50 μg/mL) was inoculated with a single colony of *E. coli* XL1-Blue cells containing recombinant plasmid pQE-80L with *dapA* or *dapB* genes, and incubated with shaking at 37 °C until cultures reached an OD_{600} of 0.5 - 0.6. Protein expression was induced by addition of isopropyl β-D-1-thiogalactopyranoside to a final concentration 0.5 mM. The cell culture was incubated with shaking (250 rpm) at 15 °C for 15 h, and then centrifuged at 5,180 × g for 30 min. The resulting cell pellet was resuspended in 10 ml of binding buffer (20 mM Tris-HCl, 5 mM imidazole, 500 mM NaCl, 12.5% glycerol, pH 7.9) and sonicated using a Virsonic 600 Ultrasonic Cell Disrupter (VirTis). The sample was chilled in an ice bath during all manipulations. The crude lysate was separated from cell debris by centrifugation at 27,000 × g for 30 min at 4 °C. The supernatant containing DHDPS or DHDPR was filtered through a 0.45 μm syringe filter and loaded onto a 1 ml HiTrap™ IMAC FF column (GE Healthcare), prepared according to the manufacture's procedure and equilibrated with 5 ml of binding buffer. The column was washed with 5 ml of binding buffer, a 1:1 mixture of binding and washing (20 mM Tris-HCl, 60 mM imidazole, 500 mM NaCl, 12.5% glycerol, pH 7.9) buffers, 10 ml washing buffer, a 1:1 mixture of binding and stripping (20 mM Tris-HCl, 500 mM NaCl, 100 mM EDTA, 12.5% glycerol, pH 7.9) buffers, then 15 ml of stripping buffer. Fractions were analyzed by SDS-PAGE, and those containing purified enzyme were pooled and dialyzed at 4 °C for 24 h in storage buffer (20 mM Tris-HCl, 100 mM NaCl, 1 mM DTT, 40% glycerol, pH 7.9). The resulting proteins were concentrated to 0.37 mg/ml for DHDPS and 1.43 mg/ml for DHDPR using an Amicon Ultra-15 Centrifugal Filter (30 kDa MWCO, EMD Millipore). Enzyme concentrations were determined by NanoDrop® ND-1000 using calculated parameters (ProtParam) (*33*) (molecular weight and extinction coefficient) for DHDPS (MW 34069 Da, ε_{280}

= 18068 $M^{-1}cm^{-1}$) and for DHDPR (MW 28094 Da, ε_{280} = 15930 $M^{-1}cm^{-1}$). The proteins were aliquoted and stored at -80 °C.

2.4.4 Enzyme assays

The activity of DHDPS was measured using a coupled assay (*3*). The initial velocity of the DHDPS enzymatic reaction was determined by monitoring the decrease in absorbance at 340 nm due to oxidation of NADH (ε_{340} = 6220 $M^{-1}cm^{-1}$). All kinetic measurements were performed on a Beckman DU640 spectrophotometer at 25 °C maintained by circulating water bath. Only freshly prepared solutions of substrates were used in the assay. All measurements were made using 100 mM HEPES buffer at pH 8.0. A typical assay contained 0.16 mM NADH, 0.37 μg of DHDPS, 7.15 μg DHDPR and varying concentrations of ASA (0.06 - 2.24 mM) and pyruvate (0.12 – 3.50 mM). The excess amount of DHDPR was determined experimentally, to ensure that the DHDPS-catalyzed reaction would be rate-limiting. A 0.01M solution of (*S*)-lysine was used in inhibition experiments. Cuvettes containing the assay mixture were incubated for three minutes to equilibrate at 25 ºC before the reaction was triggered by the addition of DHDPS. The obtained kinetic data were fitted to the rate equations 2.1 - 2.4 using SigmaPlot®10.0:

$$v = V_{\max} AB \big/ (K_{M(B)} A + K_{M(A)} B + AB) \tag{2.1}$$

$$\frac{v}{V_{\max}} = \frac{\frac{[S]^n}{K_s{}^n} + \frac{\beta[S]^n[I]^h}{(\alpha K_i)^h K_s{}^n}}{1 + \frac{[S]^n}{K_s{}^n} + \frac{[I]^{h'}}{K_i{}^{h'}} + \frac{[S]^n[I]^h}{(\alpha K_i)^h K_s{}^n}} \tag{2.2}$$

$$\frac{v}{V_{\max}} = \frac{\frac{[S]}{K_s} + \frac{\beta[S][I]^h}{K_s K_i{}^h}}{1 + \frac{[S]}{K_s} + \frac{[S][I]^h}{K_s K_i{}^h}} \tag{2.3}$$

$$\frac{v}{V_{\max}} = \frac{\frac{[S]^n}{K_s{}^n} + \frac{\beta[S]^n[I]^h}{K_s{}^n K_i{}^h}}{1 + \frac{[S]^n}{K_s{}^n} + \frac{[I]^h}{K_i{}^h} + \frac{[S]^n[I]^h}{K_s{}^n K_i{}^h}} \tag{2.4}$$

where V_{max} is the maximum velocity, $K_{M(A)}$ and $K_{M(B)}$ are the Michaelis-Menten constants for two substrates, A and B are the concentrations of the substrates, v is the initial velocity. K_i is the

inhibition constant, I is the inhibitor concentration, S is the substrate concentration, K_S is the dissociation constant of the ES complex, n is the Hill coefficient for ASA (when applicable), α and β are proportionality constants, and h and h' are Hill coefficients for lysine where, depending on the substrate being bound, h' and h are cooperativity coefficients for lysine binding to E and E:pyr or F and F:ASA forms of enzyme respectively in Equation 2.2. Equation 2.1 is a rate equation for the *ping-pong bi-bi mechanism*, Equations 2.2 - 2.4 describe *mixed partial*, *uncompetitive partial* and *noncompetitive partial* mechanisms of inhibition respectively, to which the Hill coefficients, h, h' and n, have been introduced. The experiments were conducted by varying concentration of one substrate while concentration of another was saturating or at near-K_M concentration.

Equation 2.5 is the Hill equation for partial inhibition,

$$\log \frac{v_i - v_{i(sat)}}{v_0 - v_i} = \log K - h \log I \tag{2.5}$$

where v_i is the velocity in the presence of the inhibitor, v_0 is the velocity in the absence of the inhibitor, $v_{i(sat)}$ is the reaction velocity at saturating concentrations of inhibitor, and K is an apparent overall dissociation constant. For reactions in which the second substrate was at near-K_M concentration, $v_{i(sat)}$ was measured at [I] = 1.0 mM; for reactions in which the second substrate was at saturating concentration, $v_{i(sat)}$ was measured at [I] = 2.0 mM.

2.5 Results

2.5.1 Ping-pong mechanism

The kinetic mechanism of catalysis by recombinant histidine-tagged DHDPS from *C. jejuni* was assessed using the DHDPR-coupled assay described above. Note that DHDPR is not selective, in that it can utilize both NADPH and NADH; the latter was used for kinetic studies of DHDPS. Variation of the concentrations of each substrate in the presence of DHDPS and DHDPR resulted in double-reciprocal plots displaying parallel lines, consistent with the canonical ping-pong kinetic mechanism observed for DHDPS from other sources. (Supporting information, Figure S2.1, Figure S2.2). The kinetic constants are shown in Table 2.1.

Substrate inhibition by ASA, which has been reported for DHDPS from some sources and/or with some ASA preparations (*17*), was not observed. The kinetic constants of *C. jejuni* DHDPS

at the chosen assay conditions (25 °C, pH 8.0, 100 mM HEPES) are close to those of *E. coli* DHDPS (*17, 34*). No evidence for significant cooperativity of substrate binding was observed.

Table 2.1 Kinetic constants for *C. jejuni* DHDPS

$K_{M(pyr)}$	$K_{M(ASA)}$	k_{cat}	$k_{cat}/K_{M(pyr)}$	$k_{cat}/K_{M(ASA)}$
0.35 ± 0.02 mM	0.16 ± 0.01 mM	76 ± 1 s^{-1}	(2.2 ± 0.1) × 10^5 $M^{-1}s^{-1}$	(4.8 ± 0.3) × 10^5 $M^{-1}s^{-1}$

2.5.2 Lysine inhibition

C. jejuni DHDPS is strongly inhibited by lysine. A simple observation of the dependence of rate on lysine concentration at fixed substrate concentrations indicates an apparent IC_{50} value near 65 μM. (Figure 2.2). DHDPS from Gram-negative bacteria can be weakly, moderately or strongly inhibited by lysine showing IC_{50} values from micromolar to millimolar range: 53 μM for *N. meningitidis* (*16*), 0.2 mM for *E. coli* (*35*), and 0.7 mM for *S. meliloti* (*36*). Figure 2.2 also reveals two other important features of inhibition. First, the shape of the curve indicates significant cooperativity of inhibition. Second, there is approximately 10% residual activity at saturating high concentrations of lysine under conditions employed. This partial inhibition (or "hyperbolic" inhibition) is also typical of DHDPS from other sources (*13, 16, 17*).

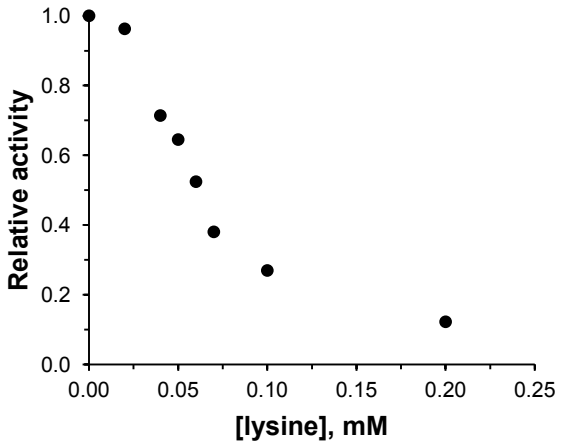

Figure 2.2 Lysine inhibition of DHDPS activity at 0.16 mM ASA and 3.5 mM pyruvate.

2.5.3 Calculation of cooperativity coefficient for lysine

A series of Hill plots were built over the range from 0.02 to 0.2 mM of lysine, where Hill plots have minimal deviation from linearity and cooperativity (slopes of Hill plots) can be considered constant. Experimentally-obtained Hill plots are normally not linear and their curvature indicates a mixture of positive and negative cooperativity (*37*). By analyzing the shape of Hill plots it is possible to estimate values of the four intrinsic association constants for the four binding steps of the ligand to the tetramer (*37*). When the concentration of inhibitor is low, the complexes with a low value of the Hill coefficient (*h*) do not contribute significantly to the initial velocity; on the other hand, at high concentrations of the inhibitor it becomes difficult to distinguish small changes in the velocity (*38*). Because the inhibition is partial, the logarithm of the ratio "inhibitable activity" in the presence and absence of lysine is plotted versus the logarithm of lysine concentration (Equation 2.5). Values of *h* are the slopes of the Hill plots. As seen in Figure 2.3, data collected at concentrations of lysine ≤0.1 mM give a straight line, but at higher concentrations the plot deviates from linearity as if values of *h* were approaching unity, i.e. cooperativity appears to dissipate at very high occupancy of the inhibitory sites. If this were the case, it would manifest itself in biphasic behavior evident from double-reciprocal plots over a wide range of concentrations of lysine.

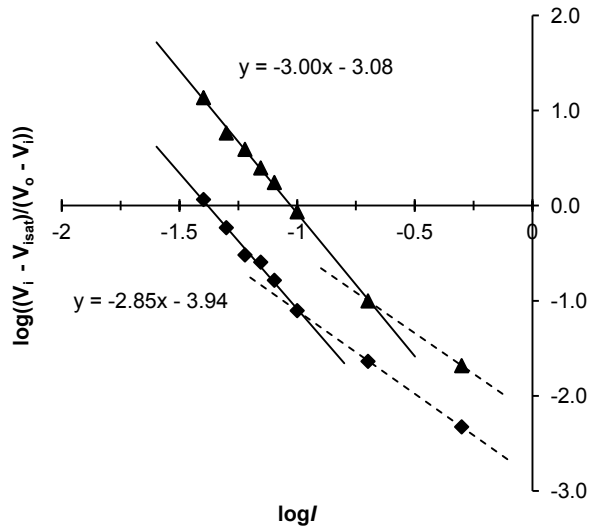

Figure 2.3 Relationship between degree of cooperativity and concentration of inhibitor. Solid line: linear area (lysine concentration 0.02 – 0.2 mM). Dashed line: apparent decrease in cooperativity at high lysine concentrations (≥ 0.2 mM). Data obtained at constant concentration of pyruvate 0.35 mM, 0.072 mM ASA (◆) and 2.0 mM ASA (▲).

Results of previous studies of DHDPS inhibition kinetics have differed in some details, but consistently have shown that the presence of pyruvate results in tighter binding of lysine to the allosteric site, suggesting that the condensation of pyruvate in the active site somehow alters the nature of the inhibitory site. Because of this, we felt that the degree of cooperativity of lysine binding need not be the same at all substrate concentrations. We therefore conducted experiments to determine cooperativity whilst varying the concentration of each substrate in the presence of both saturating and near-K_M concentrations of the other substrate (Supporting information, Figure S2.3, Figure S2.4, Figure S2.5, and Figure S2.6). When the concentration of either substrate was varied in the presence of saturating concentration of the other, the average of h was found to be 2.8 ± 0.2 for both cases. When ASA was maintained at near-K_M concentration (0.18 mM), the value of h averaged 3.0 ± 0.2, and when pyruvate was held at near-K_M concentration (0.35 mM), h = 2.3 ± 0.4. The difference in value at low concentration of pyruvate suggests that this substrate is affecting the cooperativity of lysine binding, and is consistent with a kinetic mechanism in which pyruvate binds to the enzyme before lysine does. Drawing conclusions about the kinetic mechanism based on Hill coefficients should be done with caution, however, due in part to experimental error inherent in the calculation of h.

2.5.4 Relationship of substrate and inhibitor binding

Using these Hill plots, we determined the IC_{50} of lysine under a range of conditions. From Equation 2.5, when $v_i = 0.5v_0$, the ordinate equals $\log((0.5v_0 - v_{i(sat)})/(v_0 - 0.5v_0))$ or, after rearranging, $\log(1 - (2v_{i(sat)}/v_0))$. The projection of the ordinate $\log(1 - (2v_{i(sat)}/v_0))$ from the Hill plot on the log*I* axis gives the IC_{50} value. As shown in Figure 2.4, IC_{50} values of lysine decrease with increasing pyruvate concentration up to a saturated value. Conversely, IC_{50} values increase with increasing concentration of ASA. This clearly shows that pyruvate *promotes* lysine binding while ASA *hinders* the binding of lysine.

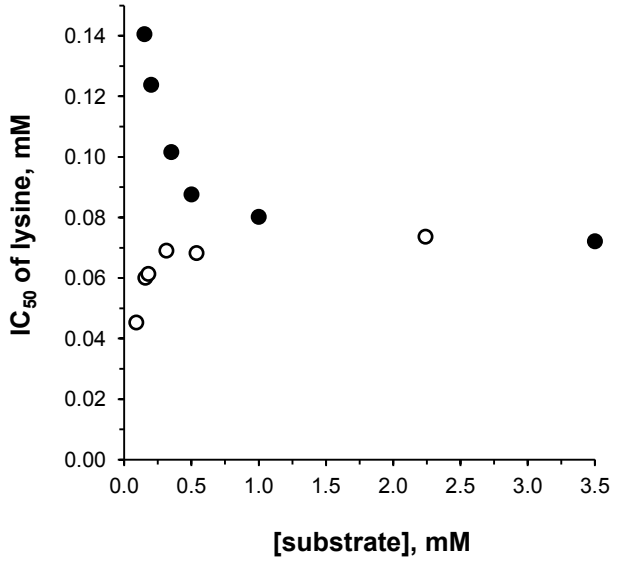

Figure 2.4 Relationship between IC_{50} of lysine and concentration substrates. (●) pyruvate is the variable substrate, concentration of ASA is 2.24 mM; (○) ASA is the variable substrate, concentration of pyruvate is 3.50 mM.

2.5.5 Analysis of Dixon and Cornish-Bowden plots

The Dixon plot (1/*v* versus *I*) and the Cornish-Bowden plot (S/*v* versus *I*) are very useful to distinguish between kinetic models of simple linear inhibition (*38, 39*), and when taken together they can provide distinctive patterns which can be attributed to a particular type of inhibition. When applying these methods to partial inhibition, a difficulty arises from the fact that the Cornish-Bowden plot and the Dixon plot are non-linear, but relatively straight plots can be obtained at concentrations of inhibitor preceding the saturation region. The effect of

cooperativity must be taken into account by raising the inhibitor concentration to the power of the Hill coefficient (*39*).

When the concentration of pyruvate was varied at constant [ASA], the plot S/v versus I^h produced a series of lines converging in the second quadrant of the Cartesian coordinate system, and the plot 1/v versus I^h yielded a series of near parallel lines (at high concentrations of lysine these lines eventually converge in the first quadrant of the coordinate system), indicative of *uncompetitive* inhibition (Supporting information, Figure S2.7 A,B). With respect to changing the concentration of ASA, the Cornish-Bowden plot produced a series of lines which cross just below the x-axis in the third quadrant, while the Dixon plot produced lines crossing in the second quadrant (Supporting information, Figure S2.8 A,B). This indicates *mixed* inhibition, with binding of lysine to the F form of the enzyme prevailing over binding to the F:ASA complex. Note for these graphs, the lines were fit independently, rather than trying to fit the data to a single model, to provide an unbiased view of the data. Given the apparent complexity of the inhibition, a global fit of the data is needed for an independent comparison to the diagnostic plots.

2.5.6 Fitting the inhibition models to observed data

A general scheme illustrating the lysine inhibition mechanism is shown in Scheme 2.1. For this model, we assumed that the formation of enzyme-pyruvate and modified enzyme-ASA complexes are reversible and rapid steps, and the breakdown of these complexes are slow, rate-limiting steps. Karsten (*21*) suggested that formation of the final product, i.e. reaction of the F form of the enzyme with the second substrate, ASA, is the rate-limiting step in the overall equilibria, therefore for this scheme $k_2 < k_1$, and our data are consistent with this. The lower part of the scheme illustrates partial inhibition, in which the enzyme-substrate-inhibitor complexes are able to convert the substrates into products at much lower rates compared to reaction rates in the absence of inhibitor ($\beta' < 1$, $\beta < 1$). Assuming that lysine can bind to each form of the enzyme, four K_i values can be determined, and based on the binding affinity of the inhibitor to a particular enzyme species, a decision about the mechanism of inhibition can be made. We have therefore used an unbiased approach and considered all applicable kinetic mechanisms of lysine inhibition with respect to each substrate.

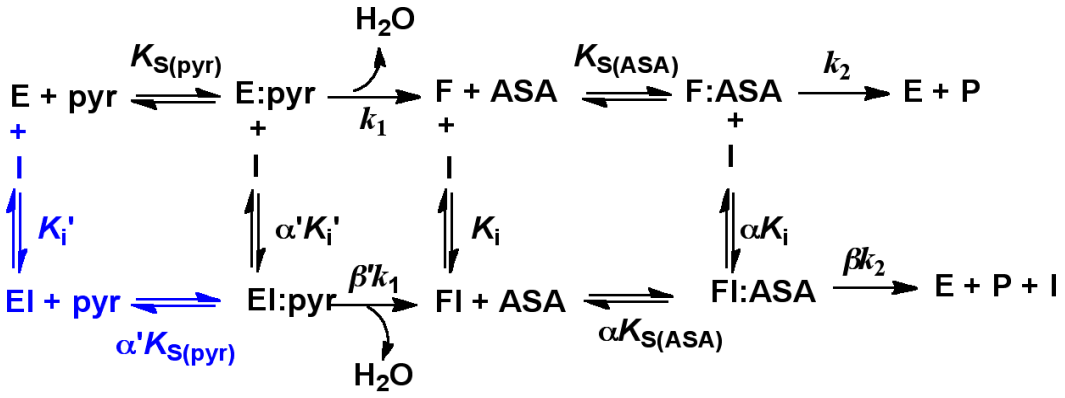

Scheme 2.1 General scheme of DHDPS lysine inhibition. The equilibria shown in blue are not observed for *C. jejuni* DHDPS. For this general scheme, there is no limit on the values of α (and α′), while β (and β′) must be < 1 for inhibition. In a purely noncompetitive partial inhibition mechanism, α and α′ = 1, whereas in a mixed partial inhibition mechanism, α and α′ > 1.

Since binding of lysine is a cooperative process, each rate equation was modified by raising the inhibitor concentration and the inhibition constants to the power of the Hill coefficient (Equations 2.2 – 2.4). Fitting of data was done using cooperativity coefficients as independent variables in the rate equations, and the resulting coefficients were compared with those found by the graphical method. Experimental data obtained by varying the concentration of pyruvate were fit using the mixed partial (hyperbolic) (Equation 2.2) and uncompetitive partial (Equation 2.3) models (Figure 2.5, Supporting information, Figure S2.9 - Figure S2.12). For the *mixed partial* model, the rate constant k_1 (Scheme 2.1) decreases (by the factor of β') and the binding affinity of lysine to the E:pyr complex increases (by α'), where $0 < \alpha' < 1$, $0 < \beta' < 1$. Two Hill coefficients, h and h', were introduced in to the rate equation to allow for different degrees of cooperativity of lysine binding to the E and E:pyr forms of the enzyme respectively. The cooperativity of pyruvate was equal to 1 (Figure S2.10, Figure S2.12). The *uncompetitive partial* model describes the situation when inhibitor produces its effect by binding only to the enzyme-substrate complex, the series of double-reciprocal plots are not parallel and the limiting plot at $I = \infty$ is a horizontal line (Figure 2.5, Supporting information, Figure S2.9, Figure S2.11). Both regression models describe the experimental data well (R^2 close to one) (Supporting information, Table S2.1). For the mixed partial model several parameters were poorly estimated: the cooperativity of lysine binding to the E:pyr complex (h exceeds the number of binding sites in the tetramer), and K_i' and α' (have high statistical error) (Supporting information, Table S2.1). Based on the information obtained, including R^2 values, distribution of residuals, and shape of secondary plots (slope and

intercept *vs.* lysine concentration - plots are not shown), preference should be given to the *uncompetitive partial* model as the model providing a good fit with fewer variables.

The most common conclusion in the recent literature is that (*S*)-lysine is a partial noncompetitive inhibitor of DHDPS with respect to ASA (*14, 16, 17*), which implies that lysine is able to bind to both F enzyme form (pyruvate-bound) and F:ASA complex with the same affinity: $K_i = \alpha K_i$ (Scheme 2.1). Assuming that the binding affinities could be different, the model of mixed partial inhibition ($1 < \alpha < \infty$, $0 < \beta < 1$) was considered as well. The family of double-reciprocal plots ($1/v$ versus 1/[ASA] at different lysine concentrations) has a mutual point of convergence near the *y*-axis when [lysine] ≤ 0.1 mM. At high lysine concentration plots have a limiting slope and look more like a set of parallel lines (Figure 2.6). Taking into account that the apparent K_M values for ASA increases at lysine concentrations less than 0.1 mM, and then slightly decrease at higher lysine concentrations, it can be concluded that the kinetic mechanism changes at saturating concentrations of lysine.

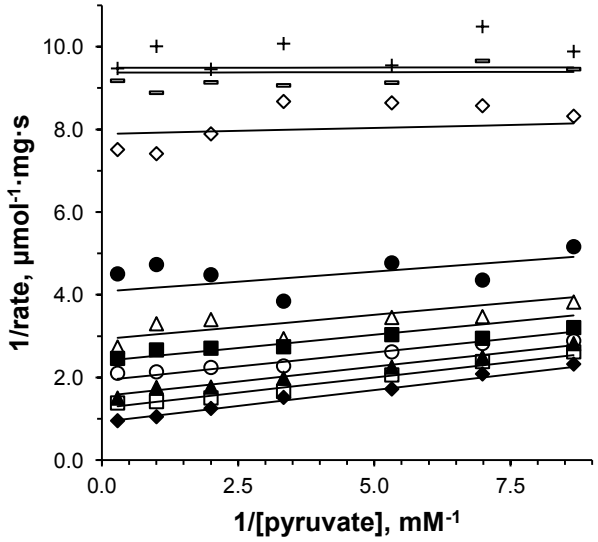

Figure 2.5 Double-reciprocal plot of data obtained at a constant ASA concentration of 0.18 mM. Concentration of lysine: (♦) 0 mM, (□) 0.04 mM, (▲) 0.05 mM, (○) 0.06 mM, (■) 0.07 mM, (△) 0.08 mM, (●) 0.10 mM. (◊) 0.20 mM, (-) 0.50 mM, (+) 1.00 mM. Solid lines are fit lines, obtained by global fitting the *uncompetitive partial* model to the data. Residuals are shown in Supporting information Figure S2.9.

The analysis of the mechanism of lysine inhibition with respect to ASA is more complex. The double-reciprocal plot in Figure 2.6 again indicates two distinct conditions: at low lysine concentrations (≤ 0.1 mM), a family of intersecting lines is evident, as is detectable curvature of

the lines; at higher lysine concentrations the lines appear parallel, with no apparent curvature. Although there are several arguments that might explain a change in behavior of an enzyme saturated with an allosteric ligand, the curvature of the lines suggests that there is lysine-induced cooperativity of ASA under some conditions. Construction of Hill plots indicated that the cooperativity coefficient for ASA is a non-linear function of lysine concentration (Figure 2.7). In the presence of lysine, and at near-K_M concentration of pyruvate, ASA binds with an average cooperativity coefficient $n = 1.3 \pm 0.3$, and this value was therefore included in Equations 2.2 and 2.4, generating the lines of fit included in Figure 2.6 at lysine concentrations ≤ 0.1 mM. At saturating concentration of pyruvate the average cooperativity coefficient for ASA is close to one (1.1 ± 0.3).

Regression analysis of the data indicated that while both noncompetitive partial (Figure S2.13 and Figure S2.14) and mixed partial (Figure 2.6, Figure S2.15 and Figure S2.16) models approximate the data, the mixed partial model has better statistical characteristics. Analysis of residual plots revealed that in the case of the noncompetitive partial model (at near-K_M concentration of pyruvate), residuals are distributed non-randomly (Figure S2.13B). This indicates that lysine is a *mixed partial* inhibitor with respect to ASA, where the inhibitor binds with higher affinity to the F form of the enzyme and with lower affinity to the F:ASA complex.

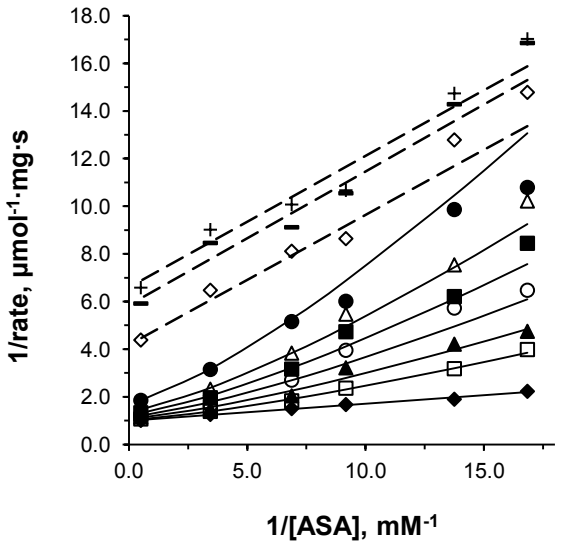

Figure 2.6 Double-reciprocal plot of data obtained at a constant pyruvate concentration of 0.35 mM fit to the mixed partial inhibiton model (Equation 2.2, $1 < \alpha < \infty$, $0 < \beta < 1$). Solid lines, Hill coefficient for ASA $n = 1.3$; dashed lines, $n = 1$. Concentration of lysine: (♦) 0 mM, (□) 0.04 mM, (▲) 0.05 mM, (○) 0.06 mM, (■) 0.07 mM, (△) 0.08 mM, (●) 0.10 mM, (◊) 0.20 mM, (-) 0.50 mM, (+) 1.00 mM.

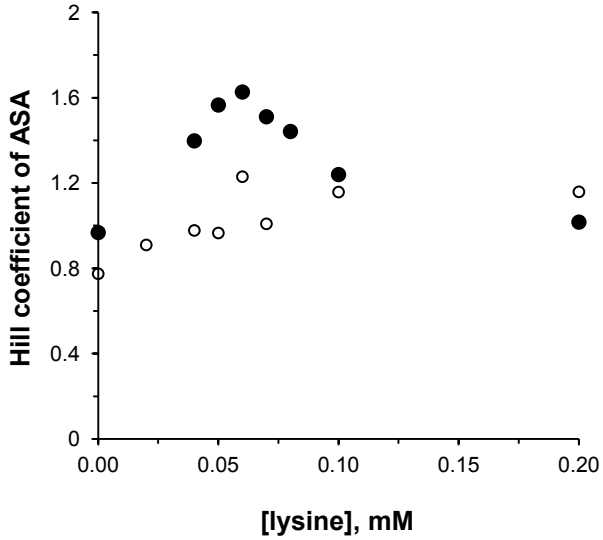

Figure 2.7 Values of the Hill coefficient of ASA at varying concentrations of (*S*)-lysine and constant pyruvate concentrations, 0.35 mM (●) and 3.50 mM (○).

The lysine inhibition results are summarized in Table 2.2. The values of dissociation constants, $K_{S(pyr)}$ and $K_{S(ASA)}$, are close to the K_M values for these substrates in Table 2.1 (for near-K_M background concentration of the second substrate, K_S values are approximately half of

those for saturating concentration of the second substrate), which suggests that the assumptions which have been made about rapid and slow steps in the overall equilibria (Scheme 2.1) are correct.

Table 2.2 Lysine inhibition kinetic parameters for *C. jejuni* DHDPS

Kinetic model	Uncompetitive partial		Mixed partial	
Variable substrate	Pyruvate		ASA	
Fixed substrate	ASA (sat.)	ASA (K_M)	Pyruvate (sat.)	Pyruvate (K_M)
$h_{E:pyr}$, lysine	2.6 ± 0.1	2.9 ± 0.1		
h_F, lysine			2.3 ± 0.2	2.2 ± 0.1
$h_{F:ASA}$, lysine			2.8 ± 0.2	3.2 ± 0.2
n, ASA			1.1 ± 0.3	1.3 ± 0.3
K_{i1}, mM[a]	0.069 ± 0.001	0.054 ± 0.001		
K_{i2}, mM[b]			0.045 ± 0.003	0.037 ± 0.001
K_{i3}, mM[c]			0.072 ± 0.009	0.100 ± 0.006
$K_{S\,(ASA)}$, mM			0.12 ± 0.01	0.073 ± 0.003
$K_{S\,(pyr)}$, mM	0.33 ± 0.01	0.17 ± 0.01		

[a] K_{i1} corresponds to $\alpha' K_i'$ in the Scheme 2.1.
[b] K_{i2} corresponds to K_i in the Scheme 2.1.
[c] K_{i3} corresponds to αK_i in the Scheme 2.1.

2.6 Discussion

Inhibition of DHDPS from various organisms has been studied, and the results of these studies have demonstrated three challenges: defining the kinetic mechanism of inhibition; understanding exactly how the binding of lysine to the regulatory site results in impaired catalysis; and the design of potent, selective inhibitors of the enzyme. The first of these challenges is addressed here for *C. jejuni* DHDPS.

Studies on the *E. coli* enzyme show that the active site contains a lysine residue, Lys161, with which pyruvate condenses in the first chemical step of the ping-pong mechanism. The reaction apparently relies on a "catalytic triad" (*34*) of Thr44, Tyr133, and Tyr107' (a residue contributed from the other polypeptide chain of the tight dimer). Arg138 has been shown to be important for

ASA binding to the enzyme (*40*). These residues are present in *C. jejuni* DHDPS as Lys166, Thr47, Tyr137, Tyr111', and Arg142. Moreover, the structure of *E. coli* DHDPS with lysine bound in the active site shows each lysine molecule making polar contacts with seven residues of the protein (Ser48, Ala49, Leu51, His56, Asn80', Glu84', and Tyr106), and, as shown in Figure 2.8, all of these residues are conserved in the allosteric site of *C. jejuni* DHDPS (Ser51, Ala52, Leu54, His59, Asn84', Glu88', and Tyr110). In short, it would be reasonable to expect these homologues to display very similar behaviour in catalysis and inhibition. We were therefore surprised to find distinct differences in the kinetic mechanism of inhibition, as demonstrated in independent kinetic analyses of the data: we observe that lysine is an uncompetitive partial inhibitor with respect to pyruvate, and a mixed partial inhibitor with respect to ASA. Kinetic mechanisms can vary among enzymes from different species, although some differences in our results may be attributed to our treatment of cooperativity in the mechanistic analysis, which was absent from recent treatments of the *E. coli* DHDPS mechanism. In arriving at our conclusions, we found the use of the combination of Cornish-Bowden and Dixon plots to be extremely helpful in differentiating the kinetic models.

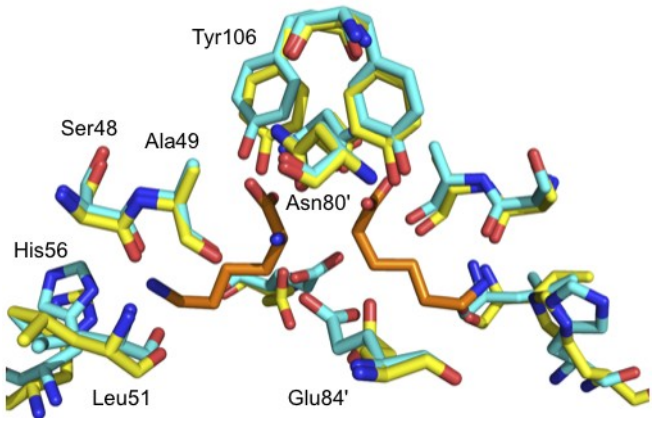

Figure 2.8 Overlay of the allosteric site residues of *C. jejuni* DHDPS (cyan), and *E. coli* DHDPS (yellow) making polar contacts with bound L-lysine (orange). Residue labels indicate *E. coli* residues making contact with one L-lysine molecule. Coordinates from RSCB PDB entries 1YXD (*E. coli*) and 3LER (*C. jejuni*). Figure generated using PyMOL Molecular Graphics System, Version 1.4.1, Schrodinger, LLC.

Binding of lysine to DHDPS has been shown to be cooperative for DHDPS from other sources, including *E. coli* (*21, 24*), *S. meliloti* (*25*), and *V. vinifera* (*23*). It is therefore surprising that although this cooperativity has been known for fifteen years, most detailed kinetic analyses

have not accounted for cooperativity. (During the preparation of this manuscript, a report describing the kinetics of inhibition of the *V. vinifera* DHDPS appeared, in which Hill coefficients were calculated and incorporated into rate equations.) In some cases perhaps, lysine cooperativity is small enough to be ignored, but the significant cooperativity evident with *C. jejuni* DHDPS made it clear that Hill coefficients would have to be incorporated into our analyses.

As described above, the degree of cooperativity was not the same in all conditions. This is not surprising: the presence of pyruvate increases the affinity of the allosteric site for lysine, while the presence of ASA decreases the affinity of the allosteric site for lysine. In each case, the properties of the site have changed, albeit subtly, and therefore there is no reason for the degree of cooperativity to remain constant. In all conditions the value of h was between 2 and 3.2. That the degree of cooperativity exceeds 2.0 is significant in that it indicates that the two allosteric sites are not entirely independent; binding of lysine to one site affects the binding of lysine at the other, showing the enzyme to be functioning as a tetrameric catalyst, rather than as a dimer of independent dimers. It is unlikely that this site-to-site communication is due to a pronounced structural change, since no evidence has been observed for such changes in the very similar *E. coli* DHDPS. Dobson *et al.* (*30*) and Reboul *et al*. (*41*) have used molecular dynamics simulations to show the likely importance of protein dynamics to DHDPS catalysis, and the role that the tetrameric structure may play in maintaining optimal active site residue conformation.

The complexity of the inhibition mechanism extends beyond the cooperativity of inhibitor binding. The behaviour of the enzyme at high concentrations of lysine can be differentiated from its behaviour at lysine concentrations below 0.1 mM. Specifically, the Lineweaver-Burk plots of Figure 2.6 show a different pattern, with the lines at high lysine concentrations near parallel. This can be understood in terms of Scheme 2.1 by considering that at high concentrations, catalysis passes largely through the lower pathway, i.e. the inhibitor-bound enzyme species. We also observe that the presence of lysine induces cooperativity in the second substrate, ASA. It may be that the presence of lysine restricts or alters the dynamics of the protein, which thereby alters several properties of catalysis, such as cooperativity of substrate binding.

In summary, although the kinetic mechanism of inhibition is complex, there are some clear conclusions to be drawn from these results. Lysine is a more effective inhibitor of *C. jejuni* DHDPS than of most DHDPS from Gram-negative bacteria, and the observed kinetic mechanism

differs from that reported recently for DHDPS from other sources. It is evident that the inhibition mechanism cannot be assessed properly without accounting for the cooperativity of lysine binding. The value of the Hill coefficient with respect to each binding event varies somewhat, but in all cases $h > 2$, indicating that the two allosteric sites are not independent. Lysine binds most effectively to the F form of *C. jejuni* DHDPS and kinetic results suggest that lysine either does not bind to the E form (this equilibrium is shown in blue in Scheme 2.1) or binding of lysine to this form does not have an effect on inhibition kinetics. Figure 2.4 clearly shows that the presence of pyruvate promotes lysine binding, while ASA and lysine have an antagonistic relationship; the presence of ASA drives up the apparent inhibition constant of lysine, and the presence of lysine drives up the apparent Michaelis constant of ASA; each hinders the binding of the other. Finally, this is the first observation of lysine-induced cooperativity of ASA. As observed previously for other DHDPS enzymes, there is no cooperativity in the absence of lysine, but the curvature of the lines in Figure 2.6 clearly demonstrates the low but significant cooperativity of the second substrate. The specifics of the signal transduction between active site and allosteric site, and between antipodal allosteric sites, remain unclear, but will be aided by biophysical studies of this protein including high-resolution crystallographic studies.

2.7 Acknowledgments

This work was funded by a Natural Sciences and Engineering Research Council of Canada (NSERC) Discovery Grant to D. R. J. P. and an NSERC PGS D Scholarship to Y. V. S, and by the Saskatchewan Health Research Foundation (SHRF) through support for the Molecular Design Research Group. The authors thank Dr. Janet Hill and Dr. Bonnie Chaban (Department of Veterinary Microbiology, Western College of Veterinary Medicine, University of Saskatchewan) for providing *C. jejuni* genomic DNA, Ken Thoms, Dr. Keith Brown, and other staff of the Saskatchewan Structural Sciences Centre, and Dr. David A. R. Sanders (Department of Chemistry) for shared equipment and helpful discussions.

2.8 References

1. Devenish, S. R., Blunt, J. W., and Gerrard, J. A. (2010) NMR studies uncover alternate substrates for dihydrodipicolinate synthase and suggest that dihydrodipicolinate reductase is also a dehydratase, *J Med Chem 53*, 4808-4812.
2. Blickling, S., Renner, C., Laber, B., Pohlenz, H. D., Holak, T. A., and Huber, R. (1997) Reaction mechanism of *Escherichia coli* dihydrodipicolinate synthase investigated by X-ray crystallography and NMR spectroscopy, *Biochemistry 36*, 24-33.
3. Yugari, Y., and Gilvarg, C. (1965) The condensation step in diaminopimelate synthesis, *J Biol Chem 240*, 4710-4716.
4. Borthwick, E. B., Connell, S. J., Tudor, D. W., Robins, D. J., Shneier, A., Abell, C., and Coggins, J. R. (1995) *Escherichia coli* dihydrodipicolinate synthase: characterization of the imine intermediate and the product of bromopyruvate treatment by electrospray mass spectrometry, *Biochem J 305 (Pt 2)*, 521-524.
5. Hutton, C. A., Southwood, T. J., and Turner, J. J. (2003) Inhibitors of lysine biosynthesis as antibacterial agents, *Mini Rev Med Chem 3*, 115-127.
6. Kobayashi, K., Ehrlich, S. D., Albertini, A., Amati, G., Andersen, K. K., Arnaud, M., Asai, K., Ashikaga, S., Aymerich, S., Bessieres, P., Boland, F., Brignell, S. C., Bron, S., Bunai, K., Chapuis, J., Christiansen, L. C., Danchin, A., Debarbouille, M., Dervyn, E., Deuerling, E., Devine, K., Devine, S. K., Dreesen, O., Errington, J., Fillinger, S., Foster, S. J., Fujita, Y., Galizzi, A., Gardan, R., Eschevins, C., Fukushima, T., Haga, K., Harwood, C. R., Hecker, M., Hosoya, D., Hullo, M. F., Kakeshita, H., Karamata, D., Kasahara, Y., Kawamura, F., Koga, K., Koski, P., Kuwana, R., Imamura, D., Ishimaru, M., Ishikawa, S., Ishio, I., Le Coq, D., Masson, A., Mauel, C., Meima, R., Mellado, R. P., Moir, A., Moriya, S., Nagakawa, E., Nanamiya, H., Nakai, S., Nygaard, P., Ogura, M., Ohanan, T., O'Reilly, M., O'Rourke, M., Pragai, Z., Pooley, H. M., Rapoport, G., Rawlins, J. P., Rivas, L. A., Rivolta, C., Sadaie, A., Sadaie, Y., Sarvas, M., Sato, T., Saxild, H. H., Scanlan, E., Schumann, W., Seegers, J. F., Sekiguchi, J., Sekowska, A., Seror, S. J., Simon, M., Stragier, P., Studer, R., Takamatsu, H., Tanaka, T., Takeuchi, M., Thomaides, H. B., Vagner, V., van Dijl, J. M., Watabe, K., Wipat, A., Yamamoto, H., Yamamoto, M., Yamamoto, Y., Yamane, K., Yata, K., Yoshida, K., Yoshikawa, H., Zuber, U., and Ogasawara, N. (2003) Essential *Bacillus subtilis* genes, *Proc Natl Acad Sci U S A 100*, 4678-4683.
7. Boughton, B. A., Hor, L., Gerrard, J. A., and Hutton, C. A. (2012) 1,3-Phenylene bis(ketoacid) derivatives as inhibitors of *Escherichia coli* dihydrodipicolinate synthase, *Bioorg Med Chem 20*, 2419-2426.
8. Boughton, B. A., Griffin, M. D., O'Donnell, P. A., Dobson, R. C., Perugini, M. A., Gerrard, J. A., and Hutton, C. A. (2008) Irreversible inhibition of dihydrodipicolinate synthase by 4-oxo-heptenedioic acid analogues, *Bioorg Med Chem 16*, 9975-9983.
9. Boughton, B. A., Dobson, R. C., Gerrard, J. A., and Hutton, C. A. (2008) Conformationally constrained diketopimelic acid analogues as inhibitors of dihydrodipicolinate synthase, *Bioorg Med Chem Lett 18*, 460-463.
10. Turner, J. J., Gerrard, J. A., and Hutton, C. A. (2005) Heterocyclic inhibitors of dihydrodipicolinate synthase are not competitive, *Bioorg Med Chem 13*, 2133-2140.
11. Turner, J. J., Healy, J. P., Dobson, R. C., Gerrard, J. A., and Hutton, C. A. (2005) Two new irreversible inhibitors of dihydrodipicolinate synthase: diethyl (E,E)-4-oxo-2,5-heptadienedioate and diethyl (E)-4-oxo-2-heptenedioate, *Bioorg Med Chem Lett 15*, 995-998.
12. Kumpaisal, R., Hashimoto, T., and Yamada, Y. (1987) Purification and characterization of dihydrodipicolinate synthase from wheat suspension cultures, *Plant Physiol 85*, 145-151.

13. Laber, B., Gomis-Ruth, F. X., Romao, M. J., and Huber, R. (1992) *Escherichia coli* dihydrodipicolinate synthase. Identification of the active site and crystallization, *Biochem J 288 (Pt 2)*, 691-695.
14. Dereppe, C., Bold, G., Ghisalba, O., Ebert, E., and Schar, H. P. (1992) Purification and characterization of dihydrodipicolinate synthase from pea, *Plant Physiol 98*, 813-821.
15. Frisch, D. A., Gengenbach, B. G., Tommey, A. M., Sellner, J. M., Somers, D. A., and Myers, D. E. (1991) Isolation and characterization of dihydrodipicolinate synthase from maize, *Plant Physiol 96*, 444-452.
16. Devenish, S. R., Huisman, F. H., Parker, E. J., Hadfield, A. T., and Gerrard, J. A. (2009) Cloning and characterisation of dihydrodipicolinate synthase from the pathogen *Neisseria meningitidis*, *Biochim Biophys Acta 1794*, 1168-1174.
17. Dobson, R. C., Griffin, M. D., Roberts, S. J., and Gerrard, J. A. (2004) Dihydrodipicolinate synthase (DHDPS) from *Escherichia coli* displays partial mixed inhibition with respect to its first substrate, pyruvate, *Biochimie 86*, 311-315.
18. Domigan, L. J., Scally, S. W., Fogg, M. J., Hutton, C. A., Perugini, M. A., Dobson, R. C., Muscroft-Taylor, A. C., Gerrard, J. A., and Devenish, S. R. (2009) Characterisation of dihydrodipicolinate synthase (DHDPS) from *Bacillus anthracis*, *Biochim Biophys Acta 1794*, 1510-1516.
19. Rice, E. A., Bannon, G. A., Glenn, K. C., Jeong, S. S., Sturman, E. J., and Rydel, T. J. (2008) Characterization and crystal structure of lysine insensitive *Corynebacterium glutamicum* dihydrodipicolinate synthase (cDHDPS) protein, *Arch Biochem Biophys 480*, 111-121.
20. Wolterink-van Loo, S., Levisson, M., Cabrieres, M. C., Franssen, M. C., and van der Oost, J. (2008) Characterization of a thermostable dihydrodipicolinate synthase from *Thermoanaerobacter tengcongensis*, *Extremophiles 12*, 461-469.
21. Karsten, W. E. (1997) Dihydrodipicolinate synthase from *Escherichia coli*: pH dependent changes in the kinetic mechanism and kinetic mechanism of allosteric inhibition by L-lysine, *Biochemistry 36*, 1730-1739.
22. Soares da Costa, T. P., Muscroft-Taylor, A. C., Dobson, R. C., Devenish, S. R., Jameson, G. B., and Gerrard, J. A. (2010) How essential is the 'essential' active-site lysine in dihydrodipicolinate synthase?, *Biochimie 92*, 837-845.
23. Atkinson, S. C., Dogovski, C., Downton, M. T., Czabotar, P. E., Dobson, R. C., Gerrard, J. A., Wagner, J., and Perugini, M. A. (2013) Structural, kinetic and computational investigation of *Vitis vinifera* DHDPS reveals new insight into the mechanism of lysine-mediated allosteric inhibition, *Plant Mol Biol 81*, 431-446.
24. Muscroft-Taylor, A. C., Soares da Costa, T. P., and Gerrard, J. A. (2010) New insights into the mechanism of dihydrodipicolinate synthase using isothermal titration calorimetry, *Biochimie 92*, 254-262.
25. Phenix, C. P., and Palmer, D. R. (2008) Isothermal titration microcalorimetry reveals the cooperative and noncompetitive nature of inhibition of *Sinorhizobium meliloti* L5-30 dihydrodipicolinate synthase by (S)-lysine, *Biochemistry 47*, 7779-7781.
26. Hughes, R. (2004) *Campylobacter jejuni* in Guillain-Barre syndrome, *Lancet Neurol 3*, 644.
27. Young, K. T., Davis, L. M., and Dirita, V. J. (2007) *Campylobacter jejuni*: molecular biology and pathogenesis, *Nat Rev Microbiol 5*, 665-679.
28. Larkin, M. A., Blackshields, G., Brown, N. P., Chenna, R., McGettigan, P. A., McWilliam, H., Valentin, F., Wallace, I. M., Wilm, A., Lopez, R., Thompson, J. D., Gibson, T. J., and Higgins, D. G. (2007) Clustal W and Clustal X version 2.0, *Bioinformatics 23*, 2947-2948.
29. Goujon, M., McWilliam, H., Li, W., Valentin, F., Squizzato, S., Paern, J., and Lopez, R. (2010) A new bioinformatics analysis tools framework at EMBL-EBI, *Nucleic Acids Res 38*, W695-699.
30. Dobson, R. C., Griffin, M. D., Jameson, G. B., and Gerrard, J. A. (2005) The crystal structures of native and (S)-lysine-bound dihydrodipicolinate synthase from *Escherichia coli* with improved

resolution show new features of biological significance, *Acta Crystallogr D Biol Crystallogr 61*, 1116-1124.
31. Roberts, S. J., Morris, J. C., Dobson, R. C. J., Baxter, C. L., and Gerrard, J. A. (2004) Two complete syntheses of (S)-aspartate semi-aldehyde and demonstration that Δ–(2)-tetrahydroisophthalic acid is a non-competitive inhibitor of dihydrodipicolinate synthase, *Arkivoc x*, 166-177.
32. Sambrook, J., and Russell, D. W. (2001) *Molecular cloning : a laboratory manual*, 3rd ed., Cold Spring Harbor Laboratory Press, Cold Spring Harbor, N.Y.
33. Walker, J. M. (2005) *The proteomics protocols handbook*, Humana Press, Totowa, N.J.
34. Dobson, R. C., Valegard, K., and Gerrard, J. A. (2004) The crystal structure of three site-directed mutants of *Escherichia coli* dihydrodipicolinate synthase: further evidence for a catalytic triad, *J Mol Biol 338*, 329-339.
35. Joerger, A. C., Mayer, S., and Fersht, A. R. (2003) Mimicking natural evolution in vitro: an N-acetylneuraminate lyase mutant with an increased dihydrodipicolinate synthase activity, *Proc Natl Acad Sci U S A 100*, 5694-5699.
36. Tam, P. H., Phenix, C. P., and Palmer, D. R. (2004) MosA, a protein implicated in rhizopine biosynthesis in *Sinorhizobium meliloti* L5-30, is a dihydrodipicolinate synthase, *J Mol Biol 335*, 393-397.
37. Cornish-Bowden, A., and Koshland, D. E. (1975) Diagnostic uses of Hill (Logit and Nernst) plots, *J Mol Biol 95*, 201-212.
38. Segel, I. H. (1975) *Enzyme kinetics : behavior and analysis of rapid equilibrium and steady state enzyme systems*, Wiley, New York.
39. Cortes, A., Cascante, M., Cardenas, M. L., and Cornish-Bowden, A. (2001) Relationships between inhibition constants, inhibitor concentrations for 50% inhibition and types of inhibition: new ways of analysing data, *Biochem. J. 357*, 263-268.
40. Dobson, R. C., Devenish, S. R., Turner, L. A., Clifford, V. R., Pearce, F. G., Jameson, G. B., and Gerrard, J. A. (2005) Role of arginine 138 in the catalysis and regulation of *Escherichia coli* dihydrodipicolinate synthase, *Biochemistry 44*, 13007-13013.
41. Reboul, C. F., Porebski, B. T., Griffin, M. D., Dobson, R. C., Perugini, M. A., Gerrard, J. A., and Buckle, A. M. (2012) Structural and dynamic requirements for optimal activity of the essential bacterial enzyme dihydrodipicolinate synthase, *PLoS Comput Biol 8*, e1002537.

2.9 Supporting Information

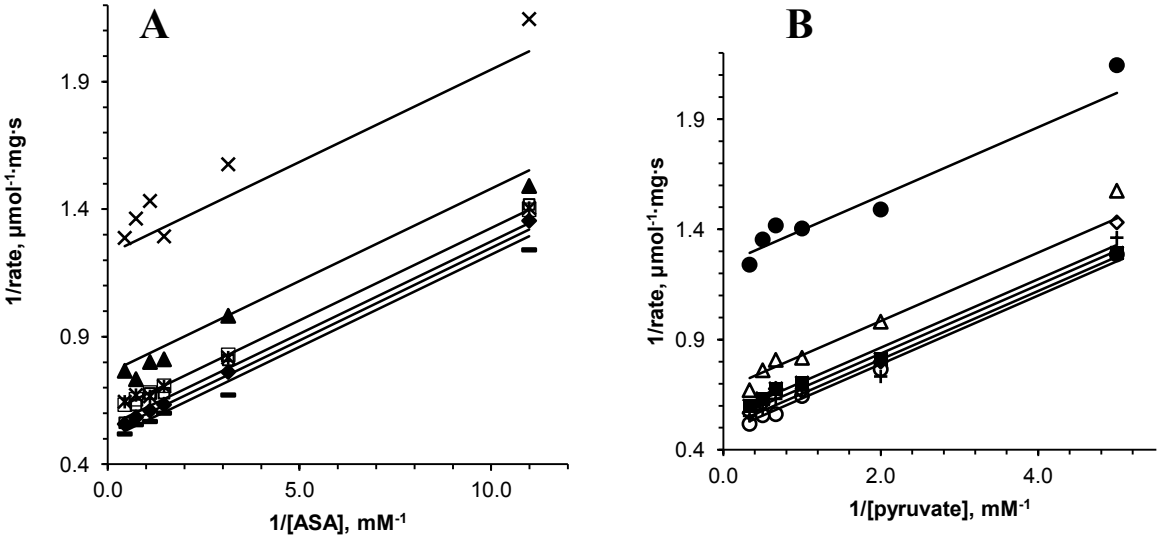

Figure S2.1 Double-reciprocal plots of the DHDPS-catalyzed reaction. Solid lines are the global fit of the data to Equation 2.1) (R^2 is 0.985703). (A) Concentration of pyruvate is varied: (✕) 0.2 mM, (▲) 0.5 mM, (✳) 1.0 mM, (□) 1.5 mM, (♦) 2.0 mM, (▬) 3.0 mM. (B) Concentration of ASA is varied: (●) 0.09 mM, (△) 0.32 mM, (■) 0.68 mM, (◊) 0.91 mM, (+) 1.37 mM, (○) 2.28 mM.

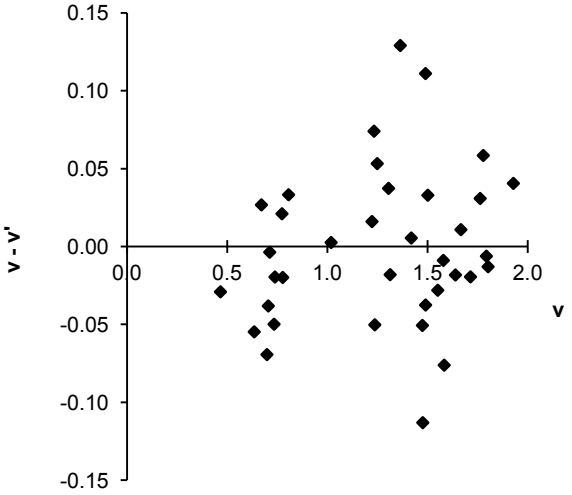

Figure S2.2 Residuals for plots in Figure S2.1.

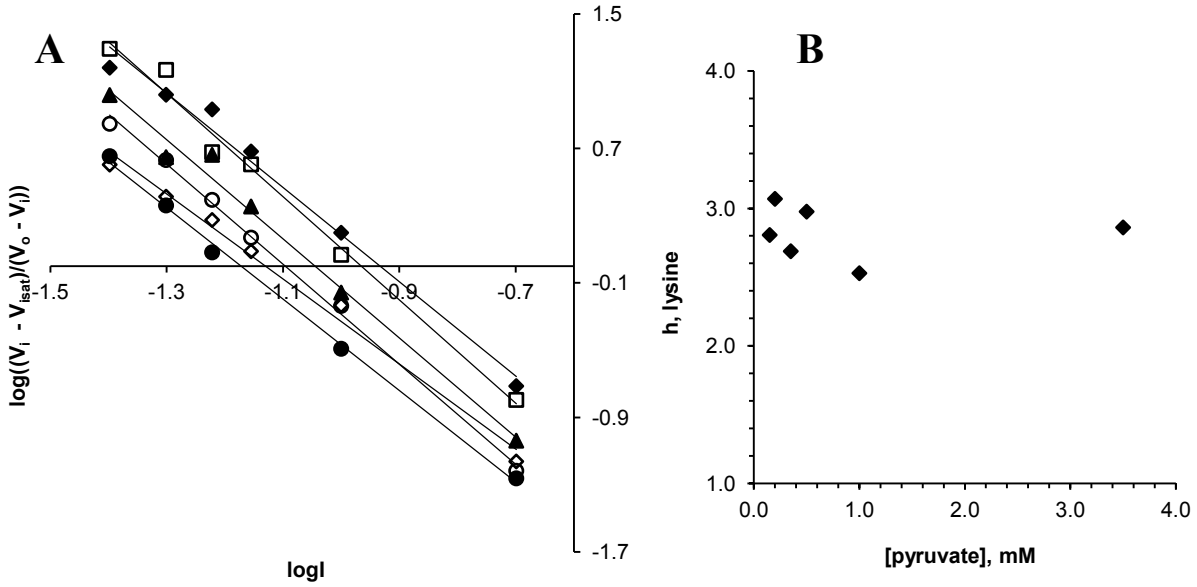

Figure S2.3 (A) Hill plots at 2.24 mM ASA and varied concentrations of pyruvate: (♦) 0.15 mM, (□) 0.20 mM, (▲) 0.35 mM, (○) 0.50 mM, (◊) 1.00 mM, (●) 3.50 mM. Solid lines were obtained by linear regression. (B) Values of the Hill coefficient of lysine at varying concentration of pyruvate.

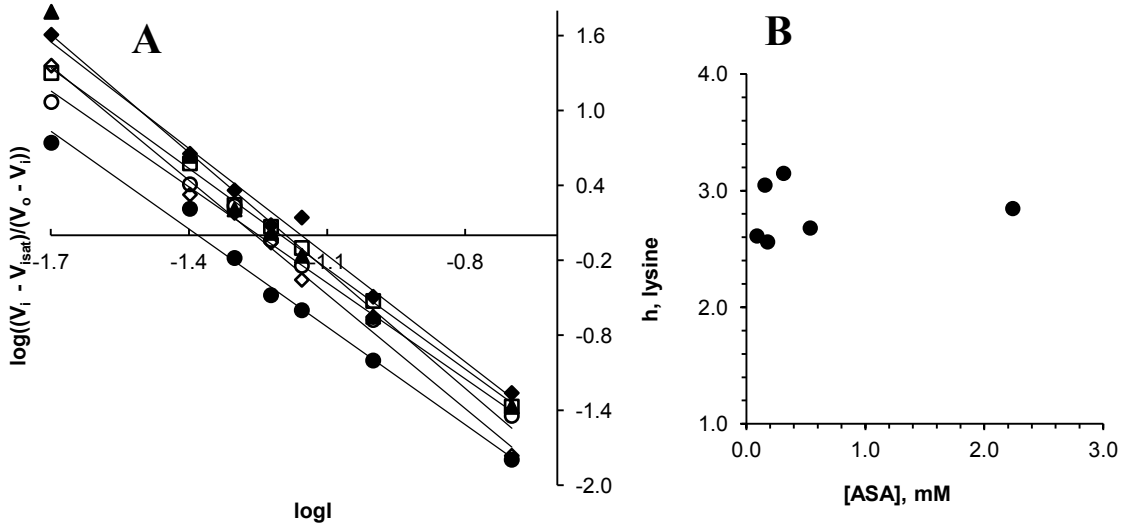

Figure S2.4 (A) Hill plots at 3.50 mM pyruvate and varied concentration of ASA: (♦) 2.24 mM, (□) 0.54 mM, (▲) 0.31 mM, (○) 0.18 mM, (◊) 0.16 mM, (●) 0.09 mM. Solid lines were obtained by linear regression. (B) Values of the Hill coefficient of lysine at varying concentrations of ASA.

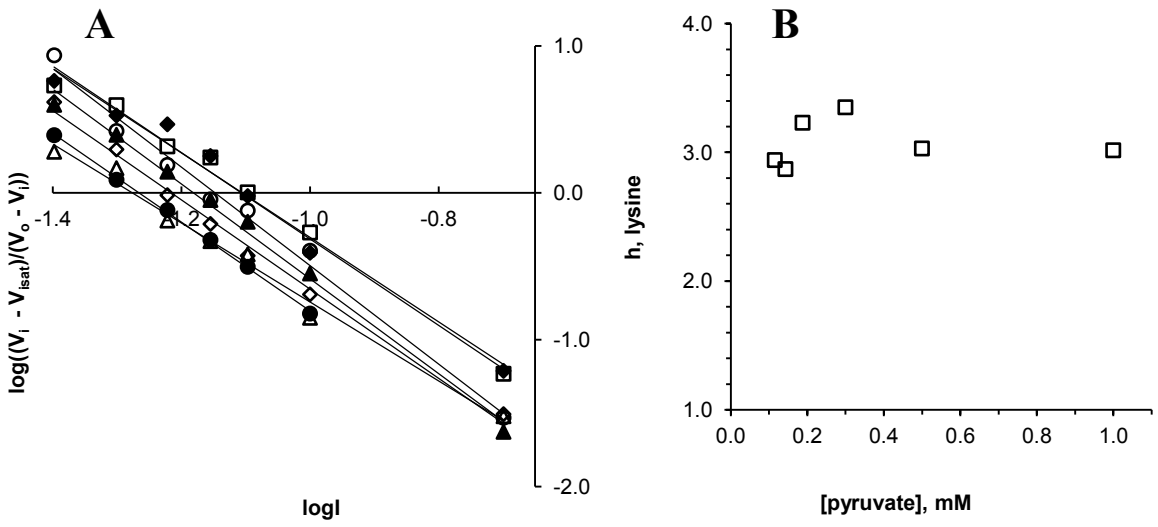

Figure S2.5 (A) Hill plots at 0.18 mM ASA and varied concentrations of pyruvate: (♦) 0.12 mM, (□) 0.14 mM, (▲) 0.19 mM, (○) 0.30 mM, (◊) 0.50 mM, (●) 1.00 mM, (△) 3.50 mM. Solid lines were obtained by linear regression. (B) Values of the Hill coefficient of lysine at varying concentrations pyruvate.

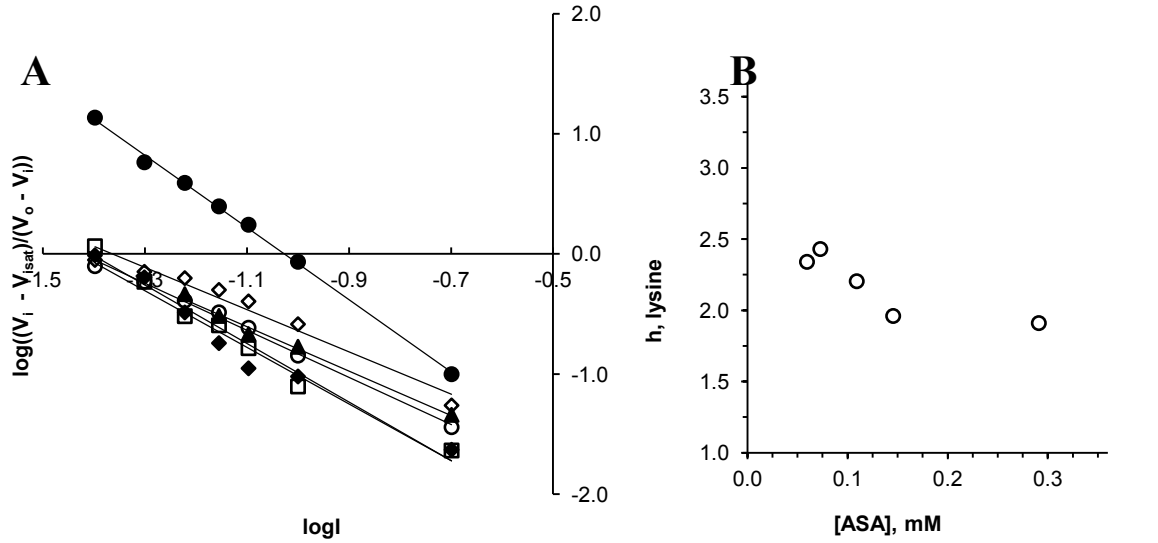

Figure S2.6 (A) Hill plots at 0.35 mM pyruvate and varied concentrations of ASA: (♦) 0.06 mM, (□) 0.07 mM, (▲) 0.11 mM, (○) 0.15 mM, (◇) 0.29 mM, (●) 2.00 mM. Solid lines were obtained by linear regression. (B) Values of the Hill coefficient of lysine at varying concentrations of ASA.

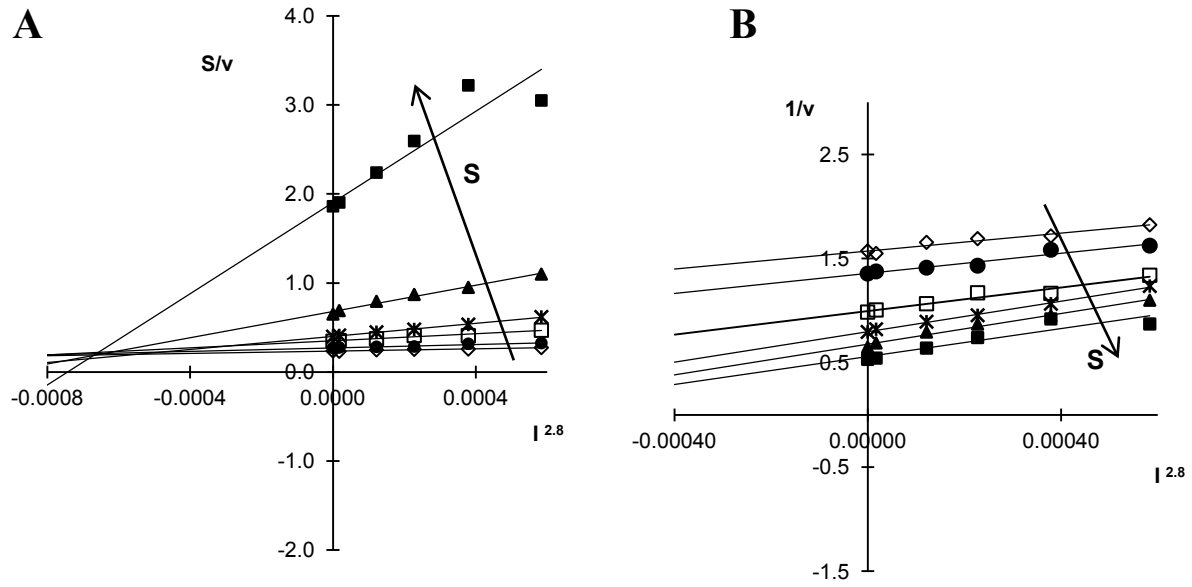

Figure S2.7 Cornish-Bowden plot (A) and Dixon plot (B) of the inhibition of the DHDPS-catalyzed reaction by lysine with respect to pyruvate. Concentration of pyruvate is 0.15 (◊), 0.20 (●), 0.35 (□), 0.50 (✳), 1.00 (▲), 3.50 (■) mM; concentration of ASA 2.24 mM. Solid lines were obtained by linear regression.

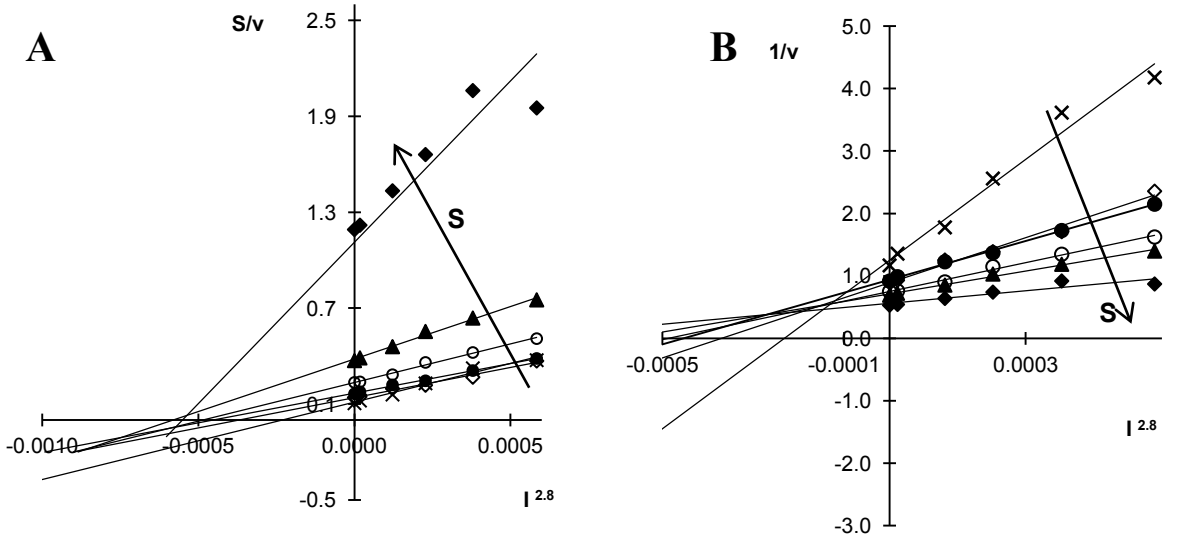

Figure S2.8 Cornish-Bowden plot (A) and Dixon plot (B) of the inhibition of the DHDPS-catalyzed reaction by lysine with respect to ASA. Concentration of ASA is 0.09 (×), 0.16 (◊), 0.18 (●), 0.31 (○), 0.54 (▲), 2.24 (◆) mM; concentration of pyruvate is 3.50 mM. Solid lines were obtained by linear regression.

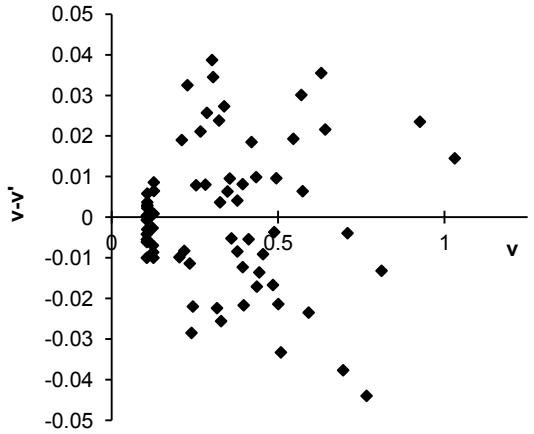

Figure S2.9 Residuals for plot in Figure 2.5.

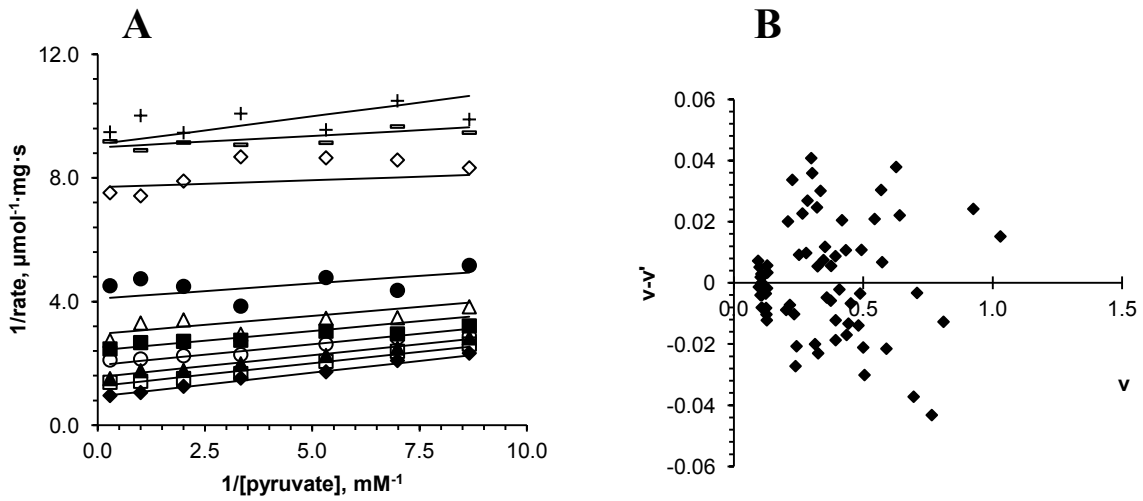

Figure S2.10 (A) Double-reciprocal plots of data obtained at a constant ASA concentration of 0.18 mM. Concentration of lysine: (♦) 0 mM, (□) 0.04 mM, (▲) 0.05 mM, (○) 0.06 mM, (■) 0.07 mM, (△) 0.08 mM, (●) 0.10 mM. (◇) 0.20 mM, (▪) 0.50 mM, (+) 1.00 mM. Solid lines are fit lines, obtained by global fitting the *mixed partial* model to the data ($0 < \alpha' < 1$, $0 < \beta' < 1$). (B) Residuals for Figure S2.10A.

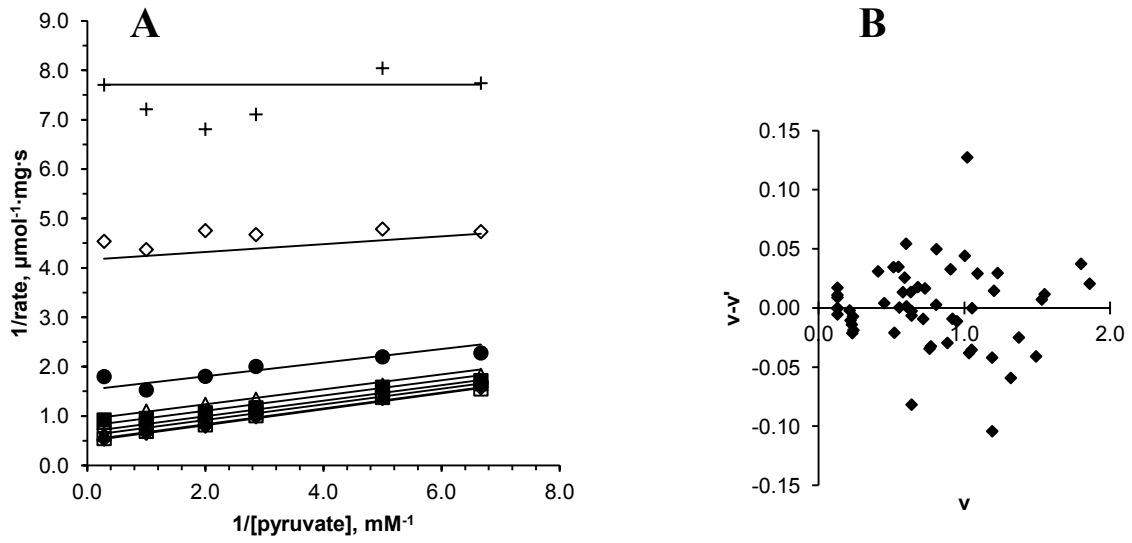

Figure S2.11 (A) Double-reciprocal plots of data obtained at a constant ASA concentration of 2.24 mM. Concentration of lysine: (♦) 0 mM, (□) 0.02 mM, (▲) 0.04 mM, (○) 0.05 mM, (■) 0.06 mM, (△) 0.07 mM, (●) 0.10 mM. (◇) 0.20 mM, (+) 2.00 mM. Solid lines are fit lines, obtained by global fitting the *uncompetitive partial* model to the data. (B) Residuals for Figure S2.11A.

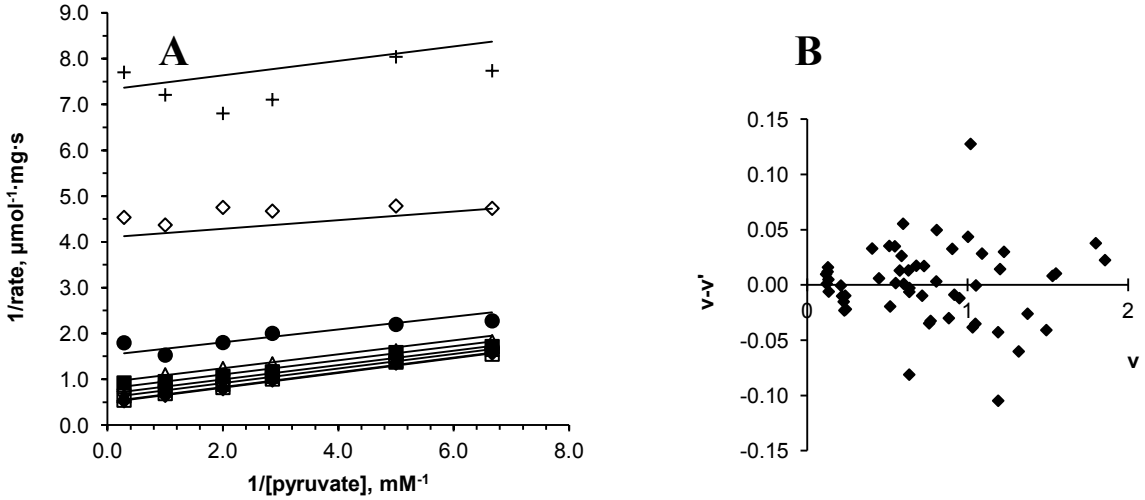

Figure S2.12 (A) Double-reciprocal plot of data obtained at a constant ASA concentration of 2.24 mM. Concentration of lysine: (♦) 0 mM, (□) 0.02 mM, (▲) 0.04 mM, (○) 0.05 mM, (■) 0.06 mM, (△) 0.07 mM, (●) 0.10 mM. (◇) 0.20 mM, (+) 2.00 mM. Solid lines are fit lines, obtained by global fitting the *mixed partial* model to the data ($0 < \alpha' < 1$, $0 < \beta' < 1$). (B) Residuals for Figure S2.12A.

Table S2.1 Comparison of kinetic constants calculated by global fitting using alternative kinetic models, showing poorly estimated parameters and poorer fits for the mixed partial model with respect to pyruvate and the noncompetitive partial model with respect to ASA.

	With respect to pyruvate				With respect to ASA			
Parameters, models	Mixed partial		Uncompetitive partial		Mixed partial		Noncompetitive partial	
Concentration of the second substrate	K_M	saturating	K_M	saturating	K_M	saturating	K_M	saturating
V_{max}, μmol·mg^{-1}·s^{-1}	1.08 ± 0.02	2.03 ± 0.03	1.08 ± 0.02	2.03 ± 0.03	1.01 ± 0.01	1.89 ± 0.04	1.22 ± 0.04	2.02 ± 0.05
K_S, mM	0.17 ± 0.01	0.33 ± 0.01	0.17 ± 0.01	0.33 ± 0.01	0.073 ± 0.003	0.12 ± 0.01	0.15 ± 0.01	0.16 ± 0.01
α					2.7 ± 0.1	1.6 ± 0.2	1	1
β					0.14 ± 0.01	0.08 ± 0.02	0.15 ± 0.02	0.086 ± 0.018
α'	0.25 ± 0.21*	0.22 ± 0.28*						
β'	0.10 ± 0.07*	0.067 ± 0.011	0.097 ± 0.004	0.064 ± 0.007				
n (ASA)					1.0, 1.3[1]	1.0, 1.1[3]	1.0, 1.3[1]	1.0, 1.1[3]
h_E (lysine)	4.2 ± 2.3*	3.3 ± 2.1*						
$h_{E:pyr}$ (lysine)	2.9 ± 0.1	2.6 ± 0.1	2.9 ± 0.1	2.6 ± 0.1				
h_F (lysine)					2.2 ± 0.1[2]	2.3 ± 0.2[4]	2.5 ± 0.3	2.6 ± 0.2
$h_{F:ASA}$ (lysine)					3.2 ± 0.2[2]	2.8 ± 0.2[4]	2.5 ± 0.3	2.6 ± 0.2
K_i'	0.22 ± 0.19*	0.31 ± 0.39*						
$\alpha' K_i'$	0.055 ± 0.066*	0.068 ± 0.122*	0.054 ± 0.007	0.069 ± 0.001				
K_i					0.037 ± 0.001	0.045 ± 0.003	0.071 ± 0.003	0.062 ± 0.002
αK_i					0.100 ± 0.006	0.072 ± 0.009	0.071 ± 0.003	0.062 ± 0.002
R^2	0.993299	0.993712	0.993341	0.993801	0.995676	0.987739	0.968191	0.981916

* Poorly estimated parameters

[1] Average Hill coefficients for ASA were used: n = 1.0 (in the absence of lysine and in the range of lysine concentrations from 0.2 to 1.0 mM), n = 1.3 (in the range of lysine concentrations from 0.04 to 0.1 mM), based on the results shown in Figure 2.7.

[2] Hill coefficients for lysine were found by global fitting of the model to data, in the range of lysine concentration from 0.2 to 1.0 mM of lysine the fit was produced by reducing Hill coefficients from 2.2 to 1.4 (h_F) and from 3.2 to 1.95 ($h_{F:ASA}$).

[3] Average Hill coefficients for ASA were used: n = 1.0 (in the absence of lysine and in the range of lysine concentrations from 0.2 to 2.0 mM), n = 1.1 (in the range of lysine concentrations from 0.02 to 0.2 mM), based on the results shown in Figure 2.7.

[4] Hill coefficients for lysine were found by global fitting of the model to data, in the range of lysine concentration from 0.2 to 2.0 mM the fit was produced by reducing Hill coefficients from 1.9 to 1.4 (h_F) and from 2.5 to 1.7 ($h_{F:ASA}$).

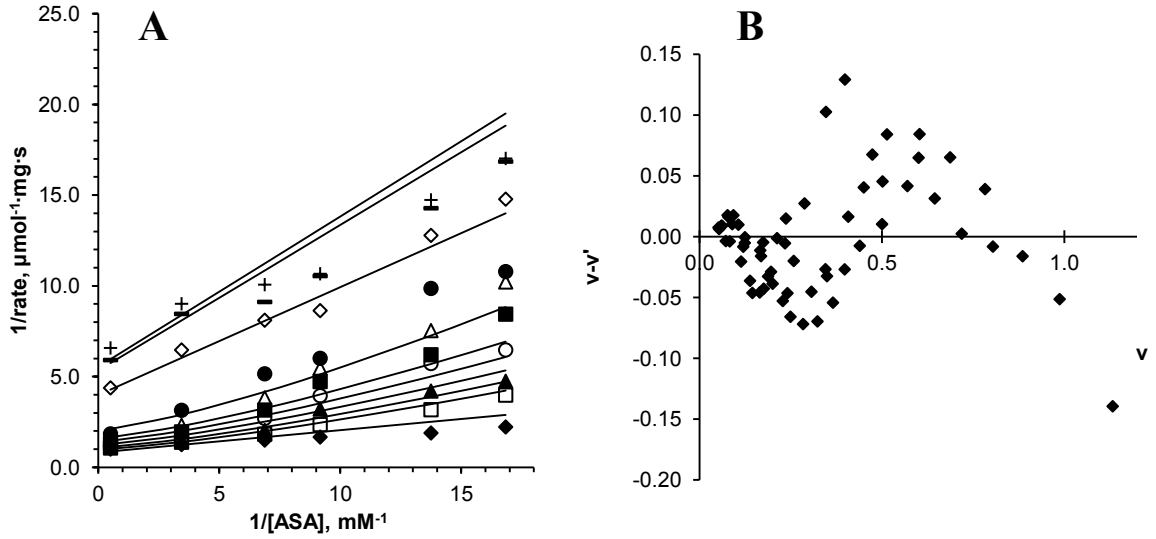

Figure S2.13 Fit of the data obtained at a constant pyruvate concentration of 0.35 mM to the *noncompetitive partial* model. (A) Double-reciprocal plot of data obtained at concentration of lysine: (♦) 0 mM, (□) 0.04 mM, (▲) 0.05 mM, (○) 0.06 mM, (■) 0.07 mM, (△) 0.08 mM, (●) 0.10 mM. Solid lines are fit lines, obtained by global fitting of the data to Equation 2.4. (B) Residuals for Figure S2.13A.

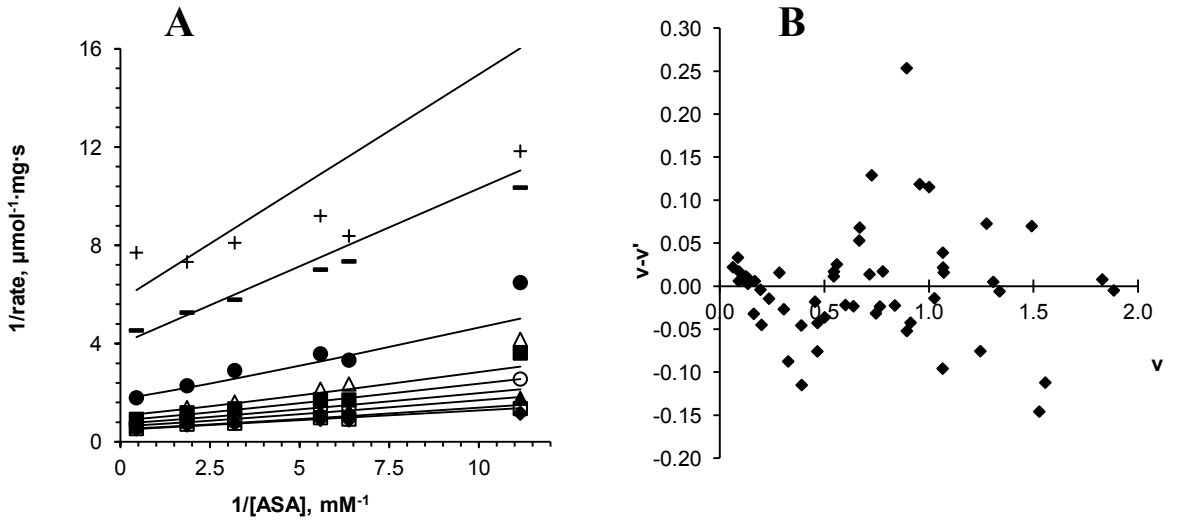

Figure S2.14 (A) Double-reciprocal plot of data obtained at a constant pyruvate concentration of 3.50 mM. Concentration of lysine: (♦) 0 mM, (□) 0.02 mM, (▲) 0.04 mM, (○) 0.05 mM, (■) 0.06 mM, (△) 0.07 mM, (●) 0.10 mM, (–) 0.20 mM, (+) 2.00 mM. Solid lines are fit lines, obtained by global fitting the *noncompetitive partial* model to the data. (B) Residuals for Figure S2.14A.

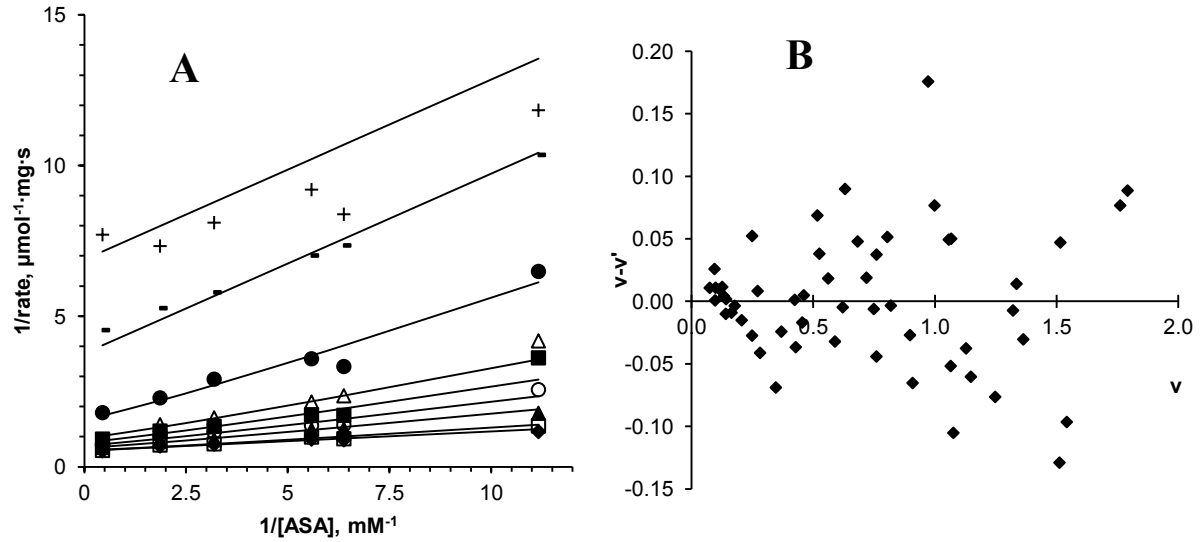

Figure S2.15 (A) Double-reciprocal plots. Data obtained at constant pyruvate concentration 3.50 mM. Concentration of lysine: (♦) 0 mM, (□) 0.02 mM, (▲) 0.04 mM, (○) 0.05 mM, (■) 0.06 mM, (△) 0.07 mM, (●) 0.10 mM, (–) 0.20 mM, (+) 2.00 mM. Solid lines are fit lines, obtained by global fitting the *mixed partial* model ($1 < \alpha < \infty$, $0 < \beta < 1$) to the data. (B) Residuals for Figure S2.15A.

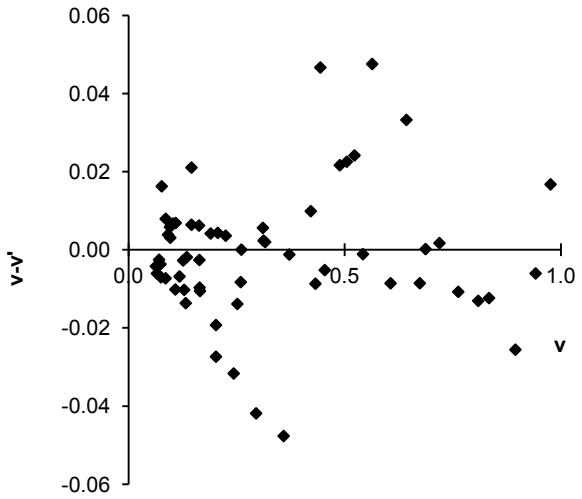

Figure S2.16 Residuals for plot in Figure 2.6.

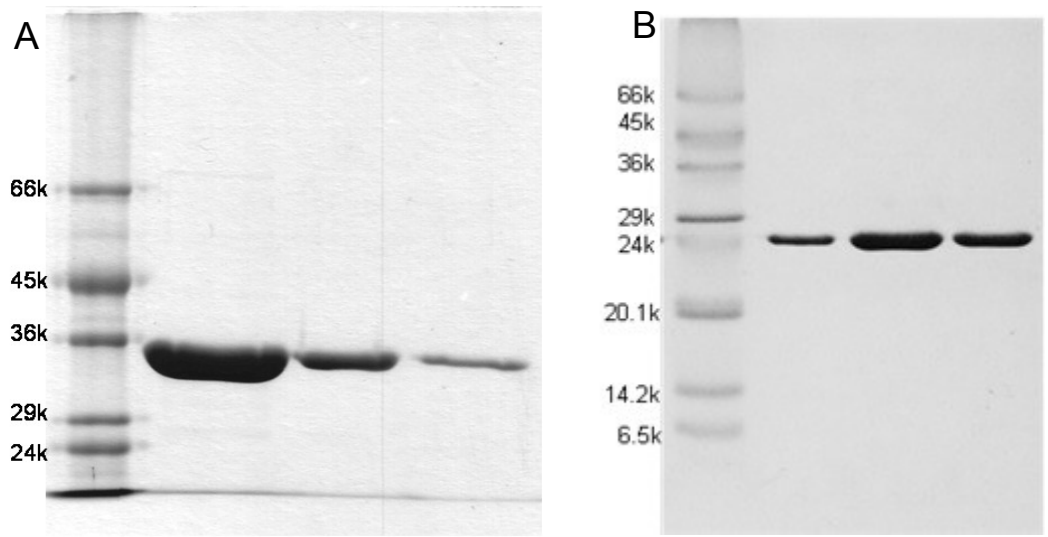

Figure S2.17 (A) 12% SDS-PAGE of *C. jejuni* DHDPS; (B) 15% SDS-PAGE of *C. jejuni* DHDPR. Left lane on A and B is M3913 Sigma Marker™ protein ladder.

CHAPTER 3. *R,R*-BISLYSINE: A POTENT, NONCOMPETITIVE SLOW-BINDING INHIBITOR OF DIHYDRODIPICOLINATE SYNTHASE FROM *CAMPYLOBACTER JEJUNI*

3.1 Introduction

Dihydrodipicolinate synthase (DHDPS, E.C. 4.2.1.52) is an enzyme catalyzing the condensation of pyruvate and (*S*)-aspartate-*β*-semialdehyde (ASA) into an unstable heterocyclic product (4*S*)-hydroxy-2,3,4,5-tetrahydro-(2*S*)-dipicolinate (HTPA), which spontaneously dehydrates into 2,3-dihydrodipicolinate (DHDP) (1, 2). DHDPS catalyzes the first committed step in L-lysine and *meso*-diaminopimelate biosynthesis in bacteria, plants and some fungi (*3-5*). L-Lysine and *meso*-diaminopimelate are essential components of bacterial cell walls (*6*). DHDPS is encoded by a *dapA* gene (*7*), and studies revealed that mutant auxotrophs for diaminopimelate undergo lysis in the absence of diaminopimelate in the medium (*8*). *E. coli* AT997 (a *dapA* mutant strain) can be maintained on nutrient medium only if the medium is supplemented with diaminopimelate (*7, 9*). As a result of studying the *B. subtilis* genome, *dapA* was classified as "essential" (*10*). Genome analysis and mapping by *in vitro* transposition in *H. influenza* putatively identified *dapA* as an "essential" gene (*11*). These results show that DHDPS is a potential target for drug development (*12*). However, Schnell *et al*. has shown that *Pseudomonas aeruginosa* mutants with *dapA* deleted are viable, implying that *dapA* is not an optimal target for drug development against that bacteria (*13*).

The activity of DHDPS is regulated by L-lysine, which binds at an allosteric site of the enzyme (*2*). DHDPS from plants and Gram-negative bacteria are more sensitive to lysine inhibition, showing micromolar or millimolar IC_{50} values (*14-18*). DHDPS from Gram-positive bacteria is weakly inhibited or insensitive to L-lysine (*19-21*).

Potent inhibitors of DHDPS have not yet been reported, despite many years effort. Various research groups focus mostly inhibitor design on the active site of the enzyme, and a number of millimolar range inhibitors have been presented in the literature. Among them are analogs of

substrates (pyruvate and ASA) (*12, 22, 23*), analogs of product (HTPA or DHDP) (*3, 12, 23-27*), and mimics of enzyme-bound condensation products of ASA and pyruvate (*28-31*).

Until now there were no attempts to design an allosteric inhibitor of DHDPS. Based on the results of isothermal titration calorimetry, Phenix and Palmer (*32*) suggested that an effective strategy of inhibitor design would be mimicking a pair of bound lysine molecules. The distance between the α-carbons of two bound L-lysines, based on the crystal structure of *E. coli* DHDPS PDB ID 1YXD is 4.1 Å. This distance appeared to be able to accommodate a two-carbon bridge connecting to the lysine molecules (Figure 3.1). The resulting molecule "bislysine" would have stereocenters designated *R*- (due to the change in substituent priorities) to mimic (*S*)-lysine. This bis-inhibitor analog we predicted would be more effective than lysine itself, because the entropic barrier to binding of the second inhibitor molecule would be eliminated.

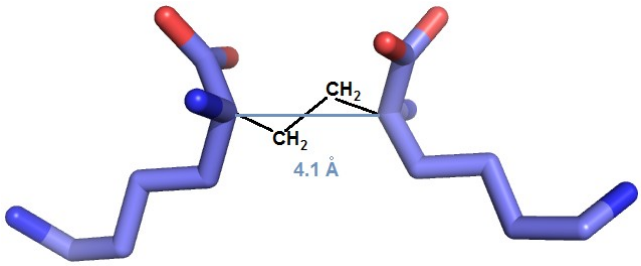

Figure 3.1 Crystal structure of two L-lysines bound at the allosteric site of *E. coli* DHDPS (PDB ID 1YXD).

Here we report the synthesis of *R,R*-bislysine, and its potent inhibition of DHDPS from *Campylobacter jejuni*. We have shown that *R,R*-bislysine is a close mimic and superior inhibitor to lysine.

The inhibitory activity of L-thialysine (*S*-aminoethyl-L-cysteine), a known weak noncompetitive inhibitor of *E. coli* DHDPS, and α-methyl-DL-lysine, a close mimic of L-lysine with a methyl substituent at the α carbon was also tested. This study will explore how tolerant the allosteric site of DHDPS is to different functionalities.

3.2 Experimental

3.2.1 General experimental procedures

Chemicals were purchased from Sigma-Aldrich Canada, Ltd (Oakville, ON) or Alfa Aesar (Ward Hill, MA). Reactions that required anhydrous conditions were conducted under a dry nitrogen atmosphere using oven-dried glassware. Dry DCM and THF were obtained using a MB-Solvent Purification System (University of Saskatchewan); diisopropylamine was freshly distilled from CaH_2. HMPA was distilled under vacuum from CaH_2 and stored over activated 4Å molecular sieves. Flash chromatography was performed using Merck silica gel 60 (230-400 mesh). Thin layer chromatography was conducted using silica gel 60 F_{254} aluminum plates; visualisation of spots was performed under UV lamp (254 nm) and by charring after treatment with cerium phosphomolybdate. NMR spectra were recorded on a Bruker 500 MHz spectrometer. Mass spectra were acquired on a Qstar XL MS/MS System Applied Biosystems/MDS Sciex and VG 70-VSE mass spectrometer (VG Analytical Inc. Ltd.) at the Saskatchewan Structural Sciences Centre.

3.2.2 α-Methyl-DL-lysine synthesis

Methyl (2*S*)-2,6-diaminohexanoate (1)

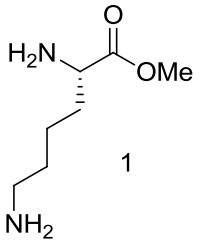

1

A round bottom flask was charged with methanol (10 ml) under a nitrogen atmosphere and cooled on ice. Acetyl chloride (1.17 ml, 16.4 mmol) was added dropwise with stirring over a period of 10 min. The solution was stirred for 5 min, then solid (*S*)-lysine (monohydrochloride) (1.0 g, 5.48 mmol) was added in one portion to the flask and the resulting suspension was slowly heated to reflux. After 2 h of refluxing (at 65 °C) the mixture was cooled down and solvent was evaporated *in vacuo* to afford a white crystalline product **1** as a dihydrochloride salt in 98% yield (1.25 g, 5.36 mmol). The product was used for the next step without further purification. ^{1}H

NMR (500 MHz, D_2O): δ 4.14 (t, *J* = 6.4 Hz, 1H), 3.82 (s, 3H), 2.98 (t, *J* = 7.6 Hz, 2H), 2.05 – 1.87 (m, 2H), 1.68 (p, *J* = 7.6 Hz, 2H), 1.57 – 1.38 (m, 2H).

Methyl (2*S*)-2,6-bis{[(tert-butoxy)carbonyl]amino}hexanoate (2)

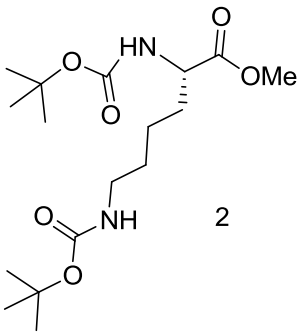

2

The starting material **1** (1.25 g, 5.37 mmol) was added to dry THF (16 ml) in a round-bottom flask under nitrogen, followed by triethylamine (2.99 ml, 21.46 mmol), and the resulting suspension was cooled on ice. A solution of di-*tert*-butyl dicarbonate (2.34 g, 10.73 mmol) in dry THF (16 ml) was added slowly over period of 1 h to the stirring suspension. The ice bath was removed and the mixture was left stirring for 14 h at rt and then warmed at 50 °C for 3 h. The solvent was removed under reduced pressure and the residue was partitioned between diethyl ether and a saturated solution of sodium bicarbonate (20 ml each). The aqueous layer was additionally extracted by diethyl ether (30 ml). The combined ethereal layer was washed with brine, dried with anhydrous sodium sulfate, and concentrated *in vacuo*. Purification by FCC (25% EtOAc:hexane) afforded a white solid **2** in quantitative yield (1.92 g, 5.33 mmol). ^{1}H NMR (500 MHz, $CDCl_3$): δ 5.08 (d, *J* = 6.9 Hz, 1H), 4.56 (bs, 1H), 4.28 (q, *J* = 7.2, Hz, 1H), 3.73 (s, 3H), 3.11 (dd, *J* = 12.3 Hz, *J* = 6.3 Hz, 2H), 1.85 – 1.75 (m, 1H), 1.69 – 1.59 (m, 1H), 1.55 – 1.45 (m, 2H), 1.44 (s, 18H), 1.40 – 1.30 (m, 2H).

Methyl (±)-2,6-bis{[(tert-butoxy)carbonyl]amino}-2-methylhexanoate (3)

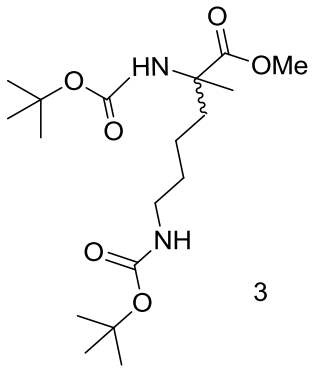

3

A dry round bottom flask was charged with dry THF (7 ml) under nitrogen. Freshly distilled diisopropylamine (0.29 ml, 2.08 mmol) was added via syringe and the flask was cooled to -78 °C in a dry ice/acetone bath. A freshly titrated solution of *n*-butyllithium (0.93 ml, 1.89 mmol) in hexanes was added dropwise over a period of 10 min, and the reaction flask was then placed on ice for 30 min to form LDA. The solution was cooled down again to -78 °C. Compound **2** (0.200 g, 0.556 mmol) was dissolved in a minimum amount of dry THF (1 ml) and the resulting solution was added slowly via syringe to the stirring solution of LDA over a period of 10 min and the reaction was left to stir for 30 min. Finally, neat methyl iodide (0.19 ml, 3.06 mmol) was added. After 1 h, the reaction was quenched by a saturated solution of NH_4Cl, and the mixture was partitioned between ethyl acetate (20 ml) and saturated NH_4Cl (20 ml). The organic phase was washed with saturated $NaHCO_3$ (25 ml) and then brine (25 ml). The organic solvent was evaporated under reduced pressure affording a yellow oily residue. FCC (20% EtOAc/hexane) afforded the title compound **3** (as a racemic mixture) in a 54% yield as colorless oil (0.112 g, 0.300 mmol).^{1}H NMR (500 MHz, $CDCl_3$): δ 5.32 (bs, 1H), 4.54 (bs, 1H), 3.72 (s, 3H), 3.09 (d, *J* = 5.2 Hz, 2H), 2.03 (bs, 1H), 1.77 (td, *J* = 13.0 Hz, *J* = 4.6, 1H), 1.50 (s, 3H), 1.48 – 1.42 (m, 1H), 1.42 (s, 9H), 1.44 (s, 9H), 1.34 – 1.22 (m, 1H), 1.18 – 1.06 (m, 1H). ^{13}C NMR (125 MHz, $CDCl_3$): δ 175.1, 156.2, 154.5, 79.5, 79.2, 59.6, 52.7, 40.1, 36.6, 30.0, 28.54, 28.48, 23.6, 21.5. HRMS *m/z* calcd. for $C_{18}H_{34}N_2O_6Na$ $[M + Na]^+$ 397.2309, found 397.2305 (ESI).

(±)-2,6-diamino-2-methylhexanoic acid (α-methyl-DL-lysine) (4)

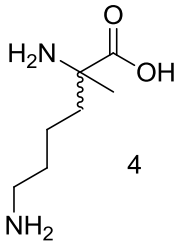

4

A 1:1 mixture of 12M HCl and MeOH (6 ml) was added to the racemic mixture **3** (0.056 g, 0.149 mmol) and stirred at rt for 1h. The solvent was evaporated *in vacuo* and 6M HCl (aqueous) (5 ml) was added to the remaining residue. The resulting solution was heated to reflux. After 8 h the solvent was evaporated under reduced pressure affording racemic mixture **4** as a yellow solid in 91% yield (0.032 g, 0.136 mmol) in a form of dihydrochloride salt. ^{1}H NMR (500 MHz, D_2O): δ 2.98 (t, *J* = 7.6 Hz, 2H), 2.00 – 1.92 (m, 1H), 1.92 – 1.83 (m, 1H), 1.68 (p, *J* = 7.6 Hz, 2H), 1.56 (s, 3H), 1.52 – 1.49 (m, 1H), 1.38 – 1.28 (m, 1H). ^{13}C NMR (125 MHz, D_2O): δ 174.4, 60.2, 39.0, 36.2, 26.6, 21.7, 20.2. HRMS *m/z* calcd. for $C_7H_{17}N_2O_2$ $[M + H]^+$ 161.1284, found 161.1279 (ESI).

3.2.3 (±)-Bislysine synthesis

Dimethyl 2,5-dibromohexanedioate (5)

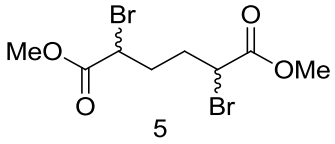

5

The procedure of obtaining *meso*-2,5-dibromohexanedioate from hexanedioyl dichloride (*33*) was reported previously (*34*). Neat thionyl chloride (40.0 g, 342 mmol) was added to hexanedioic (adipic) acid (20.0 g, 137 mmol) and refluxed under an inert atmosphere at 80 °C for 3 h. Excess thionyl chloride was removed under reduced pressure. To the remaining hexanedioyl dichloride, neat bromine (54.7 g, 342 mmol) was added and the mixture was heated to 80 °C using similar reaction setup as described by Watson and O'Neill (*34*). Additionally, a 500 Watt halogen lamp was placed approximately 10 cm from the reaction flask. The bromination reaction

was monitored by NMR and an additional 0.25 equivalents of bromine were added until the reaction was complete. After the reaction was completed (6 – 7 h) the excess bromine was removed by purging with a stream of nitrogen gas into the flask (*34*), and the crude product was added dropwise (via a syringe) to cold methanol (140 ml) on ice. The resulting suspension was left stirring for 14 h at room temperature. The product was then filtered. The product was obtained in 87% yield (39.6 g, 119 mmol). ^{1}H NMR (500 MHz, $CDCl_3$): δ 4.26 (t, J = 4.4 Hz, 2H), 3.80 (s, 3H), 2.35 – 2.26 (m, 2H), 2.12 – 2.02 (m, 2H). ^{13}C NMR (125 MHz, $CDCl_3$): δ 165.6, 54.4, 45.9, 34.6. HRMS *m/z* calcd. for $C_8H_{16}N_1Br_2O_4$ $[M + NH_4]^+$ 349.9426, found 349.9419 (CI).

Dimethyl 2,5-bis(1,3-dioxo-2,3-dihydro-1*H*-isoindol-2-yl)hexanedioate (6)

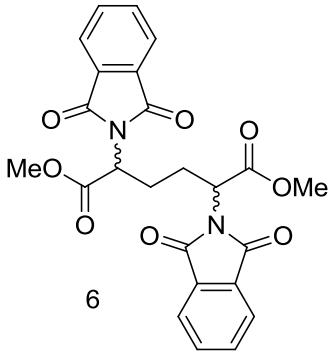

6

The mixture of stereoisomers **6** was obtained using a reported method (*35*). To a stirring solution of **5** (3.80 g, 11.4 mmol) in dry DMF (20 ml), potassium phthalimide (10.5 g, 56.7 mmol) was added in one portion. The mixture was heated to 90 °C, and the reaction continued for 2 h. Then the cooled reaction mixture was diluted with chloroform (25 ml) and the resulting solution was poured into water (100 ml). The organic layer was separated and the aqueous layer was extracted twice with chloroform. The chloroform layers were combined and the organic solvent was evaporated under reduced pressure to the point of crystallisation, followed by addition of diethyl ether (30 ml) to promote rapid crystallization. The product was washed with diethyl ether and dried *in vacuo* to obtain **6** as an off-white solid in 90% yield (4.77 g, 10.3 mmol), which was used for the next step. ^{1}H NMR (500 MHz, $CDCl_3$): δ 7.90 – 7.85 (m, 4H), 7.89 – 7.74 (m, 4H), 4.81 (t, J = 5.0, Hz, 2H,), 3.68 (s, 6H), 2.39 – 2.29 (m, 2H), 2.29 – 2.19 (m, 2H). ^{13}C NMR (125 MHz, $CDCl_3$): δ 165.2, 163.6, 131.8, 129.5, 121.7, 54.0, 53.1, 28.6. HRMS *m/z* calcd. for $C_{24}H_{20}N_2O_8$ $[M^{\bullet+}]$ 464.1220, found 464.1230 (EI).

2,5-Diaminohexanedioic acid (7)

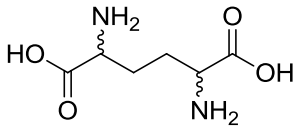

7

The reaction had been described by Sheehan (*35*), and following the reported procedure, to the mixture of stereoisomers **6** (21.9 g, 47.2 mmol), a 1:1 mixture of 48% HBr (in water) and glacial acetic acid (100 ml) was added, and the mixture was refluxed at 115 °C while stirring. After hydrolysis was completed (the reaction mixture becomes clear in approximately 14 days), the cooled reaction mixture was filtered to remove phthalic acid and the filtrate was evaporated *in vacuo*. The residue was dissolved in water (40 ml), filtered and the filtrate was neutralized with concentrated solution of ammonia. The obtained white precipitate was filtered and dried. The product mixture of stereoisomers **7** (7.9 g, 45.3 mmol) was obtained in 96% yield. ^{1}H NMR (500 MHz, CD_3OD): δ 4.09 (d, J = 2.2 Hz, 2H), 2.30 – 2.00 (m, 4H). ^{13}C NMR (125 MHz, CD_3OD): δ 165.6, 53.1, 28.5. HRMS *m/z* calcd. for $C_6H_{11}N_2O_4$ $[M - H]^-$ 175.0724, found 175.0729 (ESI).

Dimethyl 2,5-diaminohexanedioate dihydrochloride (8)

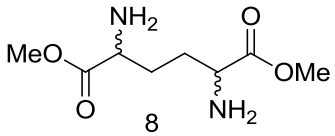

8

Esterification was carried out using a procedure described previously (*36*). A round bottom flask was charged with methanol (3.0 ml) and cooled on ice under nitrogen. Acetyl chloride (0.189 ml, 2.73 mmol) was added dropwise over a period of 10 min. The solution was stirred for 5 min, then solid compound **7** (2,5-diaminoadipic acid) (80 mg, 0.455 mmol) was added in one portion to the flask and the resulting suspension was slowly heated to reflux. After 2 h of refluxing (at 65 °C) the mixture was cooled down and solvent was evaporated *in vacuo* to afford a white crystalline product **8** as a dihydrochloride salt in quantitative yield (126 mg, 0.455 mmol). The product was used for the next step without further purification. ^{1}H NMR (500 MHz, CD_3OD): δ 4.18 – 4.15 (m, 2H), 3.87 (s, 6H), 2.25 – 1.95 (m, 4H). ^{13}C NMR (125 MHz,

CD_3OD): δ 165.6, 53.1, 28.5. HRMS *m/z* calcd. for $C_8H_{16}N_2O_4$ [$M^{\bullet+}$] 204.1110, found 204.1100 (EI).

Dimethyl 2,5-bis([(*tert*-butoxy)carbonyl]amino)hexanedioate (9)

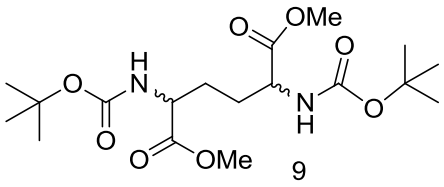

9

The protection of amino groups was carried out using a procedure reported by Dondoni (*36*). The starting material **8** (2.08 g, 7.51 mmol) was added to THF (30 ml) in a round-bottom flask under nitrogen, followed by triethylamine (4.19 ml, 30.0 mmol), and the resulting suspension was cooled on ice. A solution of di-*tert*-butyl dicarbonate (4.91 g, 22.5 mmol) in THF (30 ml) was added slowly over period of 1 h to the stirring suspension. The ice bath was removed and the mixture was left stirring for 14 h at rt and then warmed at 50 °C for 3 h. The solvent was removed under reduced pressure and the residue was partitioned between diethyl ether and a saturated solution of sodium bicarbonate (40 ml each). The aqueous layer was additionally extracted by diethyl ether (30 ml). The combined ethereal layer was washed with brine, dried with anhydrous sodium sulfate, and concentrated *in vacuo*. Purification by flash column chromatography (20% EtOAc:hexane) afforded a white crystalline solid **9** in 72% yield (2.18 g, 5.41 mmol). ^{1}H NMR (500 MHz, $CDCl_3$): δ 5.15 – 5.02 (m, 2H), 4.29 (s, 2H), 3.73 (s, 6H), 1.95 – 1.77 (m, 2H), 1.75 – 1.60 (m, 2H), 1.43 (s, 18H). ^{13}C NMR (125 MHz, $CDCl_3$): δ 168.6, 152.0, 80.1, 54.4, 53.6, 31.0, 30.6. HRMS *m/z* calcd. for $C_{18}H_{32}N_2O_8Na$ [M + Na]$^+$ 427.2050, found 427.2062 (ESI).

Mixture of dimethyl (2*R*, 5*R*)-2,5-bis([(*tert*-butoxy)carbonyl]amino)-2,5-bis(4-chlorobutyl)hexanedioate and dimethyl (2*S*, 5*S*)-2,5-bis([(*tert*-butoxy)carbonyl]amino)-2,5-bis(4-chlorobutyl)hexanedioate (10a); dimethyl (2*R*, 5*S*)-2,5-bis([(*tert*-butoxy)carbonyl]amino)-2,5-bis(4-chlorobutyl)hexanedioate (10b)

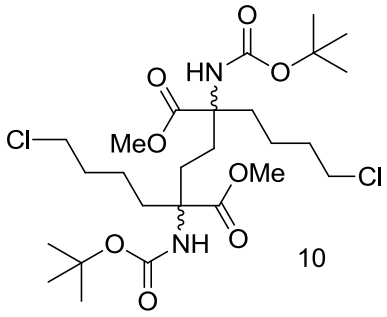

10

A dry round bottom flask was charged with a 10% solution of HMPA in dry THF (10 ml) under nitrogen. Freshly distilled diisopropylamine (0.59 ml, 4.18 mmol) was added via syringe and the flask was cooled to -78 °C in a dry ice/acetone bath. A freshly titrated solution of *n*-butyllithium (1.61 ml, 3.80 mmol) in hexanes was added dropwise over a period of 10 min, and the reaction flask was then placed on ice for 30 min to form LDA. The solution was cooled down again to -78 °C. The mixture **9** (0.349 g, 0.863 mmol) was dissolved in a minimum amount of dry THF (approximately 2 ml) and the resulting solution was added slowly via syringe to the stirring solution of LDA over a period of 20 min and the reaction was left to stir for 30 min. An additional portion of *n*-butyllithium (0.73 ml, 1.73 mmol) was added slowly, and the reaction was stirred for another 15 min. Finally, neat 1-bromo-4-chlorobutane (0.30 ml, 2.59 mmol) was added and the reaction monitored by TLC. After 45 min, the reaction was quenched by a saturated solution of NH_4Cl, and the mixture was partitioned between ethyl acetate (25 ml) and saturated NH_4Cl (25 ml). The organic phase was washed with saturated $NaHCO_3$ (25 ml) and then brine (25 ml). The organic solvent was evaporated under reduced pressure affording a yellow oily residue. Flash column chromatography (15% EtOAc/hexane) afforded the title compounds **10a** and **10b** in a 12% yield as white crystalline solids (50 mg, 0.085 mmol and 12 mg, 0.021 mmol respectively). The *meso* compound **10b** eluted first followed by the racemic mixture **10a**. One third of the starting material was recovered. Monoalkylated side products as well as some elimination side products were also observed. The *meso* compound **10b** and the racemic mixture **10a** were distinguished later, after the inhibition tests with DHDPS. **10a**: ^1H

NMR (500 MHz, $CDCl_3$): δ 5.41 (bs, 2H), 3.74 (s, 6H), 3.49 (t, *J* = 6.6 Hz, 4H), 2.30 – 2.12 (m, 4H), 1.72 (t, *J* = 6.9 Hz, 4H), 1.78 – 1.68 (m, 2H), 1.49 (t, *J* = 11.7 Hz, 2H), 1.42 (s, 18H), 1.42 – 1.32 (m, 2H), 1.22 – 1.10 (m, 2H). ^{13}C NMR (125 MHz, $CDCl_3$): δ 169.8, 150.5, 79.4, 63.7, 53.9, 46.1, 36.4, 34.3, 32.0, 30.7, 23.8. HRMS *m/z* calcd. for $C_{26}H_{46}N_2O_8Cl_2Na$ $[M + Na]^+$ 607.2523, found 607.2503 (ESI). **10b**: ^{1}H NMR (500 MHz, $CDCl_3$): δ 5.62 (bs, 2H), 3.74 (s, 6H), 3.49 (dt, *J* = 6.6 Hz, *J* = 1.3 Hz, 4H), 2.35 – 2.25 (m, 2H), 2.04 (d, *J* = 7.6 Hz, 2H), 1.75 – 1.64 (m, 8H), 1.43 (s, 18H), 1.42 – 1.35 (m, 2H), 1.17 – 1.05 (m, 2H). ^{13}C NMR (125 MHz, $CDCl_3$): δ 169.7, 150.2, 79.2, 64.1, 54.1, 46.1, 36.6, 34.3, 32.5, 30.7, 23.9. HRMS *m/z* calcd. for $C_{26}H_{46}N_2O_8Cl_2Na$ $[M + Na]^+$ 607.2523, found 607.2525 (ESI).

Mixture of dimethyl (2*R*, 5*R*)-2,5-bis([(*tert*-butoxy)carbonyl]amino)-2,5-bis[4-(1,3-dioxo-2,3-dihydro-1*H*-isoindol-2-yl)butyl]hexanedioate and dimethyl (2*S*, 5*S*)-2,5-bis([(*tert*-butoxy)carbonyl]amino)-2,5-bis[4-(1,3-dioxo-2,3-dihydro-1*H*-isoindol-2-yl)butyl]hexanedioate (11)

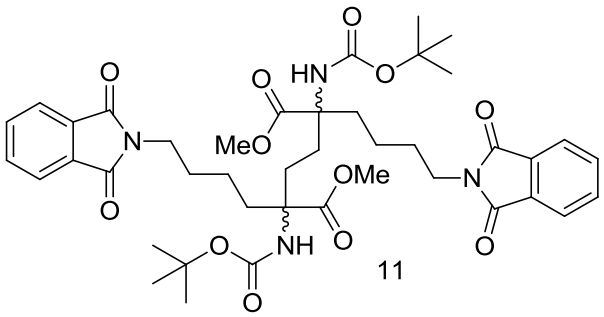

11

To a solution of **10a** (61.9 mg, 0.106 mmol) in dry DMF (4 ml), solid potassium phthalimide (98 mg, 0.522 mmol) was added in one portion, followed by finely ground potassium iodide (43.9 mg, 0.265 mmol). The mixture was heated to 90 °C under nitrogen. After 2 h, DMF was evaporated under reduced pressure, and the residue was partitioned between chloroform and water (5 ml of each), and the aqueous layer was extracted twice with chloroform (2 ml). The organic layers were combined and the solvent evaporated *in vacuo*. Flash column chromatography (40% EtOAc/hexane) gave the title mixture **11** in 50% yield (43 mg, 0.053 mmol) as colourless oil. ^{1}H NMR (500 MHz, $CDCl_3$): δ 7.82 (dd, *J* = 5.4 Hz, *J* = 3.2 Hz, 4H), 7.69 (dd, *J* = 5.4 Hz, *J* = 3.2 Hz, 4H), 5.40 (bs, 2H), 3.71 (s, 6H), 3.61(dt, *J* = 7.3 Hz, *J* = 2.8 Hz, 4H), 2.18 (bs, 4H), 1.76 (dt, *J* = 13.2 Hz, *J* = 4.4 Hz, 2H), 1.65 – 1.56 (m, 4H), 1.50 (t, *J* = 11.7 Hz, 2H), 1.38 (s, 18H), 1.30 – 1.20 (m, 2H), 1.05 (bs, 2H). ^{13}C NMR (125 MHz, $CDCl_3$): δ

174.1, 168.4, 153.9, 134.0, 132.2, 123.3, 79.4, 62.9, 52.8, 37.7, 35.0, 29.7, 28.4, 21.3. HRMS *m/z* calcd. for $C_{42}H_{54}N_4O_{12}Na$ $[M + Na]^+$ 829.3630, found 829.3638 (ESI).

Mixture of (2*R*, 5*R*)-2,5-diamino-2,5-bis(4-aminobutyl)hexanedioate tetrabromide and (2*S*, 5*S*)-2,5-diamino-2,5-bis(4-aminobutyl)hexanedioate tetrabromide (12)

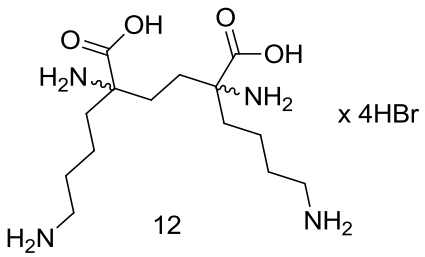

12

A 1:1 mixture of 48% HBr (in water) and glacial acetic acid (4 ml) was added to the racemic mixture **11** (33.6 mg, 0.0416 mmol) and heated to 115 °C. After 3 days the solvent was evaporated under reduced pressure and the brown residue was dissolved in distilled water (1.5 ml). Cation exchange resin, AG 50W-X2 (Bio-Rad) (acidic form), was prepared according to the manufacture's procedure and packed in a glass Pasteur pipette (6 cm high). The sample dissolved in water was slowly applied onto the column. The column was washed first with water (10 ml), then with 1M HBr (10 ml), and eluted with 2M HBr (15 ml). Fractions eluting with 2M HBr were evaporated under reduced pressure and the product **12** was obtained as a colorless solid in 88% yield (23.5 mg, 0.0366 mmol). ^{1}H NMR (500 MHz, D_2O): δ 3.05 (t, J = 7.6 Hz, 4H), 2.13 – 1.99 (m, 4H), 1.99 – 1.85 (m, 4H), 1.75 (p, J = 7.6 Hz, 4H), 1.61 – 1.59 (m, 2H), 1.43 – 1.31 (m, 2H). ^{13}C NMR (125 MHz, D_2O): δ 170.8, 65.9, 42.6, 38.4, 33.9, 30.7, 24.4. HRMS *m/z* calcd. for $C_{14}H_{31}N_4O_4$ $[M + H]^+$ 319.2339, found 319.2352 (ESI).

Mixture of dimethyl (2*R*, 5*R*)-2,5-diamino-2,5-bis[4-(1,3-dioxo-2,3-dihydro-1*H*-isoindol-2-yl)butyl]hexanedioate and dimethyl (2*S*, 5*S*)-2,5-diamino-2,5-bis[4-(1,3-dioxo-2,3-dihydro-1*H*-isoindol-2-yl)butyl]hexanedioate (13)

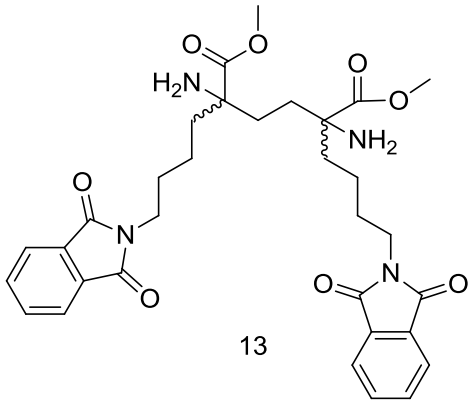

13

To the mixture **11** (23.4 mg, 0.0290 mmol) in dichloromethane (2.5 ml), TFA (2.5 ml) was added slowly and the mixture was stirred at rt for 1h. The solvent was evaporated *in vacuo* and the racemic mixture **13** was obtained in 98% yield (17.2 mg, 0.0284 mmol). ^{1}H NMR (500 MHz, CD_3OD): δ 7.88 – 7.83 (m, 4H), 7.83 – 7.79 (m, 4H), 3.85 (s, 6H), 3.69 (t, J = 6.9 Hz, 4H), 2.16 – 2.07 (m, 2H), 2.04 - 1.92 (m, 4H), 1.90 – 1.81 (m, 2H), 1.73 (m, 4H), 1.54 – 1.44 (m, 2H), 1.32 – 1.22 (m, 2H). ^{13}C NMR (125 MHz, CD_3OD): δ 171.4, 169.9, 135.5, 133.3, 124.2, 63.9, 54.2, 38.0, 36.5, 30.7, 29.2, 21.3. HRMS *m/z* calcd. for $C_{32}H_{39}N_4O_8$ $[M + H]^+$ 607.2762, found 607.2753 (ESI).

3.2.4 HPLC separation of the racemic mixture

HPLC analyses were performed on an Agilent 1100 series instrument consisting of a quaternary pump, autosampler, diode array detector (DAD) and evaporative light scattering detector (ELSD). Astec CHIROBIOTIC^{TM} T (25 cm x 10.0 mm, Supelco Analytical), a chiral semi-preparative column was used for separation of enantiomers. A 250 mM ammonium acetate buffer pH 4.5, with 70% methanol was used as a mobile phase for separation of protected **13** and deprotected **12** racemic mixtures. The mobile phase was degassed by sparging with helium for 20 min. Instrument parameters were set to the following: flow rate, 2.0 ml/min; injection volume, 25 µl; DAD, 254 nm; ELSD temperature, 50 ºC; ELSD gain, 5. Acquisition and processing of

data was done using ChemStation LC Software (Rev.B.04.02; Agilent Technologies Inc). All experiments were performed isocratically. The column was initially washed with methanol and equilibrated with the mobile phase for 30 min. For analytical separations, 1 mg/ml solutions of **13** and **12** were prepared in methanol and water, respectively. For quantitative separations a 5.3 mg/ml solution of compound **13** was prepared in methanol. Only the DAD detector was used for runs involving fraction collection. The middle fraction between peaks of enantiomers was discarded to avoid cross contamination. Fractions of each enantiomer were combined and evaporated under reduced pressure and moderate heating (40 ºC) to remove all ammonium acetate. The ^{1}H NMR spectrum of each sample was collected to confirm that ammonium acetate had been removed. Each enantiomer obtained was hydrolyzed and purified on a cation exchange column as described above in section 3.2.3 for product **12**. The purity of each enantiomer was judged by HPLC. The amount of sodium bromide in the samples was calculated using a calibration plot (Figure A 1). Each enantiomer was tested as an inhibitor of DHDPS. The active enantiomer was presumed to be the *R,R*-isomer, later confirmed by protein crystallography.

3.2.5 Expression and purification of DHDPS and DHDPR

DHDPS and DHDPR from *C. jejuni* were expressed and purified as described previously (*37*). The obtained proteins were concentrated to 0.37 mg/ml for DHDPS and 1.29 mg/ml for DHDPR. Enzyme concentrations were determined as reported (*37*), (CHAPTER 2). The proteins were aliquoted and stored at -80 °C.

3.2.6 Enzyme assays and inhibition studies

The activity of DHDPS was measured using a coupled assay (*38*). The initial velocity of the DHDPS enzymatic reaction was determined by monitoring the decrease in absorbance at 340 nm due to oxidation of NADH (ε_{340} = 6220 $M^{-1}cm^{-1}$) as described previously (*37*). All kinetic measurements were made in 100 mM HEPES buffer at pH 8.0. A one-mL assay contained 0.16 mM NADH, 0.37 μg of DHDPS, 7.15 μg DHDPR and varying concentrations of ASA (0.066 - 2.6 mM) and pyruvate (0.20 – 3.7 mM). A 0.0084 mM solution of *R,R*-bislysine was used in inhibition experiments. 0.1 M solutions of L-thialysine and α-methyl-DL-lysine were used for inhibition tests. All kinetic studies were carried out at 25 ºC and normal atmospheric pressure.

3.2.6.1 Slow-binding kinetic determination

Inhibition of DHDPS by *R,R*-bislysine happens in a time-dependent manner, and as such, experiments were performed by triggering the reaction by addition of DHDPS. Each progress curve was fit to Equation 3.1.

$$[P] = v_s t + \frac{v_z - v_s}{k_{obs}}(1 + e^{-k_{obs}t}) + d\,, \tag{3.1}$$

where v_s and v_z are velocities at steady-state and at time zero, k_{obs} is the frequency constant of the exponential phase, t is time, d is displacement or finite intercept, [P] is related to the amount of product produced.

3.2.6.2 Steady-state kinetic studies

DHDPS was preincubated with the inhibitor (and other components of the assay) for 1 min and the reaction was started with ASA. This way of conducting the experiments allows the inhibitor and the enzyme to form a complex, and the observed rate of the reaction is a steady-state velocity. The concentration of one substrate was varied, while the concentration of the other was kept constant at saturating level (2.6 mM for ASA and 3.7 mM for pyruvate). The models for *mixed partial* (Equation 3.2) and *noncompetitive partial* inhibition (Equation 3.3) were used to fit experimental data with SigmaPlot 10.0 (Systat Software, San Jose, CA).

$$\frac{v}{V_{\max}} = \frac{\dfrac{[S]}{K_s} + \dfrac{\beta[S]\,[I]^h}{K_s\,(\alpha K_i)^h}}{1 + \dfrac{[S]}{K_s} + \dfrac{[I]^{h'}}{K_i^{h'}} + \dfrac{[S]\,[I]^h}{K_s\,(\alpha K_i)^h}} \tag{3.2}$$

$$\frac{v}{V_{\max}} = \frac{\dfrac{[S]}{K_s} + \dfrac{\beta[S]\,[I]^h}{K_s\,K_i^h}}{1 + \dfrac{[S]}{K_s} + \dfrac{[I]^h}{K_i^h} + \dfrac{[S]\,[I]^h}{K_s\,K_i^h}} \tag{3.3}$$

$$\log\frac{v_i - v_{i(sat)}}{v_0 - v_i} = \log K - h\log I \tag{3.4}$$

where V_{max} is the maximum velocity, K_S is the dissociation constant of the ES complex, v is the initial velocity. K_i is the inhibition constant, I is the inhibitor concentration, S is the substrate

concentration, α and β are proportionality constants. The cooperativity coefficients h' and h correspond to *R,R*-bislysine binding to E and E:pyr respectively (Equation 3.2). For Equation 3.3, h is a cooperativity coefficient for *R,R*-bislysine binding to F and F:ASA forms of enzyme. Equation 3.4 is the Hill equation for partial inhibition, where v_i is the velocity in the presence of the inhibitor, v_0 is the velocity in the absence of the inhibitor, $v_{i(sat)}$ is the reaction velocity at saturating concentrations of inhibitor, and K is an apparent overall dissociation constant.

3.3 Results

3.3.1 Synthesis of α-methyl-DL-lysine

Synthesis of α-methyl-L-lysine in enantiomerically pure form has been described in the literature (*39*), however for the purposes of performing preliminary inhibition tests, the enantiomerically pure form of α-methyl-L-lysine was not required and therefore this method was not used. Instead, α-methyl-DL-lysine was synthesized as a racemic mixture using a simpler method involving protection of the amino and carboxyl groups, and alkylation by LDA and methyl iodide (Scheme 3.1).

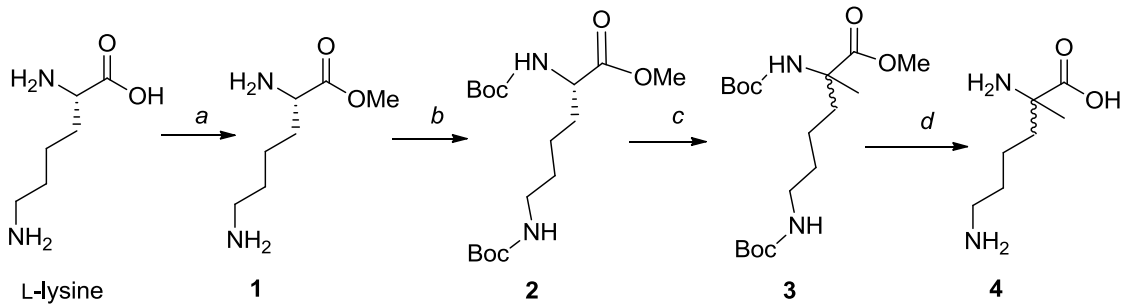

Scheme 3.1 Synthesis of α-methyl-DL-lysine.
Reagents: (a) AcCl, MeOH, 2 h, 65 °C, quant. yield; (b) DIBOC, TEA, THF, 14 h rt, 3 h 50 °C, quant. yield; (c) methyl iodide, LDA, THF, 1 h, -78 °C, 54%; (d) 1:1 12M HCl:MeOH, 1h, rt; 6M HCl (aqueous) 8 h, reflux, 91 %.

3.3.2 L-Thialysine and α-methyl-DL-lysine are weak inhibitors of DHDPS

L-Thialysine (Figure 3.2) is a very close mimic of L-lysine, having just one replacement of the methylene group for sulfur in the side chain. Despite the high structural similarity of lysine and thialysine, the latter is a weaker inhibitor with inhibition constants about one order of magnitude higher than the corresponding values for L-lysine in experiments with *E. coli* DHDPS (*40*). *C. jejuni* DHDPS is even less sensitive to L-thialysine inhibition than the *E. coli* enzyme, showing an apparent IC_{50} of 2 mM (Figure 3.3). Prior to attempting the synthesis of *R,R*-bislysine, the inhibitory properties of another lysine mimic, α-methyl-DL-lysine (Figure 3.2, Figure 3.3) were tested. These results indicate that the methyl group in the α position dramatically decreases inhibitory properties of the molecule (IC_{50}^{app} > 10 mM), possibly by preventing proper binding molecules of the inhibitor in the proximal allosteric sites.

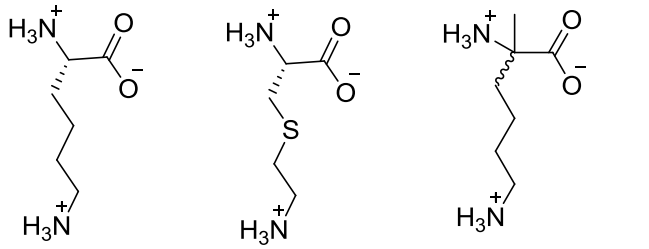

Figure 3.2 L-lysine and lysine analogs.

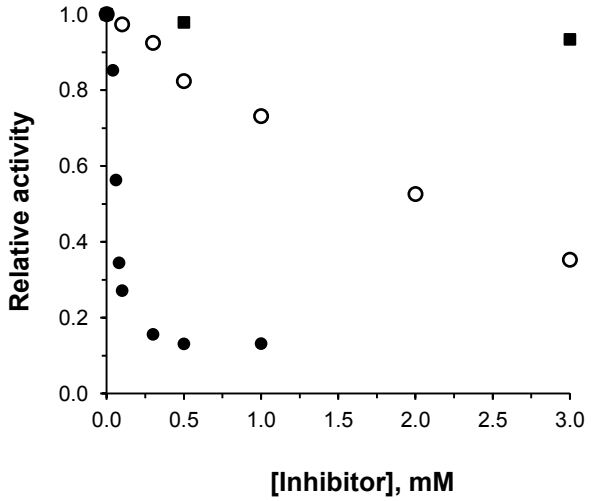

Figure 3.3 Comparison of inhibitory activity of some inhibitors. (●) L-Lysine, (○) L-thialysine, (■) α-methyl-DL-lysine. Concentrations of ASA and pyruvate 0.23 mM and 0.50 mM respectively.

3.3.3 Synthesis of (±)-bislysine

(±)-Bislysine was synthesized using a straightforward strategy: double alkylation of protected 2,5-diamino adipic acid (Scheme 3.2) using 1-bromo-4-chlorobutane followed by introduction of ε-amino groups on the side chains. Steps *a* - *e* (Scheme 3.2), which describe synthesis of 2,5-diamino adipic acid as a mixture of diastereomers, had been reported previously (*33-35*). The reported procedures of esterification of carboxyl groups and Boc protection of amino groups (*36*) were effectively applied to 2,5-diamino adipic acid (steps *f* - *g*, Scheme 3.2). Along with the required dialkylated product **10**, monoalkylated side products and products of elimination were

observed. In spite of the expected low yield of the alkylation step, (±)-bislysine was obtained in amounts sufficient for HPLC separation and inhibition kinetic studies.

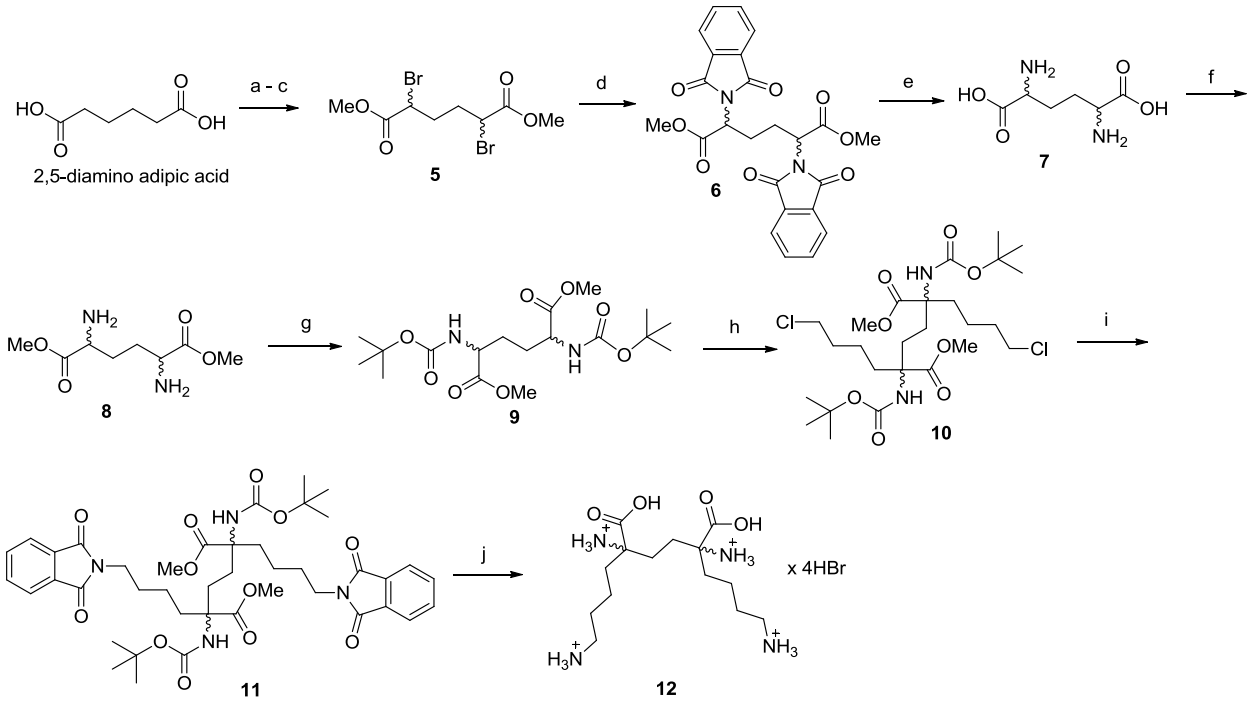

Scheme 3.2 Synthesis of (±)-bislysine.
Reagents: (a) $SOCl_2$, 80 °C, 3 h; (b) Br_2, 500 Watt, 12 h, 80 °C; (c) MeOH, 14 h, rt; a-c yield 87%; (d) potassium phthalimide, DMF, 90 °C, 2 h, 90%; (e) 1:1 48% HBr:AcOH, 14 d, 115 °C, 96%; (f) AcCl, MeOH, 2 h, 65 °C, quant. yield; (g) DIBOC, TEA, THF, 14 h rt, 3 h 50 °C, 72%; (h) 1-bromo-4-chlorobutane, LDA, THF/10% HMPA, 1 h, -78 °C, 12 %; (i) potassium phthalimide, DMF, 90 °C, 2 h, 50%; (j) 1:1 48% HBr:AcOH, 3 d, 115 °C, AG 50W-X2, 88%.

3.3.4 HPLC separation of (±)-bislysine

HPLC analysis confirmed the presence of two enantiomers in the racemic mixture of bislysine; two peaks with equal areas were detected (Figure 3.4). The separation was achieved using an Astec CHIROBIOTIC^{TM} T chiral column and 250 mM ammonium acetate buffer at pH 4.5 in 70% methanol as a mobile phase.

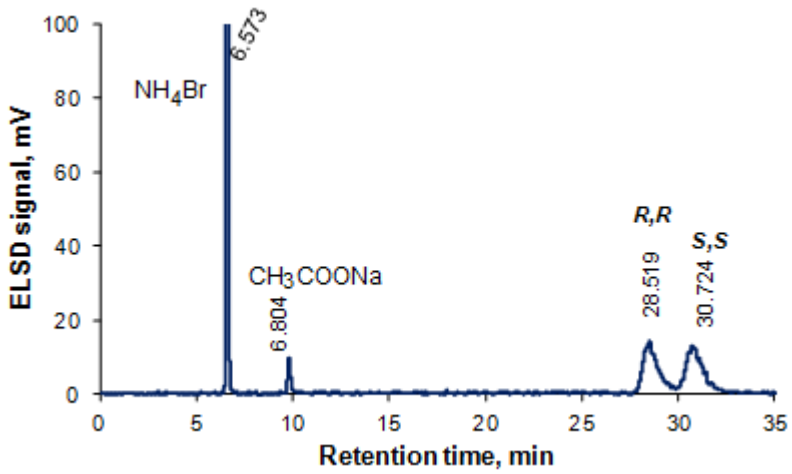

Figure 3.4 Separation of racemic mixture of bislysine, **12**. Astec CHIROBIOTIC^{TM} T column; 250 mM ammonium acetate buffer in 70% methanol, pH4.5; flow rate, 2.0 ml/min; injection volume, 25 µl; DAD, 254 nm; ELSD temperature, 50 ºC; ELSD gain, 5.

In order to obtain each individual enantiomer, (±)-bislysine in a partially protected form (Scheme 3.3) was used in quantitative HPLC separation. This racemic mixture **13** has advantages over the deprotected form **12**, such as it is UV active, which allowed us to monitor and control the collection of fractions, and it has shorter run time (Figure 3.5).

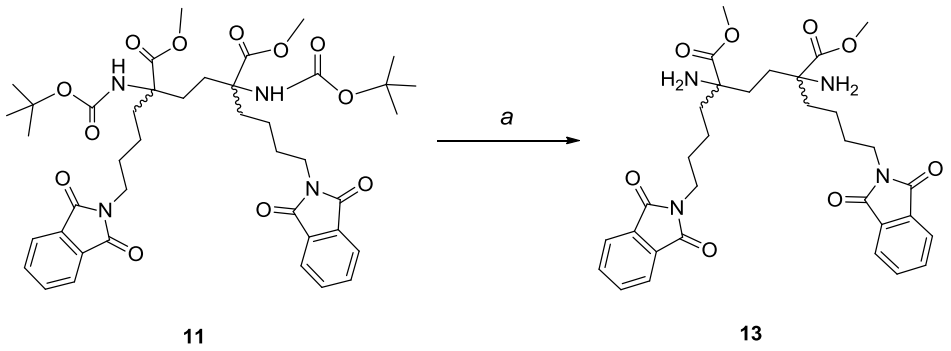

Scheme 3.3 Partial deprotection of bislysine precursor **11** to racemic mixture **13**. Reagents: (a) 1:1 DCM:TFA, rt, 1 h.

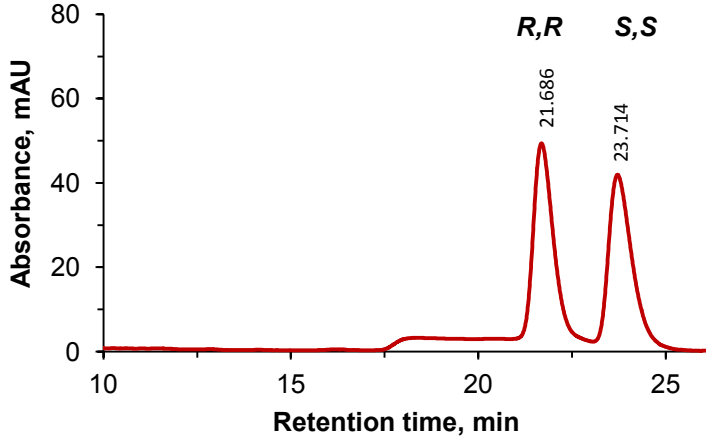

Figure 3.5 Separation of racemic mixture **13** by HPLC. Astec CHIROBIOTIC™ T column; 250 mM ammonium acetate buffer in 70% methanol, pH4.5; flow rate, 2.0 ml/min; injection volume, 25 µl; DAD, 254 nm.

After removal of ammonium acetate from samples, followed by hydrolysis and purification on an ion exchange column (as described in the experimental section 3.2.3), two individual enantiomers *R,R*- and *S,S*-bislysine were obtained, and the quality of separation was judged by HPLC (Figure 3.6, Figure 3.7).

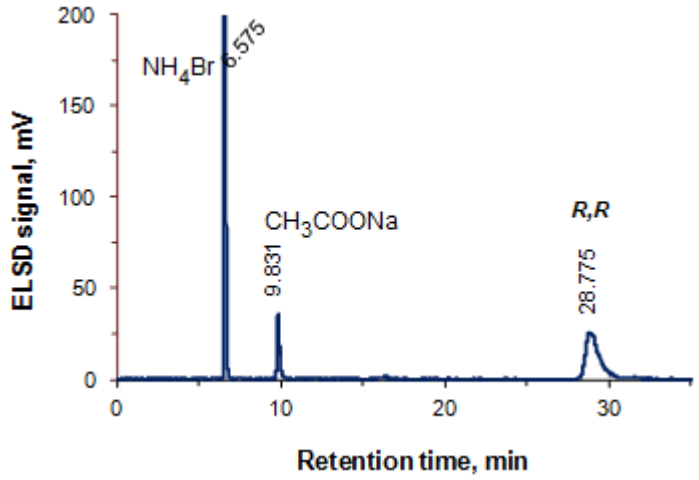

Figure 3.6 HPLC chromatogram of *R,R*-bislysine. Astec CHIROBIOTIC™ T column; 250 mM ammonium acetate buffer in 70% methanol, pH4.5; flow rate, 2.0 ml/min; injection volume, 25 µl; DAD, 254 nm; ELSD temperature, 50 ºC; ELSD gain, 5.

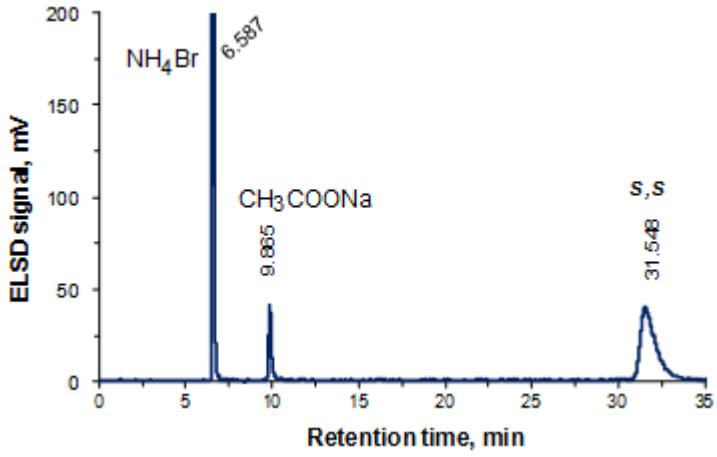

Figure 3.7 HPLC chromatogram of *S,S*-bislysine. Astec CHIROBIOTIC™ T column; 250 mM ammonium acetate buffer in 70% methanol, pH4.5; flow rate, 2.0 ml/min; injection volume, 25 µl; DAD, 254 nm; ELSD temperature, 50 ºC; ELSD gain, 5.

The samples of enantiomers were obtained as hydrobromide salts. Also, an impurity of sodium bromide was detected and calculated for each sample (Figure A 1, Table A 1, page 108). Prior to conducting inhibition kinetic studies with *R,R*-bislysine, it was found that sodium bromide in low concentrations (up to 2.0 µM) does not affect the enzymic reaction rate.

3.3.5 Slow-onset inhibition

The analysis of progress curves revealed that *R,R*-bislysine causes inhibition of DHDPS in a time dependent manner (Figure 3.8), where equilibrium between the free inhibitor and enzyme species establishes within the first minute.

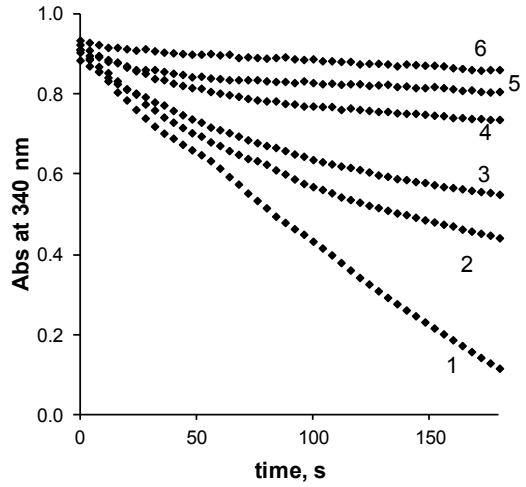

Figure 3.8 Progress curves of the enzymatic reaction in the presence of increasing concentrations of *R,R*-bislysine: (1) no inhibitor, (2) 0.084 μM, (3) 0.17 μM, (4) 0.42 μM, (5) 0.84 μM, (6) 1.7 μM. Concentrations of substrates: ASA 2.6 mM, pyruvate 3.7 mM. The curves were obtained by starting the reaction with the enzyme.

Similar to L-lysine (*37*), *R,R*-bislysine is a partial inhibitor of *C. jejuni* DHDPS. At saturating concentrations of *R,R*-bislysine (>1.7 μM) the enzyme still demonstrates 7-10% of the maximal activity (Figure A 2). Steady state velocities (slopes of the linear parts of the curves) approach the same value when triggering the reaction with either the enzyme or with ASA (Figure A 3) and therefore either method is suitable for initiating the enzymatic reaction. The inhibitor does not form any covalent bonds with the enzyme, which is supported by crystallographic data (Figure 3.12), therefore inhibition caused by *R,R*-bislysine is reversible. Two major models of slow-binding inhibition were described by Walsh (*41*), where one model describes initial fast binding of inhibitor to the enzyme, followed by slow isomerisation of [E:I] complex, and another model represents slow binding of inhibitor to the enzyme without isomerisation. The indication of the former model is a hyperbolic relationship between k_{obs} and [I], where for the latter model

the same relationship is linear. We have discovered a *linear relationship* between k_{obs} and inhibitor concentration (Figure 3.9), where formation of enzyme-inhibitor complexes are slow processes. Analysis of equations for slow-binding noncompetitive inhibition derived previously (*42, 43*) explains the linear relationship between k_{obs} and [I] (Scheme A 1, Equation A1, page 110). Additionally, the overlay of two crystal structures of DHDPS with lysine and *R,R*-bislysine (Figure A 4, page 110) shows that the structures are almost identical and there are no special structural features observed that suggests that the enzyme isomerizes upon binding of *R,R*-bislysine. This, again, suggests a one-step model of slow-binding inhibition, without isomerisation.

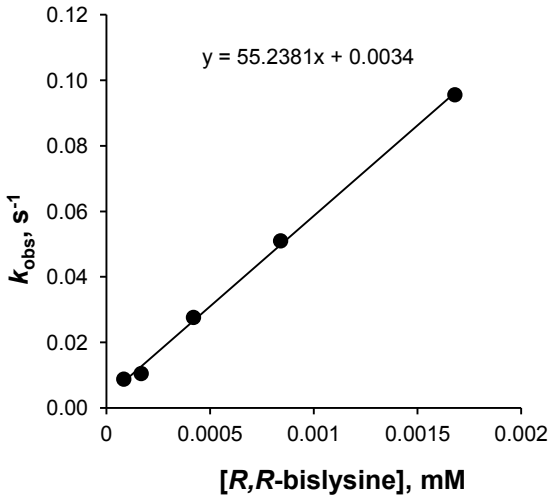

Figure 3.9 Relationship between k_{obs} and concentration of *R,R*-bislysine. Concentrations of substrates: ASA 2.6 mM, pyruvate 3.7 mM. The points were obtained by fitting Equation 3.1 to progress curves of the reactions started with DHDPS.

Assuming, that *R,R*-bislysine can bind all enzyme species, demonstrating a simple linear slow-onset inhibition, Scheme 3.4 is proposed:

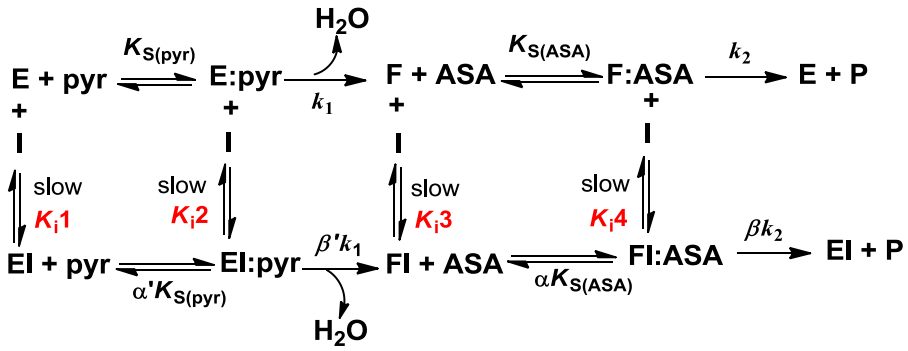

Scheme 3.4 General scheme of *R,R*-bislysine inhibition. For this scheme, there is no limit on the values of α (and α′), while β (and β′) must be <1 for inhibition. In a pure noncompetitive partial inhibition mechanism, α and α′ = 1, therefore $K_i3 = K_i4$, $K_i1 = K_i2$, whereas in a mixed partial inhibition mechanism, α and α′ ≠ 1 ($K_i1 \neq K_i2$, $K_i3 \neq K_i4$).

3.3.6 Steady-state inhibition studies

The kinetic analysis of DHDPS inhibition, triggered by the enzyme, has a disadvantage: the steady state may not be reached before a significant depletion of substrate, and as such parameters (k_{obs}, v_z, v_s), obtained by fitting Equation 3.1 to experimental progress curves at low substrate concentrations, may not be valid. Instead, we have used a short preincubation of the enzyme and the inhibitor in the assay buffer followed by addition of ASA to trigger the reaction. Equation 3.2 and Equation 3.3 were fit to the obtained steady-state velocities. The data was taken when concentration of one substrate was varied and concentration of another substrate was maintained at saturating level. Prior to global fitting, Hill coefficients were determined for *R,R*-bislysine using Equation 3.4. A series of Hill plots were built over a range of ASA and pyruvate concentrations and shown in Appendix A, Figure A 5 and Figure A 6. The average cooperativity coefficients of *R,R*-bislysine with respect to ASA and pyruvate are 1.7 ± 0.1 and 1.6 ± 0.1 respectively. The cooperativity of substrates does not change in the presence of the inhibitor and remains close to one. A *mixed partial* inhibition model successfully fit the experimental data obtained at saturating background concentration of ASA (2.6 mM) over a range of pyruvate concentrations (0.20 - 3.7 mM) (Figure 3.10).

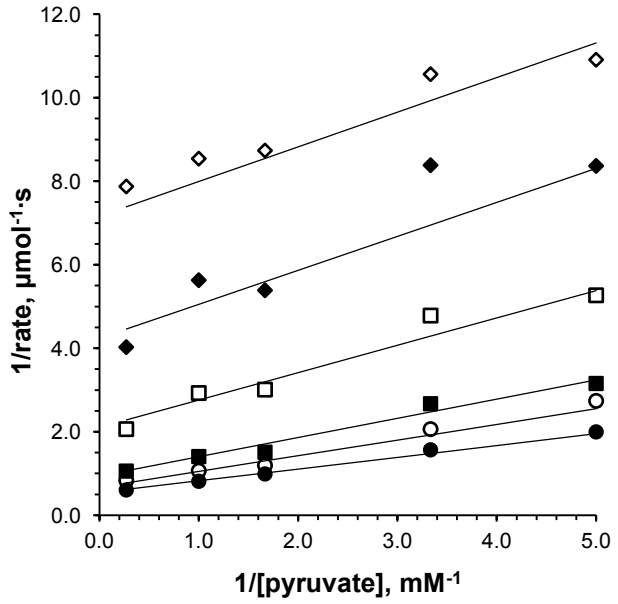

Figure 3.10 Double-reciprocal plot of data obtained after preincubating enzyme with *R,R*-bislysine for 1 min at a constant ASA concentration of 2.6 mM. Concentration of *R,R*-bislysine: (●) 0 µM, (○) 0.084 µM, (■) 0.17 µM, (□) 0.42 µM, (♦) 0.84 µM, (◇) 1.7 µM. Solid lines are fit lines, obtained by global fitting the *mixed partial* model to the data. Residuals are shown in Figure A 7.

The result of global fitting of a *noncompetitive partial* inhibition model to the data obtained at saturating concentration of pyruvate (3.7 mM) over a range of concentrations of ASA (0.066 - 2.6 mM) is presented in Figure 3.11.

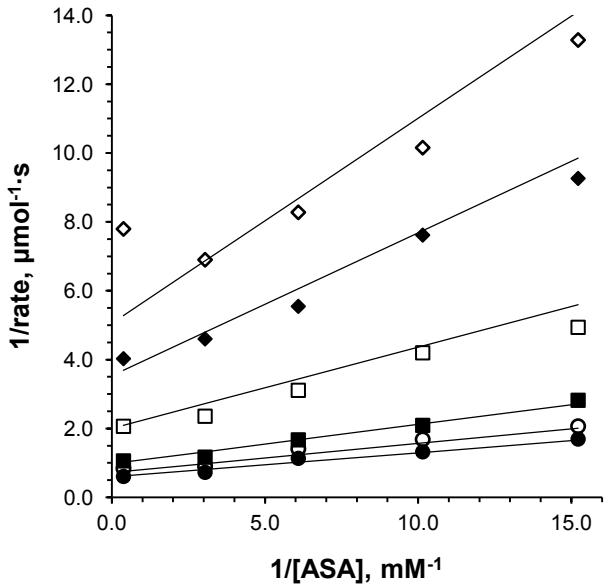

Figure 3.11 Double-reciprocal plot of data obtained after preincubating enzyme with *R,R*-bislysine for 1 min at a constant pyruvate concentration of 3.7 mM. Concentration of *R,R*-bislysine: (●) 0 µM, (○) 0.084 µM, (■) 0.17 µM, (□) 0.42 µM, (♦) 0.84 µM, (◇) 1.7 µM. Solid lines are fit lines, obtained by global fitting the *noncompetitive partial* model to the data. Residuals are shown in Figure A 8.

For the mixed partial inhibition model (with respect to pyruvate) the best fit was produced when cooperativity coefficients of *R,R*-bislysine binding to the E and E:pyr forms of the enzyme were equal 1.0 and 1.6 respectively (where the coefficient 1.6 was found by the graphical method and the coefficient 1.0 was found as a result of global fitting). Substitution of the average cooperativity coefficient of *R,R*-bislysine with respect to ASA, found by the graphical method (1.7 ± 0.1) in Equation 3.3 produces the best fit for the noncompetitive partial model. Based on information of L-lysine inhibition (*37*), the models of uncompetitive partial inhibition (where pyruvate is a varied substrate) and mixed partial model (where ASA is a varied substrate) were considered as well. Based on the comparison of statistical parameters (R^2) and analysis of diagnostic plots (Dixon and Cornish-Bowden plots are not shown) we conclude that, unlike L-lysine, *R,R*-bislysine binds (and demonstrates inhibitory properties) to both the free enzyme form E and the enzyme-pyruvate complex E:pyr with different affinities supporting the choice of the mixed partial model of inhibition. When ASA is a variable substrate, both mixed partial and noncompetitive partial models fit the data fairly well, but the noncompetitive partial model was

given a preference as a model providing a good fit with fewer variables (α = 1). The results of global fitting are summarized in the Table 3.1.

Table 3.1 *R,R*-bislysine inhibition kinetic results for *C. jejuni* DHDPS[a].

Kinetic model	Mixed partial	Noncompetitive partial
Variable substrate	Pyruvate	ASA
h_E	1.0 ± 0.2	
$h_{E:pyr}$	1.6 ± 0.1	
h_F		1.7 ± 0.1
$h_{F:ASA}$		1.7 ± 0.1
K_i1, nM	240 ± 50	
K_i2, nM	170 ± 70	
K_i3, nM		200 ± 20
K_i4, nM		200 ± 20

[a]These inhibition constants correspond to those in Scheme 3.4.

3.4 Discussion

Inhibition studies of DHDPS with L-thialysine showed that its apparent IC_{50} is approximately 30 times higher than that of lysine. The substitution of C-4 of lysine with sulfur slightly affects the length and volume of the side chain due to the larger atomic radius of sulfur, as well as the pK_a of the terminal amino group, which is lower than the pK_a of the corresponding group in lysine (9.52 and 10.53 respectively (*44, 45*)). α-Methyl-DL-lysine is a very poor inhibitor of DHDPS with an apparent IC_{50} value higher than 10 mM, which suggests that a steric clash between methyl groups prevents proper binding of this molecule. These results indicate that the allosteric site of *C. jejuni* DHDPS is very selective and proper distance between α carbons is required for inhibitory activity of "bridged" inhibitors, which is supported by these studies with *R,R*-bislysine.

Until this present work there were no inhibitors reported having stronger inhibitory properties than the natural inhibitor L-lysine. *R,R*-bislysine is the first inhibitor of DHDPS that is active in the submicromolar concentration range. In this study we have proven that it is possible to design a potent allosteric inhibitor of DHDPS mimicking binding of two lysine molecules in the

adjacent allosteric sites. The results of this study open new perspectives into the design and synthesis of allosteric inhibitors of DHDPS from different organisms. A straightforward, non-stereoselective synthetic route of bislysine synthesis was developed to confirm the validity of an idea that "bridging" of two lysine molecules would make a better inhibitor.

R,R-bislysine is a partial inhibitor of *C. jejuni* DHDPS. The minimal residual activity of the enzyme inhibited by *R,R*-bislysine is similar to that of L-lysine (7 - 10%) (*37*). Binding of *R,R*-bislysine is cooperative and the values of Hill coefficients (1.6 and 1.7) indicate that simultaneous binding of one molecule of *R,R*-bislysine at one pair of adjacent allosteric sites in the dimer promotes binding of another molecule of *R,R*-bislysine at the allosteric site of the other dimer. In other words, *C. jejuni* DHDPS demonstrates inter-dimer cooperativity upon binding of *R,R*-bislysine. The cooperativity coefficients of *R,R*-bislysine were introduced into equations of inhibition models. The mixed partial and noncompetitive partial models provide the best fit of the data, where the varied substrates are pyruvate and ASA, respectively. Analyzing the inhibition constants, presented in the Table 3.1, we conclude that *R,R*-bislysine binds with similar affinity to all enzyme species, with an average inhibition constant 200 nM. The inhibitory activity of *R,R*-bislysine is approximately 310 times higher than that of L-lysine, which allows us conclude that the design of a molecule that fits both adjacent allosteric sites in the dimer is a beneficial strategy in the development of new inhibitors of DHDPS. The crystal structure of *C. jejuni* DHDPS with *R,R*-bislysine bound at the allosteric site was solved at 2.2 Å resolution. The electron density confirms that the inhibitor in the allosteric site has *R* configuration of both stereogenic centers (Figure 3.12) (*Conly et al*., Unpublished work). Similar to lysine, *R,R*-bislysine makes hydrogen bonds with Ser51, Ala52, His59, Asn84', Glu88', Tyr110 and Ser51', Ala52', His59', Asn84, Glu88, Tyr110' and cation-π interactions with His56 and His56' (Figure 3.10). The distances between terminal amino groups of *R,R*-bislysine and the backbone carbonyls of Leu54 and Leu54' are longer compared to L-lysine in *C. jejuni* DHDPS (4.0 – 4.2 Å), and they are no longer able to make hydrogen bonds. The overlay of *R,R*-bislysine and two L-lysines bound in *C. jejuni* DHDPS shown in Figure 3.13.

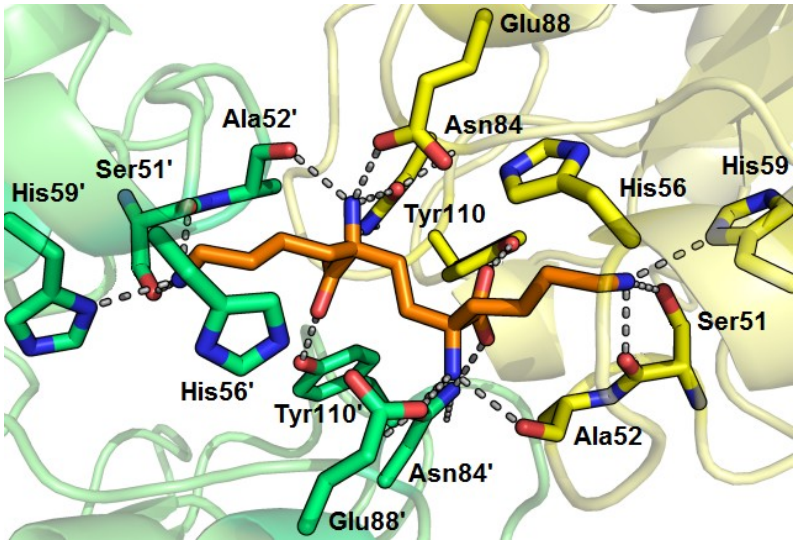

Figure 3.12 The crystal structure of *C. jejuni* DHDPS with *R,R*-bislysine bound at the allosteric site.

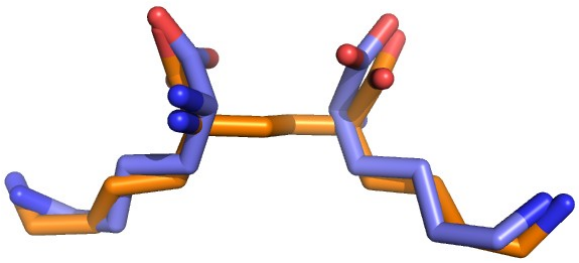

Figure 3.13 The overlay of crystal structures of *R,R*-bislysine and L-lysine bound at the allosteric site of *C. jejuni* DHDPS. L-Lysine is blue and *R,R*-bislysine is orange.

The loss of entropy upon binding of one *R,R*-bislysine molecule is lower than that of two molecules of L-lysine, which increases the total entropy of the system, and decreases the free energy of the system. The latter is likely the reason for the significant increase in an inhibitory activity of *R,R*-bislysine. The two carbon bridge in the molecule of *R,R*-bislysine does not make any polar or nonpolar contacts with the enzyme (does not change the enthalpy factor), which supports the assumption that binding affinity increases mostly due to the entropy factor.

S,S-bislysine and *R,S*-bislysine (*meso*-bislysine, obtained similar to (±)-bislysine from the product **10b**, described in 3.2.3) were tested in the assay and apparent IC_{50} values were estimated: ~50 μM and ~2 mM correspondingly. The low inhibitory activity of the *meso* compound is explained by its structural similarity to both L-lysine (a good inhibitor) and D-lysine

(a poor inhibitor (*16*)). *S,S*-bislysine is structurally similar to D-lysine and therefore its inhibitory activity should be lower than that of the *meso* compound. While it is possible for *S,S*-bislysine to inhibit DHDPS, the observed IC_{50} value being lower than that of the *meso* compound can be due to a slight contamination of *S,S*-bislysine with *R,R*-bislysine. Even a small amount of *R,R*-bislysine (below the HPLC detection limit) would decrease the IC_{50} of *S,S*-bislysine.

The design of the two carbon bridge in *R,R*-bislysine was a successful strategy to improve the effectiveness of the inhibitor; however its ability to rotate about the carbon bridge likely reduces its binding efficiency. The next step would be to design an inhibitor with "fixed" conformation and less freedom of rotation, and to decrease polarity of the molecule by replacing the carboxyl and amino groups with suitable isosteres.

3.5 References

1. Devenish, S. R., Blunt, J. W., and Gerrard, J. A. (2010) NMR studies uncover alternate substrates for dihydrodipicolinate synthase and suggest that dihydrodipicolinate reductase is also a dehydratase, *J Med Chem 53*, 4808-4812.
2. Blickling, S., Renner, C., Laber, B., Pohlenz, H. D., Holak, T. A., and Huber, R. (1997) Reaction mechanism of *Escherichia coli* dihydrodipicolinate synthase investigated by X-ray crystallography and NMR spectroscopy, *Biochemistry 36*, 24-33.
3. Walters, D. R., McPherson, A., and Robins, D. J. (1997) Inhibition of lysine biosynthesis in *Phytophthora infestans*, *Mycological Research 101*, 329-333.
4. Scapin, G., and Blanchard, J. S. (1998) Enzymology of bacterial lysine biosynthesis, *Advances in Enzymology, Vol 72 72*, 279-324.
5. Brock, T. D. (1974) *Biology of microorganisms*, 2d ed., Prentice-Hall, Englewood Cliffs, N.J.
6. Cummins, C. S., and Harris, H. (1956) The chemical composition of the cell wall in some gram-positive bacteria and its possible value as a taxonomic character, *J Gen Microbiol 14*, 583-600.
7. Yeh, P., Sicard, A. M., and Sinskey, A. J. (1988) General organization of the genes specifically involved in the diaminopimelate-lysine biosynthetic pathway of *Corynebacterium glutamicum*, *Mol Gen Genet 212*, 105-111.
8. Neidhardt, F. C., and Curtiss, R. (1996) *Escherichia coli and Salmonella: cellular and molecular biology*, 2nd ed., ASM Press, Washington, D.C.
9. Bukhari, A. I., and Taylor, A. L. (1971) Genetic analysis of diaminopimelic acid- and lysine-requiring mutants of *Escherichia coli*, *J Bacteriol 105*, 844-854.
10. Kobayashi, K., Ehrlich, S. D., Albertini, A., Amati, G., Andersen, K. K., Arnaud, M., Asai, K., Ashikaga, S., Aymerich, S., Bessieres, P., Boland, F., Brignell, S. C., Bron, S., Bunai, K., Chapuis, J., Christiansen, L. C., Danchin, A., Debarbouille, M., Dervyn, E., Deuerling, E., Devine, K., Devine, S. K., Dreesen, O., Errington, J., Fillinger, S., Foster, S. J., Fujita, Y., Galizzi, A., Gardan, R., Eschevins, C., Fukushima, T., Haga, K., Harwood, C. R., Hecker, M., Hosoya, D., Hullo, M. F., Kakeshita, H., Karamata, D., Kasahara, Y., Kawamura, F., Koga, K., Koski, P., Kuwana, R., Imamura, D., Ishimaru, M., Ishikawa, S., Ishio, I., Le Coq, D., Masson, A., Mauel, C., Meima, R., Mellado, R. P., Moir, A., Moriya, S., Nagakawa, E., Nanamiya, H., Nakai, S., Nygaard, P., Ogura, M., Ohanan, T., O'Reilly, M., O'Rourke, M., Pragai, Z., Pooley, H. M., Rapoport, G., Rawlins, J. P., Rivas, L. A., Rivolta, C., Sadaie, A., Sadaie, Y., Sarvas, M., Sato, T., Saxild, H. H., Scanlan, E., Schumann, W., Seegers, J. F., Sekiguchi, J., Sekowska, A., Seror, S. J., Simon, M., Stragier, P., Studer, R., Takamatsu, H., Tanaka, T., Takeuchi, M., Thomaides, H. B., Vagner, V., van Dijl, J. M., Watabe, K., Wipat, A., Yamamoto, H., Yamamoto, M., Yamamoto, Y., Yamane, K., Yata, K., Yoshida, K., Yoshikawa, H., Zuber, U., and Ogasawara, N. (2003) Essential *Bacillus subtilis* genes, *Proc Natl Acad Sci U S A 100*, 4678-4683.
11. Akerley, B. J., Rubin, E. J., Novick, V. L., Amaya, K., Judson, N., and Mekalanos, J. J. (2002) A genome-scale analysis for identification of genes required for growth or survival of *Haemophilus influenzae*, *Proc Natl Acad Sci U S A 99*, 966-971.
12. Hutton, C. A., Southwood, T. J., and Turner, J. J. (2003) Inhibitors of lysine biosynthesis as antibacterial agents, *Mini Rev Med Chem 3*, 115-127.
13. Schnell, R., Oehlmann, W., Sandalova, T., Braun, Y., Huck, C., Maringer, M., Singh, M., and Schneider, G. (2012) Tetrahydrodipicolinate N-succinyltransferase and dihydrodipicolinate synthase from *Pseudomonas aeruginosa*: structure analysis and gene deletion, *PLoS One 7*, e31133.
14. Kumpaisal, R., Hashimoto, T., and Yamada, Y. (1987) Purification and characterization of dihydrodipicolinate synthase from wheat suspension cultures, *Plant Physiol 85*, 145-151.

15. Dereppe, C., Bold, G., Ghisalba, O., Ebert, E., and Schar, H. P. (1992) Purification and characterization of dihydrodipicolinate synthase from pea, *Plant Physiol 98*, 813-821.
16. Frisch, D. A., Gengenbach, B. G., Tommey, A. M., Sellner, J. M., Somers, D. A., and Myers, D. E. (1991) Isolation and characterization of dihydrodipicolinate synthase from maize, *Plant Physiol 96*, 444-452.
17. Devenish, S. R., Huisman, F. H., Parker, E. J., Hadfield, A. T., and Gerrard, J. A. (2009) Cloning and characterisation of dihydrodipicolinate synthase from the pathogen *Neisseria meningitidis*, *Biochim Biophys Acta 1794*, 1168-1174.
18. Dobson, R. C., Griffin, M. D., Roberts, S. J., and Gerrard, J. A. (2004) Dihydrodipicolinate synthase (DHDPS) from *Escherichia coli* displays partial mixed inhibition with respect to its first substrate, pyruvate, *Biochimie 86*, 311-315.
19. Domigan, L. J., Scally, S. W., Fogg, M. J., Hutton, C. A., Perugini, M. A., Dobson, R. C., Muscroft-Taylor, A. C., Gerrard, J. A., and Devenish, S. R. (2009) Characterisation of dihydrodipicolinate synthase (DHDPS) from *Bacillus anthracis*, *Biochim Biophys Acta 1794*, 1510-1516.
20. Rice, E. A., Bannon, G. A., Glenn, K. C., Jeong, S. S., Sturman, E. J., and Rydel, T. J. (2008) Characterization and crystal structure of lysine insensitive *Corynebacterium glutamicum* dihydrodipicolinate synthase (cDHDPS) protein, *Arch Biochem Biophys 480*, 111-121.
21. Wolterink-van Loo, S., Levisson, M., Cabrieres, M. C., Franssen, M. C., and van der Oost, J. (2008) Characterization of a thermostable dihydrodipicolinate synthase from *Thermoanaerobacter tengcongensis*, *Extremophiles 12*, 461-469.
22. Coulter, C. V., Gerrard, J. A., Kraunsoe, J. A. E., Moore, D. J., and Pratt, A. J. (1996) (*S*)-Aspartate semi-aldehyde: Synthetic and structural studies, *Tetrahedron 52*, 7127-7136.
23. Coulter, C. V., Gerrard, J. A., Kraunsoe, J. A. E., and Pratt, A. J. (1999) *Escherichia coli* dihydrodipicolinate synthase and dihydrodipicolinate reductase: kinetic and inhibition studies of two putative herbicide targets, *Pesticide Science 55*, 887-895.
24. Couper, L., McKendrick, J. E., Robins, D. J., and Chrystal, E. J. T. (1994) Pyridine and piperidine-derivatives as inhibitors of dihydrodipicolinic acid synthase, a key enzyme in the diaminopimelate pathway to L-lysine, *Bioorg Med Chem Lett 4*, 2267-2272.
25. Hutton, C. A., Jaber, R., Otaegui, M., Turner, J. J., Turner, P., White, J. M., and Bacskay, G. B. (2002) Stereochemical and conformational consequences of the oxidation of 1,4-thiazane-3,5-dicarboxylates, *Journal of the Chemical Society-Perkin Transactions 2*, 1066-1071.
26. Turner, J. J., Gerrard, J. A., and Hutton, C. A. (2005) Heterocyclic inhibitors of dihydrodipicolinate synthase are not competitive, *Bioorg Med Chem 13*, 2133-2140.
27. Mitsakos, V., Dobson, R. C., Pearce, F. G., Devenish, S. R., Evans, G. L., Burgess, B. R., Perugini, M. A., Gerrard, J. A., and Hutton, C. A. (2008) Inhibiting dihydrodipicolinate synthase across species: towards specificity for pathogens?, *Bioorg Med Chem Lett 18*, 842-844.
28. Boughton, B. A., Dobson, R. C., Gerrard, J. A., and Hutton, C. A. (2008) Conformationally constrained diketopimelic acid analogues as inhibitors of dihydrodipicolinate synthase, *Bioorganic & Medicinal Chemistry Letters 18*, 460-463.
29. Boughton, B. A., Griffin, M. D. W., O'Donnell, P. A., Dobson, R. C. J., Perugini, M. A., Gerrard, J. A., and Hutton, C. A. (2008) Irreversible inhibition of dihydrodipicolinate synthase by 4-oxo-heptenedioic acid analogues, *Bioorg Med Chem 16*, 9975-9983.
30. Turner, J. J., Healy, J. P., Dobson, R. C. J., Gerrard, J. A., and Hutton, C. A. (2005) Two new irreversible inhibitors of dihydrodipicolinate synthase: diethyl (E,E)-4-oxo-2,5-heptadienedioate and diethyl (E)-4-oxo-2-heptenedioate, *Bioorg Med Chem Lett 15*, 995-998.
31. Boughton, B. A., Hor, L., Gerrard, J. A., and Hutton, C. A. (2012) 1,3-Phenylene bis(ketoacid) derivatives as inhibitors of *Escherichia coli* dihydrodipicolinate synthase, *Bioorg Med Chem 20*, 2419-2426.

32. Phenix, C. P., and Palmer, D. R. (2008) Isothermal titration microcalorimetry reveals the cooperative and noncompetitive nature of inhibition of *Sinorhizobium meliloti* L5-30 dihydrodipicolinate synthase by (S)-lysine, *Biochemistry 47*, 7779-7781.
33. Guha, P. C., and Sankaran, D. K. (1946) Muconic acid, *Organic Syntheses 26*, 57-60.
34. Watson, H. A., and O'Neill, B. T. (1990) A reinvestigation and improvement in the synthesis of *meso*-2,5-dibromoadipates by appication of Le Chateliers principle, *Journal of Organic Chemistry 55*, 2950-2952.
35. Sheehan, J. C., and Bolhofer, W. A. (1950) An improved procedure for the condensation of potassium phthalimide with organic halides, *J Am Chem Soc 72*, 2786-2788.
36. Dondoni, A., and Perrone, D. (2000) Synthesis of 1,1-dimethylethyl (*S*)-4-formyl-2,2-dimethyl-3-oxazolidinecarboxylate by oxidation of the alcohol, *Organic Syntheses 77*, *6*4-70.
37. Skovpen, Y. V., and Palmer, D. R. (2013) Dihydrodipicolinate synthase from *Campylobacter jejuni*: kinetic mechanism of cooperative allosteric inhibition and inhibitor-induced substrate cooperativity, *Biochemistry 52*, 5454-5462.
38. Yugari, Y., and Gilvarg, C. (1965) The condensation step in diaminopimelate synthesis, *J Biol Chem 240*, 4710-4716.
39. Gander-Coquoz, M., and Seebach, D. (1988) Synthesis of enantiomerically pure, alpha-alkylated lysine, ornitine, and tryptophan derivatives, *Helvetica Chimica Acta 71*, 224-236.
40. Karsten, W. E. (1997) Dihydrodipicolinate synthase from *Escherichia coli*: pH dependent changes in the kinetic mechanism and kinetic mechanism of allosteric inhibition by L-lysine, *Biochemistry 36*, 1730-1739.
41. Morrison, J. F., and Walsh, C. T. (1988) The behavior and significance of slow-binding enzyme inhibitors, *Adv Enzymol Relat Areas Mol Biol 61*, 201-301.
42. Baici, A. (2013) Slow-onset enzyme inhibition and inactivation, In *5th International Beilstein Symposium on Experimental Standard Conditions of Enzyme Characterizations*.
43. Cha, S. (1975) Tight-binding inhibitors-I. Kinetic behavior, *Biochem Pharmacol 24*, 2177-2185.
44. Li, C., and Gershon, P. D. (2006) pKa of the mRNA cap-specific 2'-O-methyltransferase catalytic lysine by HSQC NMR detection of a two-carbon probe, *Biochemistry 45*, 907-917.
45. Hermann, P., and Lemke, K. (1968) Ionization constants and stability constants of the copper(II)-complexes of some amino acids and their sulfur-containing analogs, *Hoppe Seylers Z Physiol Chem 349*, 390-394.

CHAPTER 4. MUTAGENESIS STUDY OF DIHYDRODIPICOLINATE SYNTHASE FROM *CAMPYLOBACTER JEJUNI*: HOW MUTATIONS IN THE ALLOSTERIC SITE AFFECT BINDING OF NONCOMPETITIVE INHIBITORS

4.1 Introduction

Antibiotic resistance of bacteria is a big concern that has emerged in the latter half of the last century (*1*). Therefore the discovery of new targets for antibiotic design is one of the primary tasks of medicinal chemistry (*2*). Inhibitors of bacterial cell wall synthesis are proven to be successful antibiotics (*3*). Bacterial cell walls require *meso*-diaminopimelate (or L-lysine for some organisms) for cross-linking of peptidoglycan chains (*4, 5*), therefore the enzymes of the *meso*-diaminopimelate and L-lysine biosynthetic pathways are potential targets for drug development (*6-8*).

Dihydrodipicolinate synthase is an enzyme of the bacterial *meso*-diaminopimelate and L-lysine biosynthetic pathway, also found in plants and some fungi (*9-11*). It catalyses the aldol condensation of pyruvate and (*S*)-aspartate-*β*-semialdehyde (ASA) into an unstable heterocyclic product, (4*S*)-hydroxy-2,3,4,5-tetrahydro-(2*S*)-dipicolinate (HTPA), which spontaneously dehydrates into dihydrodipicolinate (DHDP) (*12, 13*). Genetic studies showed that DHDPS is an essential enzyme for many bacterial species (*14-18*). The assumption is that effective inhibition of DHDPS will impair bacterial cell wall synthesis. To prove this hypothesis a number of research groups are working on design and synthesis of inhibitors of DHDPS (*7, 9, 19-27*). DHDPS is an allosteric enzyme and its natural allosteric modulator is L-lysine. DHDPS from plants are inhibited by L-lysine in low micromolar IC_{50} range (*28-30*). DHDPS from Gram-negative bacteria are moderately or weakly inhibited by L-lysine (micromolar or millimolar IC_{50} values) (*31-33*). DHDPS from Gram-positive bacteria show no inhibition by L-lysine (*34-37*). The reason for this difference is a distinct variation in structural organization of the allosteric sites in DHDPS from Gram-positive bacteria.

The proposed catalytic triad (Thr44, Tyr107', Tyr133), the key residue required for Schiff base formation (Lys161), and a residue responsible for ASA binding, Arg138, (*E. coli* numbering) are conserved for all DHDPS (*12, 38, 39*). Several crystal structures of DHDPS with

lysines bound at the allosteric sites have been obtained (*E. coli*, PDB code 1YXD; *P. aeruginosa*, 3PUO; *V. vinifera*, 4HNN; *C. jejuni*, 4M19; *S. pneumoniae*, 4FHA), and the residues responsible for lysine binding were determined (*12, 40, 41*). A few examples of homologous amino acids forming the allosteric sites of DHDPS from Gram-negative, Gram-positive bacteria, and plants are listed in Table 4.1. A sequence alignment of DHDPS from different groups of species reveals conserved (Tyr106) and variable (Ser48, Ala49, Leu51, His53, His56, Asn80', Glu84') allosteric site residues (Figure B 1, Figure B 2 and Figure B 3, pages 139-141). Tyr106 participates in lysine binding by donating a hydrogen bond to the carboxyl group of L-lysine, while Tyr 107 is a part of the catalytic triad. It is likely that signal transduction happens via Tyr106 movement upon binding of lysine, where a shift of Tyr106 affects the position of catalytic Tyr107 and alters the catalytic activity of the enzyme (Figure 4.1). Mutation of Tyr106 to Phe would reduce the binding affinity of lysine and decrease or eliminate signal transduction to the active site.

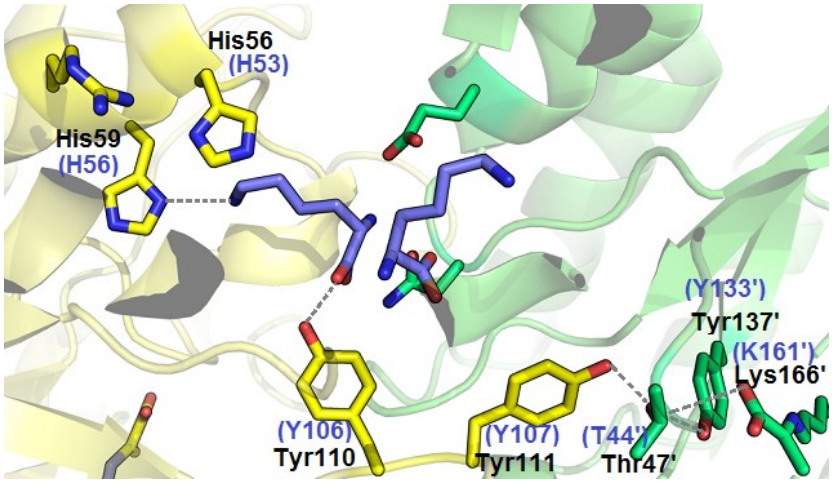

Figure 4.1 The element of signal transduction in DHDPS from allosteric to active site. Crystal structure of *C. jejuni* DHDPS with two L-lysine molecules bound at the allosteric site. *E. coli* numbering is shown in blue and *C. jejuni* numbering is shown in black. Dotted lines represent hydrogen bonds.

Table 4.1 Examples of allosteric site amino acid residues in different species[a].

Allosteric site residues in *E. coli* DHDPS Interactions with lysine in *E. coli* DHDPS	Ser48[b] H-bond with ε-amino group	Ala49[b] H-bond with α-amino group	Leu51[b] H-bond with ε-amino group	His53 cation-π interaction	His56 H-bond with ε-amino group	Asn80' H-bonds with α-amino and carboxyl groups	Glu84' H-bond with α-amino group	Tyr106 H-bond with carboxyl group
Homologous residues in different species								
Gram-negative:								
C. jejuni	Ser	Ala	Leu	His	His	Asn	Glu	Tyr
N. meningitides	Ser	Ala	Leu	Val	His	Asn	Glu	Tyr
R. typhi	Ala	Asn	Leu	Phe	Tyr	Asn	Tyr	Tyr
S. meliloti	Ser	Ala	Leu	Lys	His	Asn	Glu	Tyr
M. mediterranea	Ala	Ala	Leu	Asp	Ala	Asn	Lys	Tyr
Plants:								
V. vinifera	Gly	Gln	Met	Trp	His	Asn	Glu	Tyr
N. silvestris	Gly	Gln	Met	Trp	His	Ile	Glu	Tyr
Z. mays	Gly	His	Met	Trp	His	Asn	Glu	Tyr
T. aestivum	Gly	His	Met	Trp	His	Asn	Glu	Tyr
T. cacao	Gly	Gln	Met	Trp	His	Asn	Glu	Tyr
Gram-positive:								
B. anthracis	Ser	Pro	Leu	Ser	Lys	Asn	Ala	Tyr
S. aureus	Ser	Pro	Leu	Thr	Lys	Asn	Lys	Tyr
C. glutamicum	Ser	Pro	Thr	Ala	Lys	Asn	Thr	Tyr
L. ruminis	Gly	Pro	Leu	Glu	Lys	Asn	Thr	Tyr
C. botulinum	Ala	Thr	Met	Glu	Arg	Asn	Ala	Tyr

[a] sequence alignments are shown in Appendix B, Figure B 1, Figure B 2 and Figure B 3.
[b] interactions with the main chain.

His56 is often present in Gram-negative bacteria and it is a conserved residue in plant DHDPS, but in Gram-positive bacteria this position is mostly occupied by Lys (Table 4.1); the last is likely one of the reasons for the noted insensitivity to allosteric regulation by lysine (*37*). Lys56 in Gram-positive bacterial DHDPS points into the allosteric site, creating a steric clash with the allosteric inhibitor. Additionally, the repulsion of positively charged ε-amino groups would prevent lysine binding. His53 is not a conserved residue in DHDPS from Gram-negative and Gram-positive bacteria, but plant DHDPS contain conserved tryptophan in the same position. The replacement of Trp53 for Arg in mutagenesis studies on plant DHDPS resulted in complete insensitivity of the enzyme to lysine inhibition (*42*). Apparently, Trp53 in plants makes a significant contribution to the increased affinity of the allosteric site to L-lysine.

Campylobacter jejuni is a Gram-negative pathogen found in humans and animals (*43, 44*). The kinetic properties and lysine inhibition kinetics of DHDPS from *C. jejuni* have been

described previously (*33*). The remarkable inhibitory activity of *R*,*R*-bislysine against *C. jejuni* DHDPS raises interest in how mutations in the allosteric site would affect binding of the natural allosteric inhibitor L-lysine and the potent synthetic inhibitor *R*,*R*-bislysine.

Displacements of His56 and His59 (the corresponding residues in *E. coli* DHDPS are His53 and His56) were observed upon lysine binding, which is shown in the DHDPS crystal structures overlay (Figure 4.2). As a result of lysine binding, His56 and His59 move toward the center of the allosteric site creating a new hydrogen bond network.

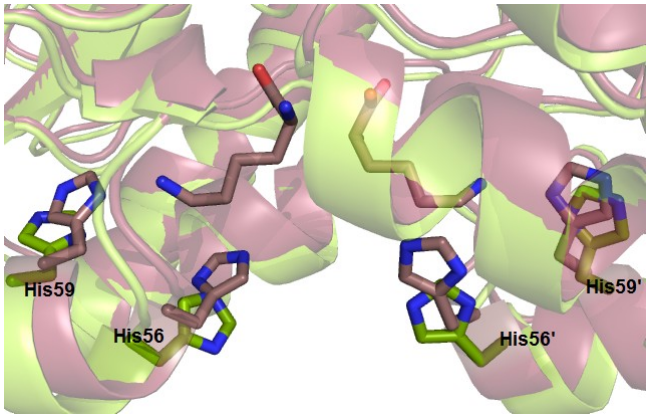

Figure 4.2 Overlay of *C. jejuni* DHDPS structures: DHDPS-pyruvate complex, PDB ID 4LY8 (green) and DHDPS-pyruvate with lysine bound at the allosteric site, PDB ID 4M19 (purple).

In this work we show how mutations of Y110, His56 and His 59 affect the catalytic activity of *C. jejuni* DHDPS, as well as how the inhibitory ability of noncompetitive inhibitors (L-lysine, *R*,*R*-bislysine) changes when they bind to the modified allosteric site.

4.2 Materials and Methods

Pyruvate, L-lysine and NADH were obtained from Sigma-Aldrich Canada, Ltd (Oakville, ON), (N-2-hydroxyethylpiperazine-N-2-ethanesulfonic acid (HEPES) was purchased from BDH (Mississauga, ON). (*S*)-Aspartate-*β*-semialdehyde (ASA) was synthesized according to the reported procedure (*45*). The concentration of each newly prepared work solution of ASA was determined using the DHDPS-DHDPR coupled kinetic assay (*33, 46*), in the presence of excess NADH. *R,R*-Bislysine was synthesized as described in Chapter 3 (3.2.3).

4.2.1 Site-directed mutagenesis

Y110F, H56A, H56N, H59A, and H59N mutations were generated using KAPA HiFi^{TM} PCR Kit (Kapa Biosystems) according to manufacturer's recommendations. Mutagenic primers were designed to introduce the required mutations:

5'-GATTTTAAGTGTGGC***G***CCGT**T**TTATAATAAACCTACGCAACAAG-3',

5'-GTGCAACTTTAACC**GC**TGAAGAACATAGAAC***A***TGCATAGAAATAGCC-3',

5'-GTGCAACTTTAACC**AA**TGAAGAACATAGAAC***A***TGCATAGAAATAGCC-3',

5'-CTTTAACCCATGAAGAA**GC**TAGAAC***A***TGCATAGAAATAGCCGTTG-3',

5'-CTTTAACCCATGAAGAA**AA**TAGAAC***A***TGCATAGAAATAGCCGTTG-3'.

Mutations shown in bold introduce phenylalanine for Y110F, alanine and asparagine for H56A and H56N, alanine and asparagine for H59A and H59N respectively. Additional silent mutations (shown in bold italic) were made to generate new restriction sites (underlined) NarI (Y110F) and NsiI (H56A, H56N, H59A, H59N) for the purpose of screening *E. coli* XL1-Blue transformants. Isolated plasmid DNA from selected clones was sequenced by the DNA Technologies Unit of the National Research Council, Saskatoon, Canada.

4.2.2 Expression and purification of mutants and DHDPR

Y110F, H56A, H56N, H59A, H59N and DHDPR proteins were expressed, purified and concentrated to 1.2, 0.81, 1.0, 0.28, 0.88 and 1.29 mg/ml respectively as previously described for *Wt*-DHDPS from *C. jejuni* (*33*). The proteins were aliquoted and stored at -80 °C.

4.2.3 Enzyme assay

The activity of mutants was measured using a coupled assay (*46*). The assay was conducted in 100 mM HEPES buffer at pH 8.0 and 25 °C as previously described for the wild-type enzyme (*33*). The amounts of Y110F, H56A, H56N, H59A and H59N used in the assay were 1.2 µg, 0.81 µg, 1.0 µg, 1.4 µg and 0.88 µg respectively. The obtained kinetic data were fitted to the rate Equation 4.1 (ping-pong kinetic mechanism) using SigmaPlot 10.0 (Systat Software, San Jose, CA):

$$v = V_{\max} AB \big/ (K_{M(B)} A + K_{M(A)} B + AB) \qquad (4.1)$$

where V_{max} is the maximum velocity, $K_{M(A)}$ and $K_{M(B)}$ are the Michaelis-Menten constants for two substrates, A and B are the concentrations of the substrates, and v is the initial velocity.

Lysine inhibition studies were conducted at constant saturating level of one of the substrates (2.5 mM for ASA and 3.7 mM for pyruvate). The models for the *mixed partial* ($\alpha \neq 1$, $0 < \beta < 1$), *noncompetitive partial* ($\alpha = 1$, $0 < \beta < 1$) (Equation 4.2) or *uncompetitive partial* inhibition ($0 < \beta < 1$) (Equation 4.3) were used to fit experimental data, as indicated in the results section,

$$\frac{v}{V_{\max}} = \frac{\frac{[S]}{K_s} + \frac{\beta[S]\,[I]^h}{K_s\,(\alpha K_i)^h}}{1 + \frac{[S]}{K_s} + \frac{[I]^{h'}}{K_i^{h'}} + \frac{[S]\,[I]^h}{K_s\,(\alpha K_i)^h}} \tag{4.2}$$

$$\frac{v}{V_{\max}} = \frac{\frac{[S]}{K_s} + \frac{\beta[S][I]^h}{K_s K_i^{\,h}}}{1 + \frac{[S]}{K_s} + \frac{[S][I]^h}{K_s K_i^{\,h}}} \tag{4.3}$$

$$\log \frac{v_i - v_{i(sat)}}{v_0 - v_i} = \log K - h \log[I] \tag{4.4}$$

$$\log \frac{v}{V_{\max} - v} = n \log[S] - \log K' \tag{4.5}$$

where K_i is the inhibition constant, $[I]$ is the inhibitor concentration, S is the substrate concentration, α and β are proportionality constants. Cooperativity coefficients h' and h are for lysine binding to Schiff-base enzyme and Schiff-base-ASA complex (Equation 4.2). For Equation 4.3, h is the cooperativity coefficient for lysine binding to the E:pyr form of the enzyme. Equation 4.4 is the Hill equation for partial inhibition, where v_i is the velocity in the presence of the inhibitor, v_0 is the velocity in the absence of the inhibitor, $v_{i(sat)}$ is the reaction velocity at saturating concentrations of inhibitor, and K is an apparent overall dissociation constant. Equation 4.5 is the Hill equation for cooperative substrate binding, where v_i is velocity, V_{max} is maximal apparent velocity at saturated concentration of the variable substrate, K' is an apparent overall affinity constant of the substrate, n is Hill coefficient of the substrate, and [S] is the concentration of the variable substrate. When cooperativity of ASA is noticed, Equation 4.2 should be modified by introducing the cooperativity coefficient of ASA n, and therefore terms [S] and K_s would be changed to $[S]^n$ and K_s^n respectively.

The enzymatic reaction was triggered by the addition of DHDPS in lysine inhibition studies, while in *R,R*-bislysine inhibition experiments DHDPS was preincubated with the inhibitor within one minute, and the reaction was triggered with ASA. This technique helps to avoid a time-dependent phase of slow-binding, so *R,R*-bislysine would form a complex with the enzyme prior to reaction initiation.

The inhibition by L-lysine and *R,R*-bislysine were tested in the range of lysine concentration (0 - 40 mM) and *R,R*-bislysine concentration (0 – 3.4 μM) at saturating concentration of pyruvate and a near-K_M concentration of ASA.

4.3 Results and Discussion

4.3.1 Ping-pong kinetics of mutants

Kinetic data for Y110F, H56A, H56N, H59A, and H59N were obtained and the ping-pong model (Equation 4.1) was fitted to the experimental values. Similar to *Wt*-DHDPS, all mutants display a ping-pong mechanism, and demonstrate approximately half of the enzymatic activity of wild-type (Table 4.2, Appendix B, Figure B 4 - Figure B 13, pages 142-146).

Table 4.2 Kinetic constants for Y110F, H56A, H56N, H59A, H59N in comparison with *Wt*-DHDPS.

	$K_{M(pyr)}$, mM	$K_{M(ASA)}$, mM	k_{cat}, s^{-1}	$k_{cat}/K_{M(pyr)}$, $M^{-1}s^{-1}$	$k_{cat}/K_{M(ASA)}$, $M^{-1}s^{-1}$
Wt[a]	0.35 ± 0.02	0.16 ± 0.01	76 ± 1	$(2.2 \pm 0.1) \times 10^5$	$(4.8 \pm 0.3) \times 10^5$
Y110F	0.19 ± 0.01	0.12 ± 0.01	33 ± 1	$(1.8 \pm 0.1) \times 10^5$	$(2.7 \pm 0.1) \times 10^5$
H56A	0.26 ± 0.02	0.16 ± 0.01	40 ± 1	$(1.5 \pm 0.1) \times 10^5$	$(2.5 \pm 0.1) \times 10^5$
H56N	0.39 ± 0.02	0.20 ± 0.01	54 ± 1	$(1.4 \pm 0.1) \times 10^5$	$(2.6 \pm 0.2) \times 10^5$
H59A	0.31 ± 0.02	0.15 ± 0.01	31 ± 1	$(1.0 \pm 0.1) \times 10^5$	$(2.1 \pm 0.2) \times 10^5$
H59N	0.40 ± 0.02	0.12 ± 0.01	36 ± 1	$(0.9 \pm 0.1) \times 10^5$	$(2.9 \pm 0.2) \times 10^5$

[a] Reference (*33*)

4.3.2 L-lysine inhibition of mutants

The lysine IC_{50} for Y110F was found to be approximately 40 mM (Figure 4.3), which indicates that Y110F mutation dramatically changes the ability of the enzyme to be inhibited by

lysine. This mutation makes the enzyme insensitive to L-lysine regulation at its physiological concentrations.

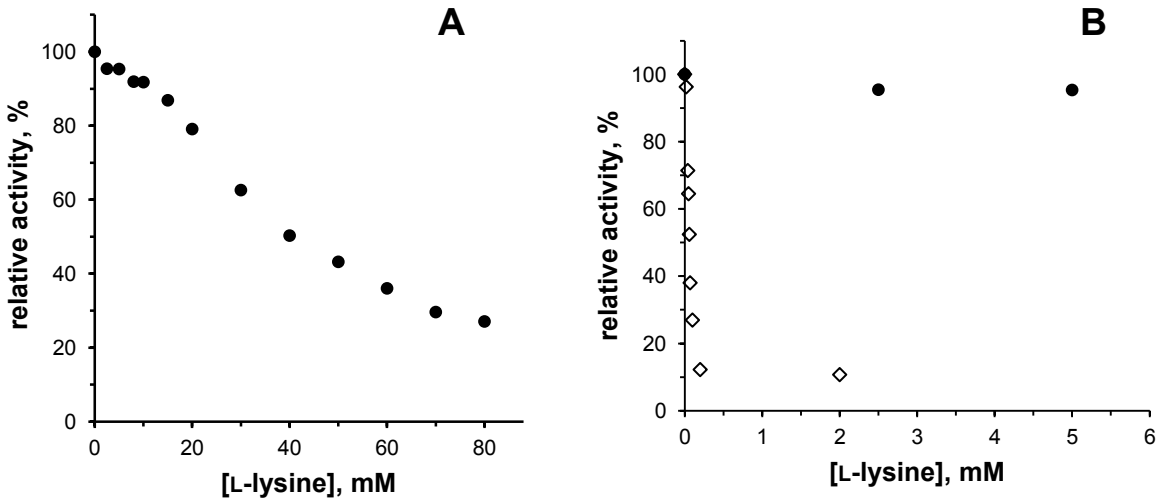

Figure 4.3 (A) Lysine inhibition curve for Y110F, (ASA 0.12 mM, pyruvate 3.7 mM); (B) Comparison of lysine inhibition for Y110F (●) and wild-type (◇), (ASA 0.16 mM, pyruvate 3.5 mM).

His56 does not make hydrogen bonds with a bound allosteric lysine directly, but it participates in a hydrogen bond network in the allosteric site. Also, His56 is situated within a favorable distance to make a cation-π interaction with the ε-amino group of L-lysine. Mutation of His56 to Ala would eliminate all polar interactions with the side chain. Mutation of His56 to Asn might maintain hydrogen-bonding interactions, but will not be able to make the cation-π interaction with lysine. His56A and His56N mutations are therefore expected to decrease the binding affinity of lysine. Lysine inhibition studies for these mutants were carried out in the range of lysine concentration 0 – 5.0 mM, at saturating background concentration of one of the substrates. Lysine binds cooperatively to both mutants and a series of Hill plots were built at various concentrations of pyruvate and ASA (Appendix B, Figure B 14 – Figure B 17, pages 147-148). The average cooperativity coefficients of lysine were 2.0 ± 0.2 and 1.6 ± 0.4 for H56A, and 2.0 ± 0.3 and 2.3 ± 0.3 for H56N, where the first value corresponds to the condition when ASA is varied substrate and the second when pyruvate is varied. A slight curvature in the Lineweaver–Burk plots (Figure 4.5 and Figure 4.7) indicates cooperativity of ASA binding in the presence of lysine. The same observation has been reported for wild-type DHDPS (*33*). The average cooperativity coefficients of ASA for H56A and H56N mutants in the presence of lysine

were found to be 1.2 ± 0.1 and 1.3 ± 0.1, respectively (Appendix B, Figure B 18, Figure B 19, pages 149-150). The cooperativity coefficients of lysine and ASA found by graphical methods are in agreement with the values obtained by global fitting (Table 4.3). The *uncompetitive partial* and *mixed partial* models provided the best fit of the experimental data of L-lysine inhibition for the H56A mutant (Figure 4.4, Figure 4.5, Appendix B, Figure B 20 and Figure B 21, page 151). For the H56N mutant, the *uncompetitive partial* model fits well the experimental data with respect to pyruvate (Figure 4.6, Appendix B, Figure B22, page 151), and the best fit with respect to ASA was obtained when the *mixed partial* model was simplified to *noncompetitive partial* ($\alpha = 1$, Equation 4.2) (Figure 4.7, Appendix B, Figure B 23, page 152).

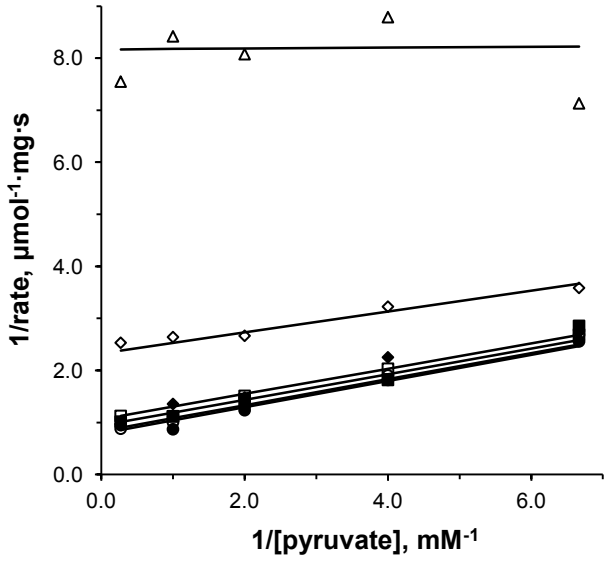

Figure 4.4 Double-reciprocal plot of data obtained at a constant ASA concentration of 2.5 mM for H56A. Concentration of lysine: (●) 0 mM, (○) 0.080 mM, (■) 0.10 mM, (□) 0.15 mM, (♦) 0.20 mM, (◇) 0.50 mM, (△) 5.0 mM. Solid lines are fit lines, obtained by global fitting the *uncompetitive partial* model (Equation 4.3, $0 < \beta < 1$) to the data. Residuals are shown in Figure B 20.

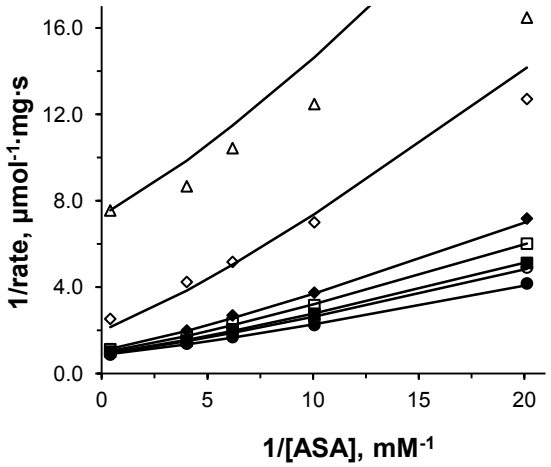

Figure 4.5 Double-reciprocal plot of data obtained at a constant pyruvate concentration of 3.7 mM fit to the *mixed partial* inhibiton model (Equation 4.2, $1 < \alpha < \infty$, $0 < \beta < 1$) for H56A. Concentration of lysine: (●) 0 mM, (○) 0.080 mM, (■) 0.10 mM, (□) 0.15 mM, (♦) 0.20 mM, (◇) 0.50 mM, (△) 5.0 mM. Solid lines are fit lines. Residuals are shown in Figure B 21.

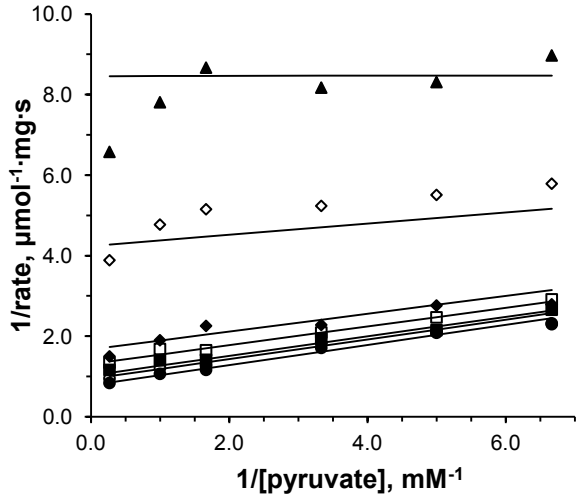

Figure 4.6 Double-reciprocal plot of data obtained at a constant ASA concentration of 2.5 mM for H56N. Concentration of lysine: (●) 0 mM, (○) 0.080 mM, (■) 0.10 mM, (□) 0.15 mM, (♦) 0.20 mM, (◇) 0.50 mM, (▲) 5.0 mM. Solid lines are fit lines, obtained by global fitting the *uncompetitive partial* model (Equation 4.3, $0 < \beta < 1$) to the data. Residuals are shown in Figure B 22.

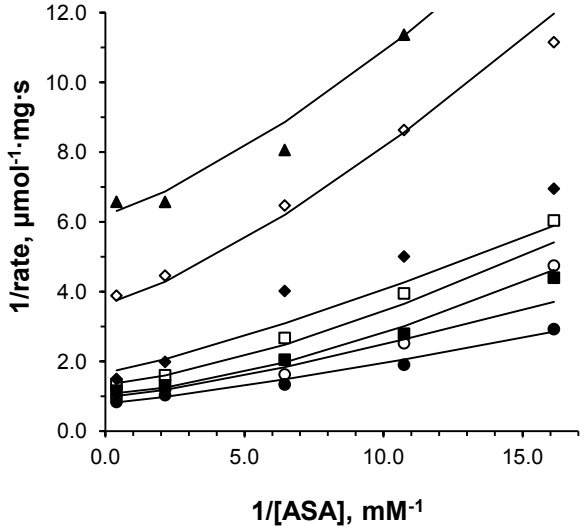

Figure 4.7 Double-reciprocal plot of data obtained at a constant pyruvate concentration of 3.7 mM fit to the *noncompetitive partial* inhibiton model (Equation 4.2, $\alpha = 1$, $0 < \beta < 1$) for H56N. Concentration of lysine: (●) 0 mM, (○) 0.080 mM, (■) 0.10 mM, (□) 0.15 mM, (♦) 0.20 mM, (◇) 0.50 mM, (▲) 5.0 mM. Solid lines are fit lines. Residuals are shown in Figure B 23.

His59 forms a hydrogen bond with the ε-amino group of lysine and therefore replacement of it with Ala or Asn would reduce the binding ability of lysine. Asparagine could donate or accept a H-bond, but the pK_a value of this residue is different from histidine. The lysine inhibition curves for H59A and H59N mutants are shown in Figure 4.8.

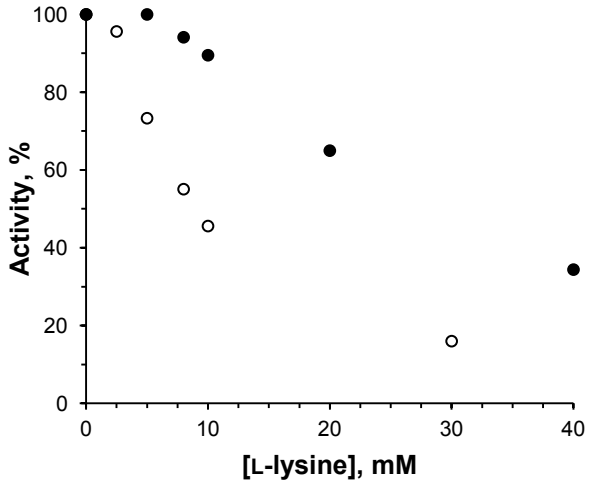

Figure 4.8 Lysine inhibition curves for H59A (•) and H59N (○) at saturating concentration of pyruvate 3.7 mM, and 0.15 mM ASA.

The apparent IC_{50} values of L-lysine for H59A and H59N were estimated ~25 mM and ~10 mM respectively. Significant decrease in lysine inhibitory activity was expected, and the fact that the IC_{50} value of H59N is smaller than that of H59A is in agreement with the suggestion that H59N is able to make more polar contacts with the inhibitor than H59A. The lysine inhibition results for the mutants are summarized in Table 4.3.

Table 4.3 Lysine inhibition kinetics results (K_i or $IC_{50}{}^{app}$) for the DHDPS mutants.

Kinetic parameters	Wt[e]	Y110F	H56A	H56N	H59A	H59N
$h_{E:pyr}$, lysine[a]	2.6 ± 0.1		2.1 ± 0.3	2.0 ± 0.1		
h_F, lysine[a]	2.3 ± 0.2		1.5 ± 0.2	1.7 ± 0.3		
$h_{F:ASA}$, lysine[a]	2.8 ± 0.2		2.0 ± 0.3	1.9 ± 0.2		
h, ASA[a]	1.1 ± 0.1		1.2 ± 0.1	1.3 ± 0.1		
K_i (1), mM[b]	0.069 ± 0.001		0.31 ± 0.03	0.17 ± 0.01		
K_i (2), mM[c]	0.045 ± 0.003		0.21 ± 0.04	0.16 ± 0.01		
K_i (3), mM[d]	0.072 ± 0.009		0.37 ± 0.10	0.16 ± 0.01		
$IC_{50}{}^{app}$, mM		~40*			~25*	~10*

*due to very weak lysine inhibition, only $IC_{50}{}^{app}$ was estimated
[a] cooperativity coefficients were found by global fitting
[b] K_i (1) inhibition constant of binding to *E:pyr* complex
[c] K_i (2) inhibition constant of binding to *F* (Schiff base enzyme form)
[d] K_i (3) inhibition constant of binding to *F:ASA* complex
[e] Reference (*33*)

4.3.3 *R,R*-bislysine inhibition

R,R-bislysine is a potent submicromolar inhibitor of wild type *C. jejuni* DHDPS with an average K_i of 200 nM (Chapter 3). *R,R*-Bislysine resembles two molecules of L-lysine connected via a carbon-carbon bridge (Figure 4.9). The initial assumption was that because of the structural similarity of lysine and *R,R*-bislysine, the latter would demonstrate similar inhibition behavior with DHDPS mutants as L-lysine, but with proportionally higher binding affinities.

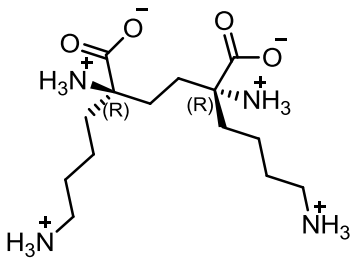

Figure 4.9 Molecule of *R,R*-bislysine.

Surprisingly, strong inhibition by *R,R*-bislysine was observed for mutants which were almost insensitive to lysine inhibition. The inhibitory efficiency of *R,R*-bislysine toward Y110F was almost as high as for wild-type DHDPS (Figure 4.10). *R,R*-bislysine binds to Y110F approximately 100,000 times stronger than lysine.

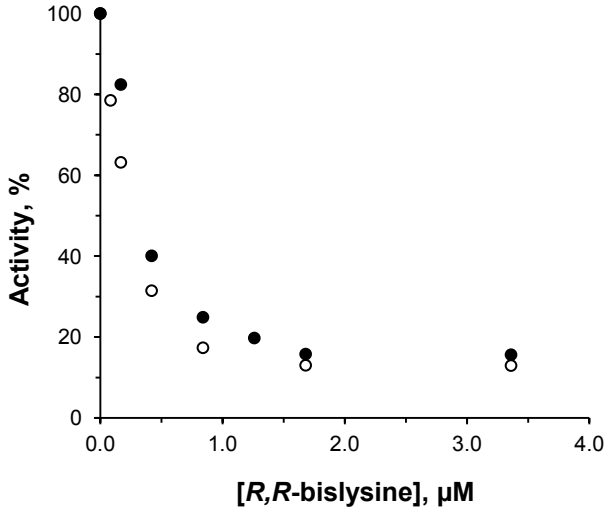

Figure 4.10 *R,R*-bislysine inhibition curves for *Wt*-DHDPS (○) and Y110F (●) at 3.7 mM pyruvate and 0.1 mM ASA.

Also, strong inhibition by *R,R*-bislysine was observed for H56A, H56N and H59N, where apparent IC_{50} values of the inhibitor are within the range 0.2 – 0.6 μM (Figure 4.11). The lowest binding affinity of *R,R*-bislysine was observed for H59A ($IC_{50}^{app} \approx 4$ μM), yet it still binds to this mutant approximately 6,250 times stronger than lysine.

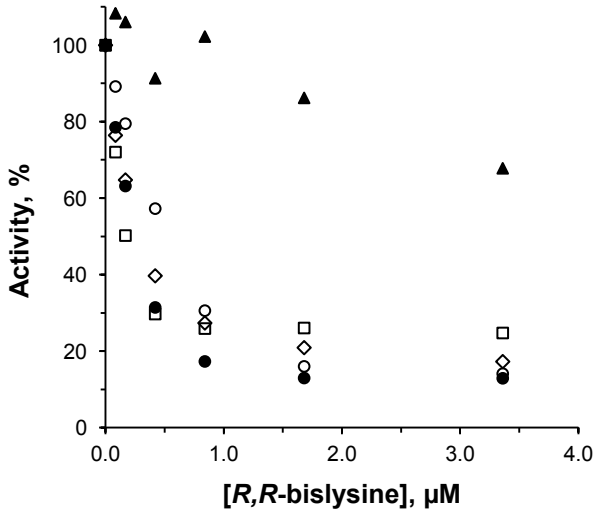

Figure 4.11 *R,R*-bislysine inhibition curves for *Wt*-DHDPS (●), H59N (○), H59A (▲), H56A (◇), and H56N (□) at 3.7 mM pyruvate and 0.1 mM ASA.

The inhibition results have shown that Tyr110 and His59 are important for lysine binding and inhibition, but they are not crucial for *R,R*-bislysine. The high inhibitory effectiveness of *R,R*-bislysine against Y110F indicates that Tyr110 is not the only essential component of the signal transduction system in *C. jejuni* DHDPS. The replacement of His56 for Ala and Asn has decreased binding affinity of lysine approximately by five and three times, respectively, however they do not significantly change apparent IC_{50} of *R,R*-bislysine. The *R,R*-bislysine inhibition curve for H56N has a distinct partial inhibition pattern (Figure 4.11) and shows more than 20% of residual activity under conditions employed, while wild-type, Y110F, H59A and H56A demonstrate less than 20% of residual activity at saturating levels of *R,R*-bislysine. The properties of the amino acid side chain in position 56 (53 in *E. coli* DHDPS) may be responsible for the partial inhibition profile. Atkinson *et al.* (*41*) pointed out the importance of a Trp residue in the corresponding position in plant DHDPS. Replacement of Trp for His in bacterial DHDPS changes the exposure of the allosteric site to solvent (*41*).

The results suggest that lysine inhibition is extremely dependent on the amount of polar contacts with residues in the allosteric site (Tyr110 and His59 in particular), but inhibition by *R,R*-bislysine remains strong even with fewer polar interactions.

4.3.4 Conclusions

The Y110F, H59A, H59N, H56A and H56N mutations in the allosteric site of *C. jejuni* DHDPS cause a decrease in catalytic activity of the enzyme, which is approximately half of activity of wild-type in each case. Y110F, H59A and H59N mutations make the enzyme almost insensitive to L-lysine inhibition. The binding affinity of lysine to H56A and H56N decreases by five and three times respectively when compared to the wild-type. However, *R,R*-bislysine inhibition of Y110F, H59N, H56A and H56N is comparable to that of wild-type, showing apparent IC_{50} values in the 0.2 – 0.6 μM range. H59A is less sensitive to *R,R*-bislysine inhibition, and its binding affinity decreases almost ten-fold relative to the wild-type. The *R,R*-bislysine inhibition results suggest some possible modifications that can be made to *R,R*-bislysine molecule. For instance, hydrogen bonding between Tyr110 and the carboxyl group of the inhibitor is not essential for inhibition and, therefore, can be replaced. On the other hand, hydrogen bonding between His59 and ε-amino group of the inhibitor plays an important role in inhibition.

4.4 References

1. Stanton, T. B. (2013) A call for antibiotic alternatives research, *Trends Microbiol 21*, 111-113.
2. Lewis, K. (2013) Platforms for antibiotic discovery, *Nat Rev Drug Discov 12*, 371-387.
3. Tipper, D. J. (1985) Mode of action of beta-lactam antibiotics, *Pharmacol Ther 27*, 1-35.
4. Bugg, T. D., and Walsh, C. T. (1992) Intracellular steps of bacterial cell wall peptidoglycan biosynthesis: enzymology, antibiotics, and antibiotic resistance, *Nat Prod Rep 9*, 199-215.
5. Cummins, C. S., and Harris, H. (1956) The chemical composition of the cell wall in some gram-positive bacteria and its possible value as a taxonomic character, *J Gen Microbiol 14*, 583-600.
6. Cox, R. J., Sutherland, A., and Vederas, J. C. (2000) Bacterial diaminopimelate metabolism as a target for antibiotic design, *Bioorg Med Chem 8*, 843-871.
7. Hutton, C. A., Southwood, T. J., and Turner, J. J. (2003) Inhibitors of lysine biosynthesis as antibacterial agents, *Mini Rev Med Chem 3*, 115-127.
8. Hutton, C. A., Perugini, M. A., and Gerrard, J. A. (2007) Inhibition of lysine biosynthesis: an evolving antibiotic strategy, *Mol Biosyst 3*, 458-465.
9. Walters, D. R., McPherson, A., and Robins, D. J. (1997) Inhibition of lysine biosynthesis in *Phytophthora infestans*, *Mycological Research 101*, 329-333.
10. Scapin, G., and Blanchard, J. S. (1998) Enzymology of bacterial lysine biosynthesis, *Advances in Enzymology, Vol 72 72*, 279-324.
11. Brock, T. D. (1974) *Biology of microorganisms*, 2d ed., Prentice-Hall, Englewood Cliffs, N.J.
12. Blickling, S., Renner, C., Laber, B., Pohlenz, H. D., Holak, T. A., and Huber, R. (1997) Reaction mechanism of *Escherichia coli* dihydrodipicolinate synthase investigated by X-ray crystallography and NMR spectroscopy, *Biochemistry 36*, 24-33.
13. Devenish, S. R., Blunt, J. W., and Gerrard, J. A. (2010) NMR studies uncover alternate substrates for dihydrodipicolinate synthase and suggest that dihydrodipicolinate reductase is also a dehydratase, *J Med Chem 53*, 4808-4812.
14. Neidhardt, F. C., and Curtiss, R. (1996) *Escherichia coli and Salmonella: cellular and molecular biology*, 2nd ed., ASM Press, Washington, D.C.
15. Yeh, P., Sicard, A. M., and Sinskey, A. J. (1988) General organization of the genes specifically involved in the diaminopimelate-lysine biosynthetic pathway of *Corynebacterium glutamicum*, *Mol Gen Genet 212*, 105-111.
16. Bukhari, A. I., and Taylor, A. L. (1971) Genetic analysis of diaminopimelic acid- and lysine-requiring mutants of *Escherichia coli*, *J Bacteriol 105*, 844-854.
17. Kobayashi, K., Ehrlich, S. D., Albertini, A., Amati, G., Andersen, K. K., Arnaud, M., Asai, K., Ashikaga, S., Aymerich, S., Bessieres, P., Boland, F., Brignell, S. C., Bron, S., Bunai, K., Chapuis, J., Christiansen, L. C., Danchin, A., Debarbouille, M., Dervyn, E., Deuerling, E., Devine, K., Devine, S. K., Dreesen, O., Errington, J., Fillinger, S., Foster, S. J., Fujita, Y., Galizzi, A., Gardan, R., Eschevins, C., Fukushima, T., Haga, K., Harwood, C. R., Hecker, M., Hosoya, D., Hullo, M. F., Kakeshita, H., Karamata, D., Kasahara, Y., Kawamura, F., Koga, K., Koski, P., Kuwana, R., Imamura, D., Ishimaru, M., Ishikawa, S., Ishio, I., Le Coq, D., Masson, A., Mauel, C., Meima, R., Mellado, R. P., Moir, A., Moriya, S., Nagakawa, E., Nanamiya, H., Nakai, S., Nygaard, P., Ogura, M., Ohanan, T., O'Reilly, M., O'Rourke, M., Pragai, Z., Pooley, H. M., Rapoport, G., Rawlins, J. P., Rivas, L. A., Rivolta, C., Sadaie, A., Sadaie, Y., Sarvas, M., Sato, T., Saxild, H. H., Scanlan, E., Schumann, W., Seegers, J. F., Sekiguchi, J., Sekowska, A., Seror, S. J., Simon, M., Stragier, P., Studer, R., Takamatsu, H., Tanaka, T., Takeuchi, M., Thomaides, H. B., Vagner, V., van Dijl, J. M., Watabe, K., Wipat, A., Yamamoto, H., Yamamoto, M., Yamamoto, Y., Yamane, K., Yata, K., Yoshida, K., Yoshikawa, H., Zuber, U., and Ogasawara, N. (2003) Essential *Bacillus subtilis* genes, *Proc Natl Acad Sci U S A 100*, 4678-4683.

18. Akerley, B. J., Rubin, E. J., Novick, V. L., Amaya, K., Judson, N., and Mekalanos, J. J. (2002) A genome-scale analysis for identification of genes required for growth or survival of *Haemophilus influenzae*, *Proc Natl Acad Sci U S A 99*, 966-971.
19. Coulter, C. V., Gerrard, J. A., Kraunsoe, J. A. E., Moore, D. J., and Pratt, A. J. (1996) (*S*)-Aspartate semi-aldehyde: Synthetic and structural studies, *Tetrahedron 52*, 7127-7136.
20. Coulter, C. V., Gerrard, J. A., Kraunsoe, J. A. E., and Pratt, A. J. (1999) *Escherichia coli* dihydrodipicolinate synthase and dihydrodipicolinate reductase: kinetic and inhibition studies of two putative herbicide targets, *Pesticide Science 55*, 887-895.
21. Couper, L., McKendrick, J. E., Robins, D. J., and Chrystal, E. J. T. (1994) Pyridine and piperidine-derivatives as inhibitors of dihydrodipicolinic acid synthase, a key enzyme in the diaminopimelate pathway to L-lysine, *Bioorg Med Chem Lett 4*, 2267-2272.
22. Hutton, C. A., Jaber, R., Otaegui, M., Turner, J. J., Turner, P., White, J. M., and Bacskay, G. B. (2002) Stereochemical and conformational consequences of the oxidation of 1,4-thiazane-3,5-dicarboxylates, *Journal of the Chemical Society-Perkin Transactions 2*, 1066-1071.
23. Turner, J. J., Gerrard, J. A., and Hutton, C. A. (2005) Heterocyclic inhibitors of dihydrodipicolinate synthase are not competitive, *Bioorg Med Chem 13*, 2133-2140.
24. Boughton, B. A., Dobson, R. C., Gerrard, J. A., and Hutton, C. A. (2008) Conformationally constrained diketopimelic acid analogues as inhibitors of dihydrodipicolinate synthase, *Bioorganic & Medicinal Chemistry Letters 18*, 460-463.
25. Boughton, B. A., Griffin, M. D. W., O'Donnell, P. A., Dobson, R. C. J., Perugini, M. A., Gerrard, J. A., and Hutton, C. A. (2008) Irreversible inhibition of dihydrodipicolinate synthase by 4-oxo-heptenedioic acid analogues, *Bioorg Med Chem 16*, 9975-9983.
26. Turner, J. J., Healy, J. P., Dobson, R. C. J., Gerrard, J. A., and Hutton, C. A. (2005) Two new irreversible inhibitors of dihydrodipicolinate synthase: diethyl (E,E)-4-oxo-2,5-heptadienedioate and diethyl (E)-4-oxo-2-heptenedioate, *Bioorg Med Chem Lett 15*, 995-998.
27. Boughton, B. A., Hor, L., Gerrard, J. A., and Hutton, C. A. (2012) 1,3-Phenylene bis(ketoacid) derivatives as inhibitors of *Escherichia coli* dihydrodipicolinate synthase, *Bioorg Med Chem 20*, 2419-2426.
28. Kumpaisal, R., Hashimoto, T., and Yamada, Y. (1987) Purification and characterization of dihydrodipicolinate synthase from wheat suspension cultures, *Plant Physiol 85*, 145-151.
29. Dereppe, C., Bold, G., Ghisalba, O., Ebert, E., and Schar, H. P. (1992) Purification and characterization of dihydrodipicolinate synthase from pea, *Plant Physiol 98*, 813-821.
30. Frisch, D. A., Gengenbach, B. G., Tommey, A. M., Sellner, J. M., Somers, D. A., and Myers, D. E. (1991) Isolation and characterization of dihydrodipicolinate synthase from maize, *Plant Physiol 96*, 444-452.
31. Devenish, S. R., Huisman, F. H., Parker, E. J., Hadfield, A. T., and Gerrard, J. A. (2009) Cloning and characterisation of dihydrodipicolinate synthase from the pathogen *Neisseria meningitidis*, *Biochim Biophys Acta 1794*, 1168-1174.
32. Dobson, R. C., Griffin, M. D., Roberts, S. J., and Gerrard, J. A. (2004) Dihydrodipicolinate synthase (DHDPS) from *Escherichia coli* displays partial mixed inhibition with respect to its first substrate, pyruvate, *Biochimie 86*, 311-315.
33. Skovpen, Y. V., and Palmer, D. R. (2013) Dihydrodipicolinate synthase from *Campylobacter jejuni*: kinetic mechanism of cooperative allosteric inhibition and inhibitor-induced substrate cooperativity, *Biochemistry 52*, 5454-5462.
34. Domigan, L. J., Scally, S. W., Fogg, M. J., Hutton, C. A., Perugini, M. A., Dobson, R. C., Muscroft-Taylor, A. C., Gerrard, J. A., and Devenish, S. R. (2009) Characterisation of dihydrodipicolinate synthase (DHDPS) from *Bacillus anthracis*, *Biochim Biophys Acta 1794*, 1510-1516.

35. Rice, E. A., Bannon, G. A., Glenn, K. C., Jeong, S. S., Sturman, E. J., and Rydel, T. J. (2008) Characterization and crystal structure of lysine insensitive *Corynebacterium glutamicum* dihydrodipicolinate synthase (cDHDPS) protein, *Arch Biochem Biophys 480*, 111-121.
36. Wolterink-van Loo, S., Levisson, M., Cabrieres, M. C., Franssen, M. C., and van der Oost, J. (2008) Characterization of a thermostable dihydrodipicolinate synthase from *Thermoanaerobacter tengcongensis*, *Extremophiles 12*, 461-469.
37. Burgess, B. R., Dobson, R. C., Bailey, M. F., Atkinson, S. C., Griffin, M. D., Jameson, G. B., Parker, M. W., Gerrard, J. A., and Perugini, M. A. (2008) Structure and evolution of a novel dimeric enzyme from a clinically important bacterial pathogen, *J Biol Chem 283*, 27598-27603.
38. Dobson, R. C., Valegard, K., and Gerrard, J. A. (2004) The crystal structure of three site-directed mutants of *Escherichia coli* dihydrodipicolinate synthase: further evidence for a catalytic triad, *J Mol Biol 338*, 329-339.
39. Dobson, R. C., Devenish, S. R., Turner, L. A., Clifford, V. R., Pearce, F. G., Jameson, G. B., and Gerrard, J. A. (2005) Role of arginine 138 in the catalysis and regulation of *Escherichia coli* dihydrodipicolinate synthase, *Biochemistry 44*, 13007-13013.
40. Dobson, R. C., Griffin, M. D., Jameson, G. B., and Gerrard, J. A. (2005) The crystal structures of native and (S)-lysine-bound dihydrodipicolinate synthase from *Escherichia coli* with improved resolution show new features of biological significance, *Acta Crystallogr D Biol Crystallogr 61*, 1116-1124.
41. Atkinson, S. C., Dogovski, C., Downton, M. T., Czabotar, P. E., Dobson, R. C., Gerrard, J. A., Wagner, J., and Perugini, M. A. (2013) Structural, kinetic and computational investigation of *Vitis vinifera* DHDPS reveals new insight into the mechanism of lysine-mediated allosteric inhibition, *Plant Mol Biol 81*, 431-446.
42. Vauterin, M., Frankard, V., and Jacobs, M. (2000) Functional rescue of a bacterial dapA auxotroph with a plant cDNA library selects for mutant clones encoding a feedback-insensitive dihydrodipicolinate synthase, *Plant J 21*, 239-248.
43. Hughes, R. (2004) *Campylobacter jejuni* in Guillain-Barre syndrome, *Lancet Neurol 3*, 644.
44. Young, K. T., Davis, L. M., and Dirita, V. J. (2007) *Campylobacter jejuni*: molecular biology and pathogenesis, *Nat Rev Microbiol 5*, 665-679.
45. Roberts, S. J., Morris, J. C., Dobson, R. C. J., Baxter, C. L., and Gerrard, J. A. (2004) Two complete syntheses of (*S*)-aspartate semi-aldehyde and demonstration that Δ^2-tetrahydroisophthalic acid is a non-competitive inhibitor of dihydrodipicolinate synthase, *Arkivoc x*, 166-177.
46. Yugari, Y., and Gilvarg, C. (1965) The condensation step in diaminopimelate synthesis, *J Biol Chem 240*, 4710-4716.

CHAPTER 5. DISCUSSION, CONCLUSIONS AND FUTURE WORK

5.1 From L-lysine and weak allosteric inhibitors of DHDPS to potent *R,R*-bislysine

The present study is a comprehensive analysis of an allosteric enzyme DHDPS and its allosteric inhibitors. A detailed lysine inhibition study has been presented for the first time with *C. jejuni* DHDPS. The results suggest that *C. jejuni* DHDPS is several times more sensitive to lysine inhibition than *E. coli* DHDPS (*1*) and has inhibition constants 69 ± 1, 45 ± 3, and 72 ± 9 μM, for when lysine binds to the E:pyr, F, and F:ASA complexes, respectively. Comparison of mixed partial and uncompetitive partial kinetic models for lysine inhibition with respect to pyruvate allowed us to conclude that lysine is an uncompetitive partial inhibitor, which is in agreement with work of Karsten (1) and Soares da Costa *et al.* (2), who studied *E. coli* DHDPS. This kinetic model does not exclude the capability of lysine to bind to the free enzyme form E, but rather indicates that if this E:I complex exists, it doesn't affect binding of the first substrate pyruvate. The results of lysine inhibition with respect to ASA indicates a mixed partial model of inhibition (which is a type of noncompetitive inhibition where binding affinities for lysine of F and F:I complexes are different). This conclusion, again in agreement with the work of Karsten (*1*), and somewhat different from the results of Gerrard and co-workers (*3*), who reported a noncompetitive partial model (meaning that F and F:I complexes have the same binding affinities for lysine). A possible reason for disagreement between research groups in reporting kinetic models is in the different approaches to kinetic data analysis. While a pure noncompetitive partial model provides a decent fit with fewer variables, the mixed partial model, having additional coefficient α, has a better fit and statistical characteristics. To provide an unbiased approach to discrimination between kinetic models, we found it useful to plot the kinetic data in Cornish-Bowden and Dixon plots and determine their inhibition patterns. Therefore uncompetitive and mixed models were selected for further kinetic analysis. Although this approach has been known for full types of inhibition (for which it is definitely more accurate), we have applied it to the case of partial inhibition. Straight plots can be obtained at inhibitor concentrations which precede the saturating region.

We found that lysine binds to the enzyme cooperatively and therefore cooperativity coefficients of lysine were calculated. The average cooperativity coefficients were found by graphical methods (2.8 ± 0.2) and cooperativity was also calculated as a result of global fitting (2.6 ± 0.1, 2.3 ± 0.2, 2.8 ± 0.2, Table 2.2). The results obtained by different methods are in a good agreement. This highly cooperative manner of binding cannot be ignored while fitting the experimental data, therefore concentrations of inhibitor and inhibition constants in the rate equations must be raised to the power of cooperativity coefficients (*4*). Atkinson *et al.* (*5*), who studied lysine inhibition kinetics of DHDPS from *V. vinifera* came to the same conclusion. The rate equations, modified with cooperativity coefficients, were successfully used in studying the kinetics of DHDPS inhibition by *R,R*-bislysine, as well as lysine inhibition of H56A and H56N. An interesting feature, lysine-induced ASA cooperativity, was noticed not only for wild-type DHDPS, but also for H56A and H56N mutants. To our knowledge this observation is rare, although there is precedent in the literature (*6*).

L-Thialysine and α-methyl-DL-lysine are very weak inhibitors of DHDPS. Despite small structural differences between lysine and L-thialysine, the latter is a much poorer inhibitor. To find the exact reason for this decreased inhibitory activity of L-thialysine is one of the subjects of future work. Possibly, changes in pK_a of the α- and terminal amino groups, as well as carboxyl group of L-thialysine results in weaker hydrogen bonding between L-thialysine and residues of the allosteric site. On the other hand, the thioether fragment in L-thialysine is larger than the corresponding methylene group in lysine, and therefore unfavourable steric interactions with amino acid residues of the allosteric site can be the reason of weaker inhibitory activity of L-thialysine. If the last statement is valid, then this can be a serious obstacle for future inhibitor design to introduce bulky aromatic rings in the inhibitor structure instead of lysine or *R,R*-bislysine side chains (design of new inhibitors of DHDPS is discussed in section 5.3). The overlay of the crystal structures of L-lysine and L-thialysine bound at the allosteric site of *C. jejuni* DHDPS is shown in Figure 5.1.

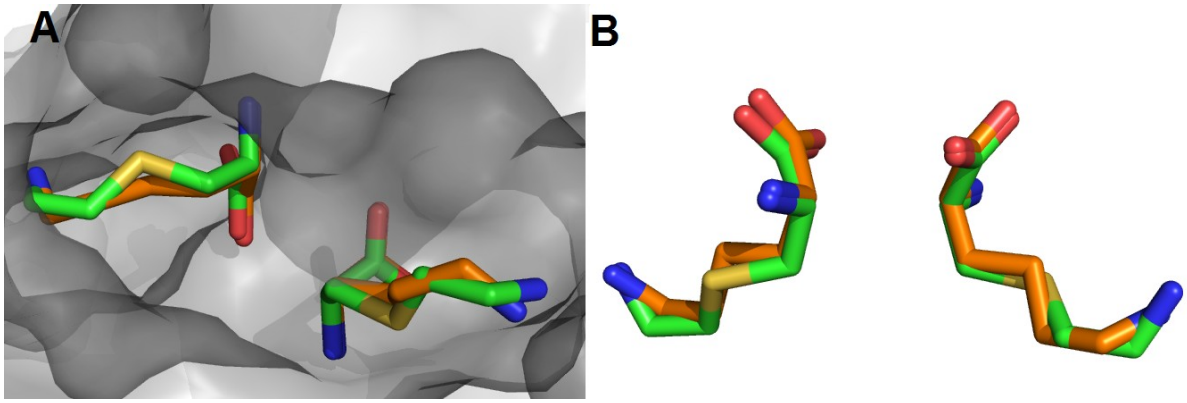

Figure 5.1 Overlay of crystal structures of L-lysine (orange) and L-thialysine (green) bound at the allosteric site of *C. jejuni* DHDPS. (A) Position of overlaid ligands in the allosteric pocket; (B) The same overlay rotated 90°.

The α-methyl group in α-methyl-DL-lysine prevents proper binding of the inhibitor at the adjacent lysine binding pockets in the allosteric site of DHDPS, therefore correct spacing between two inhibitor molecules or between binding fragments within a symmetrical molecule of inhibitor is required. The inhibition tests with α-methyl-DL-lysine suggest indirectly that the allosteric site of DHDPS will not tolerate homologs of *R,R*-bislysine with three- or four-carbon bridges in the structure.

The design of *R,R*-bislysine was based on the hypothesis that a symmetrical molecule, targeting two lysine binding pockets in the allosteric site, would have an energy benefit as a result of the decrease in binding entropy. The principle of using one inhibitor molecule to target multiple protein sites has been used before and discussed in the literature. There are inhibitors, binding within one protein subunit, but targeting two receptor sites, such as vorinostat, a histone deacetylase inhibitor, where the two amide groups in the inhibitor were linked together with a spacer, resulting in stronger binding due to a chelating effect (*7*). There are also bisubstrate inhibitors, which mimics binding of two substrates to an enzyme using a linker. For instance, Shen *et al.* reported a peptide-ATP conjugate against insulin receptor kinase which occupied both peptide and nucleotide binding sites (*8*). Bisubstrate analogue inhibitors of 6-hydroxymethyl-7,8-dihydropterin pyrophosphokinase were developed by placing a piperidine-containing linkage between pterin and adenosine moieties (*9*). Another example of bisubstrate inhibitors is the estradiol/adenosine hybrid EM-1745 which is potent against 17b-hydroxysteroid dehydrogenase (*10*). Bivalent or polyvalent inhibitors are able to target two or more protein subunits by one inhibitor molecule. As an example, the carbohydrate ligand (STARFISH) was

designed against Shiga-like toxin I with subnanomolar inhibitory activity (*11*). The inhibitor coordinates with five protein subunits and has a million times higher inhibitory activity than that of univalent ligands (*11*). Applying the concept of bivalent inhibitor design, Duggineni e*t al.* synthesized several dimeric peptides capable of binding simultaneously to two EphA2 receptor molecules, and this strategy resulted in an increase of binding affinity of these ligands (*12*). The result of using bisubstrate, bivalent or polyvalent inhibitors instead of univalent inhibitors depends on various factors including proper spacing of the moieties of the complex inhibitor. An optimal linker would provide a favourable conformation and promote a correct positioning of functional groups of the inhibitor with the protein molecule(s). The design of linked inhibitors has entropy advantages, moreover a linker part can also participate in hydrogen bonding, which would also result in a favourable enthalpy change (*9*).

R,R-bislysine is an example of a divalent inhibitor, in that one molecule targets two protein subunits. The results of this work show that the strategy of inhibitor design is valid and we observed more than 300 times stronger inhibition of wild-type *C. jejuni* DHDPS by *R,R*-bislysine than by L-lysine, where the average inhibition constant of *R,R*-bislysine is 200 nM. The two-carbon bridge in *R,R*-bislysine structure is optimal to allow the molecule to bind in the two adjacent lysine binding pockets, providing 3.93 Å distance between α-carbons, mimicking the enzyme-lysine structure nearly perfectly. *R,R*-bislysine demonstrates a slow-binding inhibition behaviour, where equilibrium between the inhibitor and the enzyme establishes within 1-1.5 min after mixing. The frequency constant of the exponential phase, k_{obs}, has a linear relationship with the concentration of *R,R*-bislysine, which is an indication that *R,R*-bislysine binds slowly to the enzyme species, without enzyme isomerisation, which is also confirmed by crystallography results. Unlike L-lysine, *R,R*-bislysine binds to the free form of enzyme E, and therefore the mixed partial model of inhibition with respect to pyruvate provides the best fit to the experimental data. With respect to ASA, *R,R*-bislysine was found to be a noncompetitive partial inhibitor. Binding of *R,R*-bislysine to all forms of enzyme (except free form of enzyme, E) is cooperative and cooperativity coefficients were found to be 1.6 and 1.7 (Table 3.1), which indicates a highly cooperative manner of binding of *R,R*-bislysine to the dimeric subunits in the tetramer. The noncompetitive nature of *R,R*-bislysine is also beneficial when compared with competitive inhibitors, such that high concentrations of substrates cannot compete with the inhibitor for the binding site.

To explore the inhibitory potential of *R,R*-bislysine and L-lysine, the allosteric site of DHDPS was modified by Y110F, H56A, H56N, H59A and H59N mutations. The expectations were that mutations would decrease the binding affinity of inhibitors to a certain extent. Surprisingly, this prediction turned out to be valid only for lysine, but not for *R,R*-bislysine. Thus, Y110F, H59A and H59N were almost insensitive to lysine inhibition, and H56A and H56N were five- and three- times respectively less sensitive to lysine than the wild-type. Unlike lysine, *R,R*-bislysine showed exceptional inhibitory properties against Y110F, H56A, H56N and H59N mutants, with apparent IC_{50} values in the submicromolar range. These studies revealed, however, that binding of *R,R*-bislysine is dependent on His59. The H59A mutation, which eliminated hydrogen bonding between the terminal amino groups of *R,R*-bislysine and the histidines in the allosteric site, caused an approximately ten-fold increase in the apparent IC_{50} value.

5.2 Design of new symmetrical inhibitors of DHDPS

The results of this study now open new perspectives in the development of noncompetitive inhibitors of DHDPS. The strategy of designing symmetrical inhibitors targeting two lysine pockets in the allosteric site was shown to be successful. *R,R*-bislysine inhibition studies with mutants allows us to conclude that hydrogen bonding between the carboxyl group of the inhibitor and Tyr110 is not crucial for inhibitory effectiveness, whereas a hydrogen bond between His59 and the ε-amino group of the inhibitor is essential, as was indicated previously. The importance of the α-amino groups in *R,R*-bislysine for inhibition is the subject for future work. Modification of *R,R*-bislysine is necessary for designing drug-like compounds, which are able to pass through bacterial cell walls. This optimization could include the replacement of carboxyl groups with suitable isosteres, design of a new spacer instead of the two-carbon bridge, which would fix the molecule in favorable conformation and reduce the number of rotatable bonds, introduce aromatic rings to the structure to increase lipophilicity, etc. The activity of *R,R*-bislysine against mutants of *C. jejuni* DHDPS, which are insensitive to lysine inhibition, means that *R,R*-bislysine would also likely be active against DHDPS from different species with a similar architecture of allosteric sites. The validity of this statement would be interesting to verify in future studies.

5.3 DHDPS from Gram-positive bacteria: inhibition of difficult targets

It is a difficult task to inhibit lysine-insensitive DHDPS from Gram-positive bacteria. The major obstacle preventing binding of lysine and its mimics is Lys (or Arg) in position 56 (H59 in *C. jejuni* DHDPS). As discussed above, substitution of His59 for Ala in *C. jejuni* DHDPS resulted in tenfold decrease in inhibitory activity of *R,R*-bislysine. Therefore a favorable interaction of the amino acid residue in this position with the inhibitor is important for signal transduction from the allosteric to active site. Lys56 in DHDPS from Gram-positive bacteria prevents binding of L-lysine due to a steric clash and repulsion of positively charged Lys56 and the ε-amino group of the inhibitor. *R,R*-bislysine would have the same unfavorable interactions with the enzyme. For that reason a symmetrical molecule, having the same 2,5-diamino adipic acid scaffold as has *R,R*-bislysine, but with shorter side chains and polar, non-positively charged functional groups at the end of side chains would be a good candidate for preliminary studies of inhibition of DHDPS from Gram-positive bacteria.

5.4 References

1. Karsten, W. E. (1997) Dihydrodipicolinate synthase from *Escherichia coli*: pH dependent changes in the kinetic mechanism and kinetic mechanism of allosteric inhibition by L-lysine, *Biochemistry 36*, 1730-1739.
2. Soares da Costa, T. P., Muscroft-Taylor, A. C., Dobson, R. C., Devenish, S. R., Jameson, G. B., and Gerrard, J. A. (2010) How essential is the 'essential' active-site lysine in dihydrodipicolinate synthase?, *Biochimie 92*, 837-845.
3. Dobson, R. C., Griffin, M. D., Roberts, S. J., and Gerrard, J. A. (2004) Dihydrodipicolinate synthase (DHDPS) from *Escherichia coli* displays partial mixed inhibition with respect to its first substrate, pyruvate, *Biochimie 86*, 311-315.
4. Cortes, A., Cascante, M., Cardenas, M. L., and Cornish-Bowden, A. (2001) Relationships between inhibition constants, inhibitor concentrations for 50% inhibition and types of inhibition: new ways of analysing data, *Biochem J 357*, 263-268.
5. Atkinson, S. C., Dogovski, C., Downton, M. T., Czabotar, P. E., Dobson, R. C., Gerrard, J. A., Wagner, J., and Perugini, M. A. (2013) Structural, kinetic and computational investigation of *Vitis vinifera* DHDPS reveals new insight into the mechanism of lysine-mediated allosteric inhibition, *Plant Mol Biol 81*, 431-446.
6. Kohlhaw, G., Leary, T. R., and Umbarger, H. E. (1969) Alpha-isopropylmalate synthase from *Salmonella typhimurium*. Purification and properties, *J Biol Chem 244*, 2218-2225.
7. Marks, P. A., and Breslow, R. (2007) Dimethyl sulfoxide to vorinostat: development of this histone deacetylase inhibitor as an anticancer drug, *Nat Biotechnol 25*, 84-90.
8. Shen, K., Hines, A. C., Schwarzer, D., Pickin, K. A., and Cole, P. A. (2005) Protein kinase structure and function analysis with chemical tools, *Biochim Biophys Acta 1754*, 65-78.
9. Shi, G., Shaw, G., Li, Y., Wu, Y., Yan, H., and Ji, X. (2012) Bisubstrate analog inhibitors of 6-hydroxymethyl-7,8-dihydropterin pyrophosphokinase: new lead exhibits a distinct binding mode, *Bioorg Med Chem 20*, 4303-4309.
10. Fournier, D., Poirier, D., Mazumdar, M., and Lin, S. X. (2008) Design and synthesis of bisubstrate inhibitors of type 1 17beta-hydroxysteroid dehydrogenase: overview and perspectives, *Eur J Med Chem 43*, 2298-2306.
11. Kitov, P. I., Sadowska, J. M., Mulvey, G., Armstrong, G. D., Ling, H., Pannu, N. S., Read, R. J., and Bundle, D. R. (2000) Shiga-like toxins are neutralized by tailored multivalent carbohydrate ligands, *Nature 403*, 669-672.
12. Duggineni, S., Mitra, S., Lamberto, I., Han, X., Xu, Y., An, J., Pasquale, E. B., and Huang, Z. (2013) Design and Synthesis of Potent Bivalent Peptide Agonists Targeting the EphA2 Receptor, *ACS Med Chem Lett 4*.

APPENDIX A

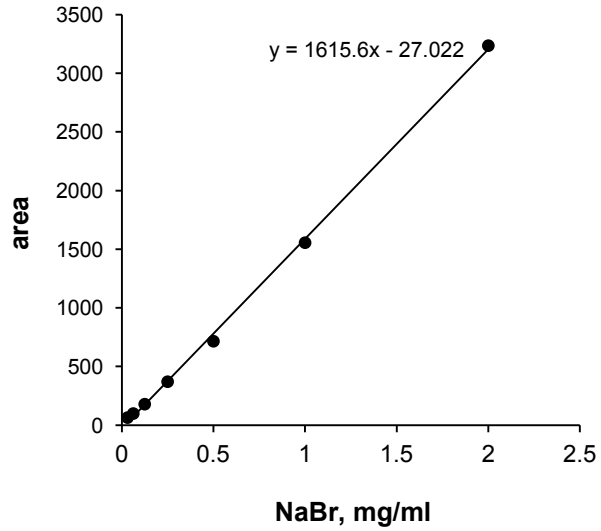

Figure A 1 Calibration plot for sodium bromide.

Table A 1 Calculated amounts of sodium bromide in the samples.

#	Sample	Sample concentration, mg/ml	NaBr peak area	% NaBr (w/w)
1	*R,R*-bislysine	1.5	365.8	16
2	*S,S*-bislysine	1.2	423.6	20

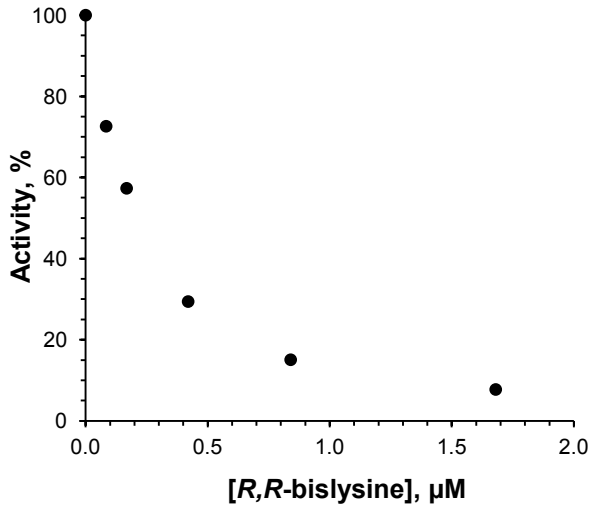

Figure A 2 An inhibition curve of DHDPS by *R,R*-bislysine (at 2.6 mM of ASA and 3.7 mM of pyruvate).

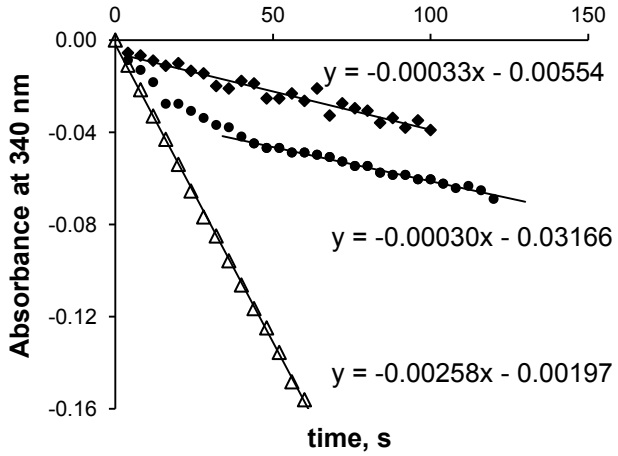

Figure A 3 Progress curves of the enzymatic reaction: (△) in the absence of *R,R*-bislysine; in the presence of *R,R*-bislysine (0.84 µM): (●) reaction started with DHDPS, (◆) reaction started with ASA. Concentrations of substrates: ASA 0.16 mM, pyruvate 3.7 mM.

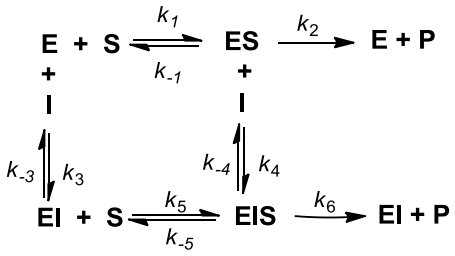

Scheme A 1 A general equilibrium scheme for noncompetitive (including pure noncompetitive and mixed) partial inhibition (similar to the noncompetitive inhibition mechanism reported by Cha (Cha, S. (1975) Tight-binding inhibitors-I. Kinetic behavior, *Biochem Pharmacol 24*, 2177-2185). Assumptions: $K_M >> K_i$, $k_{-1} >> k_{-3}$, $k_{-1} >> k_{-4}$, $k_1S >> k_3I$, $k_1S >> k_4I$. Definitions: $K_M = (k_{-1} + k_2)/k_1$; $K_M' = (k_{-5} + k_6)/k_5$; $K_i1 = k_{-3}/k_3$, $K_i2 = k_{-4}/k_4$.

Equation A1 The equation shows linear relationship between k_{obs} and [I], and can be expressed in a linear form $k_{obs} = k_{on}[I] + k_{off}$ at constant concentration of [S], where k_{on} and k_{off} are apparent microscopic rate constants, which represent a slope and an intercept of the linear plot.

$$k_{obs} = \frac{(k_3 + \frac{k_4[S]}{K_M})[I]}{1 + \frac{[S]}{K_M}} + \frac{k_{-3} + \frac{k_{-4}[S]}{K_M'}}{1 + \frac{[S]}{K_M'}} \qquad \text{(A1)}$$

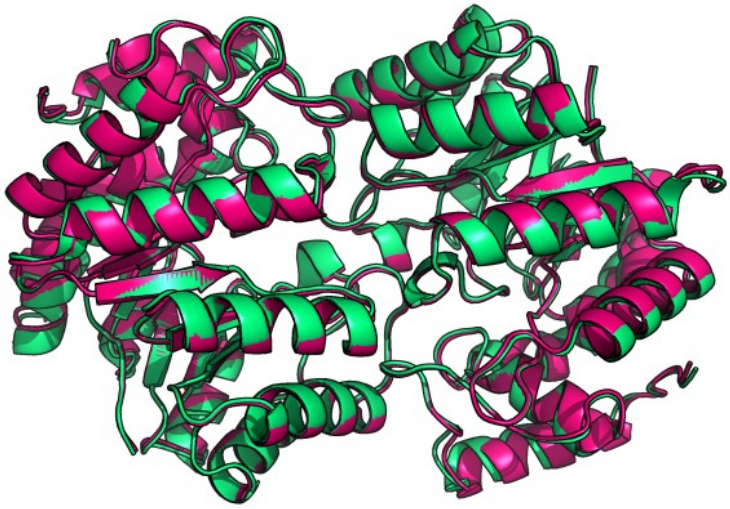

Figure A 4 Overlay of crystal structures *C. jejuni* DHDPS with L-lysine (magenta) and *R,R*-bislysine (green) (Conly *et al*., Unpublished work).

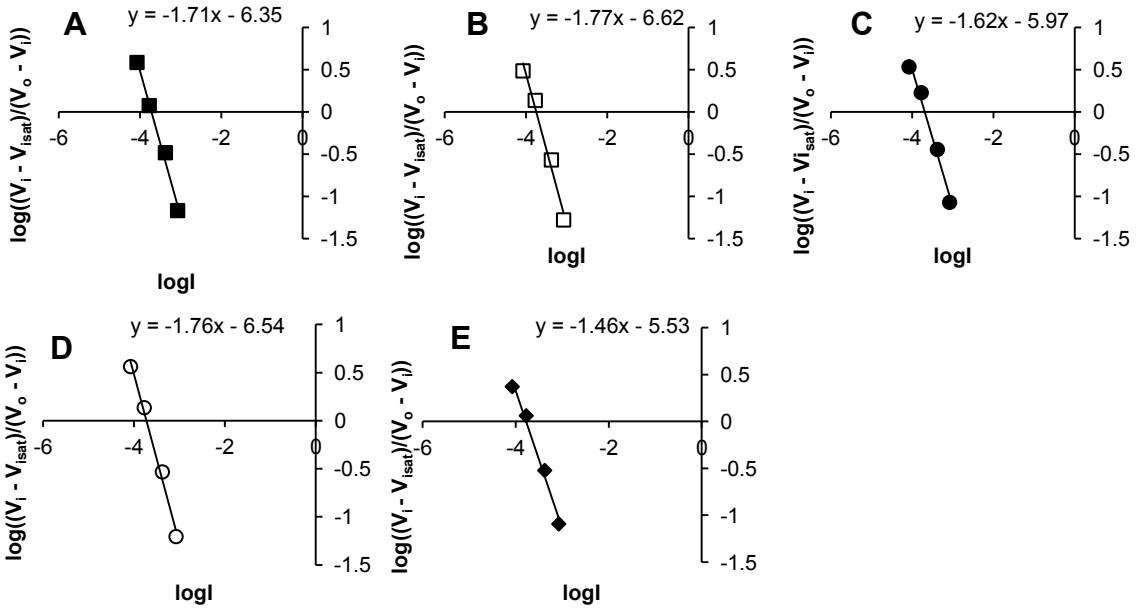

Figure A 5 Hill plots at 3.7 mM pyruvate and varied concentrations of ASA: (A) 0.066 mM, (B) 0.099 mM, (C) 0.16 mM, (D) 0.33 mM, and (E) 2.6 mM. Solid lines were obtained by linear regression.

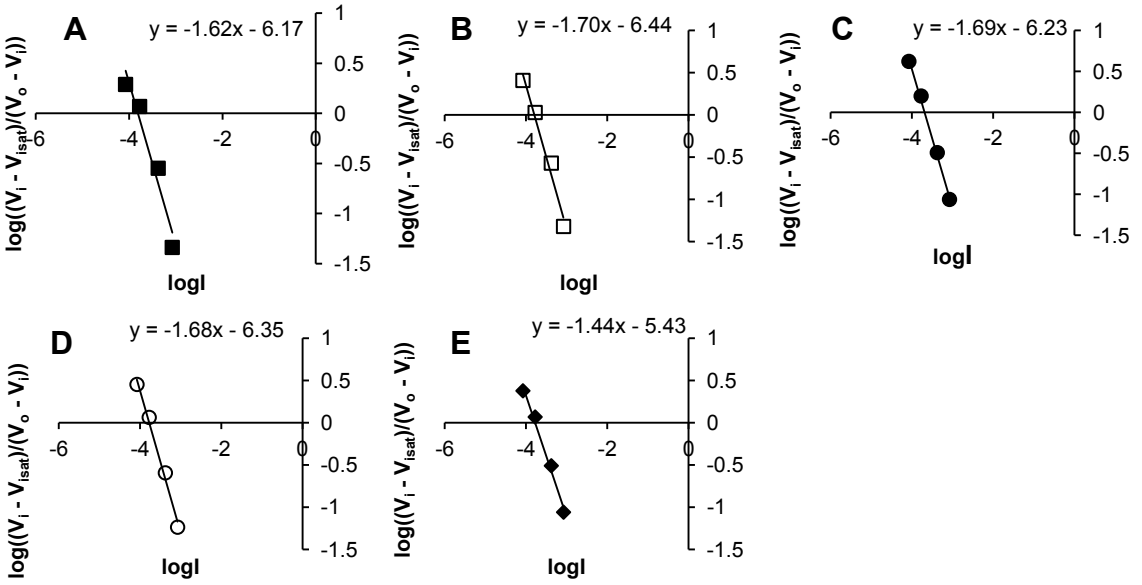

Figure A 6 Hill plots at 2.6 mM ASA and varied concentrations of pyruvate: (A) 0.20 mM, (B) 0.30 mM, (C) 0.60 mM, (D) 1.0 mM, and (E) 3.7 mM. Solid lines were obtained by linear regression.

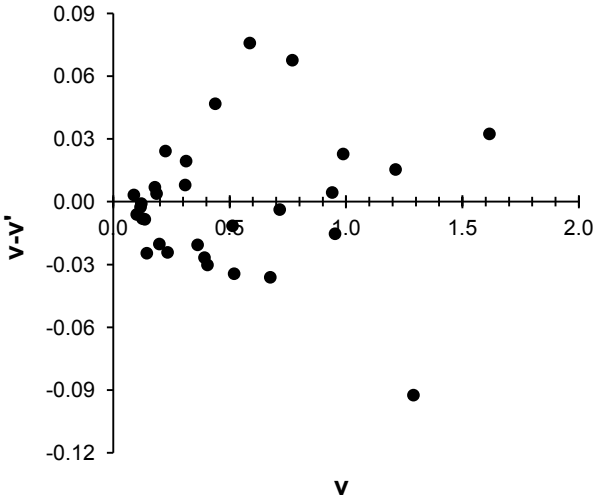

Figure A 7 Residuals for plot in Figure 3.10.

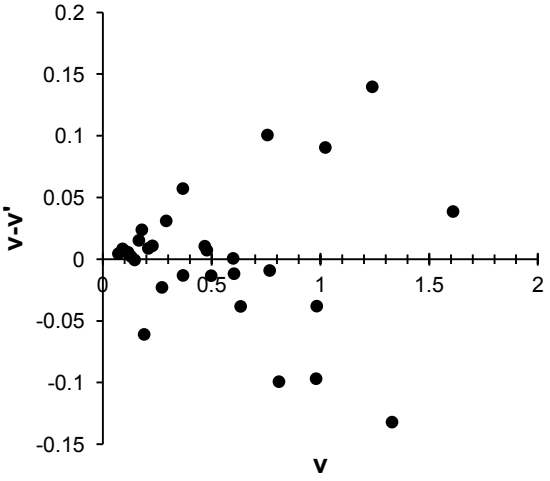

Figure A 8 Residuals for plot in Figure 3.11.

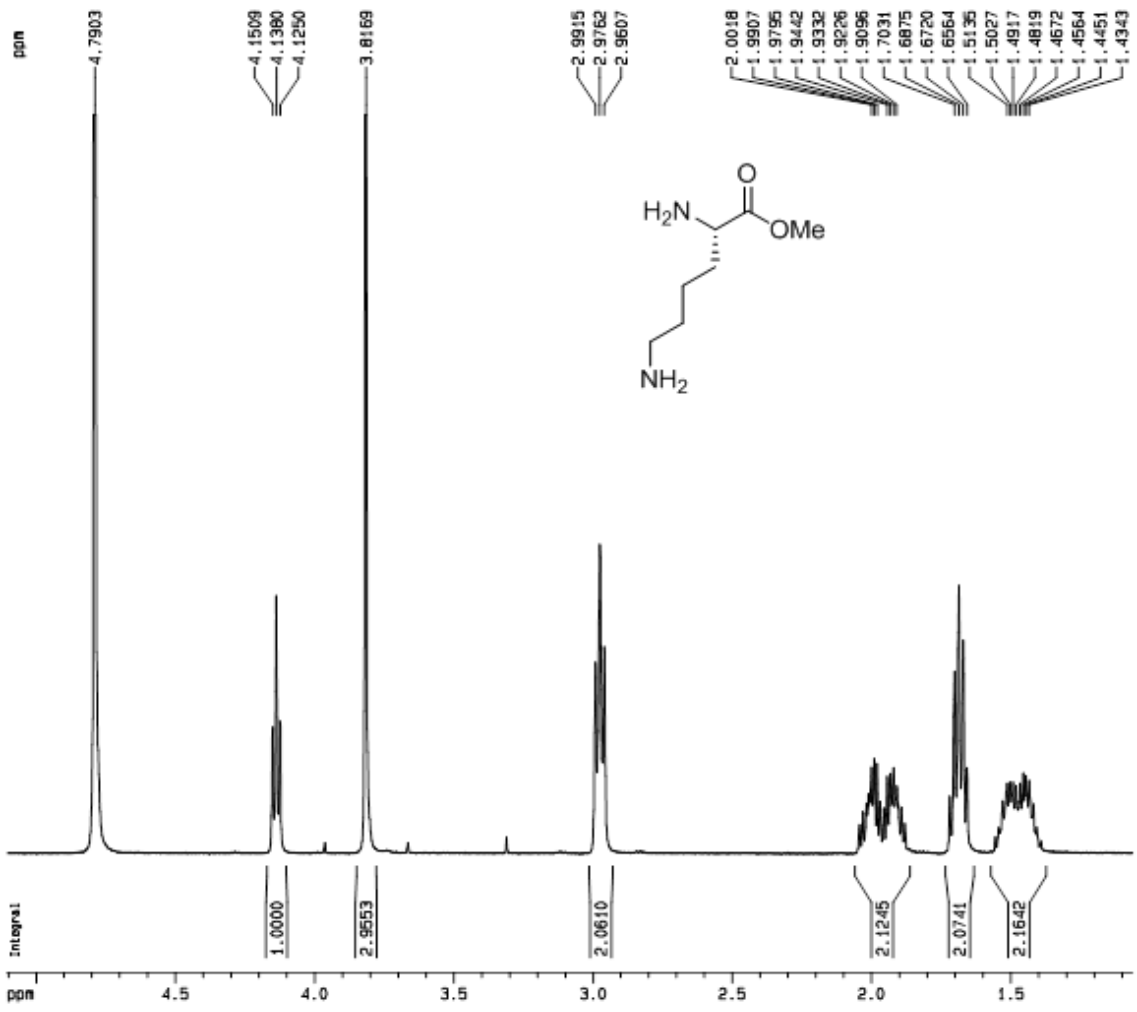

Spectrum A1-1 500 MHz ^{1}H NMR spectrum of methyl (2*S*)-2,6-diaminohexanoate (**1**) in D_2O.

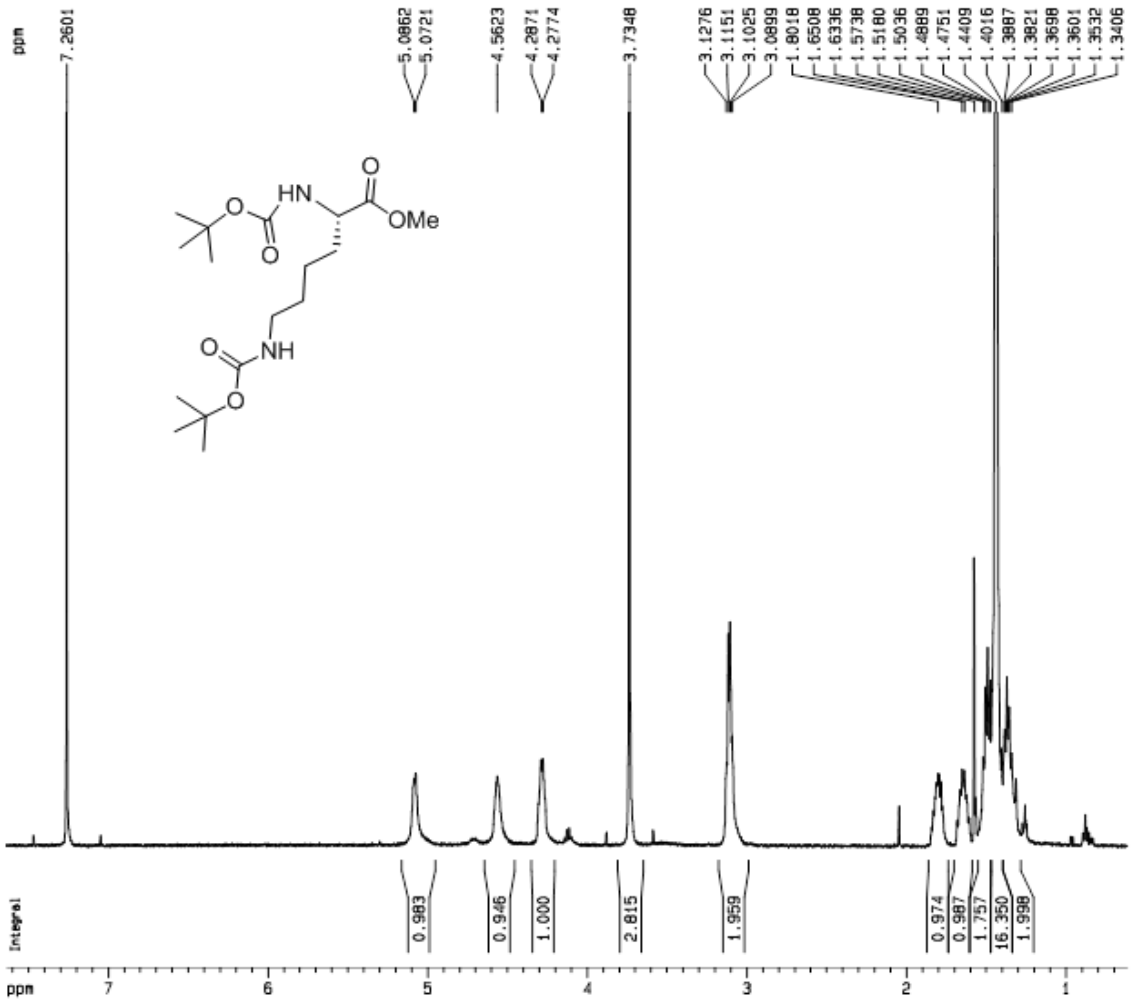

Spectrum A2-1 500 MHz ^{1}H NMR spectrum of methyl (2*S*)-2,6-bis{[(tert-butoxy)carbonyl]amino}hexanoate (**2**) in $CDCl_3$.

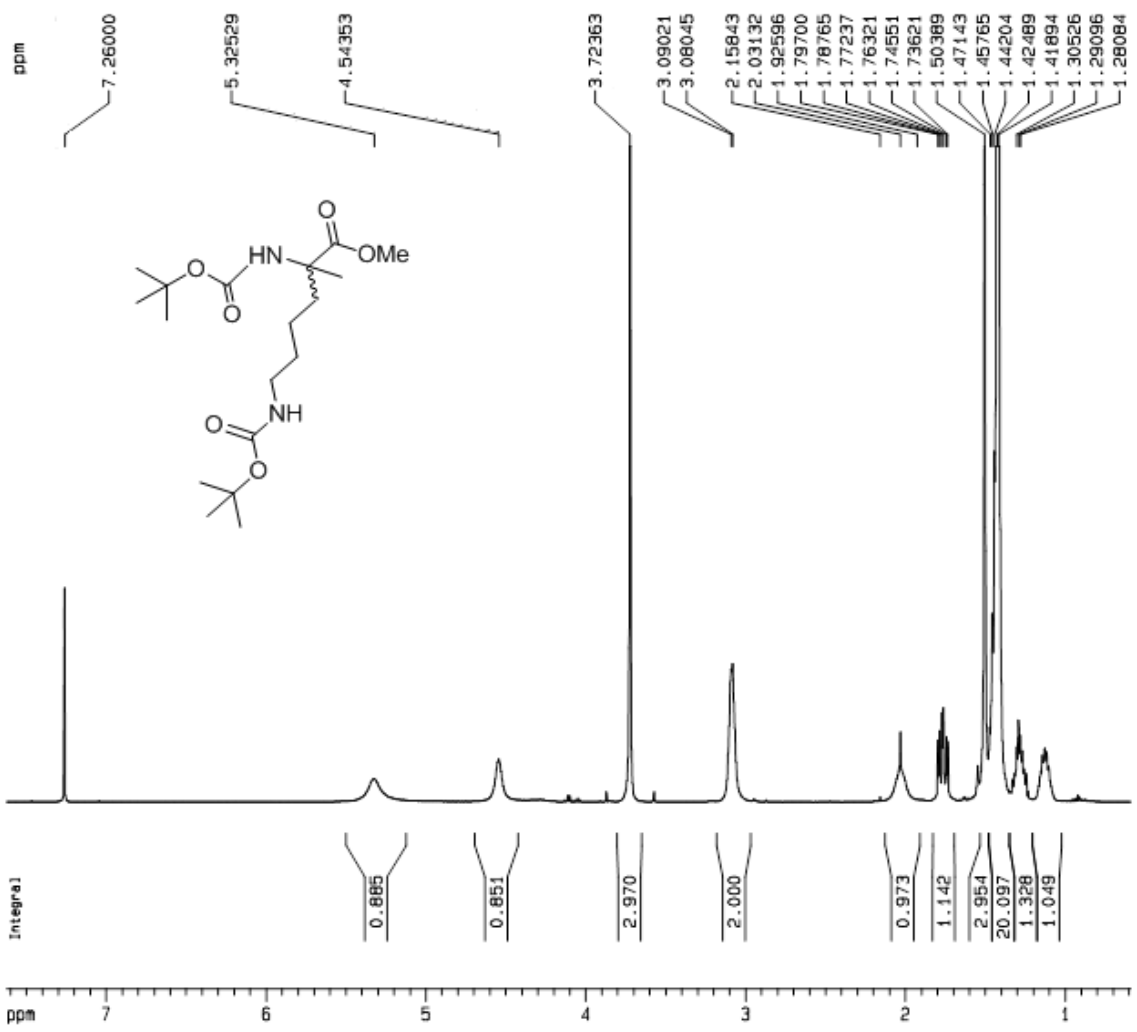

Spectrum A3-1 500 MHz ^{1}H NMR spectrum of methyl (±)-2,6-bis{[(tert-butoxy)carbonyl]amino}-2-methylhexanoate (**3**) in $CDCl_3$.

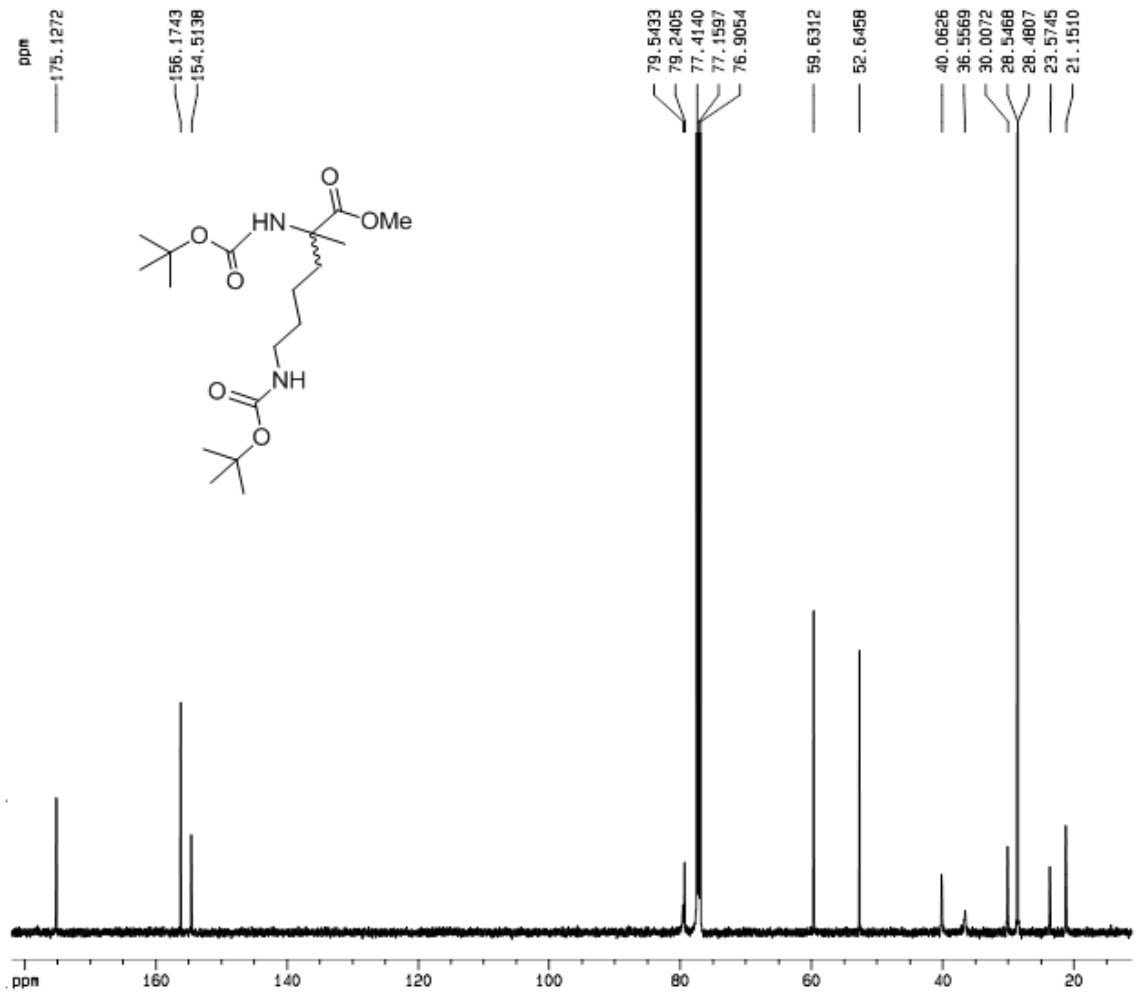

Spectrum A3-2 125 MHz ^{13}C NMR spectrum of methyl (±)-2,6-bis{[(tert-butoxy)carbonyl]amino}-2-methylhexanoate (**3**) in $CDCl_3$.

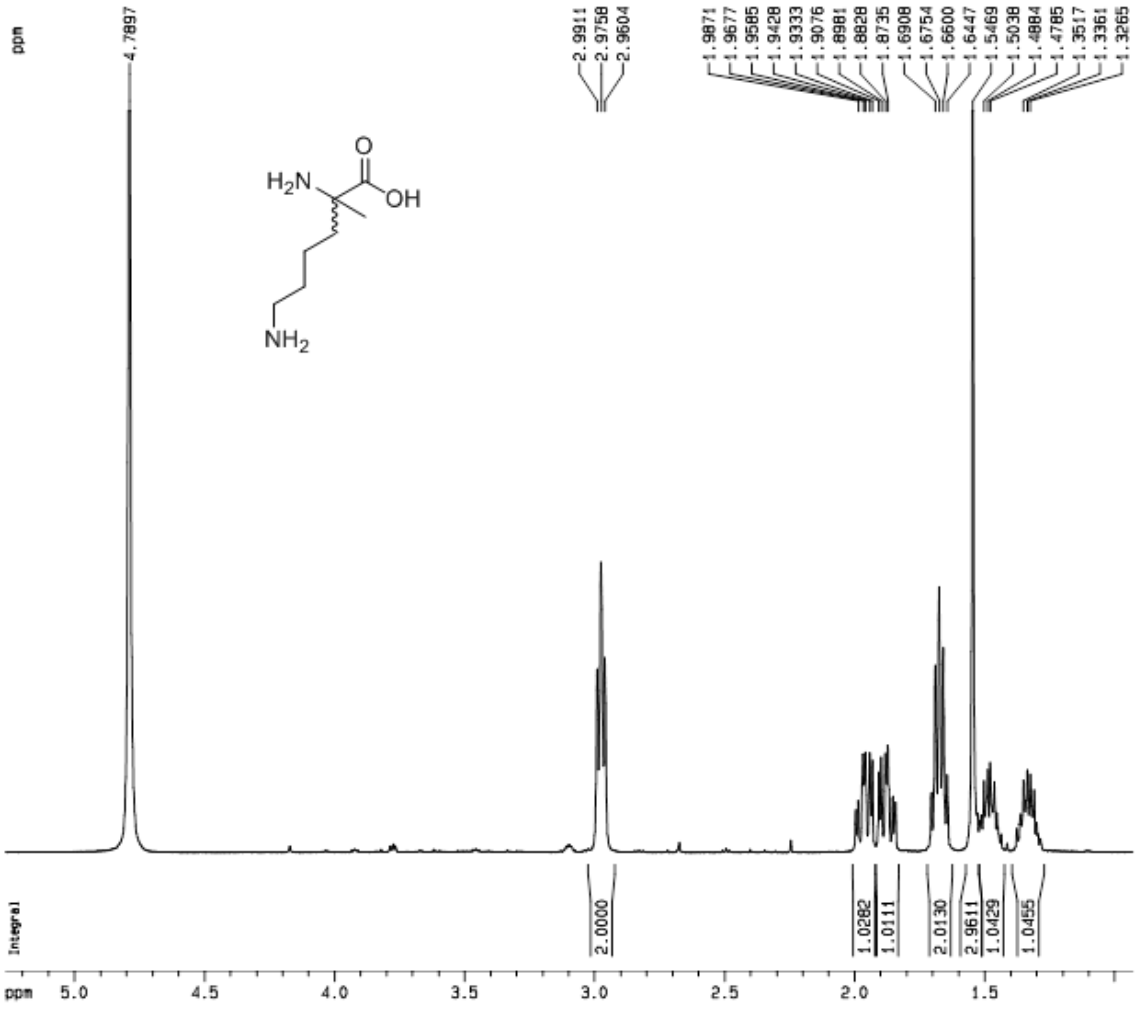

Spectrum A4-1 500 MHz ^{1}H NMR spectrum of methyl (±)-2,6-diamino-2-methylhexanoic acid (**4**) in D_2O.

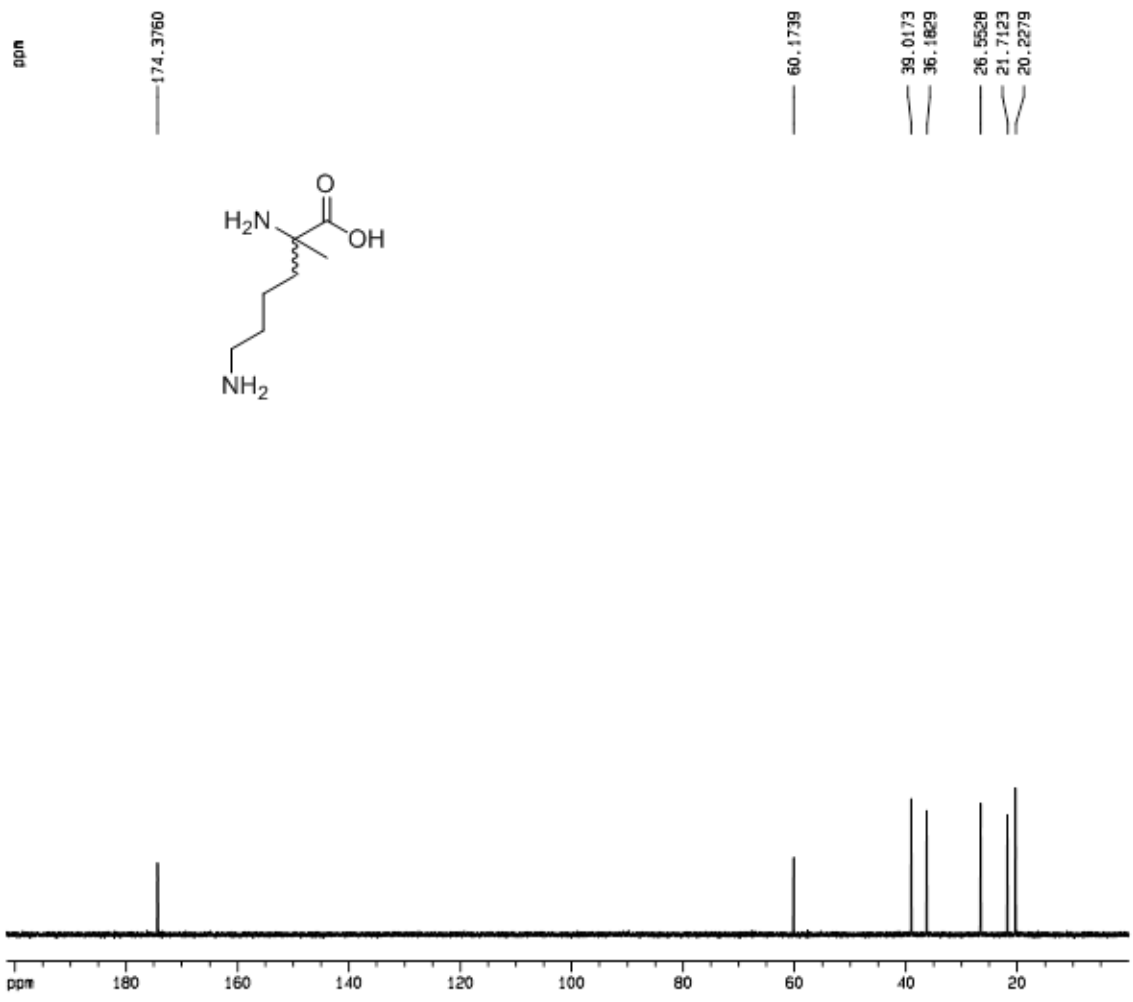

Spectrum A4-2 125 MHz ^{13}C NMR spectrum of methyl (±)-2,6-diamino-2-methylhexanoic acid (**4**) in D_2O.

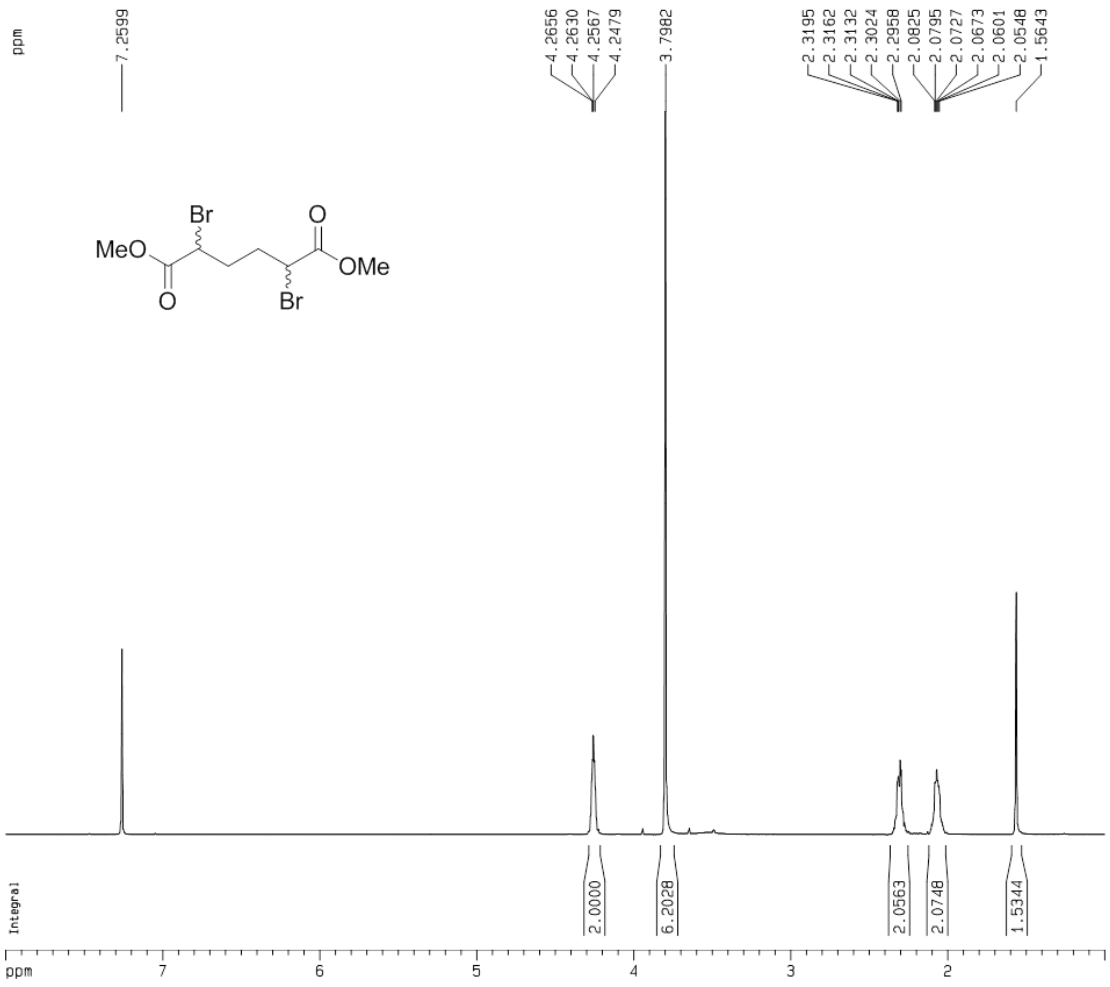

Spectrum A5-1 500 MHz ^{1}H NMR spectrum of dimethyl 2,5-dibromohexanedioate (**5**) in $CDCl_3$

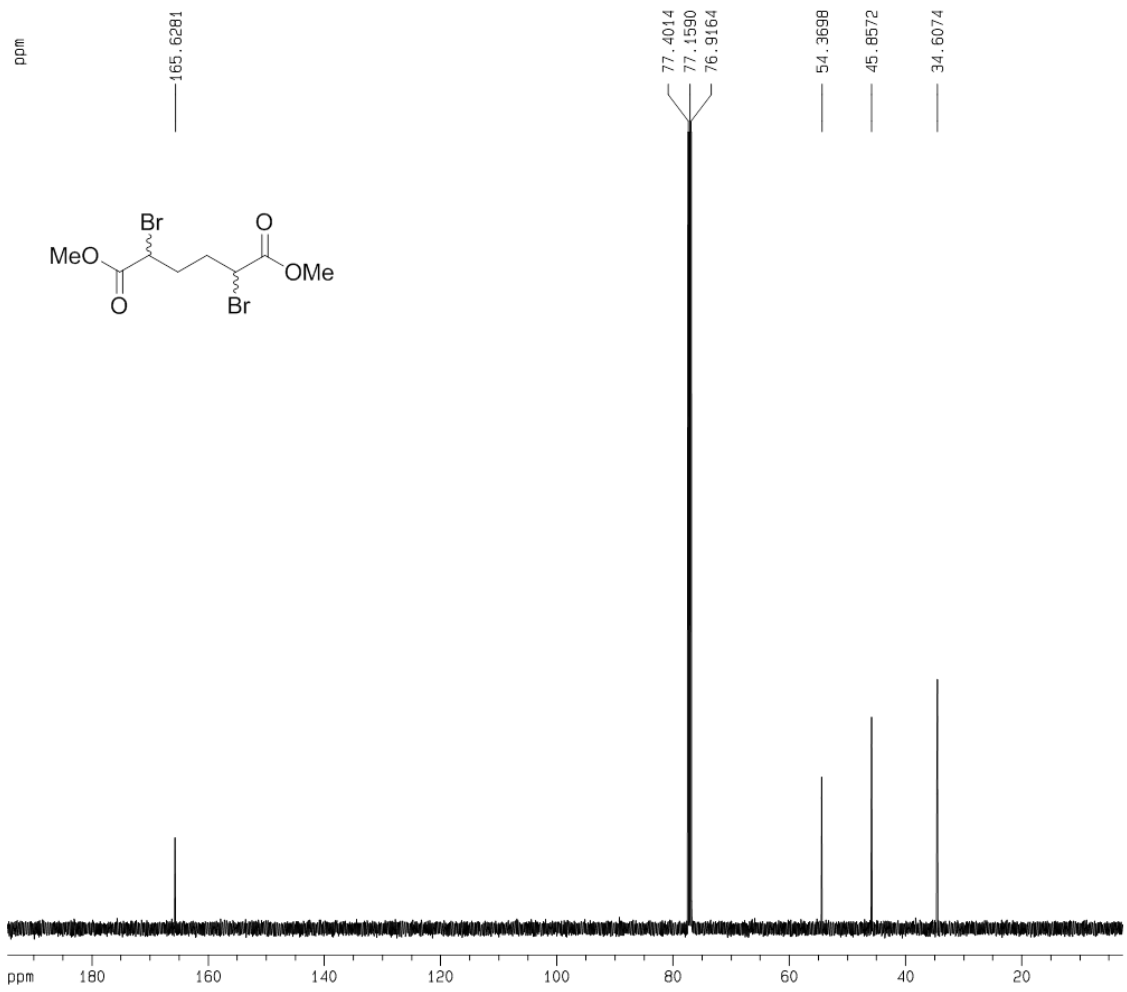

Spectrum A5-2 125 MHz ^{13}C NMR spectrum of dimethyl 2,5-dibromohexanedioate (**5**) in $CDCl_3$

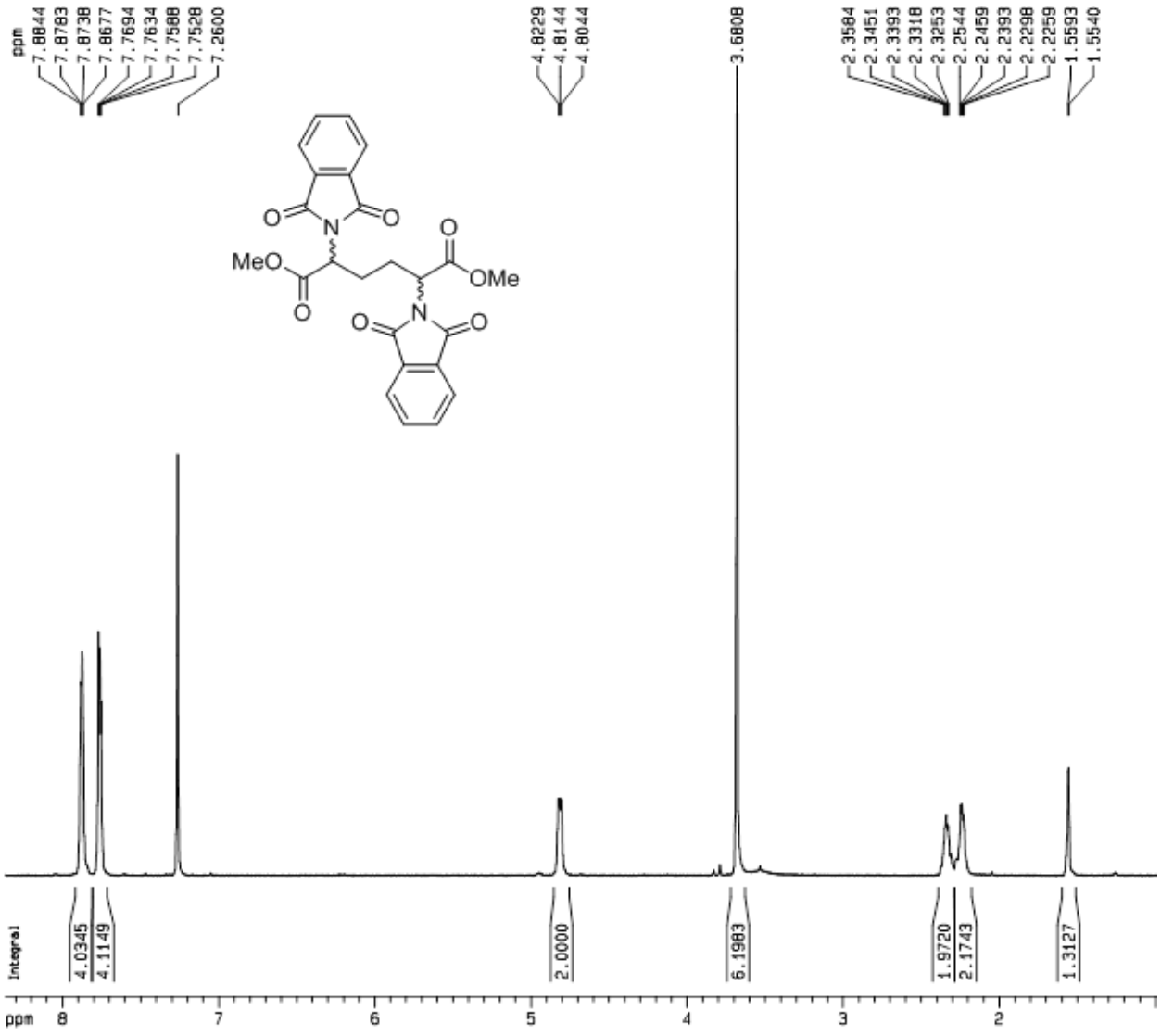

Spectrum A6-1 500 MHz ^{1}H NMR spectrum of dimethyl 2,5-bis(1,3-dioxo-2,3-dihydro-1*H*-isoindol-2-yl)hexanedioate (**6**) in $CDCl_3$.

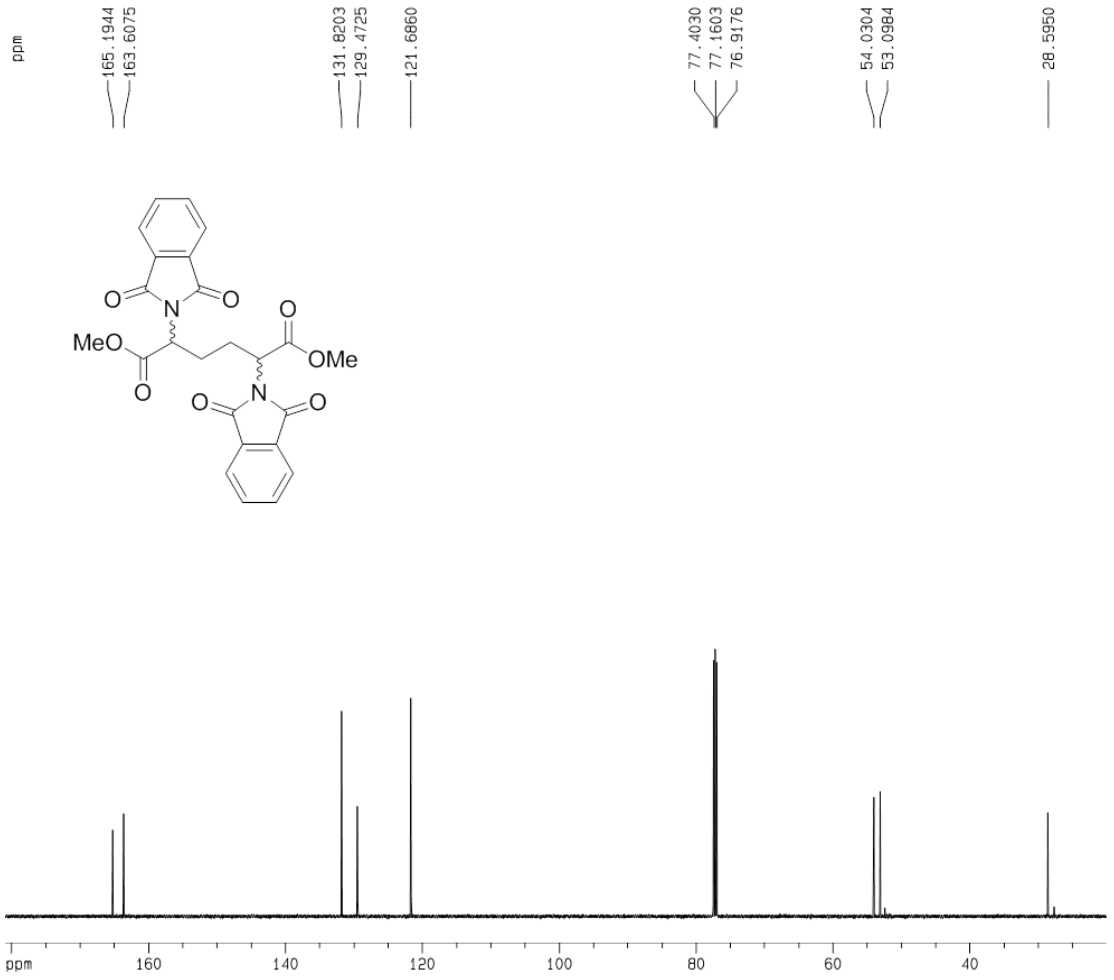

Spectrum A6-2 125 MHz ^{13}C NMR spectrum of 1,6-dimethyl-2,5-bis(1,3-dioxo-2,3-dihydro-1*H*-isoindol-2-yl)hexanedioate (**6**) in $CDCl_3$.

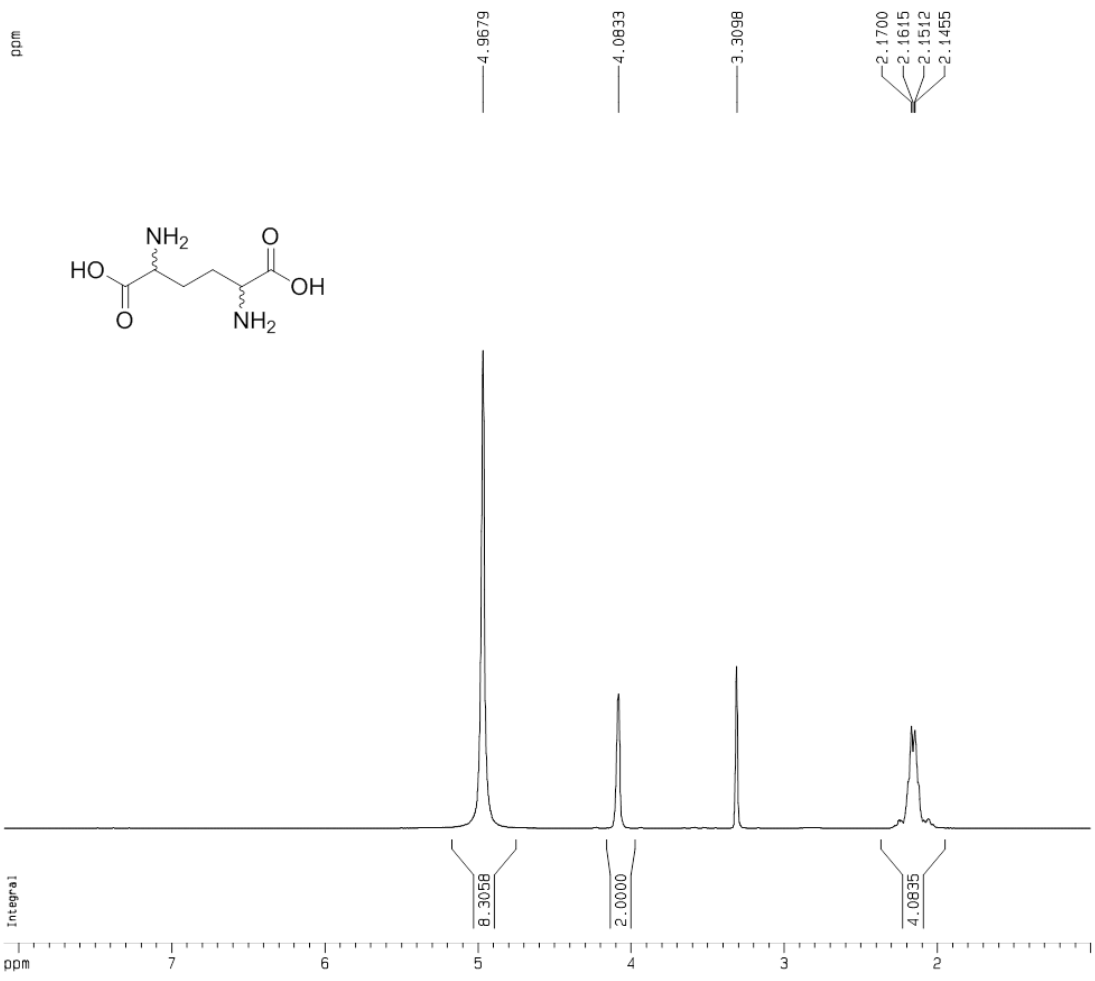

Spectrum A7-1 500 MHz ^{1}H NMR spectrum of 2,5-diaminohexanedioic acid (**7**) in MeOD.

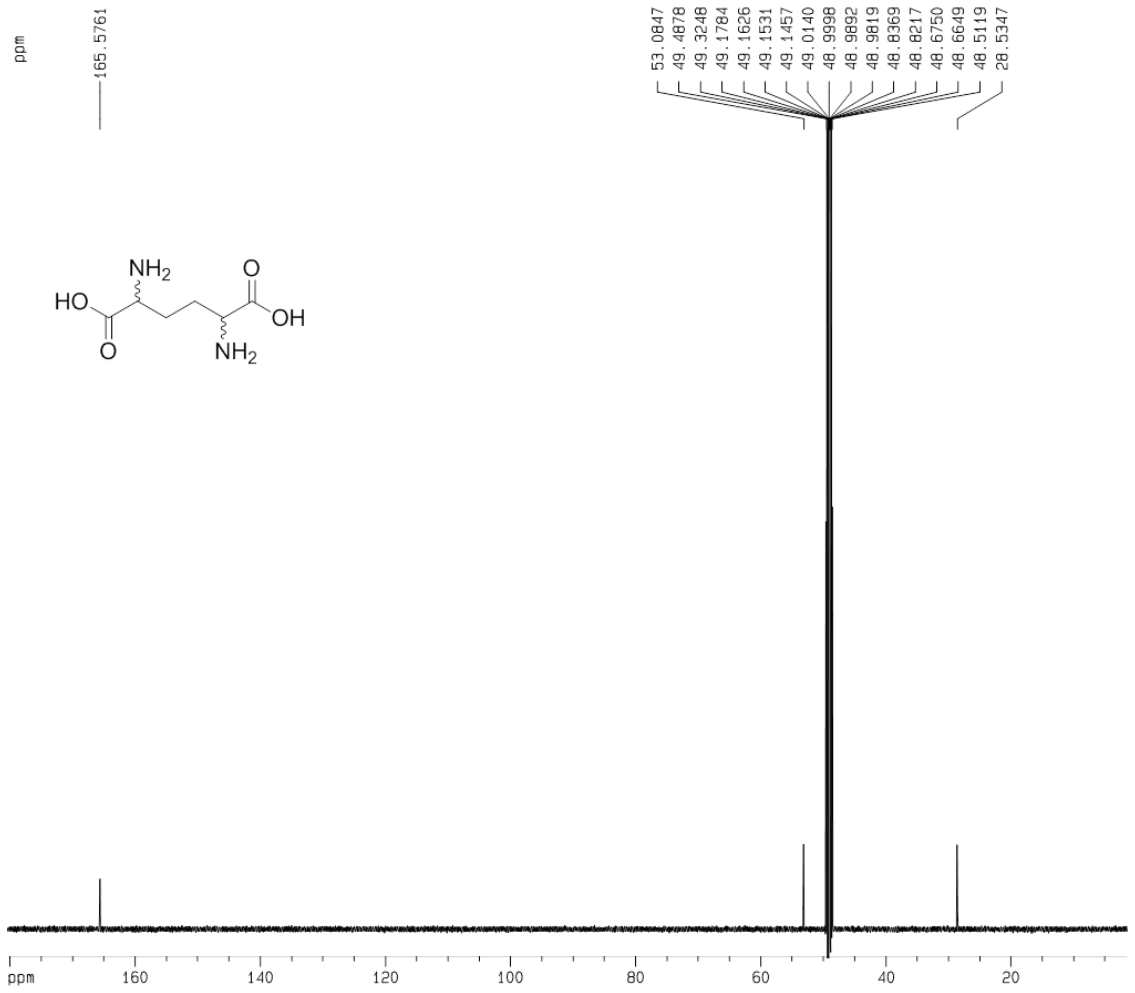

Spectrum A7-2 125 MHz ^{13}C NMR spectrum of 2,5-diaminohexanedioic acid (**7**) in MeOD.

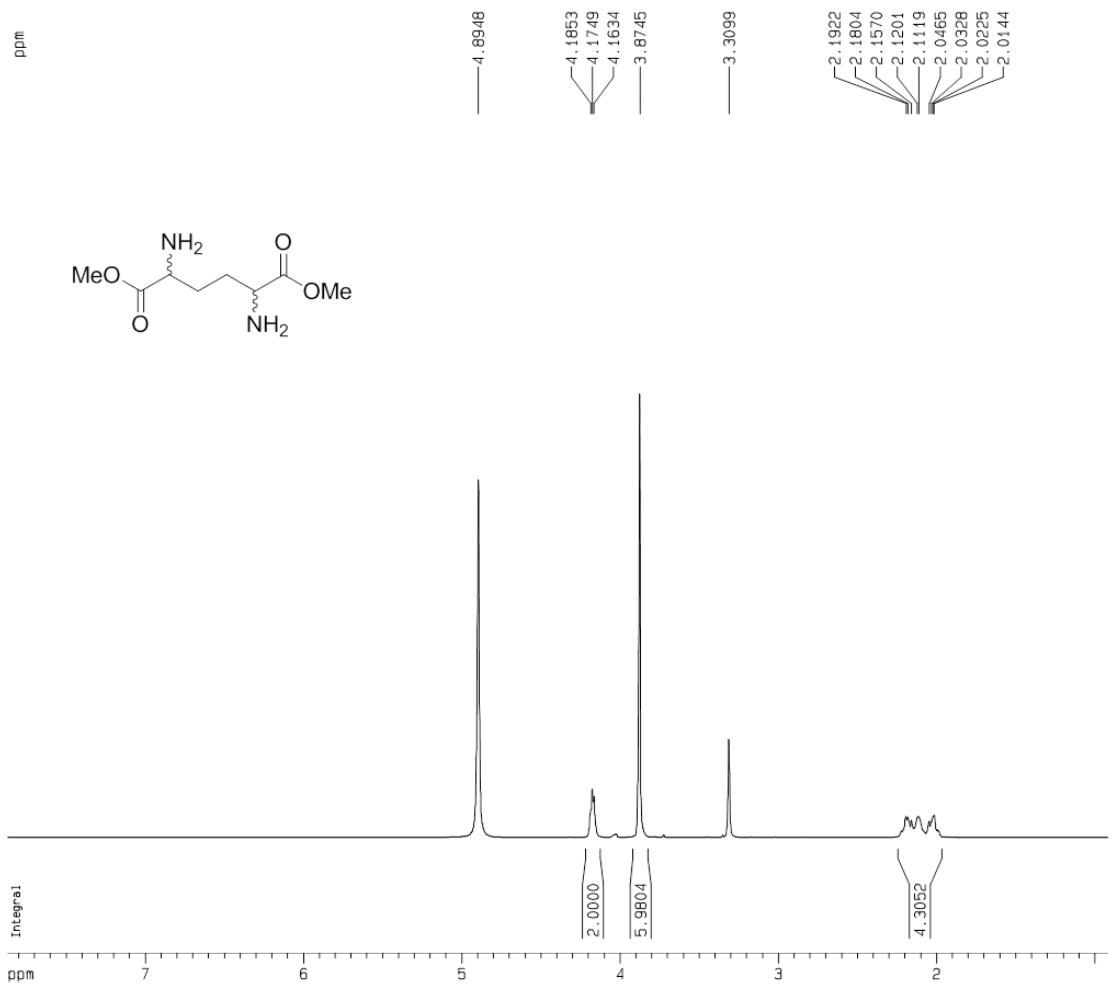

Spectrum A8-1 500 MHz ^{1}H NMR spectrum of dimethyl 2,5-diaminohexanedioate dihydrochloride (**8**) in MeOD.

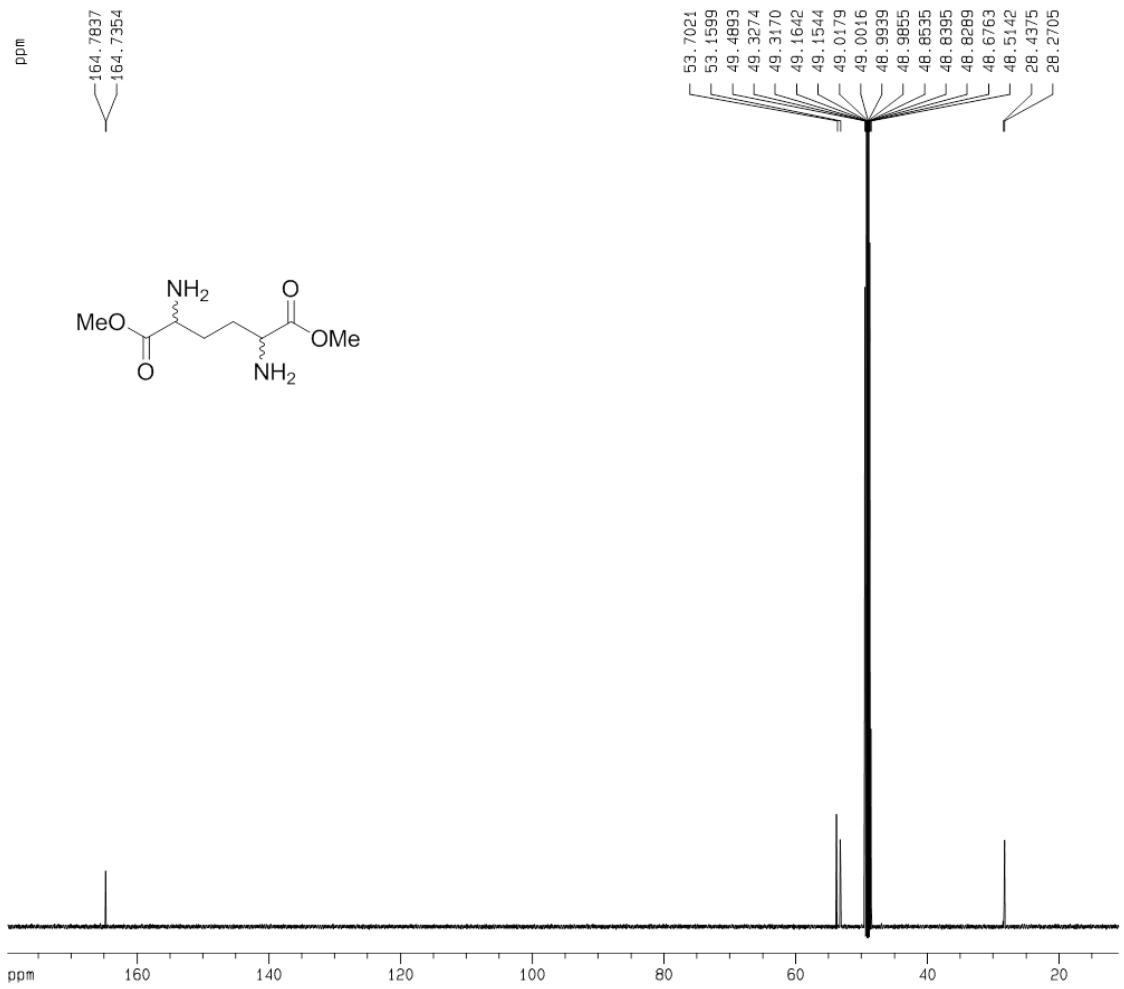

Spectrum A8-2 125 MHz ^{13}C NMR spectrum of dimethyl 2,5-diaminohexanedioate dihydrochloride (**8**) in MeOD.

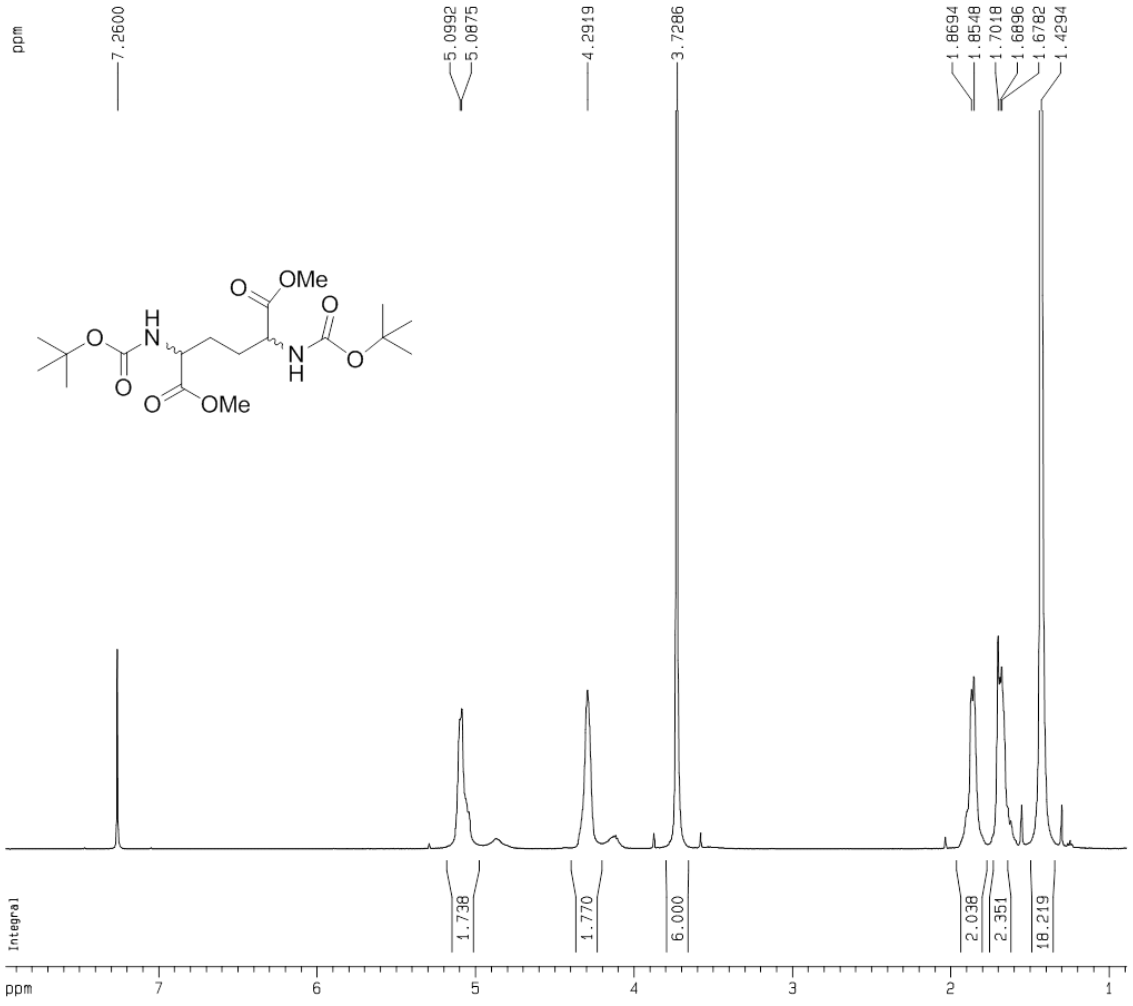

Spectrum A9-1 500 MHz ^{1}H NMR spectrum of dimethyl 2,5-bis([(*tert*-butoxy)carbonyl]amino)hexanedioate (**9**) in $CDCl_3$.

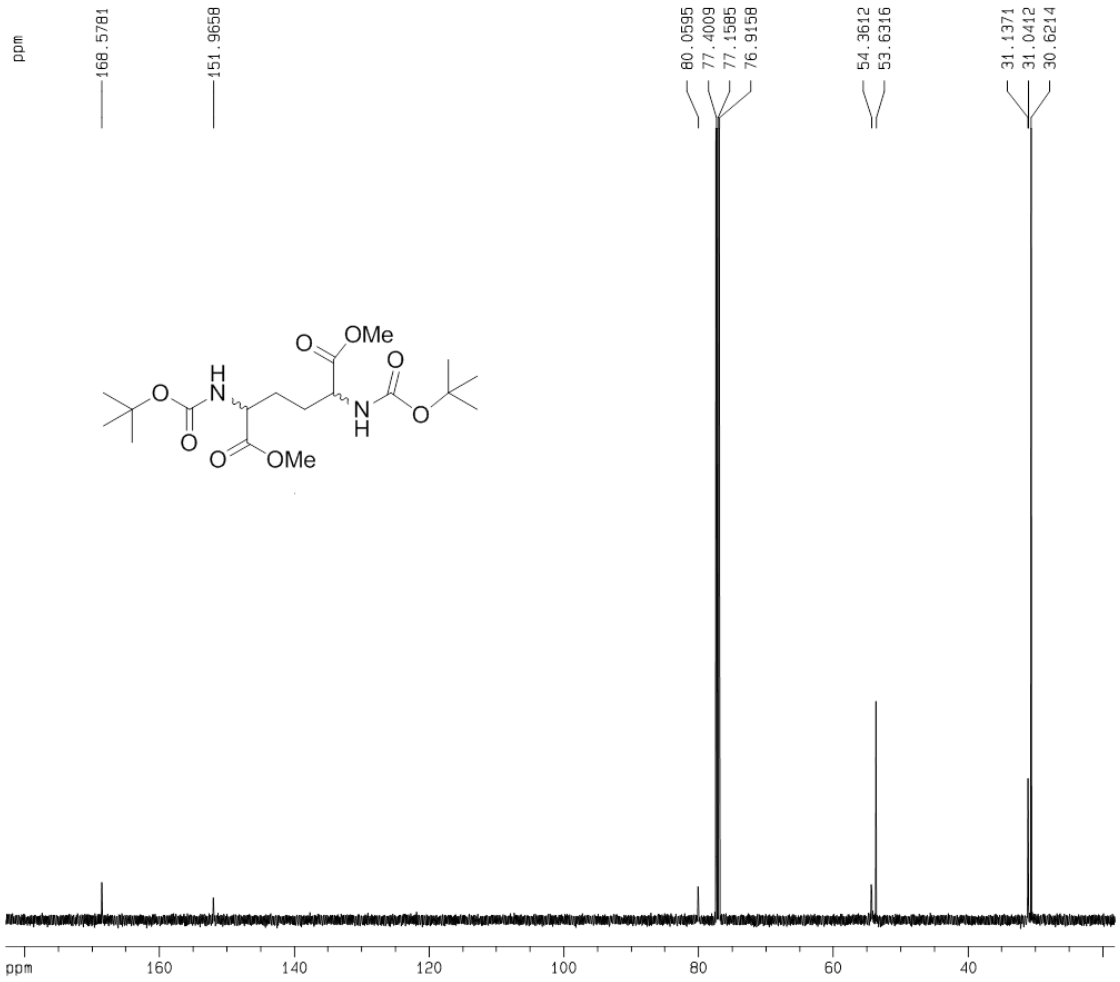

Spectrum A9-2 125 MHz ^{13}C NMR spectrum of dimethyl 2,5-bis([(*tert*-butoxy)carbonyl]amino)hexanedioate (**9**) in $CDCl_3$.

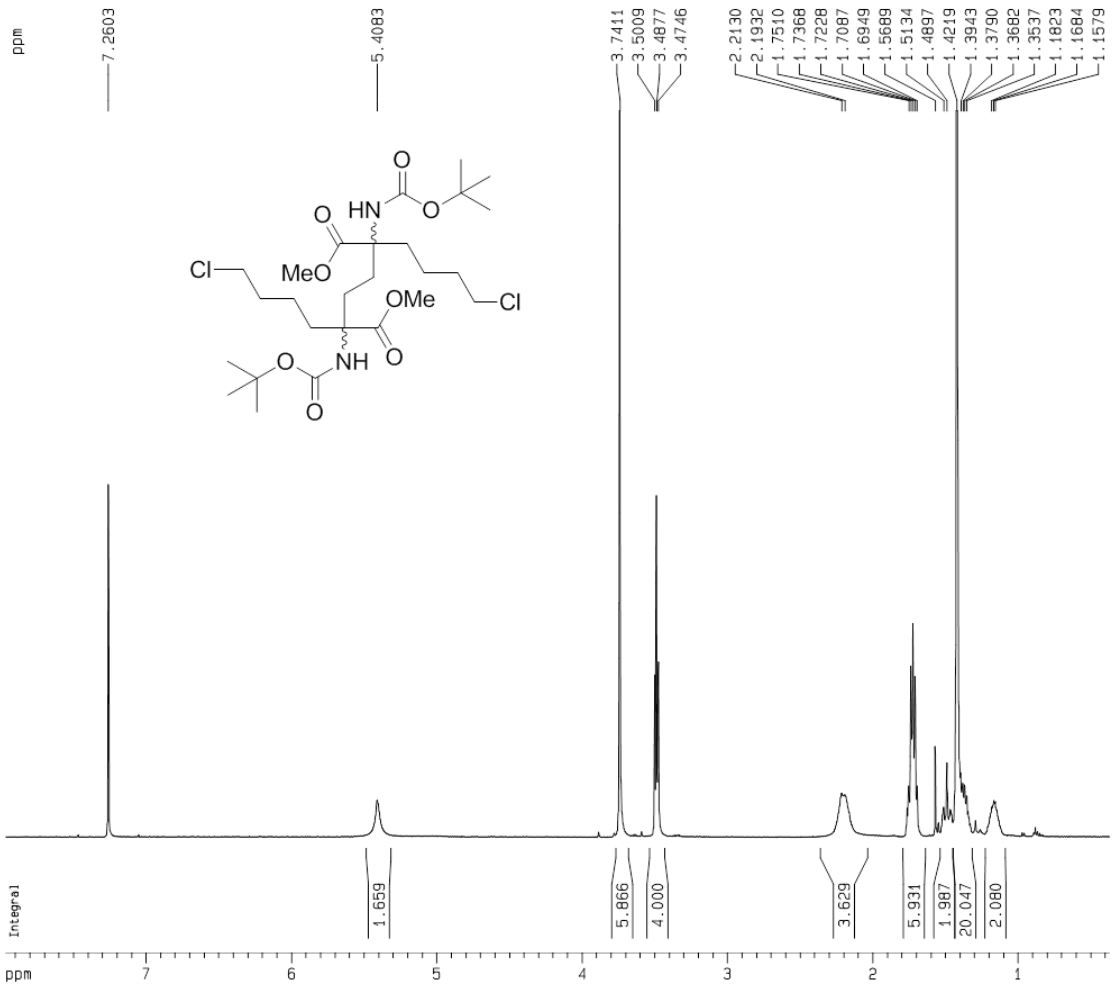

Spectrum A10-1 500 MHz ^{1}H NMR spectrum of mixture of dimethyl (2*R*, 5*R*)-2,5-bis([(*tert*-butoxy)carbonyl]amino)-2,5-bis(4-chlorobutyl)hexanedioate and dimethyl (2*S*, 5*S*)-2,5-bis([(*tert*-butoxy)carbonyl]amino)-2,5-bis(4-chlorobutyl)hexanedioate (**10a**) in $CDCl_3$.

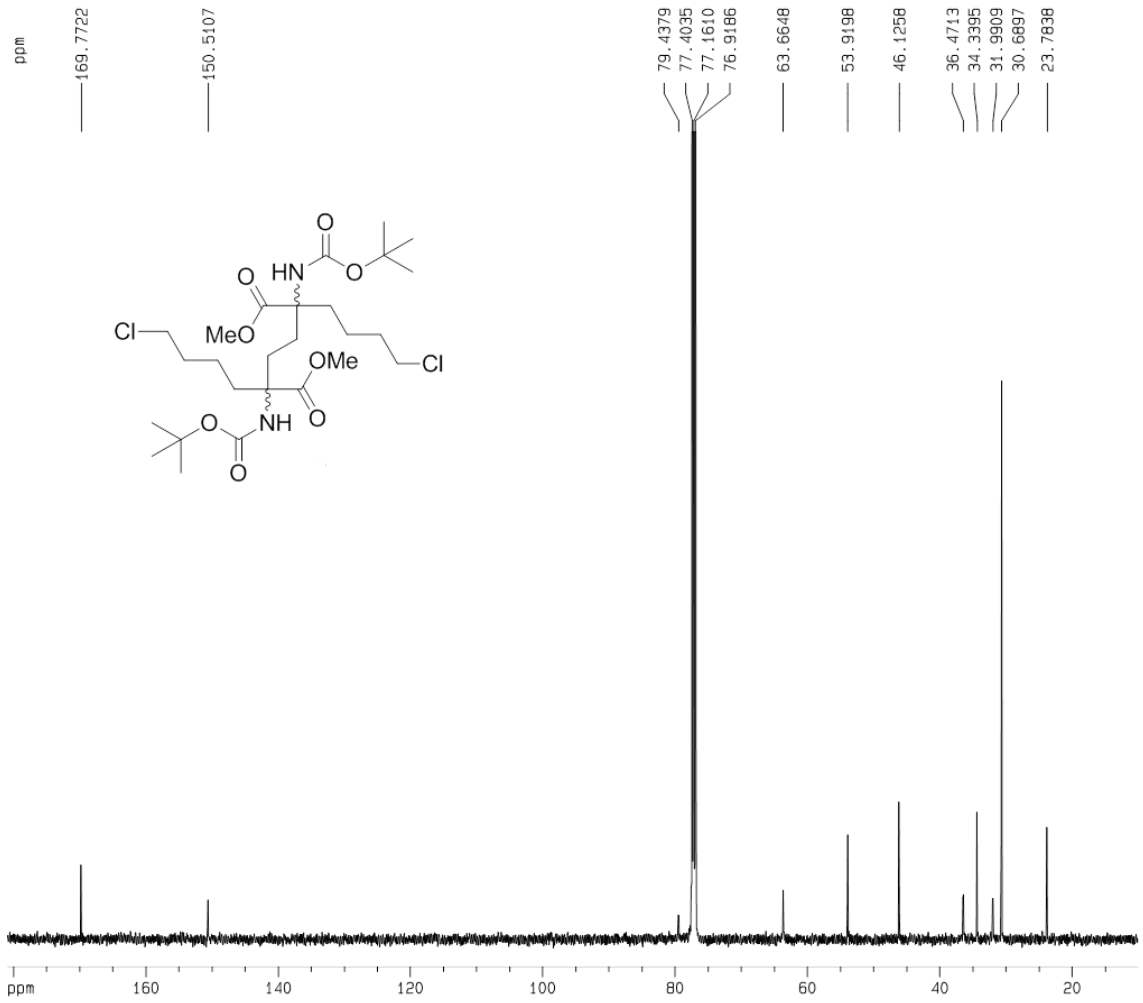

Spectrum A10-2 125 MHz ^{13}C NMR spectrum of mixture of dimethyl (2*R*, 5*R*)-2,5-bis([(*tert*-butoxy)carbonyl]amino)-2,5-bis(4-chlorobutyl)hexanedioate and dimethyl (2*S*, 5*S*)-2,5-bis([(*tert*-butoxy)carbonyl]amino)-2,5-bis(4-chlorobutyl)hexanedioate (**10a**) in $CDCl_3$.

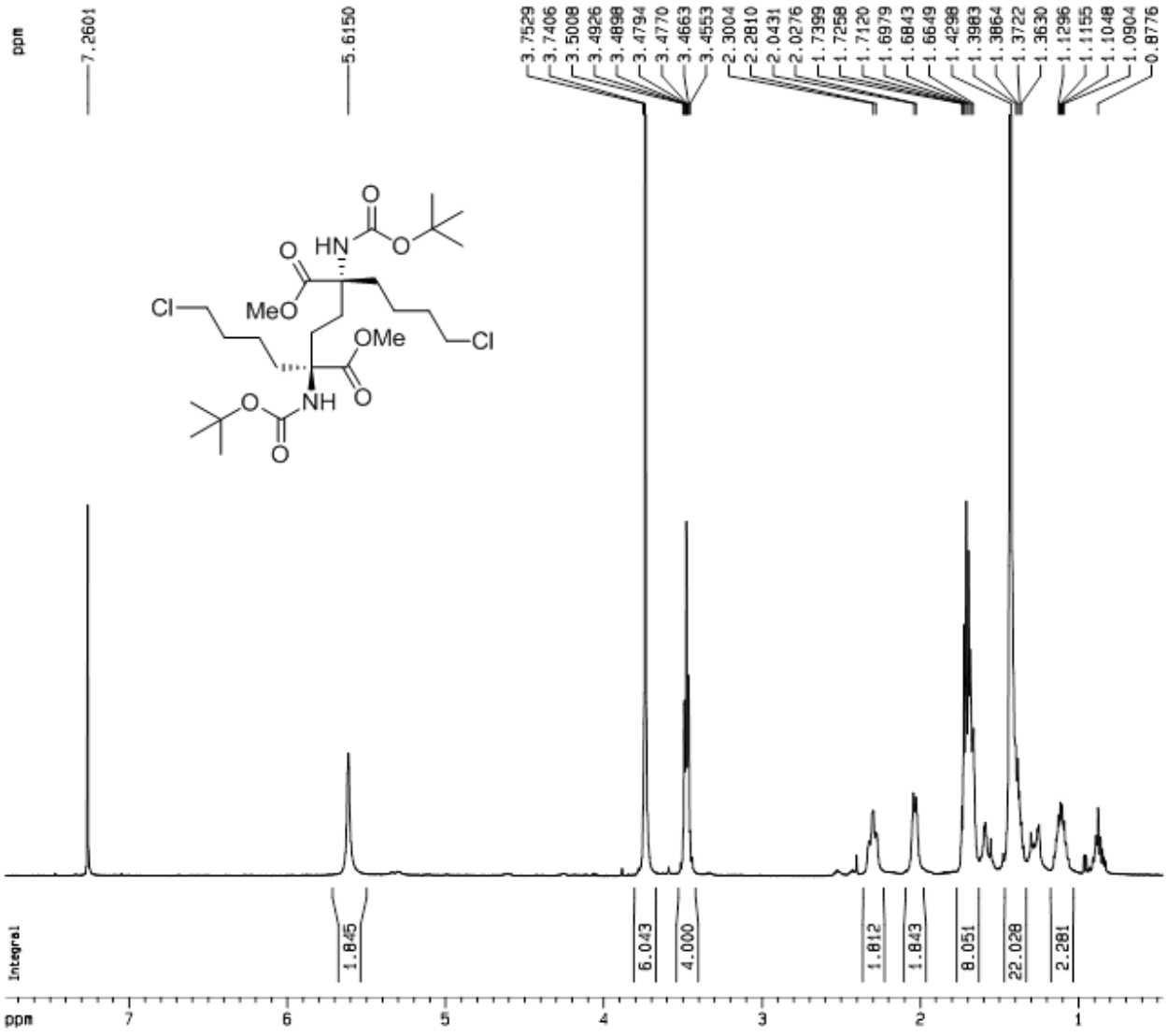

Spectrum A10-3 500 MHz ^{1}H NMR spectrum of dimethyl (2*R*, 5*S*)-2,5-bis([(*tert*-butoxy)carbonyl]amino)-2,5-bis(4-chlorobutyl)hexanedioate (**10b**) in $CDCl_3$.

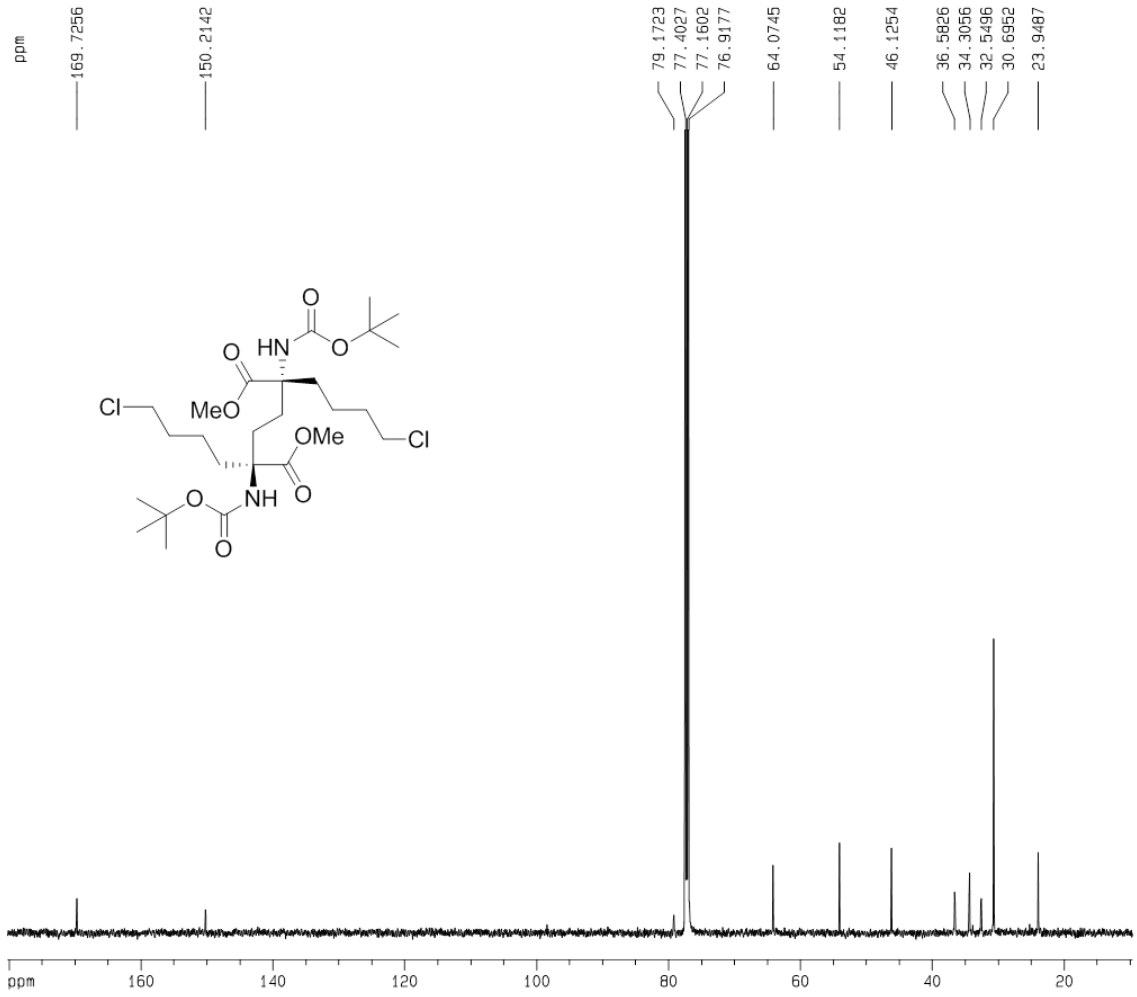

Spectrum A10-4 125 MHz ^{13}C NMR spectrum of dimethyl (2*R*, 5*S*)-2,5-bis([(*tert*-butoxy)carbonyl]amino)-2,5-bis(4-chlorobutyl)hexanedioate (**10b**) in $CDCl_3$.

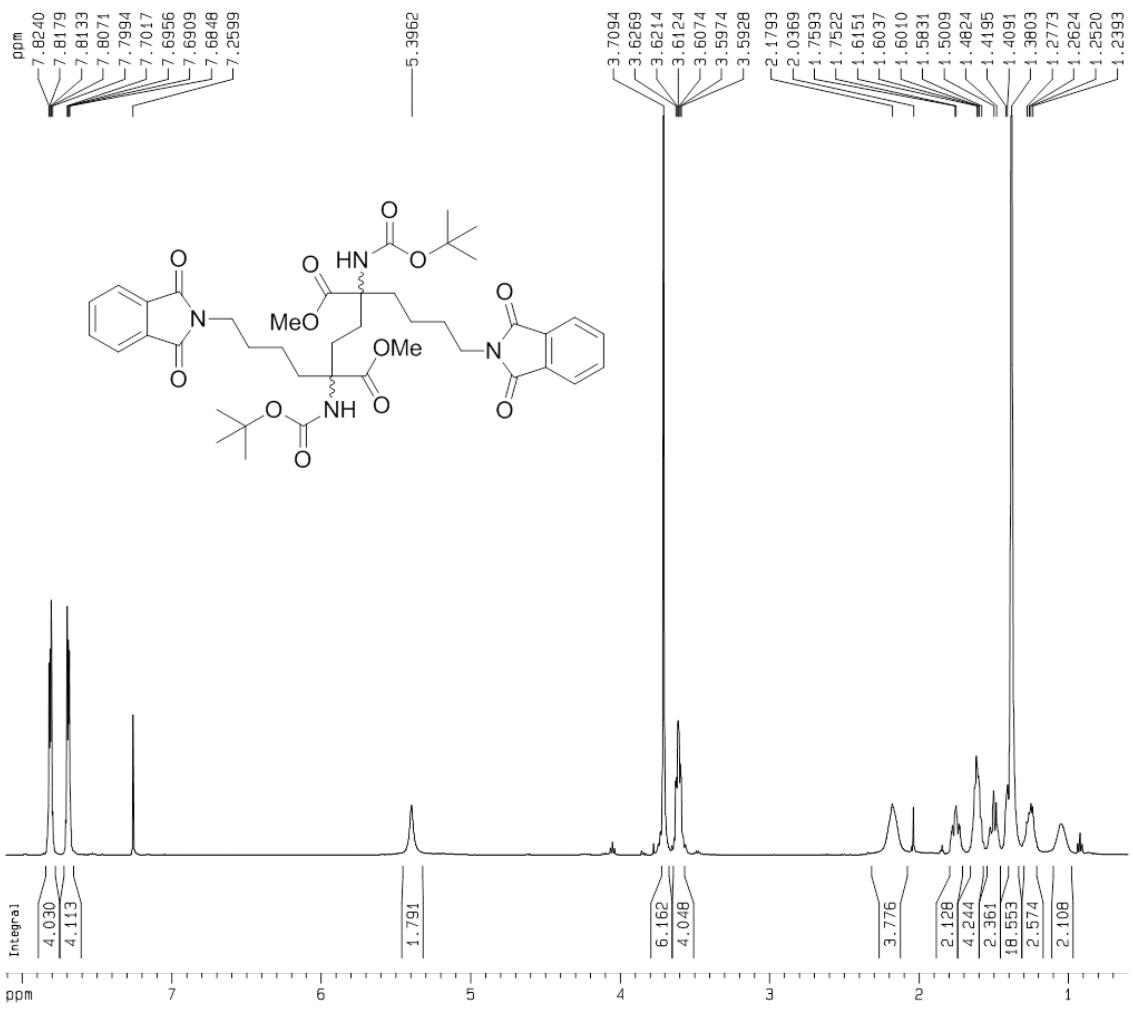

Spectrum A11-1 500 MHz ^{1}H NMR spectrum of mixture of dimethyl (2*R*, 5*R*)-2,5-bis([(*tert*-butoxy)carbonyl]amino)-2,5-bis[4-(1,3-dioxo-2,3-dihydro-1*H*-isoindol-2-yl)butyl]hexanedioate and dimethyl (2*S*, 5*S*)-2,5-bis([(*tert*-butoxy)carbonyl]amino)-2,5-bis[4-(1,3-dioxo-2,3-dihydro-1*H*-isoindol-2-yl)butyl]hexanedioate (**11**) in $CDCl_3$.

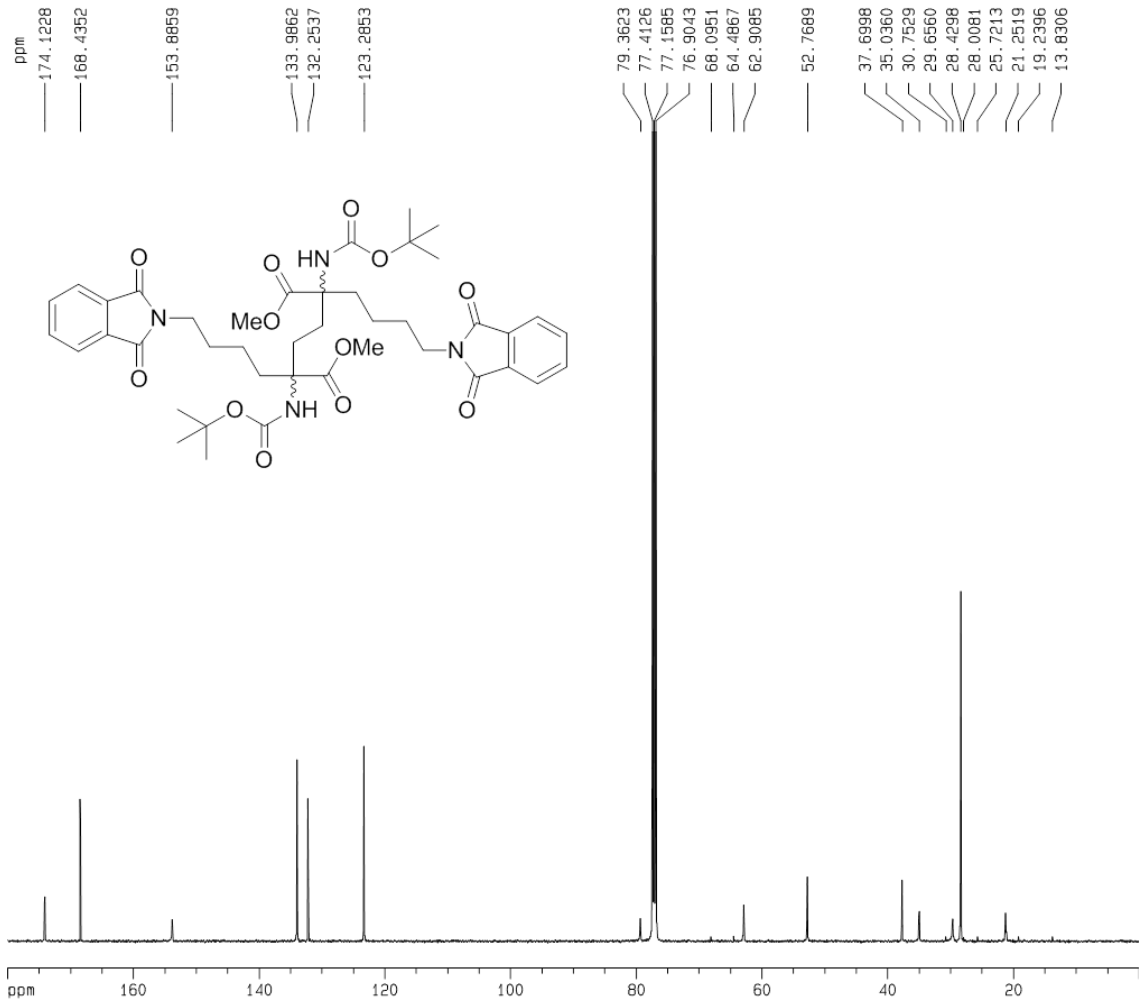

Spectrum A11-2 125 MHz ^{13}C NMR spectrum of mixture of dimethyl (2*R*, 5*R*)-2,5-bis([(*tert*-butoxy)carbonyl]amino)-2,5-bis[4-(1,3-dioxo-2,3-dihydro-1*H*-isoindol-2-yl)butyl]hexanedioate and dimethyl (2*S*, 5*S*)-2,5-bis([(*tert*-butoxy)carbonyl]amino)-2,5-bis[4-(1,3-dioxo-2,3-dihydro-1*H*-isoindol-2-yl)butyl]hexanedioate (**11**) in $CDCl_3$.

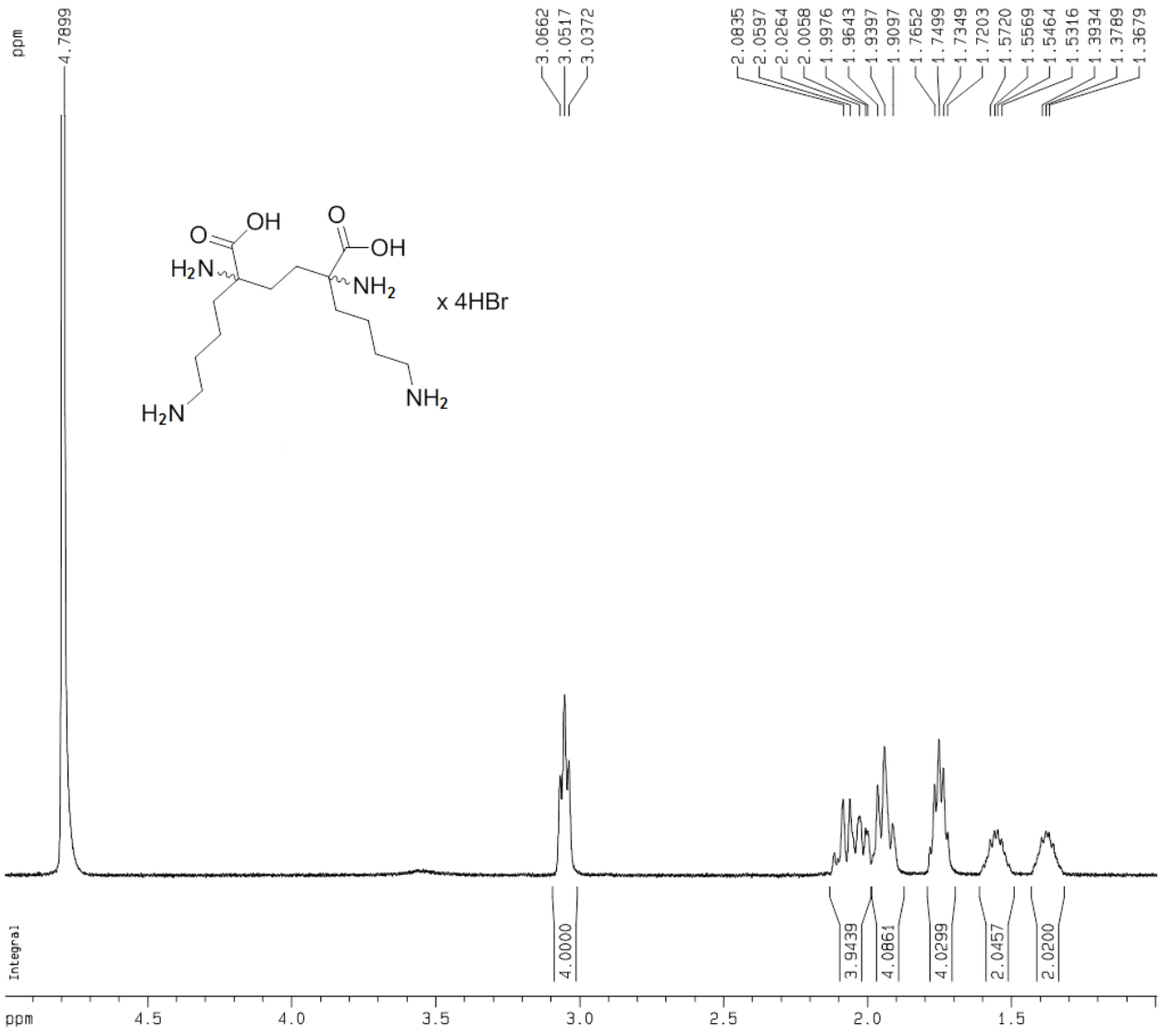

Spectrum A12-1 500 MHz ^{1}H NMR spectrum of mixture of (2*R*, 5*R*)-2,5-diamino-2,5-bis(4-aminobutyl)hexanedioate tetrabromide and (2*S*, 5*S*)-2,5-diamino-2,5-bis(4-aminobutyl)hexanedioate tetrabromide (**12**) in D_2O.

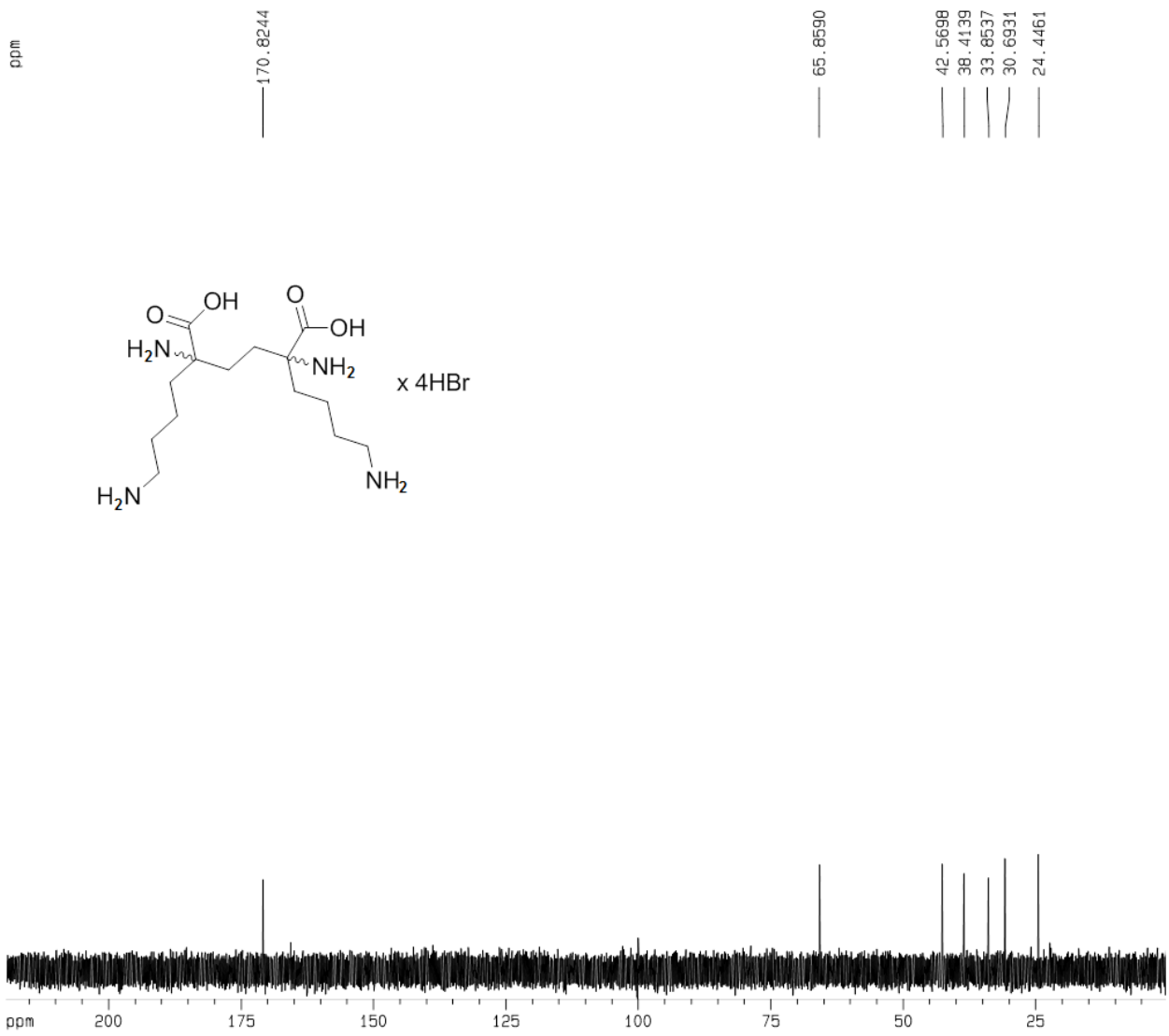

Spectrum A12-2 125 MHz ^{13}C NMR spectrum of mixture of (2*R*, 5*R*)-2,5-diamino-2,5-bis(4-aminobutyl)hexanedioate tetrabromide and (2*S*, 5*S*)-2,5-diamino-2,5-bis(4-aminobutyl)hexanedioate tetrabromide (**12**) in D_2O.

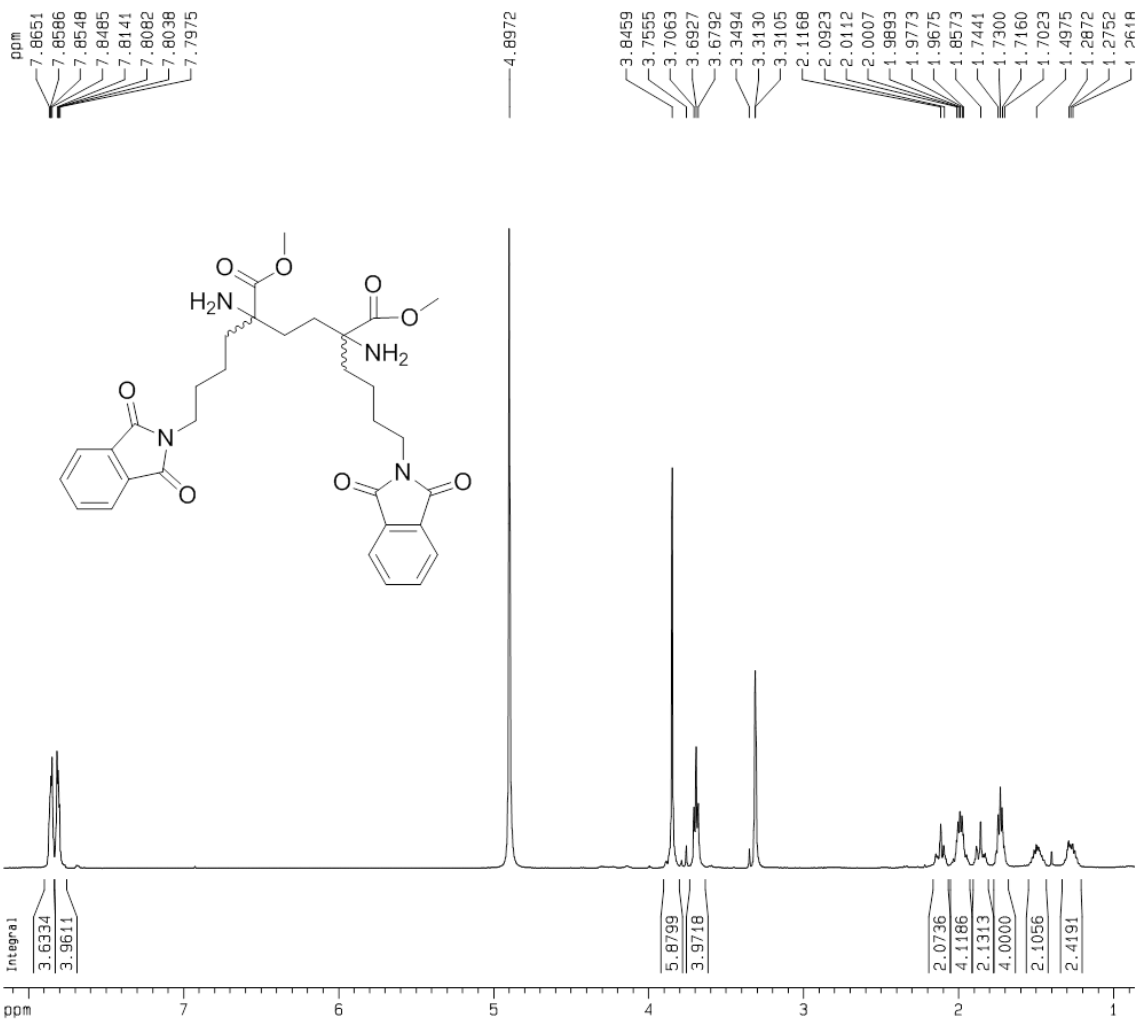

Spectrum A13-1 500 MHz ^{1}H NMR spectrum of mixture of dimethyl (2*R*, 5*R*)-2,5-diamino-2,5-bis[4-(1,3-dioxo-2,3-dihydro-1*H*-isoindol-2-yl)butyl]hexanedioate and dimethyl (2*S*, 5*S*)-2,5-diamino-2,5-bis[4-(1,3-dioxo-2,3-dihydro-1*H*-isoindol-2-yl)butyl]hexanedioate (**13**) in MeOD.

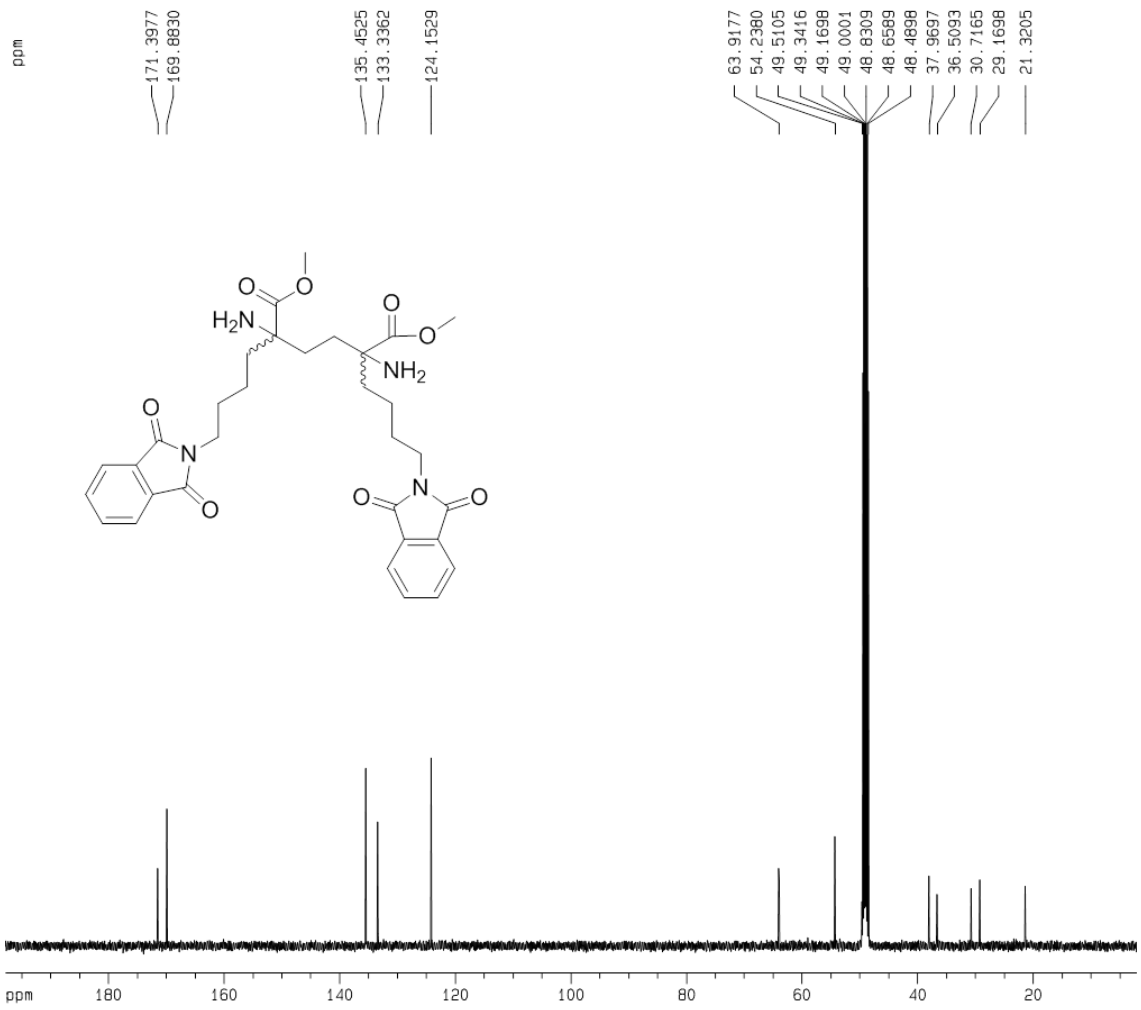

Spectrum A13-2 125 MHz ^{13}C NMR spectrum of mixture of dimethyl (2*R*, 5*R*)-2,5-diamino-2,5-bis[4-(1,3-dioxo-2,3-dihydro-1*H*-isoindol-2-yl)butyl]hexanedioate and dimethyl (2*S*, 5*S*)-2,5-diamino-2,5-bis[4-(1,3-dioxo-2,3-dihydro-1*H*-isoindol-2-yl)butyl]hexanedioate (**13**) in MeOD

APPENDIX B

Figure B 1 Sequence alignment of DHDPS from some Gram-negative bacteria[a].

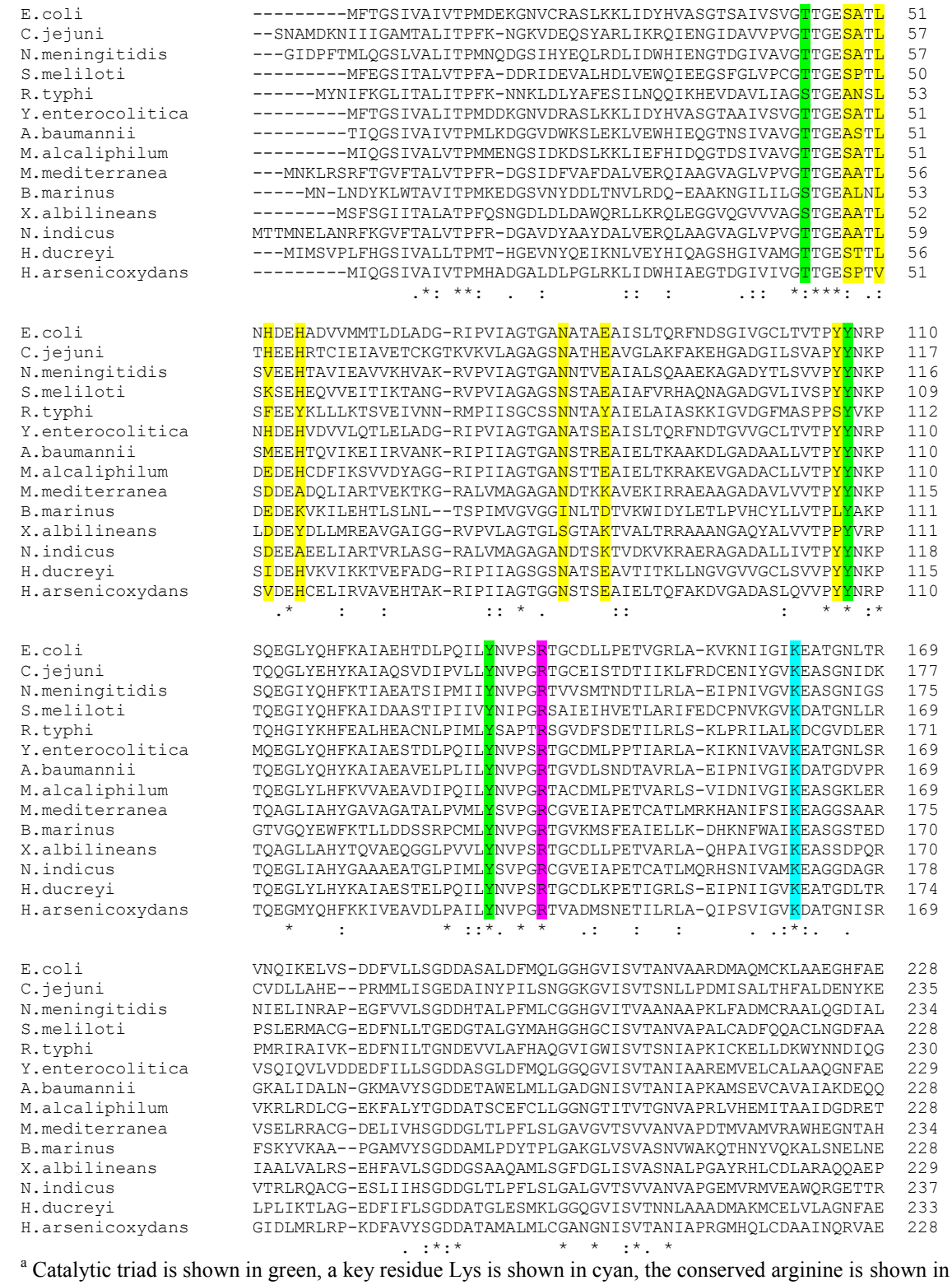

[a] Catalytic triad is shown in green, a key residue Lys is shown in cyan, the conserved arginine is shown in magenta, selected residues of the allosteric site are shown in yellow.

Figure B 2 Sequence alignment of DHDPS from some plants[a].

```
V.vinifera        LPMRSFEVKNRTSVDDIKSLRLITAIKTPYLPDGRFDLEAYDALVNMQIVDGAEGVIVGG      87
N.sylvestris      ----------TFADDIKALRLITAIKTPYLPDGRFDLEAYDTLVNLQIENGAEGVIVGG      49
Z.mays            LPMRSTEVKNRTLTGDITSLRLITAVKTPYLPDGRFDLEAYDSLINMQIEGGSEGVIVGG      118
Z.latifolia       --MRSSEVKNRTSTADITSLRLITAVKTPYLPDGRFDLEAYDSLINMQVDGGAEGVIVGG      58
A.thaliana        LPMRSLEVKNRTNTDDIKALRVITAIKTPYLPDGRFDLEAYDDLVNIQIQNGAEGVIVGG      106
T.aestivum        LPMRSTEVKNRTSVDGIKSLRLITAVKTPYLPDGRFDLEAYDSLINTQINGGAEGVIVGG      118
T.cacao           LPMRSFEVKNRTSSEDIKSLRLITAIKTPYLPDGRFDLEAYDGLVNMQIENGAEGVIVGG      106
O.sativa          LPMRSSEVKNRTSTGDITSLRVITAVKTPYLPDGRFDLEAYDSLINMQIEGGAEGVIVGG      88
                            *    *.:**:***:**************** *:* *:  *:*******

V.vinifera        TTGEGQLMSWDEHIMLIGHTVNCFGGSIKVIGNTGSNSTREAIHATEQGFAVGMHAALHI      147
N.sylvestris      TTGEGQLMSWDEHIMLIGHTVNCFGGSIKVIGNTGSISTREAIHATEQGFAVGMHAALHI      109
Z.mays            TTGEGHLMSWDEHIMLIGHTVNCFGTRIKVIGNTGSNSTREAVHATEQGFAVGMHAALHI      178
Z.latifolia       TTGEGHLMSWDEHIMLIGHTVNCFGTKIKVIGNTGSNSTREAIHATEQGFAVGMHAALHI      118
A.thaliana        TTGEGQLMSWDEHIMLIGHTVNCFGGSIKVIGNTGSNSTREAIHATEQGFAVGMHAALHI      166
T.aestivum        TTGEGHLMSWDEHIMLIGHTVNCFGTNIKVIGNTGSNSTREAIHASEQGFAVGMHAALHV      178
T.cacao           TTGEGQLMSWDEHIMLIGHTVNCFGGSIKVIGNTGSNSTREAIHATEQGFAVGMHAALHI      166
O.sativa          TTGEGHLMSWDEHIMLIGHTVNCFGTKIKVVGNTGSNSTREAIHATEQGFAVGMHAALHI      148
                  *****:*******************  ***:***** *****:**:**************:

V.vinifera        NPYYGKTSLEGLVSHFESVLPMGPTVIYNVPSRTGQDIPPGVIHTVAQSANLAGVKECVG      207
N.sylvestris      NPYYGKTSLEGLISHFESVLPMGPTIIYNVPSRTGQDIPPRVIQTMAKSPNLAGVKECVG      169
Z.mays            NPYYGKVSTEGLISHFEAVLPMGPTIIYNVPSRSGQDIPPQVIETLSGYPNMAGVKECVG      238
Z.latifolia       NPYYGKTSIEGLISHFEAVLPMGPTIIYNVPSRTGQDIPPAVIEAVSSFSNMAGVKECVG      178
A.thaliana        NPYYGKTSIEGLIAHFQSVLHMGPTIIYNVPGRTGQDIPPRAIFKLSQNPNLAGVKECVG      226
T.aestivum        NPYYGKTSTAGLISHFDEVLPMGPTIIYNVPSRTGQDIPPAVIEALSTYPNMAGVKECVG      238
T.cacao           NPYYGKTSLEGLVSHFDSVLPMGPTIIYNVPSRTGQDIPPRVINTVAQSPNLAGVKECVG      226
O.sativa          NPYYGKTSVEGLISHFEAVLPMGPTIIYNVPSRDWQDIPPPVIEAVSSYTNMAGVKECVG      208
                  ******.*  **::**: ** ****:*****.*  ***** .*  ::   *:********

V.vinifera        NDRIKQYTDNRIVVWSGNDDQCHDAKWDYGATGVISVTSNLIPGLMRQLLFKGKNPSLNA      267
N.sylvestris      NDRVEQYTSNGIVVWSGNDDECHVSRWDYGATGVISVTSNLVPGLMRELMFGGKNLALNS      229
Z.mays            HERVKCYTDKGITVWSGNDDECHDSRWKYGATGVISVASNLVPGLMRSLMYEGENALLNE      298
Z.latifolia       HERVKCYTDKGITIWSGNDDECHDSRWKHGATGVISVASNLVPGLMHNLMYEEQTAVLNE      238
A.thaliana        NKRVEEYTENGVVVWSGNDDECHDSRWDYGATGVISVTSNLVPGLMRKLMFEGRNSSLNS      286
T.aestivum        HERVKCYTDKGITIWSGNDDECHDSRWKYGATGVISVTSNLVPGLMRSLMFEGENAALNE      298
T.cacao           NDRIEQYTDNGIVVWSGNDDQCHDARWSHGATGVISVTSNLIPGLMRELMFGGKNPSLNV      286
O.sativa          HERVKCYADRGISIWSGNDDECHESRWKYGATGVISVASNLIPGLMHSLMYEGENAALND      268
                  ..*:: *:.. : :******:** ::*.:********:***:****:.*::  ..  **

V.vinifera        KIMPLVNWLFEEPNPIGLNTALAQLGVVRPVFRLPYVPLPLAKRVEFVNIVKEIGRENFV      327
N.sylvestris      KLMPLVEWLFHEPNPIALNTAFAQLGVVRPVFRLPYVPLTKAKREEFVKIVKDIGRENFI      289
Z.mays            KLLPLTKWLFCLPNPIALNTALAQLGVARPVFRLPYVPLPLEKRIEFVRIVEAIGRGNFV      358
Z.latifolia       KLLPLMKWLFCQPNPIALNTALAQLGVVRPVFRLPYVPLPREKRVEFVRIVESIGRENFV      298
A.thaliana        KLLPLMAWLFHEPNPIGINTALAQLGVSRPVFRLPYVPLPLSKRLEFVKLVKEIGREHFV      346
T.aestivum        KLLPLMKWLFSEPNPIGLNTALAQLGVVRPVFRRPYAPLSLEKRTEFVRIVEAIGRENFV      358
T.cacao           KLLPLIEWLFEEPNPIGLNTALAQLGVVRPVFRLPYVPLPLAKRVEFVNLVRQIGRQNFV      346
O.sativa          KLLPLMKWLFCQPNPIALNTALAQLGVARPVFRLPYVPLPLEKRVEFVRIVESIGRENFV      328
                  *::**  ***  ****.:***:***** ***** **.**   ** ***.:*. *** .*:
```

[a] Catalytic triad is shown in green, the key residue Lys is shown in cyan, the conserved arginine is shown in magenta, selected residues of the allosteric site are shown in yellow.

Figure B 3 Sequence alignment of DHDPS from some Gram-positive bacteria[a].

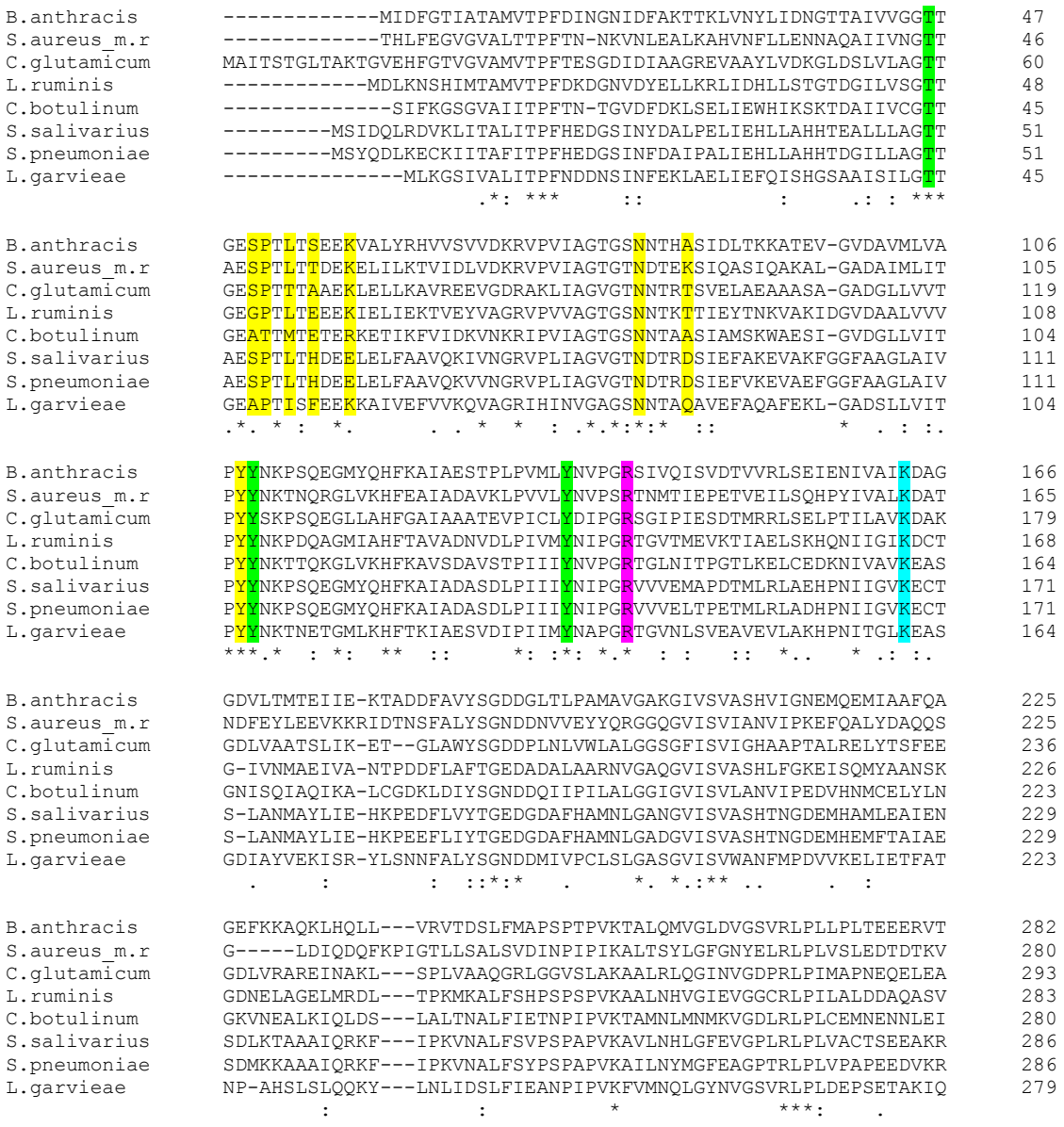

[a] Catalytic triad is shown in green, the key residue Lys is shown in cyan, the conserved arginine is shown in magenta, selected residues of the allosteric site are shown in yellow[a].

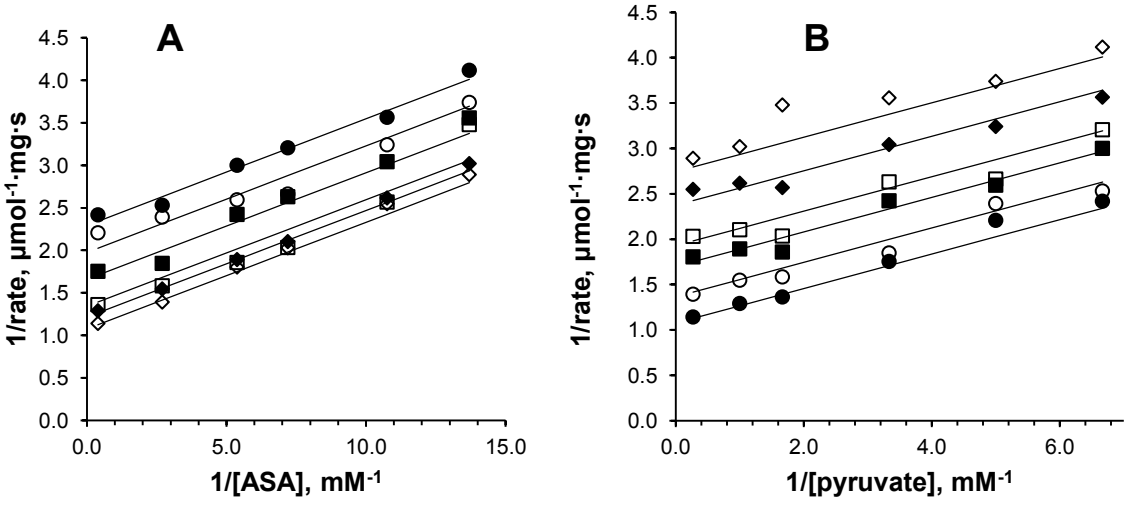

Figure B 4 Double-reciprocal plots of the Y110F-catalyzed reaction. Solid lines are the global fit of Equation 4.1 to the data. (A) Concentration of pyruvate: (●) 0.15 mM, (○) 0.20 mM, (■) 0.30 mM, (□) 0.60 mM, (♦) 1.0 mM, (◇) 3.7 mM; (B) Concentration of ASA: (◇) 0.073 mM, (♦) 0.093 mM, (□) 0.14 mM, (■) 0.19 mM, (○) 0.37 mM, (●) 2.6 mM.

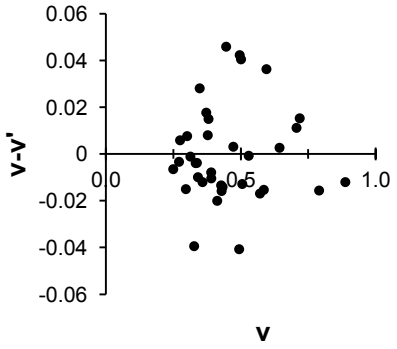

Figure B 5 Residuals for plots in Figure B 4.

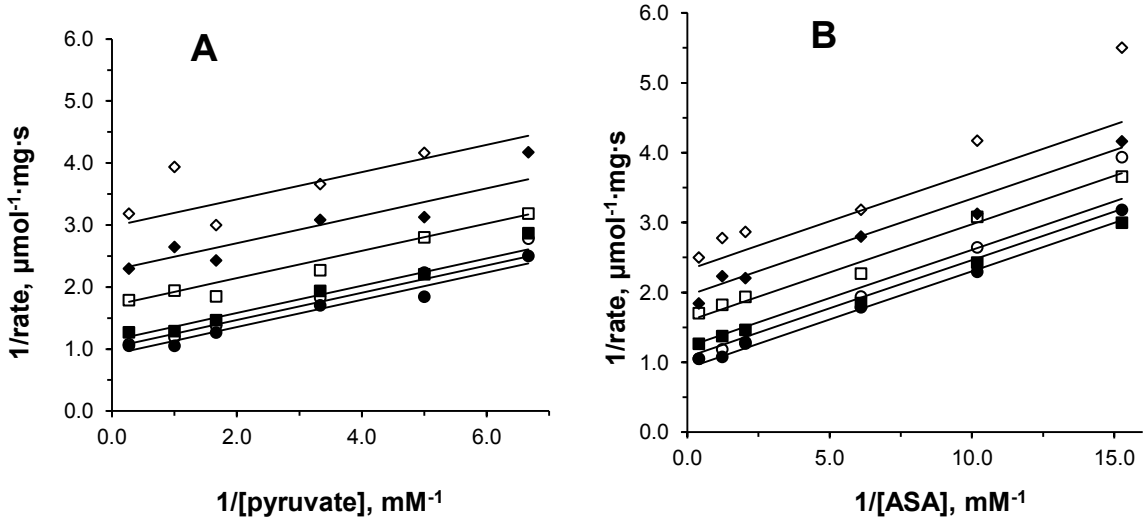

Figure B 6 Double-reciprocal plots of the H56A-catalyzed reaction. Solid lines are the global fit of Equation 4.1 to the data. (A) Concentration of ASA: (●) 2.5 mM, (○) 0.82 mM, (■) 0.49 mM, (□) 0.16 mM, (♦) 0.098 mM, (◇) 0.066 mM; (B) Concentration of pyruvate: (◇) 0.15 mM, (♦) 0.20 mM, (□) 0.30 mM, (■) 0.60 mM, (○) 1.0 mM, (●) 3.7 mM.

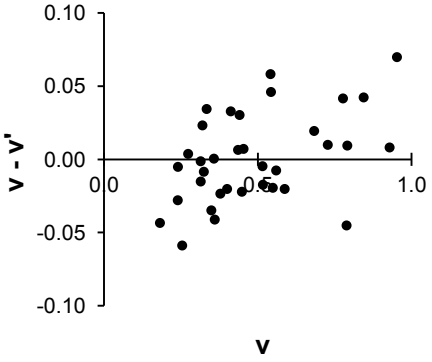

Figure B 7 Residuals for plots in Figure B 6.

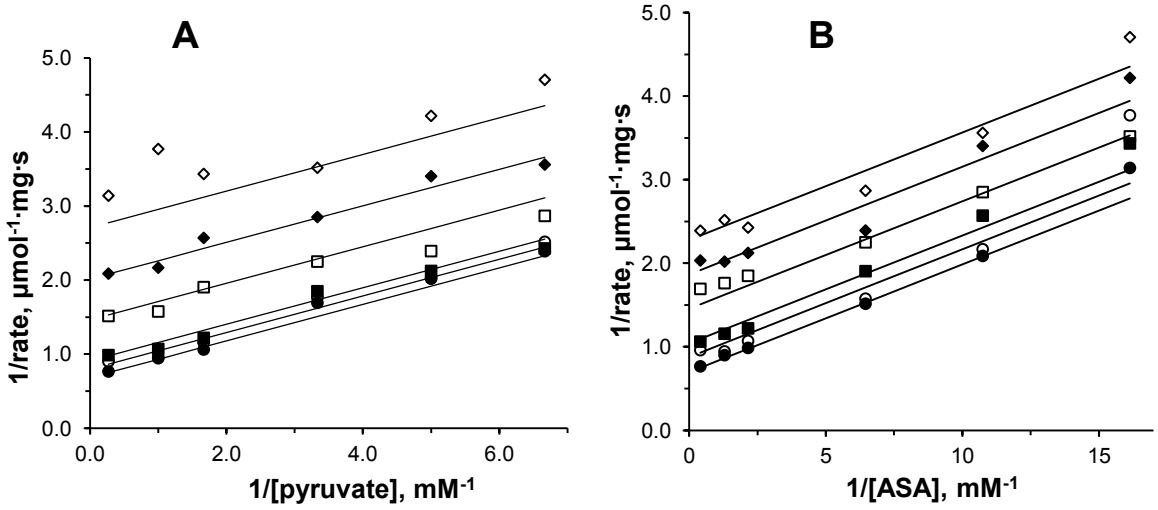

Figure B 8 Double-reciprocal plots of the H56N-catalyzed reaction. Solid lines are the global fit of Equation 4.1 to the data. (A) Concentration of ASA: (●) 2.5 mM, (○) 0.76 mM, (■) 0.47 mM, (□) 0.16 mM, (♦) 0.093 mM, (◇) 0.062 mM; (B) Concentration of pyruvate: (◇) 0.15 mM, (♦) 0.20 mM, (□) 0.30 mM, (■) 0.60 mM, (○) 1.0 mM, (●) 3.7 mM.

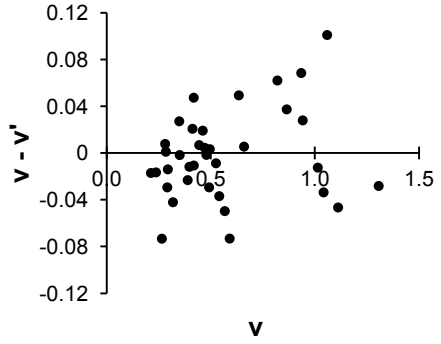

Figure B 9 Residuals for plots in Figure B 8.

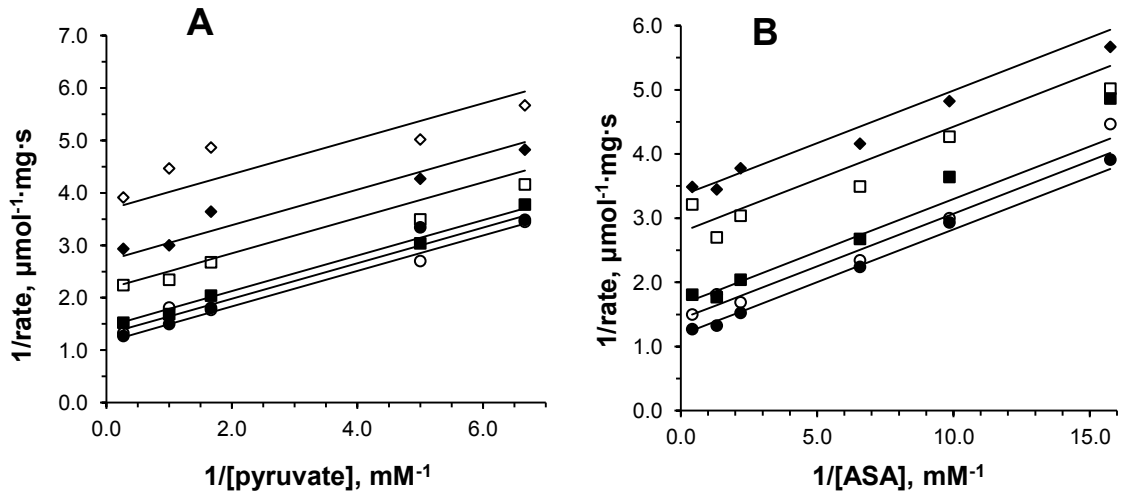

Figure B 10 Double-reciprocal plots of the H59A-catalyzed reaction. Solid lines are the global fit of Equation 4.1 to the data. (A) Concentration of ASA: (●) 2.4 mM, (○) 0.76 mM, (■) 0.46 mM, (□) 0.15 mM, (♦) 0.10 mM, (◇) 0.064 mM; (B) Concentration of pyruvate: (♦) 0.15 mM, (□) 0.20 mM, (■) 0.60 mM, (○) 1.0 mM, (●) 3.7 mM.

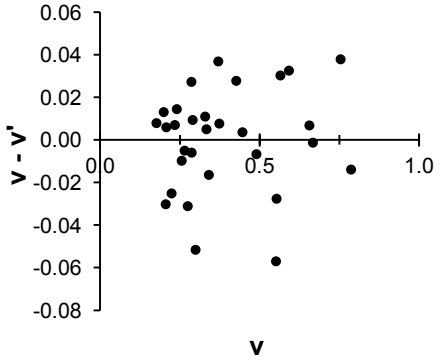

Figure B 11 Residuals for plots in Figure B 10**.**

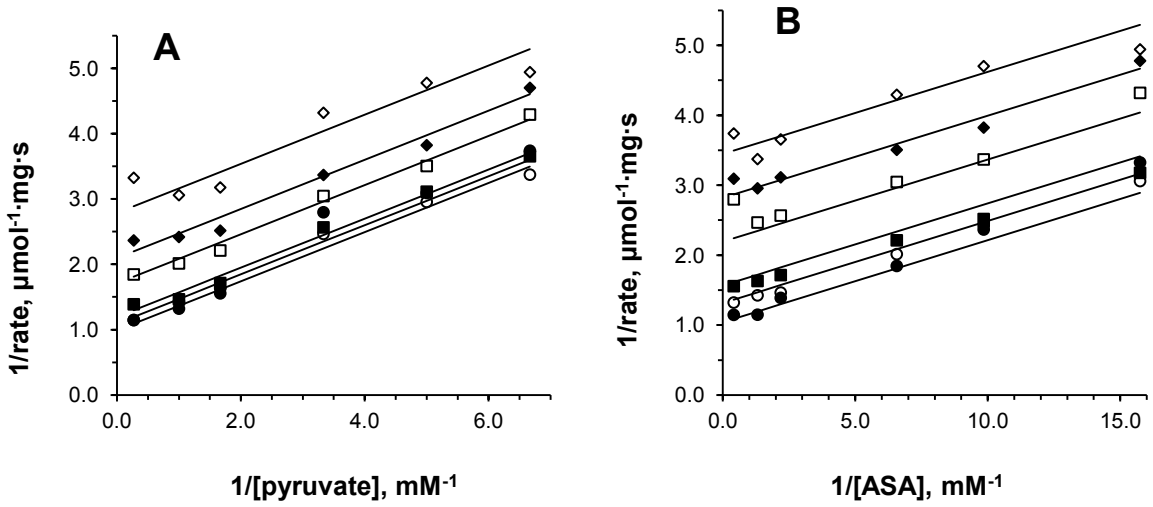

Figure B 12 Double-reciprocal plots of the H56N-catalyzed reaction. Solid lines are the global fit of Equation 4.1 to the data. (A) Concentration of ASA: (●) 2.4 mM, (○) 0.76 mM, (■) 0.46 mM, (□) 0.15 mM, (♦) 0.10 mM, (◇) 0.064 mM; (B) Concentration of pyruvate: (◇) 0.15 mM, (♦) 0.20 mM, (□) 0.30 mM, (■) 0.60 mM, (○) 1.0 mM, (●) 3.7 mM.

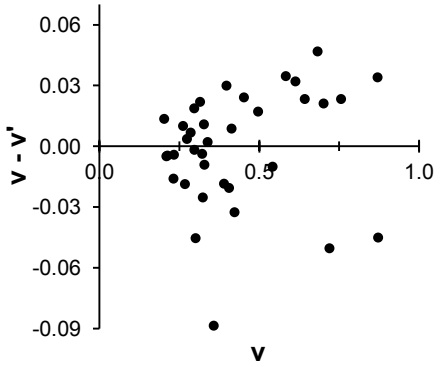

Figure B 13 Residuals for plots in Figure B 12.

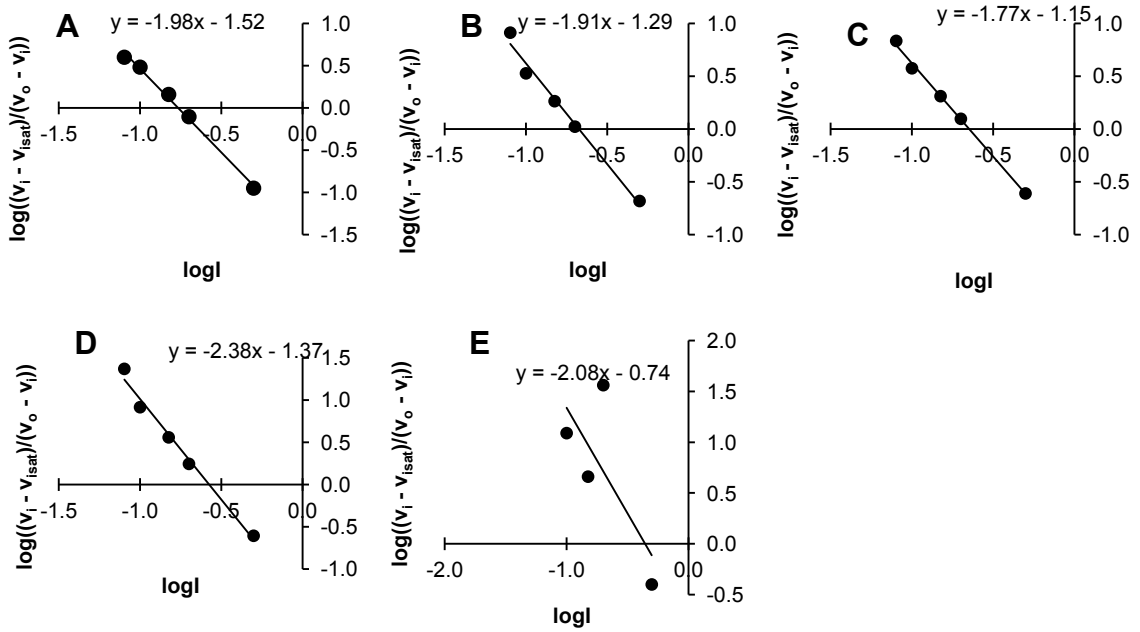

Figure B 14 Hill plots at 3.7 mM pyruvate and varied concentrations of ASA for H56A mutant: (A) 0.050 mM, (B) 0.099 mM, (C) 0.16 mM, (D) 0.25 mM, (E) 2.5 mM. Solid lines were obtained by linear regression.

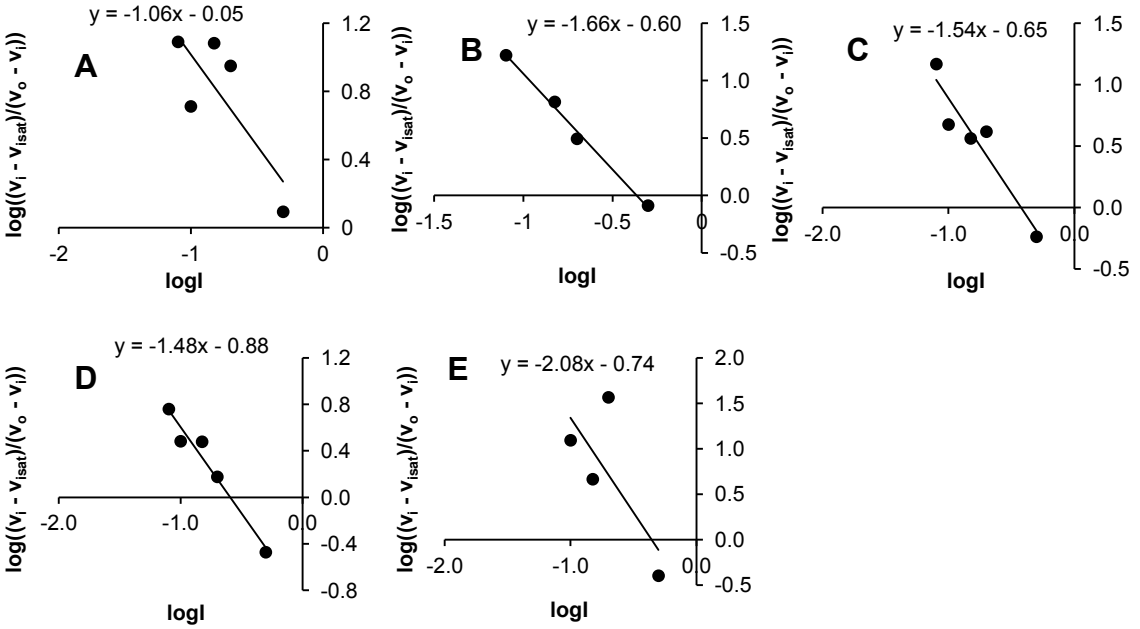

Figure B 15 Hill plots at 2.5 mM ASA and varied concentrations of pyruvate for H56A mutant: (A) 0.15 mM, (B) 0.25 mM, (C) 0.50 mM, (D) 1.0 mM, (E) 3.7 mM. Solid lines were obtained by linear regression.

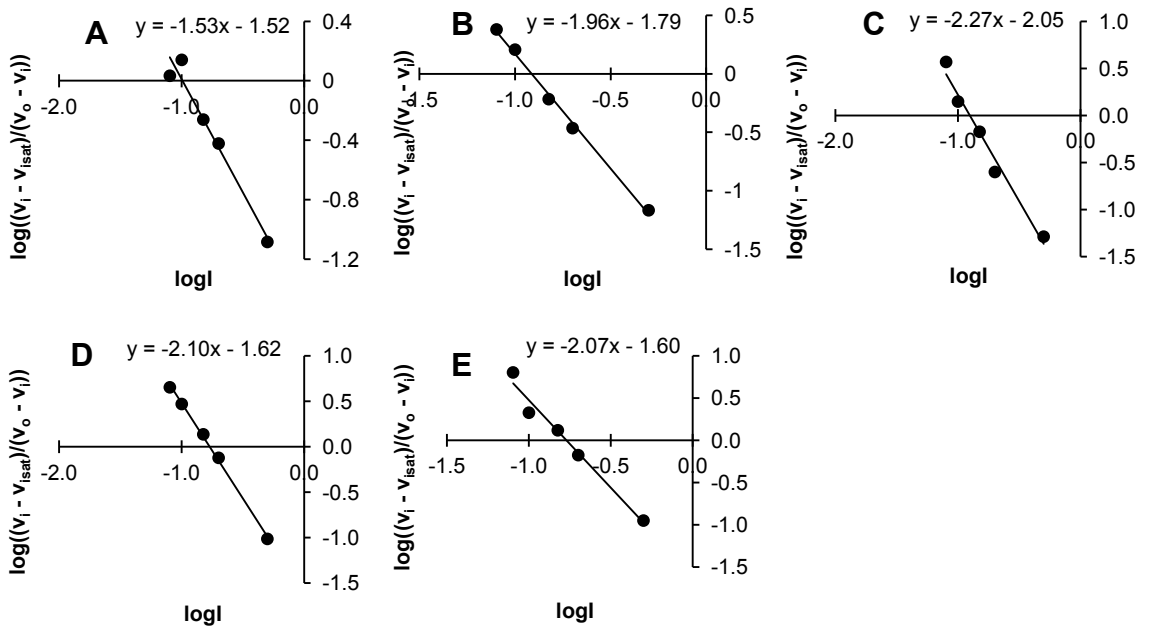

Figure B 16 Hill plots at 3.7 mM pyruvate and varied concentrations of ASA for H56N mutant: (A) 0.062 mM, (B) 0.093 mM, (C) 0.16 mM, (D) 0.47 mM, (E) 2.5 mM. Solid lines were obtained by linear regression.

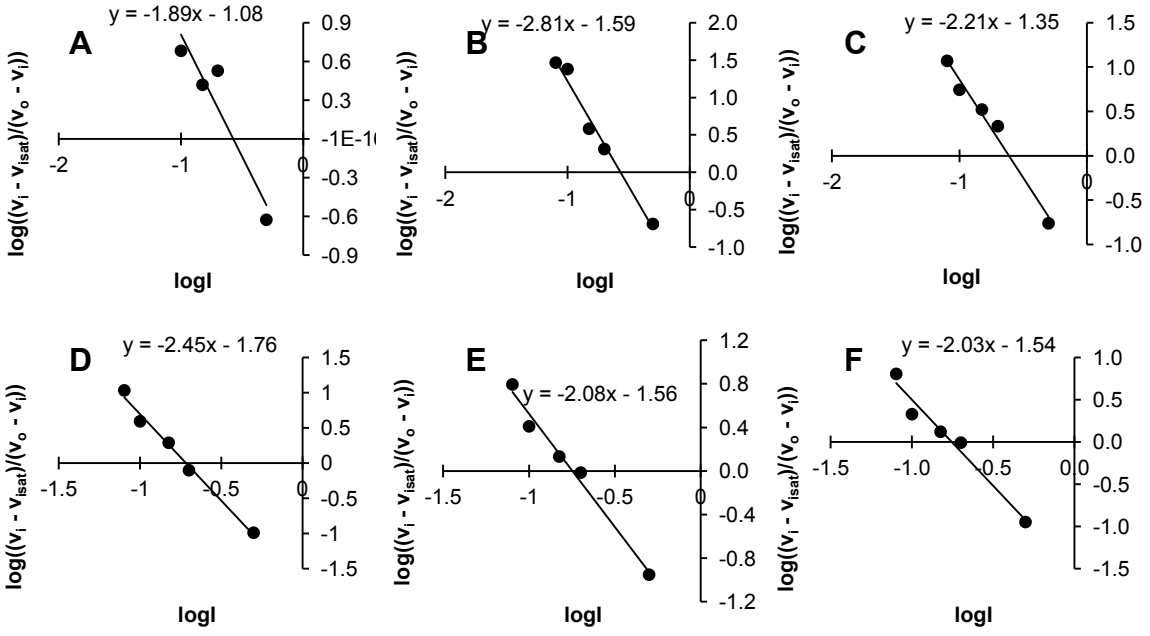

Figure B 17 Hill plots of at 2.5 mM ASA and varied concentrations of pyruvate for H56N mutant: (A) 0.15 mM, (B) 0.20 mM, (C) 0.30 mM, (D) 0.60 mM, (E) 1.0, (F) 3.7 mM. Solid lines were obtained by linear regression.

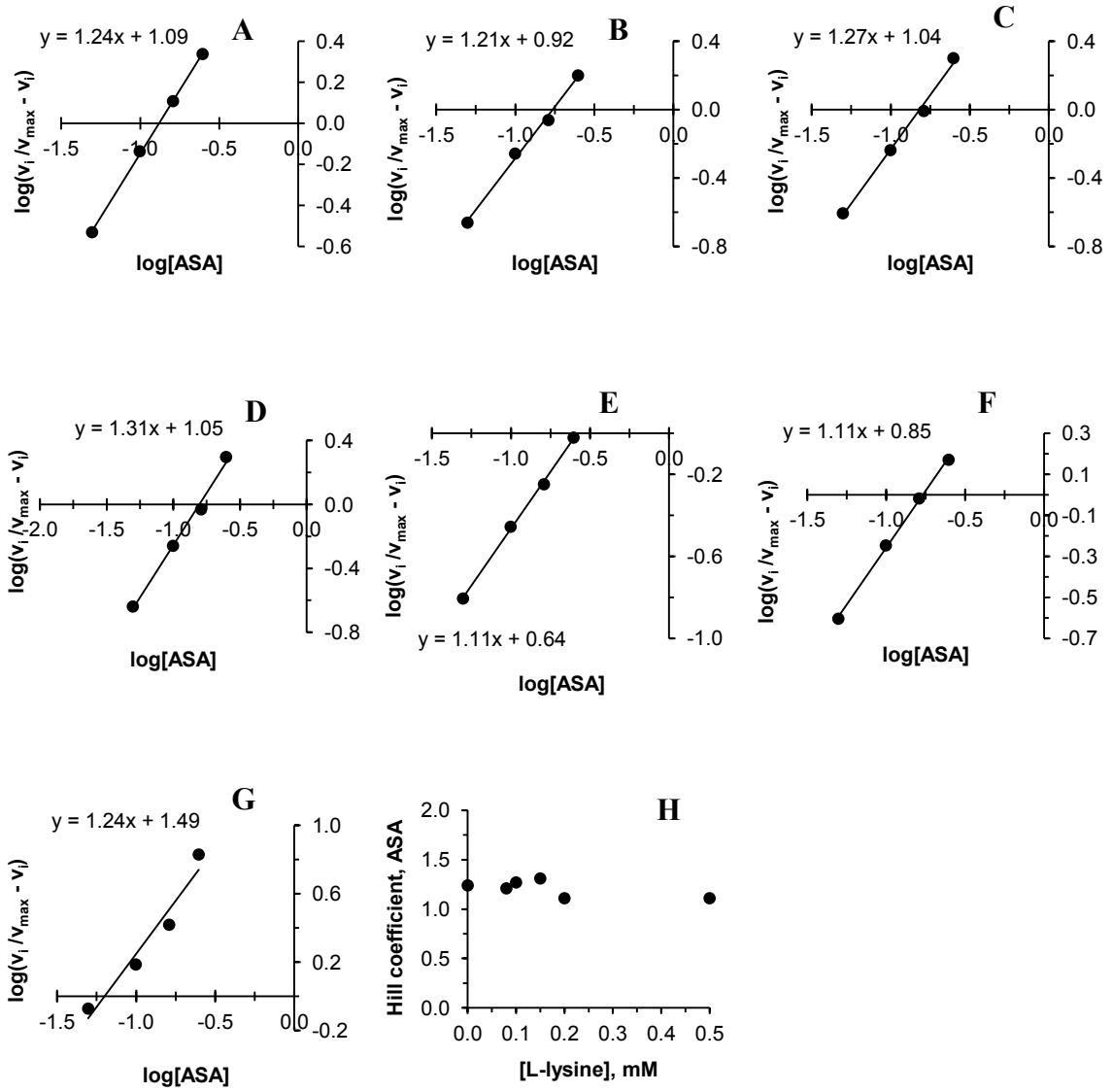

Figure B 18 Hill plots at 3.7 mM pyruvate and varied concentrations of lysine for H56A mutant: (A) 0 mM, (B) 0.08 mM, (C) 0.10 mM, (D) 0.15 mM, (E) 0.20, (F) 0.50, (G) 5.0 mM. Solid lines were obtained by linear regression. (H) Plot *n*(ASA) *vs*. [L-lysine]

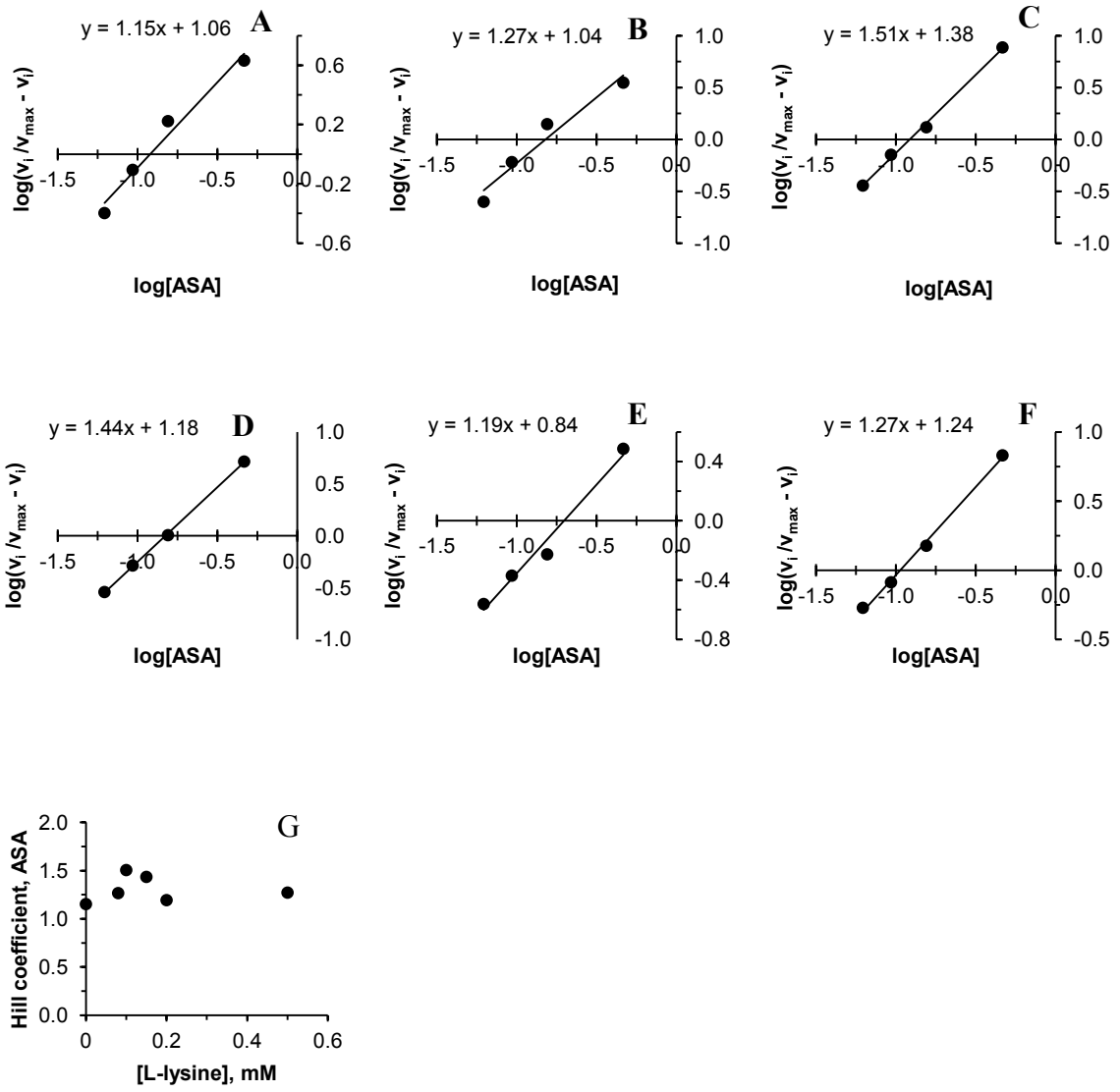

Figure B 19 Hill plots at 3.7 mM pyruvate and varied concentrations of lysine for H56N mutant: (A) 0 mM, (B) 0.08 mM, (C) 0.10 mM, (D) 0.15 mM, (E) 0.20, (F) 0.50 mM. Solid lines were obtained by linear regression. (G) Plot *n*(ASA) *vs*. [L-lysine]

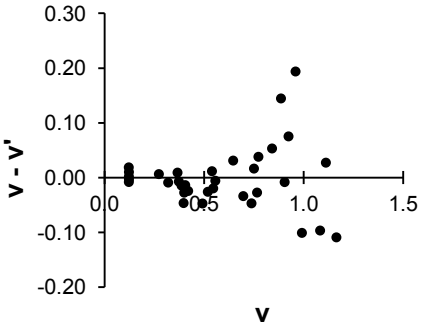

Figure B 20 Residuals for plots in Figure 4.4.

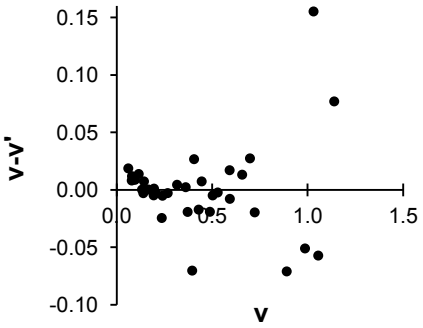

Figure B 21 Residuals for plots in Figure 4.5.

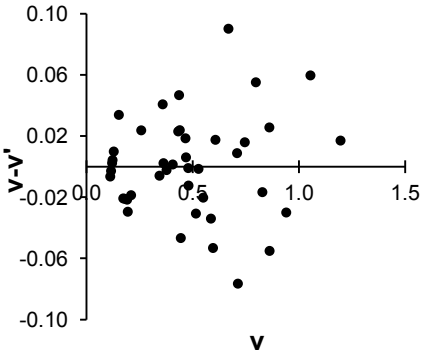

Figure B 22 Residuals for plots in Figure 4.6.

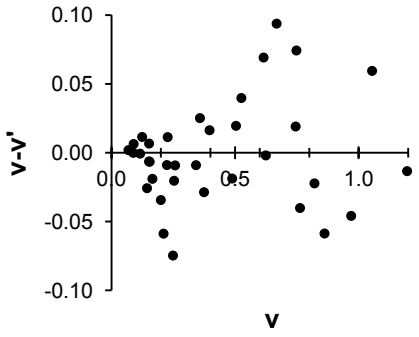

Figure B 23 Residuals for plots in Figure 4.7.